Eva Morava
Matthias Baumgartner
Marc Patterson
Shamima Rahman
Johannes Zschocke
Verena Peters *Editors*

JIMD Reports

Volume 27

SSIEM

Springer

JIMD Reports
Volume 27

Eva Morava
Editor-in-Chief

Matthias Baumgartner · Marc Patterson · Shamima Rahman · Johannes Zschocke
Editors

Verena Peters
Managing Editor

JIMD Reports
Volume 27

Springer

SSIEM

Editor-in-Chief
Eva Morava
Tulane University Medical School
New Orleans
Louisiana
USA

Editor
Matthias Baumgartner
Division of Metabolism and Children's Research Centre
University Children's Hospital Zurich
Zurich
Switzerland

Editor
Marc Patterson
Division of Child and Adolescent Neurology
Mayo Clinic
Rochester
Minnesota
USA

Editor
Shamima Rahman
Clinical and Molecular Genetics Unit
UCL Institute of Child Health
London
UK

Editor
Johannes Zschocke
Division of Human Genetics
Medical University Innsbruck
Innsbruck
Austria

Managing Editor
Verena Peters
Center for Child and Adolescent Medicine
Heidelberg University Hospital
Heidelberg
Germany

ISSN 2192-8304 ISSN 2192-8312 (electronic)
JIMD Reports
ISBN 978-3-662-50408-6 ISBN 978-3-662-50409-3 (eBook)
DOI 10.1007/978-3-662-50409-3

© SSIEM and Springer-Verlag Berlin Heidelberg 2016
This work is subject to copyright. All rights are reserved by the Publisher, whether the whole or part of the material is concerned, specifically the rights of translation, reprinting, reuse of illustrations, recitation, broadcasting, reproduction on microfilms or in any other physical way, and transmission or information storage and retrieval, electronic adaptation, computer software, or by similar or dissimilar methodology now known or hereafter developed.
The use of general descriptive names, registered names, trademarks, service marks, etc. in this publication does not imply, even in the absence of a specific statement, that such names are exempt from the relevant protective laws and regulations and therefore free for general use.
The publisher, the authors and the editors are safe to assume that the advice and information in this book are believed to be true and accurate at the date of publication. Neither the publisher nor the authors or the editors give a warranty, express or implied, with respect to the material contained herein or for any errors or omissions that may have been made.

Printed on acid-free paper

This Springer imprint is published by Springer Nature
The registered company is Springer-Verlag GmbH Berlin Heidelberg

Contents

JIMD Reports
DOI 10.1007/8904_2015_491

RESEARCH REPORT

Detailed Biochemical and Bioenergetic Characterization of *FBXL4*-Related Encephalomyopathic Mitochondrial DNA Depletion

Ghadi Antoun • Skye McBride • Jason R. Vanstone • Turaya Naas • Jean Michaud • Stephanie Redpath • Hugh J. McMillan • Jason Brophy • Hussein Daoud • Pranesh Chakraborty • David Dyment • Martin Holcik • Mary-Ellen Harper • Matthew A. Lines

Received: 06 May 2015 / Revised: 24 July 2015 / Accepted: 30 July 2015 / Published online: 25 September 2015
© SSIEM and Springer-Verlag Berlin Heidelberg 2015

Abstract Mutations of *FBXL4*, which encodes an orphan mitochondrial F-box protein, are a recently identified cause of encephalomyopathic mtDNA depletion. Here, we describe the detailed clinical and biochemical phenotype of a neonate presenting with hyperlactatemia, leukoencephalopathy, arrhythmias, pulmonary hypertension, dysmorphic features, and lymphopenia. Next-generation sequencing in the proband identified a homozygous frameshift, c.1641_1642delTG, in *FBXL4*, with a surrounding block of SNP marker homozygosity identified by microarray. Muscle biopsy showed a paucity of mitochondria with ultrastructural abnormalities, mitochondrial DNA depletion, and profound deficiency of all respiratory chain complexes. Cell-based mitochondrial phenotyping in fibroblasts showed mitochondrial fragmentation, decreased basal and maximal respiration, absence of ATP-linked respiratory and leak capacity, impaired survival under obligate aerobic respiration, and reduced mitochondrial inner membrane potential, with relative sparing of mitochondrial mass. Cultured fibroblasts from the patient exhibited a more oxidized glutathione ratio, consistent with altered cellular redox poise. High-resolution respirometry of permeabilized muscle fibers showed marked deficiency of oxidative phosphorylation using a variety of mitochondrial energy substrates and inhibitors. This constitutes the fourth and most detailed report of *FBXL4* deficiency to date. In light of our patient's clinical findings and genotype (homozygous frameshift), this phenotype likely represents the severe end of the *FBXL4* clinical spectrum.

Communicated by: Shamima Rahman, FRCP, FRCPCH, PhD

Competing interests: None declared

Electronic supplementary material: The online version of this chapter (doi:10.1007/8904_2015_491) contains supplementary material, which is available to authorized users.

G. Antoun · M.-E. Harper
Department of Biochemistry, Microbiology, and Immunology, Faculty of Medicine, University of Ottawa, Ottawa, ON, Canada

S. McBride · J.R. Vanstone · T. Naas · S. Redpath · H.J. McMillan · J. Brophy · H. Daoud · P. Chakraborty · D. Dyment · M. Holcik · M.A. Lines (✉)
Children's Hospital of Eastern Ontario Research Institute, Ottawa, ON, Canada
e-mail: mlines@cheo.on.ca

J. Michaud
Department of Pathology and Laboratory Medicine, Children's Hospital of Eastern Ontario and Faculty of Medicine, University of Ottawa, Ottawa, ON, Canada

T. Naas · P. Chakraborty
Newborn Screening Ontario, Ottawa, ON, Canada

Introduction

Autosomal recessive mutations of *FBXL4* (F-box and leucine-rich repeat-containing protein 4) cause a recently described form of encephalomyopathic mitochondrial DNA (mtDNA) depletion (OMIM #615471). Clinical findings in all patients described to date variably include: lactic acidosis, hyperammonemia, encephalopathy (hypotonia, microcephaly, white matter changes, and severe developmental delay), dysmorphic features, congenital cataract, and premature death in infancy or childhood (Bonnen et al. 2013; Gai et al. 2013; Huemer et al. 2015). Multiple deficiencies of respiratory chain activities are observed, with associated mtDNA depletion occurring via an unknown mechanism. Cells from patients with *FBXL4* deficiency exhibit a number of further

mitochondrial phenotypes such as reduced spare respiratory capacity and inner membrane potential, fragmentation of the mitochondrial network, and aberrant (enlarged) nucleoids. Because the function of FBXL4 and the molecular pathophysiology of this condition are unknown, a rational treatment strategy has not yet been devised, and current management is supportive.

The existing literature surrounding FBXL4 deficiency consists of only three reports (Bonnen et al. 2013; Gai et al. 2013; Huemer et al. 2015) primarily concerned with the clinical and molecular features of this rare condition. Here, we present the detailed clinical, molecular, biochemical, and bioenergetic findings in a female neonate with a homozygous *FBXL4* frameshift mutation predicted to result in a total loss of protein activity. The observed phenotype in this case, which includes hyperlactatemia, periventricular cysts, cardiomyopathy, failure to thrive, panleukopenia, profound impairment of cellular respiration, loss of inner membrane potential, altered cellular redox balance, and mitochondrial network fragmentation, demonstrates the severe and pleiotropic effects of FBXL4 deficiency on a wide range of mitochondrial functions.

Materials and Methods

Subject Recruitment and Clinical Investigations

Please refer to "Compliance with Ethical Guidelines," above, for details regarding study design and recruitment. Clinically standard investigations (conventional serum chemistries, amino acids, acylcarnitines, organic acids, histology and histochemistry, electron microscopy, spectrophotometric respiratory chain testing, and measurement of lactate to pyruvate ratio in fibroblasts) were performed on a clinical basis according to established protocols. Fibroblast cell lines were established from a small sterile skin biopsy, maintained in standard growth medium (DMEM containing 25 mM glucose, 4 mM glutamine, 10% fetal calf serum, 100 μg/ml streptomycin, and 100U/ml penicillin), and all subsequent analyses were performed at low passage (≤11) with a same-day passage-matched experimental control. Genomic analyses were carried out on whole blood lymphocyte DNA. Next-generation sequencing and mtDNA depletion studies were performed by Baylor College Medical Genetics Laboratories on a clinical basis. Microarray was performed clinically (Affymetrix CytoScan HD) according to standard protocols.

High-Resolution Respirometry

High-resolution respirometry was performed as previously described (Krumschnabel et al. 2015). Briefly, muscle was quickly transferred into ice-cold relaxation medium (BIOPS – 10 mM Ca-EGTA buffer, 0.1 μM free calcium, 20 mM imidazole, 20 mM taurine, 50 mM K-MES, 0.5 mM DTT, 6.56 mM $MgCl_2$, 5.77 mM ATP, 15 mM phosphocreatine, pH 7.1). After mechanical separation of individual fibers, chemical permeabilization was performed by agitating the fibers for 30 min in ice-cold BIOPS solution containing 50 μg/ml of saponin. Fibers were subsequently washed in ice-cold mitochondrial respiration medium (MiR05 – 0.5 mM EGTA, 3 mM $MgCl_2$, 60 mM K-lactobionate, 20 mM taurine, 10 mM KH_2PO_4, 20 mM HEPES, 110 mM sucrose, and 1 g/l BSA essentially fatty acid-free, pH 7.1), weighed, and transferred to the respirometer (Oxygraph-2k; Oroboros Instruments, Innsbruck, Austria). During the experiment, the oxygen concentration was maintained between 200 and 400 nmol/ml. Two multiple-substrate and multiple-inhibitor protocols were employed, with sequential addition of compounds into the chambers (Table 1). Data were corrected to wet weight of muscle fibers.

Micro-oximetry

Mitochondrial oxygen consumption rate (OCR) and extracellular acidification rate (ECAR) were measured in skin-derived fibroblasts as previously described (Invernizzi et al. 2012) using the Seahorse XF-24 Extracellular Flux Analyzer (Seahorse Biosciences, Massachusetts, USA). For the assessment of mitochondrial function, cells were seeded at 50,000 cells/well 1 day before the assay. On the day of the assay, growth medium was replaced with HCO_3-free DMEM containing 25 mM D-glucose, 4 mM glutamine, and 1 mM sodium pyruvate, and cells were incubated in a CO_2-free environment. Measurements of OCR were taken at 7-minute intervals following the sequential addition of 1 μg/ml oligomycin, 1 μM CCCP, and 1 μM antimycin A with 0.5 μM rotenone. All reported values for OCR are corrected to non-mitochondrial oxygen consumption as assessed after the addition of antimycin A. Data were normalized to total protein.

For the assessment of glycolytic function, cells were seeded at 50,000 cells/well 1 day before the assay. On the day of the assay, growth medium was replaced with HCO_3-free DMEM containing 143 mM sodium chloride, 3 mg/l phenol red, and 2 mM glutamine, and cells were incubated in a CO_2-free environment for 1 h. Measurements of ECAR were taken at 7-min intervals following the sequential addition of 10 mM glucose and 1 μg/ml oligomycin. All reported values for ECAR were corrected to basal ECAR as assessed before the injection of glucose (non-glycolytic acidification rate). Data were normalized to total protein.

Measurement of Glutathione and Glutathione Disulfide

Glutathione (GSH) and glutathione disulfide (GSSG) measurements were performed using a high-performance liquid chromatography (HPLC) method adapted from previously

Table 1 Mitochondrial respiration in permeabilized *vastus lateralis* fibers of patient as measured by high-resolution respirometry

Protocol 1: leak	Oxygen consumption (pmol/(s*mg))	Protocol 2: electron transport system (ETS)	Oxygen consumption (pmol/(s*mg))
Adenylate-free respiration		*Adenylate-free respiration*	
2 mM malate and 200 μM octanoyl carnitine	3.6204	2 mM malate and 5 mM pyruvate	2.0382
Fatty acid-supported respiration		*Complex I-supported respiration*	
5 mM ADP	4.8882	10 mM glutamate and 5 mM ADP	3.0307
Complex I-supported respiration		*Complex I+II-supported respiration*	
10 mM glutamate and 5 mM pyruvate	0.44885	10mM succinate (OXPHOS2)	22.2963
Complex I+II-supported respiration		*Maximal uncoupled respiration*	
10 mM succinate (OXPHOS1)	18.2139	0.25 μM titrations FCCP (chemical uncoupler)	22.6088
Leak respiration		*Complex I-independent oxygen consumption*	
2.5 μM oligomycin (ATP synthase inhibitor)	5.4048	0.5 μM rotenone (complex I inhibitor)	21.2964
Cytochrome C oxidase (COX) activity		*Cytochrome C oxidase (COX) activity*	
2 mM tetramethylphosphodinitrate (TMPD; COX-specific electron donors) and 2 mM ascorbate	49.15135	2 mM tetramethylphosphodinitrate (TMPD; COX-specific electron donors) and 2 mM ascorbate	75.4651

All values were corrected to non-mitochondrial oxygen consumption as measure by the addition of the complex III inhibitor, antimycin A (2.5 μM). $N = 1$

published work (Mailloux et al. 2012). Briefly, skin fibroblasts were collected, counted, and resuspended in a 1:1 solution of homogenization buffer (0.25 M sucrose, 3 mM EDTA, 10 mM Tris buffer, 0.1% trifluoroacetic acid, 10% methanol, pH 7.4) and acidified mobile phase (1.1% trifluoroacetic acid, 1% meta-phosphoric acid, 10% methanol). Samples were incubated (20 min, 4°C) and whole cells and cellular debris were removed by centrifugation (18,300 × *g* for 20 min at 4°C). Resulting samples were run on an Agilent Pursuit5 C18 column, and species were detected at 215 nm using a variable wavelength detector. Chromatographic peaks were integrated and total GSH and GSSG concentrations were determined. Data were normalized to cell number.

Characterization of Mitochondrial Content, Network, and Inner Membrane Potential

Patient and healthy adult control fibroblasts were plated 24–48 h prior to staining. Cells were stained with either 200 nM MitoTracker Green FM (Life Technologies, Carlsbad, CA) (for assessment of mitochondrial content) or 50 nM tetramethylrhodamine ethyl ester perchlorate (TMRE – Sigma, St. Louis, MO) (for assessment of mitochondrial inner membrane potential), trypsinized, and resuspended in PBS containing 0.2% BSA, and fluorescence was measured on a Cyan ADP 9 analyzer (Beckman Coulter, Mississauga, ON). Fluorescence signal from the autofluorescent control was subtracted from the mean fluorescence of the stained sample. For mitochondrial network visualization, cells were fixed with 4% paraformaldehyde and stained with 2 μg/ml TOMM20 (Abcam, Cambridge, UK) and 1:2000 Oregon Green (Life Technologies, Carlsbad, CA); secondary antibody was used in blocking buffer (3% BSA, 0.3% Triton X-100). Imaging was carried out by spinning disk confocal microscopy (Quorum Technologies, Guelph, ON).

Assessment of Cell Viability

Patient and control skin-derived fibroblasts were plated at 10,000–15,000 cells/well in 96-well plates. The following day, growth medium was replaced with new medium containing either 25 mM glucose or 10 mM galactose as the major carbon source, as well as 100 nM of YOYO-1 Iodide (Life Technologies, NY, USA). Measurements of cell death, as evidenced by YOYO-1 positive staining, were performed over 72 h using the IncuCyte ZOOM Live Cell Imaging System (Essen Bioscience, MI, USA). For end-point normalization, YOYO-1 positive cell counts were expressed as a fraction of the total number of cells.

Results

The subject, a female neonate, was born to a *gravida* 3, *para* 2 French Canadian mother, and an unidentified but reportedly nonconsanguineous father, following a term pregnancy notable only for diet-controlled gestational diabetes. The delivery was uneventful, with Apgar scores

of 8 at 1 min and 9 at 5 min. Birth weight was 2,620 g (8th centile). The initial presenting symptom was temperature instability at 12 h of age. Laboratory studies at that time showed a marked metabolic acidosis (pH 7.13; pCO2 16 mmHg; HCO_3^- 5 mmol/l; base excess –21.6 mmol/l). MRI of the brain at 1 day of age (Fig. 1a–c) showed diffuse T2 hyperintensity of the supratentorial white matter, consistent with edema, bilateral enlargement of the lateral ventricles with bilateral intraventricular and periventricular cysts as well as absent myelination of the posterior limb of the internal capsule. MR spectroscopy (TE 144) identified a lactate doublet in the basal ganglia. Echocardiography and Holter monitor showed signs consistent with suprasystemic pulmonary hypertension and atrial ectopic tachycardia, requiring treatment with flecainide. Given the working clinical diagnosis of a mitochondrial disorder, a number of biochemical and genomic investigations were undertaken, as detailed below, and the patient was started on cofactor therapy with (variously) carnitine, riboflavin, ubiquinone, biotin, and thiamine, to no obvious beneficial effect. She remained in NICU until two months of age. At four months of age, the subject's examination revealed hypotonia and dysmorphic features (Fig. 1d). By seven months of age, chronic failure to thrive, requiring chronic nasogastric feeding, was apparent, along with evidence of immunodeficiency comprising neutropenia, pan-lymphopenia, and

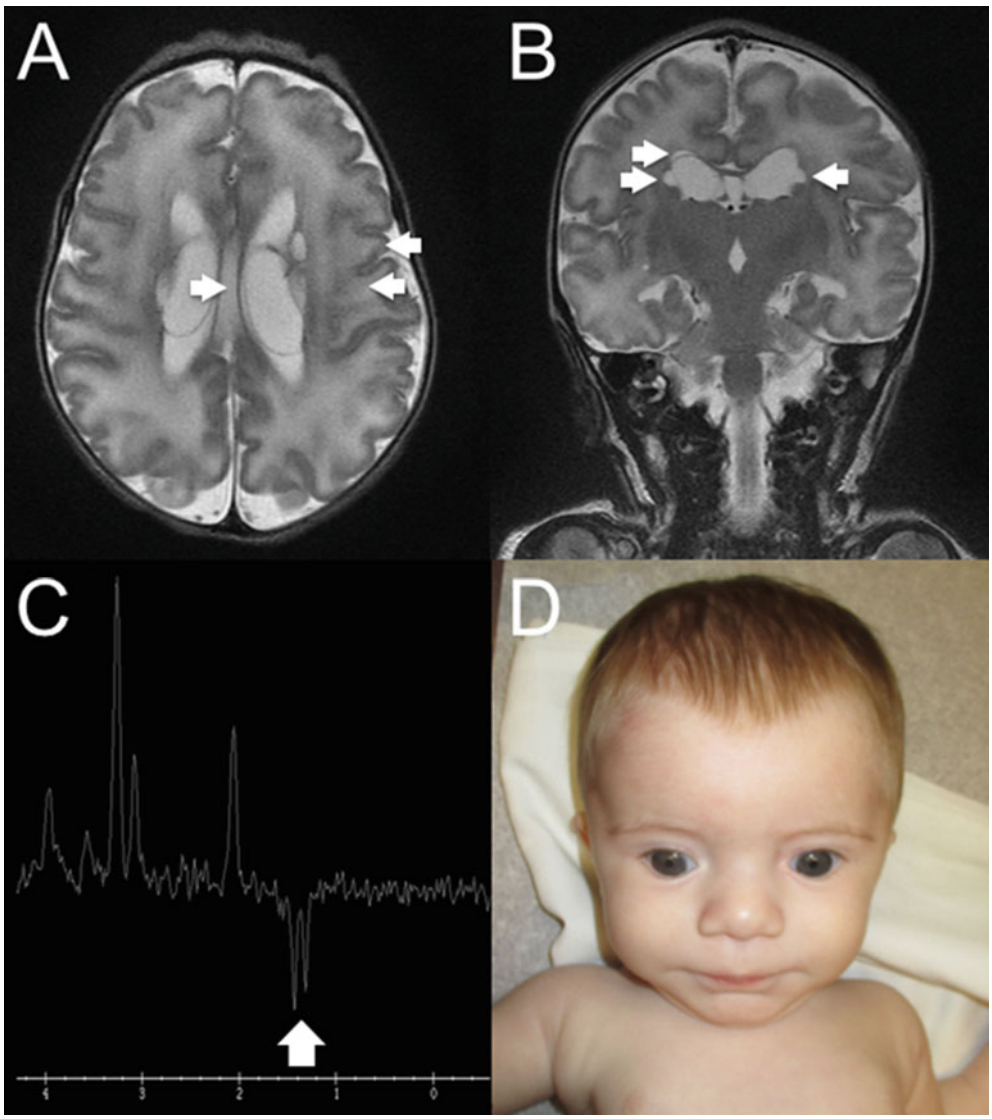

Fig. 1 Cranial MRI at five days of age showed (**a**, **b**) diffuse white matter edema with bilateral intra- and periventricular cysts, a single right occipital focus of restricted diffusion likely related to focal ischemia (not shown), and (**c**) a large lactate doublet in the left basal ganglia by MR spectroscopy. Craniofacial morphology (**d**) was notable for midface hypoplasia, short palpebral fissures, and lightly grooved philtrum. The presenting clinical features were considered to be consistent with a mitochondrial disease and/or pyruvate dehydrogenase deficiency

hypogammaglobulinemia. This presented with severe oral thrush and *Pneumocystis jirovecii* prophylaxis was initiated. Now 14 months old, she remains hypotonic and globally delayed, with milestones equivalent to a four-month-old. Immunoglobulins and neutrophil numbers improved with time and improved nutrition via NG tube feeding; further lymphocyte evaluation is underway.

Biochemical findings in the patient include: lactate, initially 21.6 mmol/l, decreased to 4.3 mmol/l by day 3 of life, and has remained elevated, 3–15 mmol/l; a normal blood lactate concentration has never been recorded in this child. Plasma amino acids showed consistently increased alanine (565–1,086 μmol/l; ref. 143–439 μmol/l), proline (286–515 μmol/l; ref. 52–298 μmol/l), and serine (227–274 μmol/l; ref. 71–186 μmol/l). Acylcarnitine profile showed diffuse elevations in short-, medium-, and long-chain acylcarnitines and acetylcarnitine and small amounts of propionylcarnitine. Urine organic acids (several occasions) have variously showed lactic, pyruvic, and ethylmalonic acids, ketone bodies, Krebs cycle intermediates, and (inconsistently) branched-chain alpha-ketoacids. A *vastus lateralis* biopsy (Supplemental Fig. 1; Supplemental Table 1) obtained at one month of age showed increased lipid droplets and intrasarcoplasmic glycogen, with deficiency of all respiratory chain activities, and particularly of cytochrome oxidase. Ultrastructurally, the mitochondria were fewer in number, some of which are larger and dysmorphic (Supplemental Fig. 1).

Genetic investigations in the patient were as follows: despite no known parental consanguinity, SNP microarray showed a single ~27 Mb region of copy-neutral loss of heterozygosity on chromosome 6 (arr[hg19] 6q13q16.3 (73958441-100963633)x2 hmz). Next-generation sequencing of a combined nuclear and mtDNA panel showed a homozygous frameshift, c.1641_1642delTG (p.C547*), in the gene *FBXL4*, which resides within the 6q marker homozygosity block. This variant has been detected 18 times in 121,202 exomes (allele frequency 0.015%) in the Exome Aggregation Consortium dataset (ExAC, Cambridge, MA, http://exac.broadinstitute.org; accessed July 2015). mtDNA copy number in skeletal muscle in the patient was 37% of control, consistent with mtDNA depletion.

To better delineate the mitochondrial pathophysiology of FBXL4 deficiency, a battery of bioenergetic studies in patient tissues and cells was next conducted. High-resolution respirometry of saponin-permeabilized muscle fibers (Table 1) showed very little respiration on complex I-, complex II-, or ETF-linked substrates. Although this analysis was hindered by the lack of a matched pediatric control specimen, we did observe that (i) all measured rates were very low (<1/3 of published healthy adult reference values) (Gnaiger 2009; authors' unpublished data), and (ii) the addition of rotenone, a complex I inhibitor, had no demonstrable effect on respiration rates, implying a near-complete absence of complex I-linked respiration. Micro-oximetry of patient fibroblasts showed reductions in oxygen consumption rate (OCR) at rest (Fig. 2a) and when stimulated with the inner membrane protonophore carbonyl cyanide m-chlorophenylhydrazone (CCCP) (maximal respiration) (Fig. 2d). This corresponded with reductions in both complex V-coupled ("phosphorylating") and uncoupled ("leak") respiration in the same assay (Fig. 2b). In contrast, the glucose- and oligomycin-stimulated extracellular acidification rate (ECAR, an indirect measure of glycolytic activity) in the cells was enhanced (Fig. 2e, f), suggesting a corresponding overreliance on glycolysis relative to oxidative phosphorylation (Fig. 2g).

The effects of the subject's profound respiratory chain defect on the mitochondrial network and cellular stress responses were further investigated. Spinning disk confocal microscopy of fixed fibroblasts immunostained for the outer membrane transporter TOMM20 (Fig. 3a) confirmed fragmentation of the mitochondrial network. Assessment of mitochondrial content and inner membrane charge in live patient fibroblasts using flow cytometric staining of the cationic lipophilic dyes MitoTracker Green and TMRE showed a reduction in inner membrane potential (Fig. 3b) with no demonstrable difference in mitochondrial content (Fig. 3c).

Assessment of cell viability by time-lapse video microscopy under normal growth conditions (Fig. 3d) showed reduced viability of patient versus control fibroblasts. This phenotype was exacerbated under mandatory aerobic respiration in a medium containing galactose as the principal energy substrate and was most apparent after 72 h (Fig. 3e). HPLC determination of glutathione (GSH) and glutathione disulfide (GSSG) in fibroblasts (Fig. 3f) showed evidence of altered redox poise, more specifically, lower levels of reduced glutathione (GSH) ($p = 0.049$) and an abnormally low GSH:GSSG ratio ($p = 0.00018$).

Discussion

We identified a homozygous frameshift mutation in *FBXL4* in a neonate with a severe mitochondrial phenotype comprising lactic acidosis, CNS, cardiac, and bone marrow involvement, and multicomplex respiratory chain dysfunction associated with mtDNA depletion. Cells from the patient exhibited profoundly deficient respiration of complex I-, II-, and ETF-linked substrates, with loss of inner mitochondrial membrane potential, mitochondrial network fragmentation, and increased cell death under obligate respiration on galactose medium. Cellular glutathione redox poise was also abnormal in patient cells, characterized by a more oxidized cellular milieu. With the exception of mitochondrial mass as assessed by flow cytometry, all other aspects of mitochondrial function were

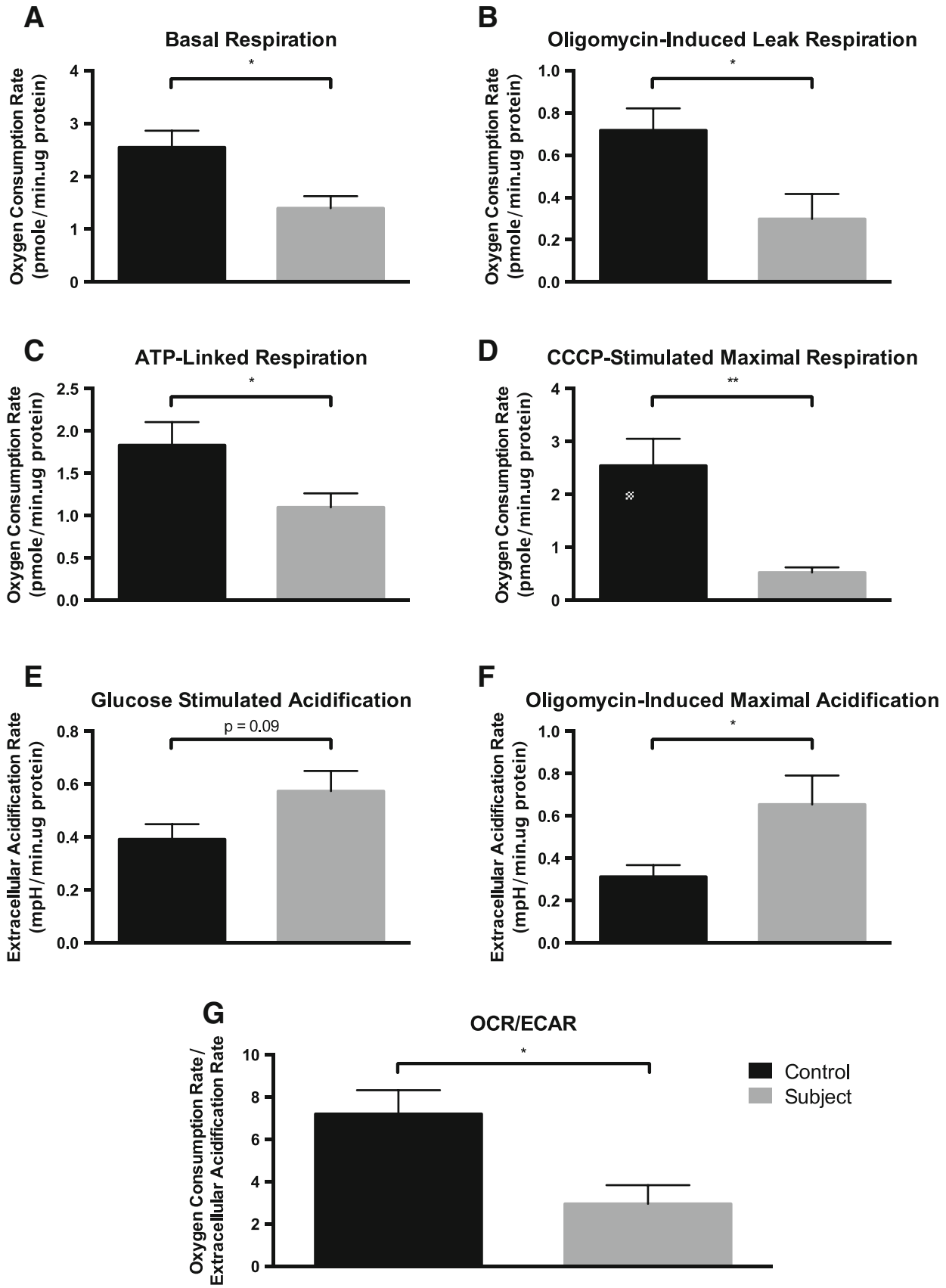

Fig. 2 Assessment of respiratory parameters in skin-derived fibroblasts by micro-oximetry. (**a**–**d**) Oxygen consumption rate (OCR) in patient and control fibroblasts in the presence of glucose, pyruvate, and glutamine. Values are corrected to non-mitochondrial OCR persisting after addition of antimycin A and rotenone. (**a**) Basal OCR. (**b**) Leak OCR measured following inhibition of complex V by

markedly abnormal, i.e., deficiency of FBXL4 had severe and pleiotropic effects on mitochondrial function. As our proband's homozygous frameshift is predicted to completely abolish FBXL4's expression, the phenotype in our patient is likely situated at the severe end of the *FBXL4* clinical spectrum. Of note, our patient did not manifest hyperammonemia, as described in a proportion of the previously described cases. Considering the few other reported individuals with two severe (truncating) *FBXL4* mutations (Huemer et al. 2015, patients 2, 3, 11, 12, 13), no clinical features can currently be consistently associated with total FBXL4 deficiency. However, some reported manifestations include craniofacial abnormalities, immune system deficiencies as well as congenital cataracts and hypoplastic cerebella.

As previously reported, (Bonnen et al. 2013; Gai et al. 2013) our micro-oximetry experiments in patient fibroblasts showed a deficiency of both basal and maximally stimulated respiration, with a simultaneous overreliance on glycolysis as approximated by ECAR. Of note, the standard clinical fibroblast lactate to pyruvate ratio in this patient was only slightly elevated (27.6) despite the patient's marked permanent hyperlactatemia and hyperalaninemia, and on this occasion micro-oximetry appeared to offer a more faithful demonstration of the patient's respiratory phenotype in cells.

A novel finding of our study is that fibroblasts from our patient exhibited a more oxidized GSH:GSSG ratio, reflecting a perturbation of glutathione-dependant redox poise. This could be caused by either an increase in reactive oxygen species (ROS) production and/or a decrease in ROS quenching capacity (Mailloux et al. 2013a). Because protein glutathionylation is known to affect the activity of various respiratory chain proteins and uncoupling proteins including UCP3 (Mailloux et al. 2013b), altered redox status could potentially have knock-on effects on the regulation of protein glutathionylation and on the glutathionylation of energy substrates such as fumarate (Sullivan et al. 2013). The potential role of excessive oxidative stress on the reduced cellular survival observed in the proband's cells under mandatory respiration requires confirmation as does the exploration of any effect of cofactor, drug, and/or antioxidant "therapy" on patient cells in vitro.

Very little is known about the actual molecular pathogenesis of FBXL4 deficiency. FBXL4 belongs to a family of leucine-rich repeat (LRR)-containing F-box proteins, other members of which are adaptor subunits of multiprotein complexes with specific (phosphorylation-dependent) E3 ubiquitin ligase activity (Skowyra et al. 1997). FBXL4, which localizes to the mitochondrial intermembrane space and participates in a 400 kDa quaternary complex, is hypothesized (but not proven) to have a similar activity. In addition, a role in mitochondrial quality control similar to the PINK1-dependent recruitment of parkin, another E3 ubiquitin ligase, has been proposed (Gai et al. 2013). If true, this model would imply that the mtDNA depletion seen in FBXL4 deficiency is secondary to altered mitophagy, mitochondrial dynamics, and/or quality control; however, apart from the relatively nonspecific observation that the mitochondrial network is fragmented in FBXL4 deficiency, this model has not yet been tested experimentally.

An effective therapeutic approach for FBXL4 deficiency is clearly wanting. Of the three available inputs to the respiratory chain, complex II-linked respiration appears to be the least profoundly impaired, at least in our patient, whereas oxidation of NADH-linked substrates appears to be poor. Empiric cofactor therapy with riboflavin, biotin, thiamine, pyridoxine, coenzyme Q, and (briefly) carnitine appears to have had no beneficial effect in our patient. We would add the important caveat that children with this condition should be evaluated for immune system dysfunction, and live vaccinations be withheld if appropriate. Patient fibroblasts, which display several "screenable" phenotypes in FBXL4 deficiency, may serve as a useful model in which to study the pathobiology of this condition, as well as its response to drugs and other pharmacologic agents.

Conclusions

Total FBXL4 deficiency in our patient was characterized clinically by severe multisystem disease including lactic acidosis, cystic white matter lesions, cardiomyopathy, arrhythmias, and immunodeficiency. The main physiological findings in cells from this patient include profound reductions in complex I-, II- and ETF-linked substrate-dependant respiration, a loss of inner membrane potential, and fragmentation of the mitochondrial network with no parallel decrease in mitochondrial content. A novel finding of this study was the marked glutathione oxidation in our patient's cells, suggesting either a failure of endogenous antioxidant defenses or increased ROS generation. We propose that cultured patient cells may serve as a convenient model in which to preclinically evaluate potential drug and/or cofactor therapies for this rare but increasingly recognized mitochondriopathy.

Fig. 2 (continued) oligomycin. (**c**) Phosphorylation-coupled OCR, estimated as the resulting decrease in OCR after oligomycin. (**e**, **f**) Extracellular acidification rate (ECAR), an indirect measure of glycolytic activity in cells. Rates are corrected to non-glycolytic acidification rate as measured prior to the addition of glucose. (**e**) Glucose-stimulated ECAR. (**f**) Maximal (oligomycin-stimulated) ECAR. (**g**) Ratio of basal OCR to glucose-stimulated ECAR. $N = 6$. Values are presented as mean ± SEM; $*p < 0.05$, $**p < 0.01$ analyzed by unpaired, two-tailed Student's *t*-test

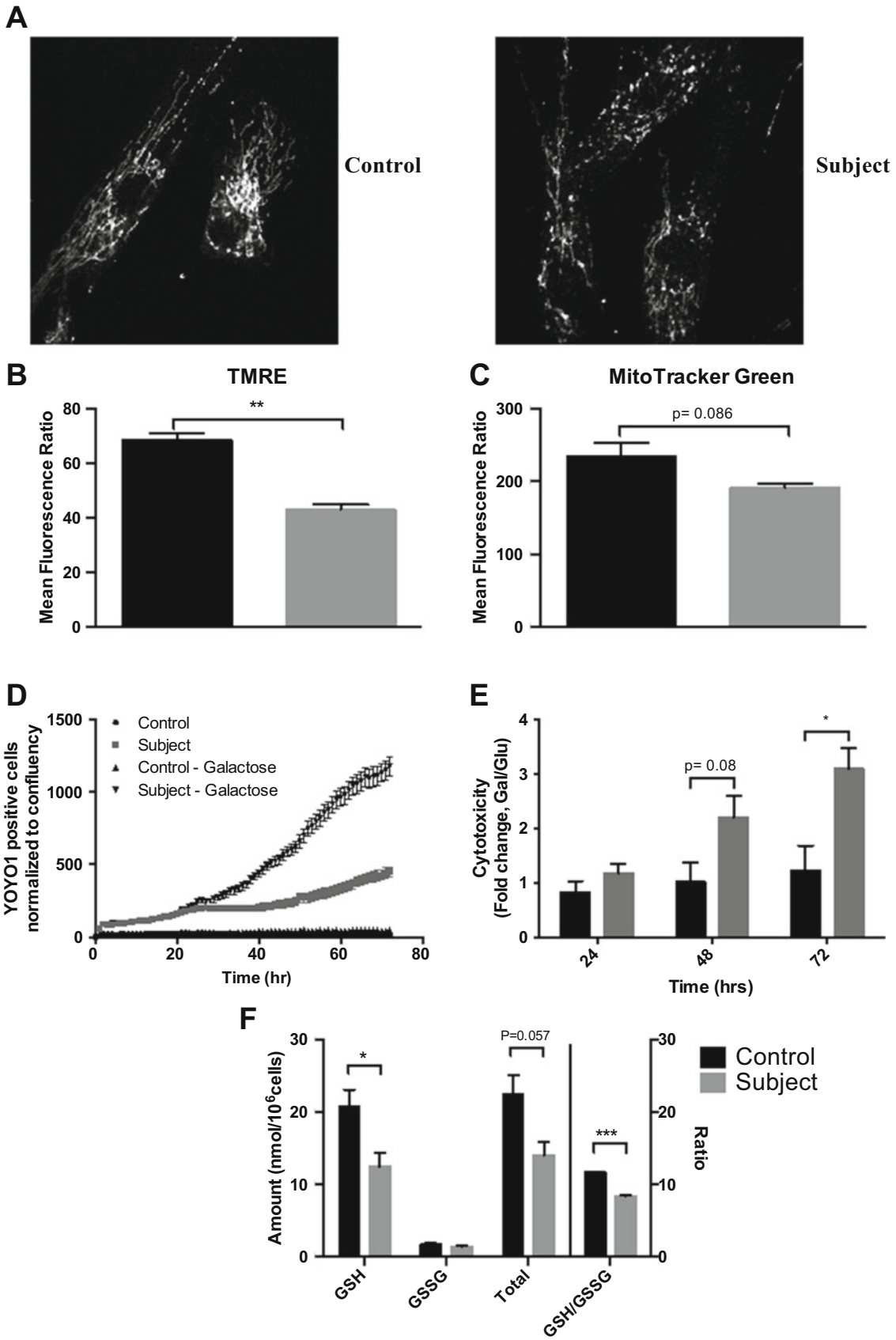

Fig. 3 Assessment of mitochondrial content, inner membrane potential, and network branching by cell staining in skin-derived fibroblasts. (**a**) Spinning disk confocal microscopy of fixed control (*left*) and patient (*right*) fibroblasts immunostained for the outer membrane transporter TOMM20. (**b**) Mitochondrial content (MitoTracker Green) ($N = 3$) and (**c**) inner membrane potential (TMRE)

One Sentence Summary

A homozygous frameshift mutation in *FBXL4* was identified in a neonate with primary lactic acidosis, in whom cell-based mitochondrial phenotyping demonstrated severe global mitochondrial dysfunction.

Compliance with Ethics Guidelines

Conflict of Interest

Ghadi Antoun, Skye McBride, Jason R. Vanstone, Turaya Naas, Jean Michaud, Stephanie Redpath, Hugh J. McMillan, Jason Brophy, Hussein Daoud, Pranesh Chakraborty, David Dyment, Martin Holcik, Mary-Ellen Harper, and Matthew A. Lines declare that they have no conflict of interest.

Informed Consent

All procedures followed were in accordance with the Tri-Council Policy Statement: Ethical Conduct for Research Involving Humans (2010) and with the Helsinki Declaration of 1975, as revised in 2000. Informed consent was obtained from all patients participating in the study. The research protocol was approved by the Children's Hospital of Eastern Ontario Research Ethics Board.

Authors' Contributions

All authors contributed to the conception and design of the study. ML, SR, JM, HJM, and JB acquired the clinical and genomic data. GA, SM, JV, and TN generated respirometry and cell-based data for mitochondrial phenotyping. Data were analyzed and interpreted by GA, SM, JV, TN, JM, MEH, and ML. The manuscript was drafted by GA, SM, MEH, and ML. Critical revisions were performed by all authors.

References

Bonnen PE, Yarham JW, Besse A et al (2013) Mutations in FBXL4 cause mitochondrial encephalopathy and a disorder of mitochondrial DNA maintenance. Am J Hum Genet 93:471–481

Gai X, Ghezzi D, Johnson MA et al (2013) Mutations in FBXL4, encoding a mitochondrial protein, cause early-onset mitochondrial encephalomyopathy. Am J Hum Genet 93:482–495

Gnaiger E (2009) Capacity of oxidative phosphorylation in human skeletal muscle: new perspectives of mitochondrial physiology. Int J Biochem Cell Biol 41:1837–1845

Huemer M, Karall D, Schossig A, et al (2015) Clinical, morphological, biochemical, imaging and outcome parameters in 21 individuals with mitochondrial maintenance defect related to FBXL4 mutations. J Inherit Metab Dis

Invernizzi F, D'Amato I, Jensen P, Ravaglia S, Zeviani M, Tiranti V (2012) Microscale oxygraphy reveals OXPHOS impairment in MRC mutant cells. Mitochondrion 12:328–335

Krumschnabel G, Fontana-Ayoub M, Sumbalova Z et al (2015) Simultaneous high-resolution measurement of mitochondrial respiration and hydrogen peroxide production. Methods Mol Biol (Clifton, NJ) 1264:245–261

Mailloux RJ, Adjeitey CN, Xuan JY, Harper ME (2012) Crucial yet divergent roles of mitochondrial redox state in skeletal muscle vs. brown adipose tissue energetics. FASEB J 26:363–375

Mailloux RJ, McBride SL, Harper ME (2013a) Unearthing the secrets of mitochondrial ROS and glutathione in bioenergetics. Trends Biochem Sci 38:592–602

Mailloux RJ, Xuan JY, Beauchamp B, Jui L, Lou M, Harper ME (2013b) Glutaredoxin-2 is required to control proton leak through uncoupling protein-3. J Biol Chem 288:8365–8379

Skowyra D, Craig KL, Tyers M, Elledge SJ, Harper JW (1997) F-box proteins are receptors that recruit phosphorylated substrates to the SCF ubiquitin-ligase complex. Cell 91:209–219

Sullivan LB, Martinez-Garcia E, Nguyen H et al (2013) The proto-oncometabolite fumarate binds glutathione to amplify ROS-dependent signaling. Mol Cell 51:236–248

Fig. 3 (continued) ($N = 3$) were measured by flow cytometry. Values are presented as mean ± SEM; $^{**}p < 0.01$ analyzed by unpaired, two-tailed Student's *t*-test. (**d**) Time course of patient and control fibroblasts showing increased cell death (as evidenced by YOYO1-positivity) of patient cells versus control cells. (**e**) This difference is magnified when cells are grown under mandatory respiration in galactose-containing medium after 72 h. $N = 3$. Values are presented as mean ± SEM; $^{*}p < 0.05$ analyzed by unpaired, two-tailed Student's *t*-test. (**f**) Levels of glutathione (GSH) and glutathione disulfide (GSSG) from skin-derived fibroblasts of control and subject. Values are corrected to cell number. $N = 3$. Values are presented as mean ± SEM; $^{*}p < 0.05$, $^{***}p < 0.001$ analyzed by unpaired, two-tailed Student's *t*-test

JIMD Reports
DOI 10.1007/8904_2015_463

CASE REPORT

Recurrent Ventricular Tachycardia in Medium-Chain Acyl-Coenzyme A Dehydrogenase Deficiency

P. Bala • S. Ferdinandusse • S.E. Olpin • P. Chetcuti • A.A.M. Morris

Received: 04 April 2015 / Revised: 12 May 2015 / Accepted: 17 May 2015 / Published online: 25 September 2015
© SSIEM and Springer-Verlag Berlin Heidelberg 2015

Abstract We report a baby with medium-chain acyl-coenzyme A dehydrogenase (MCAD) deficiency who presented on day 2 with poor feeding and lethargy. She was floppy with hypoglycaemia (1.8 mmol/l) and hyperammonaemia (182 μmol/l). Despite correction of these and a continuous intravenous infusion of glucose at 4.5–6.2 mg/kg/min, she developed generalised tonic clonic seizures on day 3. She also suffered two episodes of pulseless ventricular tachycardia, from which she was resuscitated successfully. Unfortunately, she died on day 5, following a third episode of pulseless ventricular tachycardia.

Arrhythmias are generally thought to be rarer in MCAD deficiency than in disorders of long-chain fatty acid oxidation. This is, however, the sixth report of ventricular tachyarrhythmias in MCAD deficiency. Five of these involved neonates and it may be that patients with MCAD deficiency are particularly prone to ventricular arrhythmias in the newborn period. Three of the patients (including ours) had normal blood glucose concentrations at the time of the arrhythmias and had been receiving intravenous glucose for many hours. These cases suggest that arrhythmias can be induced by medium-chain acylcarnitines or other metabolites accumulating in MCAD deficiency.

Summary Sentence Ventricular tachyarrhythmias can occur in MCAD deficiency, especially in neonates.

Abbreviations

APTT	Activated partial thromboplastin time
ECG	Electrocardiography
INR	International normalised ratio
MCAD	Medium-chain acyl-coenzyme A dehydrogenase
PCR	Polymerase chain reaction

Communicated by: Bridget Wilcken

Competing interests: None declared

P. Bala
Department of Paediatrics, Airedale General Hospital, Keighley, UK

S. Ferdinandusse
Laboratory Genetic Metabolic Diseases, Department of Clinical Chemistry, Academic Medical Center, Amsterdam, The Netherlands

S.E. Olpin
Department of Clinical Chemistry, Sheffield Children's Hospital, Sheffield, UK

P. Chetcuti
Department of Paediatrics, Leeds Teaching Hospitals NHS Trust, Leeds, UK

A.A.M. Morris (✉)
Willink Unit, Manchester Centre for Genomic Medicine, St Mary's Hospital, Oxford Road, Manchester M13 9WL, UK
e-mail: Andrew.morris@cmft.nhs.uk

Introduction

Medium-chain acyl-coenzyme A dehydrogenase (MCAD) deficiency is an autosomal recessive disorder affecting mitochondrial fatty acid oxidation. It is one of the commonest inborn errors in populations of European descent with a reported incidence ranging from 1 in 10,000 to 1 in 27,000, based on the results of newborn screening (Grosse et al. 2006). Although the commonest age of presentation is reported to be 3 months to 3 years, both neonatal and adult cases are well described, with up to one third of patients having symptoms suggestive of MCAD deficiency in the neonatal period (Grosse et al. 2006).

Case History

Our patient was a female infant, born 13 days post-term to a primigravida mother after an uncomplicated pregnancy. The parents are unrelated Caucasians. The mother's high vaginal swab was positive for group B streptococcus, and she had one dose of antibiotics 3 h before delivery; she had history of genital herpes 9 years previously. The baby's birth weight was 3.0 kg. She was breast fed and given intramuscular vitamin K according to standard policy.

At the age of 18 h, the baby was reported to be feeding poorly but clinical examination was normal and the blood glucose was 3.7 mmol/l. At 22 h of age, she was found to be floppy, mildly jaundiced and hypoglycaemic (1.8 mmol/l). She was admitted to the neonatal intensive care and started on 10% glucose at 90 ml/kg/day (6.2 mg/kg/min). The blood glucose was 2.5 mmol/l after 1 h and subsequent values were 5.5–8.3 mmol/l. She remained on an intravenous infusion of 10% glucose continuously from this time until her death. Following a partial septic screen, she was started on intravenous penicillin, gentamicin and acyclovir.

Despite normal blood glucose concentrations, she had a left focal seizure followed by generalised clonic seizures, lasting 1–2 min, at 30 h of age. Further investigations revealed normal plasma electrolytes with a low ionised calcium (0.76–0.95 mmol/l, normal >1) and a raised urea concentration (21.9 mmol/l). Liver function tests were normal apart from a plasma bilirubin of 153 μmol/l. The plasma ammonia concentration was 182 μmol/l. A full blood count was normal but clotting screen showed mild coagulopathy with INR 2.1, prothrombin time 22.5 s (control 9.5–14.0), APTT 29.5 s (control 25–50) and fibrinogen 56 (normal 150–400 mg/dl). The calcium was corrected with intravenous calcium gluconate and the ammonia concentration returned to normal after intravenous sodium benzoate (250 mg/kg infused over 90 min). A second dose of vitamin K was given and she was treated with intravenous phenobarbital (total 40 mg/kg). The rate of the intravenous infusion was reduced because of concern about possible cerebral oedema but it continued to provide glucose at 4.5 mg/kg/min. Subsequently, the CSF culture, herpes PCR and blood culture were all negative and a cranial ultrasound was normal. She had further seizures and was treated with phenytoin (60 mg) and pyridoxine (100 mg).

The baby had two cardiac arrests on day 3, during which she was noted to have pulseless ventricular tachycardia. She was treated with cardiopulmonary resuscitation and cardioversion but sinus rhythm was only restored after intravenous boluses of normal saline, adrenaline, bicarbonate and calcium. Following the second cardiac arrest, the infant was ventilated and transferred to a tertiary neonatal unit for further management. She was hypotensive and started on a dobutamine infusion. Cerebral function monitoring was normal. ECG was unremarkable with a normal QT_c interval but echocardiography showed impaired left and right ventricular function, patent ductus arteriosus, tricuspid regurgitation, systemic level of pulmonary artery pressure and a small patent foramen ovale. She had a further cardiac arrest on day 5, 14 h after transfer. Again, an ECG showed pulseless ventricular tachycardia but this time she died despite full resuscitation including cardioversion.

Post-mortem examination revealed a structurally normal heart with mild biventricular dilatation. The cardiomyocytes showed significant vacuolation of the cytoplasm and contained lipid on frozen sections. There was no cardiac inflammation or necrosis. The hepatic architecture was normal but there was evidence of severe diffuse microvesicular steatosis (confirmed on frozen sections). Examination of the kidney and skeletal muscles also showed lipid deposition on frozen sections. No other pathology was identified.

Methods

Fatty acid oxidation flux was measured in fibroblasts by the tritium release assay as previously reported (Olpin et al. 1999), using [9,10-^{3}H]myristate, [9,10-^{3}H]palmitate, [9,10-^{3}H]oleate and [2,2,3,3-^{3}H]octanoate.

A palmitate loading test was performed by loading cultured skin fibroblasts with [U-^{13}C] palmitate and L-carnitine for 96 h, followed by quantitative acylcarnitine profiling of the incubation medium by tandem mass spectrometry essentially as previously reported (Ventura et al. 1999). MCAD activity was measured in fibroblasts using phenylpropionyl-CoA as substrate, essentially as described previously (Wanders et al. 2010).

Sequence analysis of all exons and flanking intronic sequences of the *ACADM* gene was undertaken using standard techniques. DNA from both parents was analysed by multiplex ligation-dependent probe amplification (MLPA) with probes that test for deletions spanning exons 2–4 of the *ACADM* gene (Searle et al. 2013).

Results

Blood acylcarnitine analysis showed a greatly elevated octanoylcarnitine with an increased hexanoylcarnitine and an elevated C8:C10 ratio, consistent with a diagnosis of MCAD deficiency (Table 1). Urine organic analysis was also consistent with MCAD deficiency, with increased suberylglycine and dicarboxylic acids.

Fibroblast fatty acid oxidation flux using tritiated octanoate, myristate, palmitate and oleate substrates was 12%, 35%, 54% and 65%, respectively, as compared to simultaneous controls. The pattern and degree of flux reduction were entirely consistent with MCAD deficiency.

Table 1 Plasma acylcarnitine profile

Carnitine species	Notation	Results (μmol/l)	Reference values
Free carnitine	C0	31.1	15–50
Hexanoylcarnitine	C6	1.3	<0.10
Octanoylcarnitine	C8	12.7	<0.15
Decanoylcarnitine	C10:1	0.36	<0.12
Dodecenoylcarnitine	C12:1	0.21	<0.15
Dodecanoylcarnitine	C12	0.21	<0.15
	C8:C10 Ratio	15.5	<1

A palmitate loading test revealed increased [U-^{13}C]8-carnitine in the medium of the cells loaded with [U-^{13}C] palmitate. These results were also consistent with MCAD deficiency.

The MCAD activity in fibroblasts was markedly reduced (0.07 nmol/(min.mg protein)) compared to reference values (mean ± SD 0.68 ± 0.15 nmol/(min.mg protein)), confirming MCAD deficiency.

Sequence analysis of the *ACADM* gene showed that she was heterozygous for the common c.985A>G (p.Lys329-Glu) mutation, but no second pathogenic mutation was detected. For both parents, MLPA analysis excluded deletions spanning exons 2–4 of the *ACADM* gene.

Discussions

The biochemical results leave no doubt that this baby had MCAD deficiency, though the mutation on the second allele was not identified. For all genetic disorders, there are a few patients in whom causative mutations are not identified, because they are located in parts of the gene that are not tested, such as deep intronic sequences or upstream regulatory regions.

There are now newborn screening programmes for MCAD deficiency in many countries, including North America and most of Europe. These programmes prevent a number of deaths, but, unfortunately, some MCAD deficiency patients die within a few days of birth, before the results of screening are available. Indeed, death may occur before screening samples have been obtained, particularly in the UK, where samples are obtained relatively late, between postnatal days 5 and 8. In a retrospective study, Derks and colleagues found 2 neonatal deaths among 155 Dutch patients, compared with 23 deaths after the neonatal period (Derks et al. 2006). This is, however, likely to be an underestimate of the neonatal mortality, at least for other countries. Wilcken and colleagues found 4 neonatal deaths among the 81 MCAD deficiency patients diagnosed in Australia between 1994 and 2004 (Wilcken et al. 2007); they estimated that the risk of death subsequently during the first 6 years was 5–7% (Wilcken 2010). Most neonatal deaths due to MCAD deficiency occur by 72 h of age. Our patient presented with hypoglycaemia on day 2 and was successfully resuscitated; sadly, she went on to have further problems and died on day 5.

Deaths due to MCAD deficiency are almost invariably preceded by encephalopathy with poor feeding and increasing lethargy; it is often assumed that the final event is usually apnoea due to encephalopathy. Arrhythmias are well recognised in long-chain fatty acid oxidation defects but there have been relatively few reports in MCAD deficiency. Thus, in a series of 107 children with fatty acid oxidation disorders, 24 patients had a history of arrhythmias (Bonnet et al. 1999). These included ventricular tachyarrhythmias and supraventricular tachycardias; in 14 cases, the arrhythmia occurred in the newborn period. None of the patients with MCAD deficiency in this series, however, had arrhythmias.

It is possible that the arrhythmias in our patient were unrelated to the metabolic disorder but no other cause was identified. Moreover, there have been several recent reports of ventricular arrhythmias in patients with MCAD deficiency (Table 2). The first report concerned a 33-year-old alcoholic man who presented with vomiting, drowsiness, hypoglycaemia and hyperammonaemia (Feillet et al. 2003). He subsequently developed ventricular tachycardia, ventricular fibrillation and atrial fibrillation, which were managed with lidocaine, cardioversion and amiodarone, respectively; he also received glucose and haemodialysis. The other four cases were neonates, presenting with poor feeding and lethargy at 1–3 days of age. Two cases were hypoglycaemic and developed ventricular tachyarrhythmias from which they were successfully resuscitated (Rice et al. 2007; Sanatani et al. 2005). The third case had a metabolic acidosis but a normal blood glucose concentration (Maclean et al. 2005). Despite an intravenous infusion of

Table 2 Previous reports of arrhythmias in MCAD deficiency

References	Age	Presentation	Arrhythmia	Outcome
Feillet et al. (2003)	33 years	Vomiting, drowsiness, hypoglycaemia, hyperammonaemia	VT, VF, subsequently AF	Recovery after lidocaine, cardioversion, amiodarone, glucose, haemodialysis
Sanatani et al. (2005)	2 days	Poor feeding, lethargy, hypoglycaemia	VF	Recovery after cardioversion, glucose
Rice et al. (2007)	3 days	Poor feeding, hypoglycaemia	VT, torsades de pointes	Recovered with glucose, insulin, carnitine
Maclean et al. (2005)	3 days	Poor feeding, hypothermia pulmonary haemorrhage	Asystole, subsequently VT, VF	Recovery after glucose, cardioversion, lidocaine, amiodarone, carnitine
Yusuf et al. (2010)	30 h	Poor feeding, hypoglycaemia, apnoea	Recurrent VT, VF	Died aged 68 h despite glucose, lidocaine, cardioversion

VT ventricular tachycardia, *VF* ventricular fibrillation

glucose, he had a pulmonary haemorrhage associated with apnoea and an asystolic cardiac arrest. He was resuscitated and ventilated but had further cardiac arrests, associated with ventricular tachycardia and ventricular fibrillation and managed with cardioversion, lidocaine and amiodarone. The final case was particularly similar to our patient (Yusuf et al. 2010). She presented with hypoglycaemia and apnoea and was managed with ventilation and intravenous glucose. Nevertheless, she developed ventricular tachycardia and fibrillation, which responded to intravenous lidocaine. Subsequently, she was treated for hyperammonaemia and generalised seizures but ventricular tachycardia and fibrillation recurred at 65 h of age; this time the arrhythmias were resistant to antiarrhythmic drugs and cardioversion and the baby died aged 68 h.

The frequency of arrhythmias in neonates reflects the importance of fat as a fuel for the heart. This has been demonstrated by stable isotope studies in lambs (Bartelds et al. 2000) and by studying MCAD mRNA expression in rats (Kelly et al. 1989). It is interesting that arrhythmias have not been reported in older children with MCAD deficiency, although deaths most frequently occur between 6 months and 2.5 years. These deaths may result from encephalopathy and apnoea, but it is also possible that arrhythmias at this age are missed as many of the deaths occur outside hospital.

The ventricular tachyarrhythmias might potentially be induced either by increasing the automaticity of cardiomyocytes or by altering the refractory period of cardiomyocytes and allowing re-entry. The latter mechanism is favoured by the Brugada-type ECG pattern that followed the arrhythmia in one patient (Sanatani et al. 2005). Moreover, a prolonged QT_c interval has been reported in a neonate with MCAD deficiency (Wiles et al. 2014), though the QT_c interval was normal in our patient and at least one of the other patients with ventricular tachyarrhythmias (Maclean et al. 2005).

Encephalopathy and death in MCAD deficiency are often attributed to hypoglycaemia, but the accumulation of abnormal metabolites may also be responsible. Thus, there are a few reports of MCAD deficiency patients who have become encephalopathic without hypoglycaemia (Mayell et al. 2007). Our patient and that of Yusuf et al. (Yusuf et al. 2010) also had seizures at a time that their plasma glucose and ammonia concentrations were normal, several hours after brief periods of hypoglycaemia and hyperammonaemia. Cardiac arrhythmias are less likely to be directly caused by hypoglycaemia. Indeed, blood glucose concentrations were normal at the time of the arrhythmias in our patient and 2 other reports (Maclean et al. 2005; Yusuf et al. 2010). It is uncertain which metabolites contribute to the encephalopathy and cause the arrhythmias in these patients: fatty acids, acylcarnitines and acyl-CoA esters may all be responsible. Palmitoylcarnitine has been shown to affect the function of certain sodium and calcium channels in cardiomyocytes (Wu and Corr 1992; Wu and Corr 1995). Long-chain acylcarnitines at physiological concentrations (3–30 μmol/l) also affect the function of hERG potassium channels, which are involved in repolarisation (Ferro et al. 2012). These effects were not, however, observed with medium-chain acylcarnitines (Ferro et al. 2012). Fatty acids have also been shown to activate calcium channels in ventricular myocytes but, again, the effect was limited to long-chain fatty acids (Huang et al. 1992). Thus, the precise cause of the arrhythmias in MCAD deficiency remains unclear.

A sad and striking feature of our patient's history was that she continued to deteriorate with worsening ventricular tachyarrhythmias despite receiving intravenous glucose for more than 48 h. Two of the other MCAD-deficient babies were also receiving intravenous glucose (at 6.5–7 mg/kg/min) prior to their ventricular tachyarrhythmias and one had been receiving this for 35 h (Maclean et al. 2005; Yusuf et al. 2010). Most patients with MCAD deficiency

recover from acute decompensation if managed with intravenous glucose; obviously, this corrects hypoglycaemia (if present) and it is generally thought that abnormal metabolites will disappear promptly once the glucose infusion has led to a reduction in the rate of fatty acid oxidation. It is possible that the glucose infusion rates in these patients were insufficient to cause anabolism: our patient would certainly have been given more glucose if the diagnosis had been known. On the other hand, if an MCAD-deficient patient does not recover promptly with adequate intravenous glucose, it may be worth considering haemofiltration (whilst continuing the glucose infusion). Haemofiltration may have contributed to the recovery of the adult patient who presented with ventricular fibrillation (Feillet et al. 2003) as well as one with encephalopathy without hypoglycaemia (Mayell et al. 2007).

Contributions

Drs. Bala and Chetcuti looked after the patient and Dr. Bala drafted the manuscript. Dr. Morris advised on investigation of the patient and revised the manuscript. Drs. Ferdinandusse and Olpin investigated the patient and reviewed the manuscript.

Compliance with Ethics Guidelines

Conflict of Interest

Pronab Bala, Sacha Ferdinandusse, Simon Olpin, Philip Chetcuti and Andrew Morris all declare that they have no conflict of interest.

Consent

The parents of the patient reported have given written informed consent for publication.

References

Bartelds B, Knoester H, Smid GB et al (2000) Perinatal changes in myocardial metabolism in lambs. Circulation 102:926–931

Bonnet D, Martin D, De Pascale L et al (1999) Arrhythmias and conduction defects as presenting symptoms of fatty acid oxidation disorders in children. Circulation 100:2248–2253

Derks TG, Reijngoud DJ, Waterham HR, Gerver WJ, van den Berg MP, Sauer PJ, Smit GP (2006) The natural history of medium-chain acyl CoA dehydrogenase deficiency in the Netherlands: clinical presentation and outcome. J Pediatr 148:665–670

Feillet F, Steinmann G, Vianey-Saban C et al (2003) Adult presentation of MCAD deficiency revealed by coma and severe arrythmias. Intensive Care Med 29:1594–1597

Ferro F, Ouille A, Tran TA et al (2012) Long-chain acylcarnitines regulate the hERG channel. PLoS One 7, e41686

Grosse SD, Khoury MJ, Greene CL, Crider KS, Pollitt RJ (2006) The epidemiology of medium chain acyl-CoA dehydrogenase deficiency: an update. Genet Med 8:205–212

Huang JM, Xian H, Bacaner M (1992) Long-chain fatty acids activate calcium channels in ventricular myocytes. Proc Natl Acad Sci U S A 89:6452–6456

Kelly DP, Gordon JI, Alpers R, Strauss AW (1989) The tissue-specific expression and developmental regulation of two nuclear genes encoding rat mitochondrial proteins. Medium chain acyl-CoA dehydrogenase and mitochondrial malate dehydrogenase. J Biol Chem 264:18921–18925

Maclean K, Rasiah VS, Kirk EP, Carpenter K, Cooper S, Lui K, Oei J (2005) Pulmonary haemorrhage and cardiac dysfunction in a neonate with medium-chain acyl-CoA dehydrogenase (MCAD) deficiency. Acta Paediatr 94:114–116

Mayell SJ, Edwards L, Reynolds FE, Chakrapani AB (2007) Late presentation of medium-chain acyl-CoA dehydrogenase deficiency. J Inherit Metab Dis 30:104

Olpin SE, Manning NJ, Pollitt RJ, Bonham JR, Downing M, Clark S (1999) The use of [9,10-3H]myristate, [9,10-3H]palmitate and [9,10-3H]oleate for the detection and diagnosis of medium and long-chain fatty acid oxidation disorders in intact cultured fibroblasts. Adv Exp Med Biol 466:321–325

Rice G, Brazelton T 3rd, Maginot K, Srinivasan S, Hollman G, Wolff JA (2007) Medium chain acyl-coenzyme A dehydrogenase deficiency in a neonate. N Engl J Med 357:1781

Sanatani S, Mahkseed N, Vallance H, Brugada R (2005) The Brugada ECG pattern in a neonate. J Cardiovasc Electrophysiol 16: 342–344

Searle C, Andresen BS, Wraith E et al (2013) A large intragenic deletion in the ACADM gene can cause MCAD deficiency but is not detected on routine sequencing. JIMD Rep 11:13–16

Ventura FV, Costa CG, Struys EA et al (1999) Quantitative acylcarnitine profiling in fibroblasts using [U-13C] palmitic acid: an improved tool for the diagnosis of fatty acid oxidation defects. Clin Chim Acta 281:1–17

Wanders RJ, Ruiter JP, Ijlst L, Waterham HR, Houten SM (2010) The enzymology of mitochondrial fatty acid beta-oxidation and its application to follow-up analysis of positive neonatal screening results. J Inherit Metab Dis 33:479–494

Wilcken B (2010) Fatty acid oxidation disorders: outcome and long-term prognosis. J Inherit Metab Dis 33:501–506

Wilcken B, Haas M, Joy P et al (2007) Outcome of neonatal screening for medium-chain acyl-CoA dehydrogenase deficiency in Australia: a cohort study. Lancet 369:37–42

Wiles JR, Leslie N, Knilans TK, Akinbi H (2014) Prolonged QTc interval in association with medium-chain acyl-coenzyme A dehydrogenase deficiency. Pediatrics 133:e1781–e1786

Wu J, Corr PB (1992) Influence of long-chain acylcarnitines on voltage-dependent calcium current in adult ventricular myocytes. Am J Physiol 263:H410–H417

Wu J, Corr PB (1995) Palmitoylcarnitine increases [Na+]i and initiates transient inward current in adult ventricular myocytes. Am J Physiol 268:H2405–H2417

Yusuf K, Jirapradittha J, Amin HJ, Yu W, Hasan SU (2010) Neonatal ventricular tachyarrhythmias in medium chain acyl-CoA dehydrogenase deficiency. Neonatology 98:260–264

JIMD Reports
DOI 10.1007/8904_2015_494

RESEARCH REPORT

Application of an Image Cytometry Protocol for Cellular and Mitochondrial Phenotyping on Fibroblasts from Patients with Inherited Disorders

Paula Fernandez-Guerra • M. Lund • T.J. Corydon • N. Cornelius • N. Gregersen • J. Palmfeldt • Peter Bross

Received: 16 June 2015 / Revised: 13 August 2015 / Accepted: 24 August 2015 / Published online: 25 September 2015
© SSIEM and Springer-Verlag Berlin Heidelberg 2015

Abstract Cellular phenotyping of human dermal fibroblasts (HDFs) from patients with inherited diseases provides invaluable information for diagnosis, disease aetiology, prognosis and assessing of treatment options. Here we present a cell phenotyping protocol using image cytometry that combines measurements of crucial cellular and mitochondrial parameters: (1) cell number and viability, (2) thiol redox status (TRS), (3) mitochondrial membrane potential (MMP) and (4) mitochondrial superoxide levels (MSLs). With our protocol, cell viability, TRS and MMP can be measured in one small cell sample and MSL on a parallel one. We analysed HDFs from healthy individuals after treatment with various concentrations of hydrogen peroxide (H_2O_2) for different intervals, to mimic the physiological effects of oxidative stress. Our results show that cell number, viability, TRS and MMP decreased, while MSL increased both in a time- and concentration-dependent manner. To assess the use of our protocol for analysis of HDFs from patients with inherited diseases, we analysed HDFs from two patients with very long-chain acyl-CoA dehydrogenase (VLCAD) deficiency (VLCADD), one with a severe clinical phenotype and one with a mild one. HDFs from both patients displayed increased MSL without H_2O_2 treatment. Treatment with H_2O_2 revealed significant differences in MMP and MSL between HDFs from the mild and the severe patient. Our results establish the capacity of our protocol for fast analysis of cellular and mitochondrial parameters by image cytometry in HDFs from patients with inherited metabolic diseases.

Communicated by: Piero Rinaldo, MD, PhD

Competing interests: None declared

Electronic supplementary material: The online version of this chapter (doi:10.1007/8904_2015_494) contains supplementary material, which is available to authorized users.

P. Fernandez-Guerra (✉) · M. Lund · N. Cornelius · N. Gregersen · J. Palmfeldt · P. Bross (✉)
Department of Clinical Medicine, Research Unit for Molecular Medicine (MMF), Aarhus University Hospital, Brendstrupgaardsvej 100, 8200 Aarhus, Denmark
e-mail: paula.fernandez.guerra@clin.au.dk
e-mail: peter.bross@clin.au.dk

T.J. Corydon
Department of Biomedicine, Aarhus University, Aarhus, Denmark

N. Cornelius
Department of clinical Genetics, Applied Human Molecular Genetics, Kennedy Center, Copenhagen University Hospital, Rigshospitalet, Glostrup, Denmark

Introduction

Cell culture techniques allow the study of cellular mechanisms in a controlled environment. They are relevant in a wide range of studies: molecular disease mechanisms, cell metabolism and gene expression, as well as for disease prognosis and monitoring the response of treatments (Lipman et al. 1992; Sandell and Sakai 2011; Makpol et al. 2012). Human dermal fibroblasts (HDFs) are primary cells that mimic the conditions in vivo and are obtained from a non-invasive skin biopsy (Rittié and Fisher 2005; Smith 2006; Sandell and Sakai 2011). HDFs provide invaluable information for characterization of mutation defects in patients with inherited diseases (Smith 2006; Jensen 2010; Burbulla and Krüger 2012; Fernández-Guerra et al. 2014). HDFs possess the genetic composition of patients, and although HDF cultures lack the heterotypic cell–cell interactions and the three-dimensional geometry of tissues, many pathways are expressed in culture environment (Palmfeldt et al. 2009; Freshney 2011; Brand and Nicholls 2011).

Studies of molecular disease mechanisms often reveal the involvement of mitochondria; mitochondria are critical

for the viability and physiology of eukaryotic cells, especially for energy metabolism, cell cycle and programmed cell death (Burhans and Heintz 2008; Norberg et al. 2010; Brand and Nicholls 2011). Mitochondria also play a key role as regulators of cellular stress responses because they are the main producers of reactive oxygen species (ROS). At low concentrations, ROS regulate cellular signalling; however, at high concentrations, they cause damage to biomolecules (Valko et al. 2006; Murphy 2009). Thus, biomarkers for mitochondrial function are very informative parameters of cell physiology and prospective cellular viability.

There exists a variety of fluorescence-based techniques for cellular and mitochondrial phenotyping in intact cells, where mitochondria are present in their physiological environment (Brand and Nicholls 2011; Cottet-Rousselle et al. 2011). These techniques can detect cell subpopulations and study subcellular compartments in a cellular sample. One of these techniques is image cytometry (ICM) that has developed strongly in recent years due to advancements in CCD (charge-coupled device) cameras and LED (light-emitting diode) technology. ICM acquires images from cell samples producing quantitative fluorescence data from a high number of cells simultaneously, as well as gather morphological information like cell size and shape. The data analysis of the images allows for unambiguous identification of cells and cell aggregates based on their morphology or fluorescence labelling (Ozaki et al. 2010; Pierzchalski et al. 2010; Chan et al. 2011).

The purpose of the present study was to develop a cell phenotyping protocol that combines a set of cellular and mitochondrial parameters in a small cell sample, leading to a reduction in biological material, time and analytical variability. The analysed parameters were (1) cell number and viability, (2) thiol redox status (TRS), (3) mitochondrial membrane potential (MMP) and (4) mitochondrial superoxide levels (MSLs). This combination of phenotypic parameters can give a nuanced picture of mutation effects on cellular physiology in HDFs from patients with inherited diseases. To test the protocol, HDFs from healthy individuals were analysed with and without treatment with various concentrations of hydrogen peroxide (H_2O_2) at different time points. H_2O_2 is a stable ROS capable of triggering cellular stress responses when exogenously administered, thereby mimicking the physiological effects of oxidative stress (Choi et al. 2009).

To evaluate the capacity of this protocol for analysing effects of genetic changes, we analysed HDFs from patients with very long-chain acyl-CoA dehydrogenase (VLCAD, EC 1.3.99.13) deficiency (VLCADD) (MIM#201475). VLCADD is characterized by a genetic defect in the *ACADVL* gene (MIM#609575) leading to a defective activity of the mitochondrial enzyme VLCAD that is involved in fatty acid β-oxidation. This mitochondrial disorder results in a variety of clinical phenotypes ranging from relatively mild to life threatening (Houten and Wanders 2010; Schiff et al. 2013). Previous studies have suggested a relation between VLCADD and oxidative stress (Tucci et al. 2010; Cardoso et al. 2013). Therefore, we used HDFs from VLCADD patients to determine whether our protocol could detect this mitochondrial and oxidative stress implication.

Materials and Methods

Reagents

4′,6′-Diamidino-2-phenylindole (DAPI), VitaBright-48 (VB-48), 5,5′,6,6′-tetrachloro-1,1′,3,3′ tetraethylbenzimidazolylcarbocyanine iodide (JC-1), acridine orange (AO), propidium iodide (PI), Hoechst 33342 (Hoechst) and cell lysis buffer were purchased from ChemoMetec (Allerod, Denmark). Antimycin, carbonyl cyanide 3-chlorophenylhydrazone (CCCP), dimethylsulfoxide (DMSO) and hydrogen peroxide (H_2O_2) were purchased from Sigma-Aldrich (Denmark). Hank's balanced salt solution (HBSS) with calcium and magnesium and MitoSOX™ Red mitochondrial superoxide indicator (MitoSOX) were purchased from Invitrogen (Denmark).

Patients and Healthy Individuals

HDFs isolated from two healthy individuals were Cambrex #CC-2509 and ATCC #CRL-2450 which annotated NHDF-01 and NHDF-02, respectively. Patients were referred for genetic diagnosis of *ACADVL* gene (GenBank reference sequence NM_000018.3) on the basis of elevated blood C14:0, C14:1, C16:0 and C18:0 acylcarnitines. Patient one (P1) (c.[689C>T;428_467del]) presented a mild phenotype and harbours a missense mutation (p.Thr230Ile) together with a deletion leading to premature stop codon (p.Gly143Alafs*61). Patient two (P2) (c.[685C>T;685C>T]) presented a severe phenotype and harbours a nucleotide change that generates a premature stop codon (p.Arg229*). The nomenclature of the mutations is according to the Human Genome Variation Society (HGVS) (http://www.hgvs.org/mutnomen/) and has been revised with the software Mutalyzer (https://mutalyzer.nl/). The samples have been deidentified according to the regulations of the Danish Ethical Committee.

Cell Culture and H_2O_2 Treatment

HDFs were used below passage 15 and cultured with Dulbecco's modified Eagle's medium (DMEM) (Lonza,

Denmark) supplemented with 10% (v/v) foetal bovine serum (Biological Industries, Denmark), 0.29 mg/mL L-glutamine (Leo Pharmaceutical, Denmark) and 1% penicillin/streptomycin (Leo Pharmaceutical, Denmark), at 37°C in 5% CO_2. *Mycoplasma sp.* test was performed routinely (PromoKine, Heidelberg, Germany).

HDFs were seeded at 80% confluence in a T25 flask (Nunc, Roskilde, Denmark) 24 h prior to treatment with 0, 2 or 4 mmol/L H_2O_2 in serum-free DMEM for different time intervals. Then, HDFs were trypsinized and aliquoted to measure cell number and viability, TRS and MMP. MSL was measured in a parallel experiment in a 6-well plate (Nunc, Roskilde, Denmark). At least three independent experiments were performed for each measurement.

Image Cytometry

Measurements of cellular fluorescence were performed with an NC-3000 image cytometer with a 2-chamber NC-Slide A2™ (ChemoMetec, Allerod, Denmark) and a minimum of 5,000 cells analysed. The NC-3000 software (ChemoMetec, Allerod, Denmark) was used for fluorescent image acquisition, image analysis, subpopulation definition and quantification and data visualization.

Cell Number and Viability Detection Using DAPI as Nuclear Staining

HDFs (2×10^5 cells) were mixed with cell lysis buffer (1:1) and DAPI (25 μg/mL) for determination of the total cell concentration (Ct). Another aliquot was mixed with DAPI (25 μg/mL) for the non-viable cells concentration (Cnv). DAPI fluorescence was detected using peak excitation at 365 nm and emission at 470/55. Cell viability was calculated according to the following formula, viability = (Ct − Cnv)/Ct, and expressed as percentage.

Thiol Redox Status (TRS) Measurement Using VitaBright-48

VB-48 is a live permeable dye that reacts with intracellular thiol groups forming a fluorescent compound (Skindersoe et al. 2012). An aliquot of HDFs (2×10^5 cells) was mixed with VB-48, PI and AO (20, 25 and 0.06 μg/mL, respectively). VB-48 fluorescence was detected using peak excitation at 365 nm and emission at 470/55 nm, AO at 475 nm and emission at 560/35 nm and PI at 530 nm and emission at 675/75 nm. The mean fluorescence intensity (MFI) was calculated from the total fluorescence intensity detected from viable cells and divided by the number of cells.

Mitochondrial Membrane Potential (MMP) Analysis with JC-1

JC-1 has a monomer (green) and aggregate (red) state for ratiometric and semi-quantitative assessment of MMP. The red-to-green fluorescence ratio determines the amount of JC-1 inside mitochondria in relation to the cytosolic amount, serving as a control for changes in cellular dye loading (Perry et al. 2011). HDFs (5×10^5 cells/mL) were incubated with 2.5 μg/mL JC-1 for 10 min at 37°C. Then, HDFs were washed twice with PBS and mixed with DAPI. To determine the maximal MMP depolarization and the limits of the polarized/depolarized gates, an H_2O_2-untreated sample was incubated with CCCP (50 μM) together with JC-1. After exclusion of non-viable cells by DAPI staining, two gates were defined as cells with mostly polarized mitochondria and cells with mostly depolarized mitochondria. These gates correspond to the upper-left gate and lower-right gate, respectively, as shown in Fig. S2. Different incubation times were used for both JC-1 and CCCP to determine that the optimal was 10 min at 37°C. DAPI fluorescence was detected using peak excitation at 365 nm and emission at 470/55 nm, JC-1 monomers at 475 nm and emission at 560/35 nm and JC-1 aggregates at 530 nm and emission at 675/75 nm.

Measurement of Mitochondrial Superoxide Levels (MSLs) with MitoSOX

HDFs (3×10^5 cells/well) were incubated with 5 μM MitoSOX in HBSS for 20 min at 37°C. Then, HDFs were trypsinized and incubated with Hoechst (10 μg/mL) for 15 min at 37°C. Next, HDFs were stained with the non-viable cell staining RedDot2 (Biotium, Hayward, CA) diluted 1,000 times (concentration not specified). An H_2O_2-untreated sample was incubated with 150 μM antimycin for 5 min prior to MitoSOX staining, as a positive control for MitoSOX labelling. The Hoechst fluorescence was detected using peak excitation at 365 nm and emission at 470/55 nm, MitoSOX at 475 nm and emission at 675/75 nm and RedDot2 at 630 nm and emission at 740/60 nm. The mean fluorescence intensity (MFI) was calculated from the total fluorescence intensity detected from viable cells and divided by the number of cells.

Confocal Laser Scanning Microscope (CLSM)

The distribution pattern of MitoSOX fluorescence was analysed by using CLSM 710 (Zeiss, Jena, Germany) using a 63× oil-immersion objective with a numerical aperture of 1.4. MitoSOX fluorescence was detected using the 514-nm line of the multiline argon laser. HDFs were seeded at 50%

confluence in 10-cm^2 slide flasks (Nunc, Roskilde, Denmark), 24 h before the analysis. HDFs were prepared like for MSL measurement and maintained at 37°C in HBSS during imaging.

Statistical Analysis

The data were subjected to a two-tailed *t*-test analysis and a *P* value less than 0.05 was considered significant (* <0.05; ** <0.01; *** <0.001). The outliers were removed based on the interquartile range. One value is consider an outlier if it is higher than the sum of the third quartile and 1.5 times the interquartile range or it is below than the sum of the first quartile and 1.5 times the interquartile range. The statistical analysis was done using Microsoft Office Excel 2007 software.

The intraassay variation was defined as the variation in the results obtained when the same cellular suspension is measured three times in the image cytometer. The interassay variation was defined as the variation in the results obtained from three independent experiments, where the cell culture was performed in three different days from different starting material. To analyse the intraassay and interassay variability of the cell viability, TRS and MMP, we calculated the coefficient of variation (CV) defined as the ratio of the standard deviation to the mean. On the other hand, to analyse the biological differences between samples, we calculated the standard error of the mean (SEM) defined as the standard deviation divided by the square root of the sample size.

Results

This study describes a protocol for cell phenotyping by studying cellular and mitochondrial functional parameters in human dermal fibroblasts (HDFs) using image cytometry (ICM). To evaluate the protocol, HDFs from healthy individuals were analysed after treatment with 0, 2 and 4 mmol/L H_2O_2 for 1, 1½ and 2 h (Fig. 1). At these time points, we measured changes in four parameters: cell number and viability, thiol redox status (TRS), mitochondrial membrane potential (MMP) and mitochondrial superoxide levels (MSLs). The first three assays were performed with one cell sample leading to reduction in analytical variability, biological material and time (Fig. 1a). MSL was measured in a parallel cell culture (Fig. 1b).

Analysis of the Intraassay and Interassay Variation

A statistical evaluation of the intraassay and interassay variation associated with our protocol is shown in Table 1. The intraassay variation was calculated from three repeated measurements of the same sample. The coefficient of variation (CV) percentage was different in each parameter: TRS had the highest average CV, MMP the second and cell viability the lowest (12.2, 10.3 and 4.2%, respectively). The CV percentage, in the three parameters, was lower in H_2O_2-untreated samples than in the H_2O_2-treated ones. The interassay variation, caused by cell culture, was studied in four independent experiments performed with one cell line, NHDF-02. In contrast to the test of the intraassay variation, MMP had the highest average CV (56.1%) and TRS had the second highest average CV (18.4%). As in the intraassay variation, cell viability and H_2O_2-untreated showed the lowest CV. In both cases, the CV increased with the H_2O_2 concentration and incubation time. Thus, the protocol should be used carefully at 1.5 and 2 h.

Cell Number and Viability Analysis

Determining the number of cells in culture is important for standardization of culture conditions and to evaluate cell proliferation and cell death (Phelan 1998; Bie et al. 2011). Treatment with H_2O_2 led to a decrease in cell number in a time- and concentration-dependent manner (data not shown). The CV of the cell number was 15% (data from seven independent experiments with two NHDF cell lines) (data not shown). Treatment with H_2O_2 also led to decreased cell viability, in a time- and concentration-dependent manner (Fig. 2a). Incubation periods shorter than 1 h did not show decreased cell viability (data not shown). The maximal decrease occurred after treatment with 4 mmol/L H_2O_2 for 2 h (Fig. 2a).

Thiol Redox Status (TRS) Study

TRS is used to determine the cellular level of free thiols that correlates with the cellular redox state (Skindersoe et al. 2012). Only minimal effects on TRS were observed after more than 2 h of incubation (data not shown). The treatment with H_2O_2 samples resulted in decreased TRS in a concentration- and time-dependent manner (Fig. 2b). The decrease of TRS and the loss of cell viability showed a linear correlation ($R^2 = 0.90$) (Fig. S1).

Mitochondrial Membrane Potential (MMP) Analysis

MMP is an important feature of mitochondria, because it plays a central role in the oxidative phosphorylation and mitochondrial apoptosis regulation, among other pathways (Brand and Nicholls 2011). The H_2O_2-untreated samples showed MMP depolarization of 10–20% of the cell population (Fig. 2c). Cells treated with 2 mmol/L H_2O_2

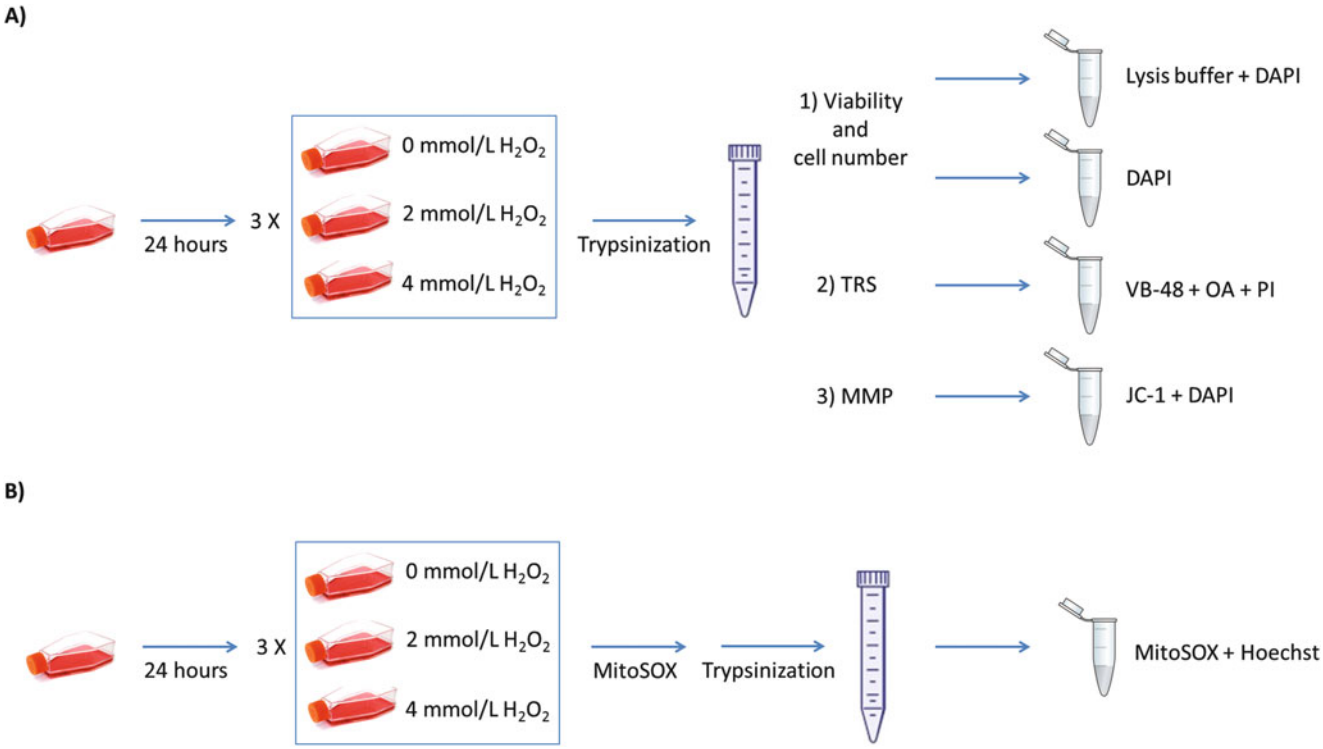

Fig. 1 Flow chart of phenotyping protocol. (**a**) Approximately 1.6×10^6 HDFs were seeded in a standard T75 cell culture flask. After 24 h, HDFs were treated with 0, 2 and 4 mmol/L H_2O_2 for 1, 1½ and 2 h. Then, HDFs were harvested by trypsinization and collected in a 15-mL Falcon. Four aliquots were taken from the Falcon for cell number, cell viability, thiol redox status (TRS) and mitochondrial membrane potential (MMP). (**b**) Approximately 3×10^5 HDFs were seeded in a standard p6-well plate. After 24 h, HDFs were treated with 0, 2 and 4 mmol/L H_2O_2 for 1, 1½ and 2 h. Then, HDFs were incubated with MitoSOX for 20 min. HDFs were harvested by trypsinization and collected in a 15-mL Falcon. Hoechst was added to the cell suspension to stain the nucleus of each cell

Table 1 Statistical analysis of the intraassay and interassay variation using the NHDF-02 control cell line

		Viability %			TRS fluorescence intensity (a.u)			MMP polarized %		
		Mean	Intraassay CV %	Interassay CV %	Mean	Intraassay CV %	Interassay CV %	Mean	Intraassay CV %	Interassay CV %
1 h	0 mmol/L H_2O_2	96.0	1.8	1.1	88.4	7.2	8.7	92.7	1.3	6.5
	2 mmol/L H_2O_2	77.4	3.3	12.3	74.7	3.2	17.9	17.7	32.2	58.7
	4 mmol/L H_2O_2	79.8	1.1	4.5	71.7	4.8	8.0	14.2	11.6	79.7
1.5 h	0 mmol/L H_2O_2	94.7	1.7	1.4	90.1	6.9	7.6	93.3	0.3	5.4
	2 mmol/L H_2O_2	46.2	16.4	38.2	59.5	5.8	12.2	27.5	10.5	75.0
	4 mmol/L H_2O_2	28.8	18.3	31.6	48.7	5.8	33.3	45.3	17.4	88.2
2 h	0 mmol/L H_2O_2	94.4	1.2	1.2	101.1	5.6	9.2	69.6	1.4	56.3
	2 mmol/L H_2O_2	35.0	14.2	47.2	51.3	33.7	31.1	41.5	10.6	57.8
	4 mmol/L H_2O_2	29.2	43.4	91.2	31.1	36.6	37.8	41.4	7.2	77.2

The intraassay variation was analysed in four independent experiments with three repeated measurements for each value. The interassay variation was studied by comparison of four independent experiments of the same cell line

for 1 h showed depolarized MMP in 81% of the cell population (Fig. 2c). There was no further decrease in MMP at 4 mmol/L H_2O_2 at any incubation times used. MMP depolarization decreased already after treatment with 2 mmol/L H_2O_2 for 30 min (Fig. S2) while TRS and cell viability showed no decrease (data not shown). These results indicated that MMP was the first parameter to change after H_2O_2 treatment.

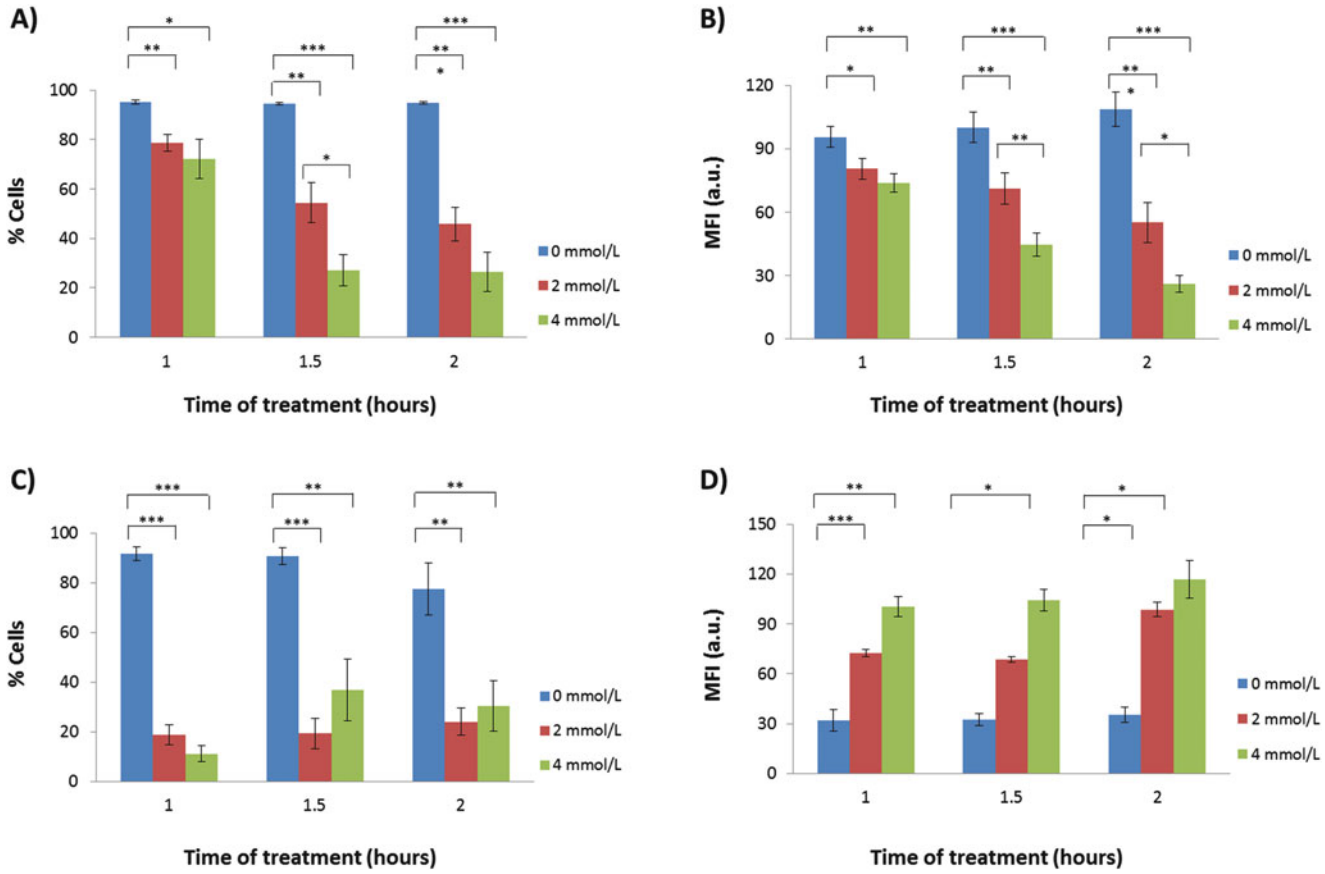

Fig. 2 Effect of exogenous H_2O_2 treatment for different time periods in two different NHDF cell lines. NHDFs were treated with 0, 2 or 4 mmol/L H_2O_2 for 1, 1½ and 2 h. (**a**) Viability quantification. Cell viability was quantified by counting DAPI-positive cells in the total cell population. (**b**) Thiol redox status (TRS). HDFs were incubated with VB-48, AO and PI. VB-48 was used to determine the levels of free thiols, AO as a nuclear staining and PI to label dead cells (removed from the analysis). The values shown correspond to the mean fluorescence intensity (MFI). (**c**) Mitochondrial membrane potential (MMP). HDFs were incubated with JC-1 to establish the percentage of cells with a depolarized MMP, and dead cells were excluded by DAPI staining. (**d**) Mitochondrial superoxide levels (MSLs) were measured by quantification of MitoSOX fluorescence intensity levels after treatment with H_2O_2. MitoSOX exhibits red fluorescence upon oxidation by superoxide anion in the mitochondrial matrix. Hoechst was used as a nuclear staining and RedDot2 to exclude non-viable cells. The values shown correspond to the mean fluorescence intensity (MFI). The columns represent the mean ± standard error of the mean (SEM). The data correspond to the mean values of at least three independent experiments for each cell line (NHDF-01 and NHDF-02). Two-tailed *t*-test analysis with **P* value <0.05; ***P* value <0.01; ****P* value <0.001

Mitochondrial Superoxide Level (MSL) Analysis

MSL was measured with MitoSOX, a probe that accumulates in the mitochondria of living cells and fluoresces red when it is oxidized by the superoxide anion (Robinson et al. 2007). We observed increased MSL in a time- and concentration-dependent manner (Fig. 2d). At high concentrations, MitoSOX can stain other organelles besides mitochondria, like the nucleus (Dingley et al. 2011). To ensure that our results reflect only mitochondrial superoxide, we performed cell-imaging experiments using the same MitoSOX incubation conditions. MitoSOX red fluorescence showed a characteristic mitochondrial pattern with no cytoplasmic background and minimal nucleus staining (Fig. S3).

Analysis of HDFs from Very Long-Chain Acyl-CoA Dehydrogenase Deficiency (VLCADD) Patients

HDFs from VLCADD patients were used to evaluate the capacity of this protocol to phenotype cellular and mitochondrial effects of mutations in the *ACADVL* gene. Based on the high interassay variation of the H_2O_2 treatment at 1.5 and 2 h, we treated the cells only for 1 h. We observed differences between HDFs from the healthy individuals and from the patients and also between the severe (P2) and the

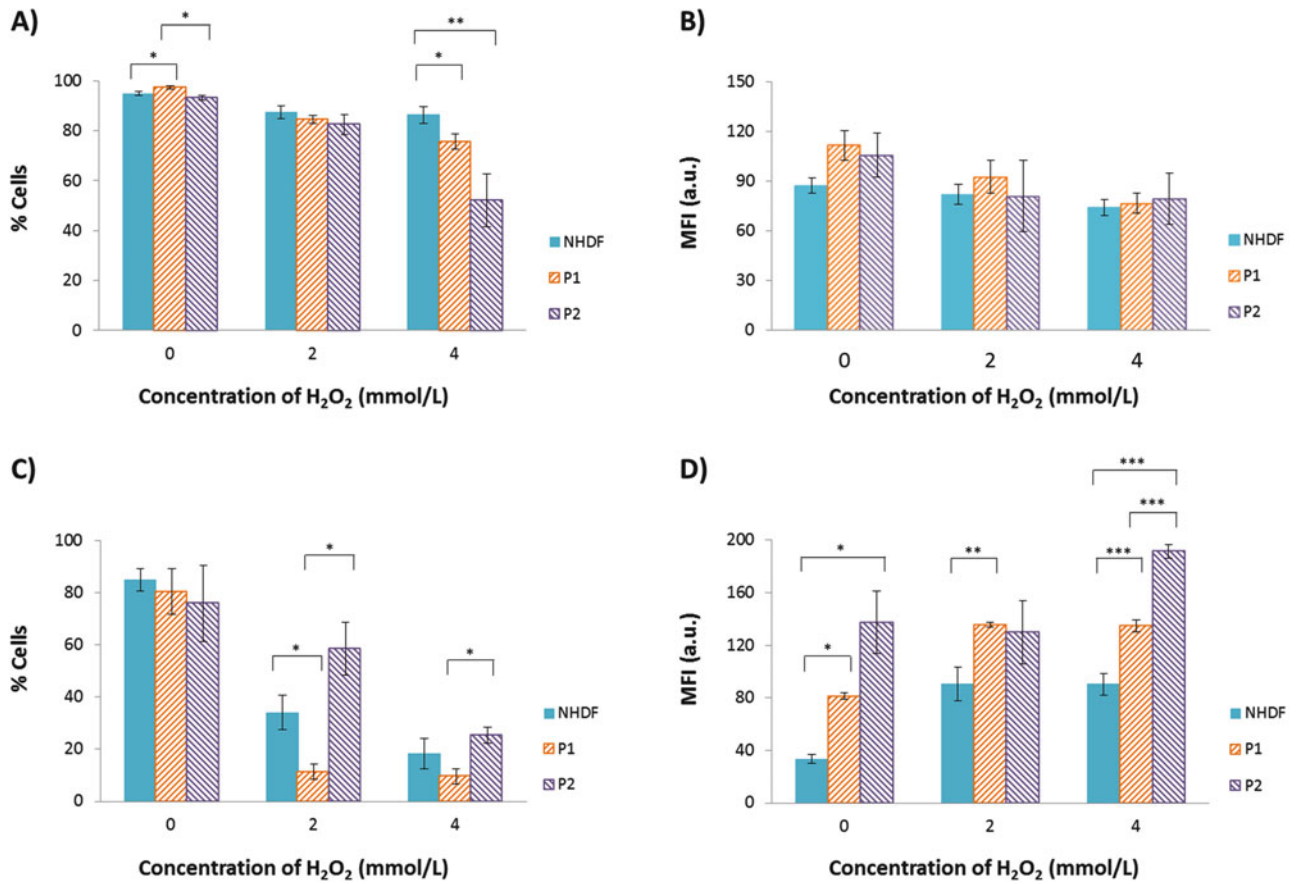

Fig. 3 Analysis of HDFs derived from VLCADD patients after treatment for 1 h with 0 mmol/L, 2 mmol/L or 4 mmol/L of H_2O_2, respectively. (**a**) Viability quantification. Cell viability was quantified by counting DAPI-positive cells in the total cell population. (**b**) Thiol redox status (TRS). HDFs were incubated with VB-48 for levels of free thiols, AO as a nuclear staining and PI to stain non-viable cells and exclude them from the analysis. The values shown correspond to the mean fluorescence intensity (MFI). (**c**) Mitochondrial membrane potential (MMP). HDFs were incubated with JC-1 to establish the percentage of cells with a depolarized MMP and with DAPI to exclude non-viable cells. (**d**) Mitochondrial superoxide levels (MSLs) were measured by quantification of MitoSOX fluorescence intensity. Hoechst was used as a nuclear staining and RedDot2 as a non-viable cell staining to exclude non-viable cells. The values shown correspond to the mean fluorescence intensity (MFI). The columns represent the mean ± standard error of the mean. The data shown correspond to at least three independent experiments for each cell line, two NHDFs (NHDF-01 and NHDF-02) and two HDFs from VLCADD patients (P1 and P2). Two-tailed *t*-test analysis with **P* value <0.05; ***P* value <0.01; ****P* value <0.001

mild (P1) patient (Fig. 3). Cell viability analysis showed statistically significant but very small increase in the H_2O_2-untreated HDFs from the mild VLCADD (P1). There were no differences in viability between patients and healthy individuals at 2 mmol/L H_2O_2, but HDFs from both VLCADD patients showed significantly decreased viability at 4 mmol/L H_2O_2 (Fig. 3a). TRS showed no significant differences between any HDFs from compared to HDFs from healthy individuals (Fig. 3b). MMP showed no differences in the H_2O_2-untreated samples and decreased with the H_2O_2 treatment, being lower in HDFs from mild VLCADD (P1) than in HDFs from severe VLCADD (P2) (Fig. 3c). MSL was significantly increased in the H_2O_2-untreated samples that further increases in the H_2O_2-treated samples with the highest levels in HDFs from the severe patient (P2) (Fig. 3d and Fig. S4).

Discussion

In this paper, we present a protocol for assessing cellular and mitochondrial parameters in human dermal fibroblasts (HDFs) by image cytometry (ICM). Using our protocol, we measured cell number, viability, TRS and MMP in one sample, reducing biological material, time and analytical variability. As a supplement, MSL was analysed in a parallel experiment (Fig. 1). The different parameters responded to induced oxidative stress by H_2O_2 in HDFs from healthy individuals in a concentration- and time-dependent manner. Furthermore, we successfully detected differences between HDFs from patients with VLCADD and healthy individuals, showing the capacity of this protocol to phenotype consequences of genetic changes in inherited diseases.

Cell viability is used to evaluate the amount of living cells in a cell population under treatments or to determine whether the expression of a mutation affects cell proliferation or promotes cell death (Phelan 1998; Bie et al. 2011). MTT (3-[4,5-dimethylthiazol-2-yl]-2,5 diphenyltetrazolium bromide) and similar assays have been widely used to determine cell viability or cell proliferation. The results of these assays are ambiguous because one cannot distinguish between changes in average enzyme activity and changes in the number of cells (Halter 2012). Our protocol for cellular phenotyping overcomes these problems because it analyses single cells (Fig. 2a). While cell count and viability are a measure of living and dead cells, parameters like MMP and TRS can offer additional information about cellular physiology (Fig. 2). MMP is a key parameter for mitochondrial function (Brand and Nicholls 2011; Cottet-Rousselle et al. 2011). In our study, MMP showed higher sensitivity to the H_2O_2 treatment than viability and TRS, allowing us to assess effects on cellular physiology at an early stage and supporting our hypothesis that mitochondrial dysfunction is an early marker of cellular stress (Fig. 2c and Fig. S2). Combining TRS and MMP gives complementary information because MMP is capable of detecting mitochondrial dysfunction while TRS reveals the status of the cellular redox balance.

Eukaryotic cells have a reducing inner environment that switches to an oxidizing environment upon oxidative stress conditions. Cellular redox homeostasis depends mostly on the size of the pool of reduced glutathione in the cytoplasm, a main cellular antioxidant whose free thiol group can act as a ROS scavenger (Skindersoe et al. 2012). Therefore, TRS is an informative parameter of the redox balance and an indirect parameter of intracellular ROS levels (Fig. 2b). Treatment with H_2O_2 increased MSL and decreased TRS but not in a linear correlation (Fig. 2b, d). This might suggest that there is a cross talk between these parameters, but other players may also be involved.

Statistical evaluation of the intraassay variation of our protocol showed that TRS had the highest CV, most likely because it was not scored as a discrete but a continuous parameter (Table 1). Evaluation of the interassay variation showed that MMP had the highest variation consistent with the notion that this is the most sensitive parameter. At the highest H_2O_2 concentration and longest treatment times, the variation was very high; thus, we suggest that 1-h treatment should be preferentially used.

We used HDFs from patients with VLCADD. VLCAD is a mitochondrial enzyme that catalyses the first step in the β-oxidation of fatty acids with a chain length of 14–20 carbons. Defects in VLCAD lead to impaired fatty acid β-oxidation and have been implicated with mitochondrial dysfunction as well as increased ROS levels (Tucci et al. 2010; Cardoso et al. 2013). VLCADD patients show different clinical phenotypes that might correlate to specific patterns of cellular phenotypes; thus, we chose both a patient with mild and a patient with severe phenotype. Indeed, already in the H_2O_2-untreated samples, we observed some differences: MSL was highest in HDFs from the severely affected VLCADD patient (P2), lower in the mild (P1) and significantly lower in the controls (Fig. 3d). The increased MLS might be linked to the observed tendency of higher TRS. The latter could be caused by a higher expression of the cellular redox markers like glutathione in response to a chronic state of oxidative stress.

An induction of survival mechanisms in the H_2O_2-untreated conditions could be caused by oxidative stress, as shown by increased MSL and cellular viability (Fig. 3a, d). Because ROS can both act as signalling molecules and as damaging species, the balance between signalling and damaging is mostly concentration dependent (Valko et al. 2006; Murphy 2009). Indeed, at 2 mmol/L and 4 mmol/L H_2O_2, we observed a different behaviour between HDFs from mild VLCADD (P1) and from severe VLCADD (P2) in all the parameters (Fig. 3 and Fig. S4b). This supports our idea of using an oxidative stressor like H_2O_2 to evaluate differences between milder and severe phenotypes.

Under oxidative stress, HDFs from the severe patient (P2), but not the mild (P1), retained a higher population of functional mitochondria measured by MMP (Fig. 3c). It has been hypothesized that VLCAD is a stabilizing factor for the supercomplexes of the respiratory chain and that absence of VLCAD protein might destabilize them (Wang et al. 2010). The HDFs from the severe VLCADD patient (P2) express mRNA with premature stop codon that either is degraded by nonsense-mediated decay (NMD) or leads to very low levels of truncated VLCAD protein. The HDFs from the severe VLCADD patient (P2) express mRNA with a premature stop codon that either is degraded by nonsense-mediated decay (NMD) or leads to very low levels of truncated VLCAD protein. This correlates with the clinical symptoms showed by the patient; a severe phenotype is caused by the lack of VLCAD enzyme activity. However, MMP in HDFs from the severe patient (P2) and from healthy individuals did not differ significantly under any of the conditions studied. Surprisingly, HDFs from the mild VLCADD patient (P1) displayed a significant disruption of the MMP after treatment with H2O2 (Fig. 3c), although this patient shows clinical symptoms that correspond to a mild phenotype. These clinical symptoms correlate with the genotype of the mild patient (P1) that harbours a missense mutation (p.Thr230Ile) that potentially can partially express both functional folded and misfolded VLCAD protein. Western blotting of protein lysates from HDFs from the mild patient (P1) indeed shows residual VLCAD protein (unpublished data) that could correspond to both some

folded and some misfolded VLCAD protein, the latter of which could interact incorrectly with the supercomplexes thus leading to a disruption of MMP.

In summary, our results from the combined analysis of cellular viability, TRS, MMP and MSL showed the potential of our protocol for cellular and mitochondrial phenotyping of HDFs from patients with inherited diseases. We observed consistency in repetitive analysis and between the different parameters. The results of this protocol have the potential to distinguish order of events and to pinpoint potential molecular pathological mechanism that then can be studied further. This establishes our protocol as efficient and highly potential for monitoring cellular and mitochondrial function in HDFs using ICM.

Acknowledgements We acknowledge Christian Knudsen, Department of Biomedicine, Aarhus University, Aarhus, for technical assistance as well as the Department of Clinical Medicine and the Faculty of Health Sciences at Aarhus University, Aarhus, for financial support.

Take-Home Message

Protocol for cellular and mitochondrial phenotyping reveals differences between fibroblasts from VLCADD patients with mild and severe gene variations.

Compliance with Ethical Guidelines

Conflict of Interest

Paula Fernandez Guerra, Martin Lund, Thomas Juhl Corydon, Nanna Cornelius, Niels Gregersen, Johan Palmfeldt and Peter Bross declare that they have no conflict of interest.

Informed Consent

All procedures followed were in accordance with the ethical standards of the responsible committee on human experimentation (institutional and national) and with the Helsinki Declaration of 1975, as revised in 2000 (5).

Details of the Contributions of Individual Authors

1. Paula Fernandez Guerra: experimental design, performance of experiments with fibroblasts from healthy individuals, data analysis and writing the first draft of the manuscript
2. Martin Lund: performance of experiments with fibroblasts from patients
3. Thomas Juhl Corydon: performance of confocal laser microscope experiments with MitoSOX
4. Nanna Cornelius: performance of confocal laser microscope experiments with MitoSOX
5. Niels Gregersen: VLCADD patient selection and hypothesis of oxidative stress in VLCADD patients
6. Johan Palmfeldt: experimental design, report editing and data analysis
7. Peter Bross: experimental design, report editing and data analysis

References

Bie AS, Palmfeldt J, Hansen J et al (2011) A cell model to study different degrees of Hsp60 deficiency in HEK293 cells. Cell Stress Chaperones 16:633–640. doi:10.1007/s12192-011-0275-5

Brand MD, Nicholls DG (2011) Assessing mitochondrial dysfunction in cells. Biochem J 435:297–312. doi:10.1113/expphysiol.2006.034330

Burbulla LF, Krüger R (2012) The use of primary human fibroblasts for monitoring mitochondrial phenotypes in the field of Parkinson's disease. J Vis Exp. doi:10.3791/4228

Burhans WC, Heintz NH (2008) The cell cycle is a redox cycle: linking phase-specific targets to cell fate. Free Radic Biol Med 47:1282–1293. doi:10.1016/j.freeradbiomed.2009.05.026

Cardoso AR, Kakimoto PA, Kowaltowski AJ (2013) Diet-sensitive sources of reactive oxygen species in liver mitochondria: role of very long chain acyl-CoA dehydrogenases. PLoS One 8:e77088. doi:10.1371/journal.pone.0077088.g001

Chan LL, Zhong X, Qiu J et al (2011) Cellometer vision as an alternative to flow cytometry for cell cycle analysis, mitochondrial potential, and immunophenotyping. Cytometry 79A:507–517. doi:10.1002/cyto.a.21071

Choi K, Kim J, Kim GW, Choi C (2009) Oxidative stress-induced necrotic cell death via mitochondria-dependent burst of reactive oxygen species. Curr Neurovasc Res 6:213–222

Cottet-Rousselle C, Ronot X, Leverve X, Mayol J-F (2011) Cytometric assessment of mitochondria using fluorescent probes. Cytometry A 79:405–425. doi:10.1002/cyto.a.21061

Dingley S, Chapman KA, Falk MJ (2011) Fluorescence-activated cell sorting analysis of mitochondrial content, membrane potential, and matrix oxidant burden in human lymphoblastoid cell lines. Methods Mol Biol 837:231–239. doi:10.1007/978-1-61779-504-6_16

Fernández-Guerra P, Birkler RID, Merinero B et al (2014) Selected reaction monitoring as an effective method for reliable quantification of disease-associated proteins in maple syrup urine disease. Mol Genet Genomic Med 2:383–392. doi:10.1002/mgg3.88

Freshney RI (2011) Introduction. Culture of animal cells. Wiley, Hoboken, pp 1–10

Halter M (2012) Modernizing the MTT assay with microfluidic technology and image cytometry. Cytometry A 81:643–645. doi:10.1002/cyto.a.22089

Houten SM, Wanders RJA (2010) A general introduction to the biochemistry of mitochondrial fatty acid β-oxidation. J Inherit Metab Dis 33:469–477. doi:10.1007/s10545-010-9061-2

Jensen BC (2010) Skin deep: what can the study of dermal fibroblasts teach us about dilated cardiomyopathy? J Mol Cell Cardiol 48:576–578. doi:10.1016/j.yjmcc.2009.11.021

Lipman J, Flint O, Bradlaw J et al (1992) Cell culture systems and in vitro toxicity testing. Cytotechnology 8:129–176. doi:10.1007/BF02525495

Makpol S, Abdul Rahim N, Kien Hui C, Wan Ngah WZ (2012) Inhibition of mitochondrial cytochrome c release and suppression of caspases by gamma-tocotrienol prevent apoptosis and delay aging in stress-induced premature senescence of skin fibroblasts. Oxid Med Cell Longev 2012:1–13. doi:10.1371/journal.pone.0004894

Murphy MP (2009) How mitochondria produce reactive oxygen species. Biochem J 417:1. doi:10.1042/BJ20081386

Norberg E, Orrenius S, Zhivotovsky B (2010) Mitochondrial regulation of cell death: processing of apoptosis-inducing factor (AIF). Biochem Biophys Res Commun 396:95–100. doi:10.1016/j.bbrc.2010.02.163

Ozaki Y-I, Uda S, Saito TH et al (2010) A quantitative image cytometry technique for time series or population analyses of signaling networks. PLoS One 5:e9955. doi:10.1371/journal.pone.0009955.t002

Palmfeldt J, Vang S, Stenbroen V et al (2009) Mitochondrial proteomics on human fibroblasts for identification of metabolic imbalance and cellular stress. Proteome Sci 7:20. doi:10.1186/1477-5956-7-20

Perry S, Norman J, Barbieri J et al (2011) Mitochondrial membrane potential probes and the proton gradient: a practical usage guide. Biotechniques 50:98–115. doi:10.2144/000113610

Phelan MC (1998) Basic techniques in mammalian cell tissue culture. Curr Protoc Cell Biol Chapter 1:Unit 1.1. doi:10.1002/0471143030.cb0101s36

Pierzchalski A, Mittag A, Tárnok A (2010) Introduction A: recent advances in cytometry instrumentation, probes, and methods–review. Methods Cell Biol 102:1–21. doi:10.1016/B978-0-12-374912-3.00001-8

Rittié L, Fisher GJ (2005) Isolation and culture of skin fibroblasts. Methods Mol Med 117:83–98. doi:10.1385/1-59259-940-0:083

Robinson KM, Janes MS, Beckman JS (2007) The selective detection of mitochondrial superoxide by live cell imaging. Nat Protoc 3:941–947. doi:10.1038/nprot.2008.56

Sandell L, Sakai D (2011) Mammalian cell culture. Curr Protoc Essent Lab Tech 4.3. 1–4.3. 32

Schiff M, Mohsen A-W, Karunanidhi A et al (2013) Molecular and cellular pathology of very-long-chain acyl-CoA dehydrogenase deficiency. Mol Genet Metab 109:21–27. doi:10.1016/j.ymgme.2013.02.002

Skindersoe ME, Rohde M, Kjaerulff S (2012) A novel and rapid apoptosis assay based on thiol redox status. Cytometry 81A:430–436. doi:10.1002/cyto.a.22032

Smith CL (2006) Mammalian cell culture. Curr Protoc Cell Biol Chapter 28:Unit 0.1. doi:10.1002/0471142727.mb2800s73

Tucci S, Primassin S, Spiekerkoetter U (2010) Fasting-induced oxidative stress in very long chain acyl-CoA dehydrogenase-deficient mice. FEBS J 277:4699–4708. doi:10.1111/j.1742-4658.2010.07876.x

Valko M, Leibfritz D, Moncol J et al (2006) Free radicals and antioxidants in normal physiological functions and human disease. Int J Biochem Cell Biol 39:44–84. doi:10.1016/j.biocel.2006.07.001

Wang Y, Mohsen A-W, Mihalik SJ et al (2010) Evidence for physical association of mitochondrial fatty acid oxidation and oxidative phosphorylation complexes. J Biol Chem 285:29834–29841. doi:10.1074/jbc.M110.139493

JIMD Reports
DOI 10.1007/8904_2015_464

CASE REPORT

SUCLA2 Deficiency: A Deafness-Dystonia Syndrome with Distinctive Metabolic Findings (Report of a New Patient and Review of the Literature)

Roeltje R. Maas · Adela Della Marina · Arjan P.M. de Brouwer · Ron A. Wevers · Richard J Rodenburg · Saskia B. Wortmann

Received: 12 February 2015 / Revised: 26 April 2015 / Accepted: 20 May 2015 / Published online: 27 September 2015
© SSIEM and Springer-Verlag Berlin Heidelberg 2015

Abstract *SUCLA2* encodes for a subunit of succinyl-coenzyme A synthase, the enzyme that reversibly synthesises succinyl-coenzyme A and ATP from succinate, coenzyme A and ADP in the Krebs cycle. Disruption of *SUCLA2* function can lead to mitochondrial DNA depletion. Patients with a *SUCLA2* mutation present with a rare but distinctive deafness-dystonia syndrome. Additionally, they exhibit elevated levels of the characteristic biochemical markers: methylmalonate, C4-dicarboxylic carnitine and lactate are increased in both plasma and urine. Thus far, eight different disease-causing *SUCLA2* mutations, of which six missense mutations and two splice site mutations, have been described in the literature. Here, we present the first patient with an intragenic deletion in *SUCLA2* and review the patients described in literature.

Communicated by: Wolfgang Sperl, MD, PhD

Competing interests: None declared

R.R. Maas · R.J. Rodenburg · S.B. Wortmann (✉)
Amalia Children's Hospital, Radboud University Nijmegen, Nijmegen, The Netherlands
e-mail: saskia-wortmann@gmx.de

A.D. Marina
Department of Neuropediatrics, Developmental Neurology and Social Pediatrics, University of Essen, Essen, Germany

A.P.M. de Brouwer
Department of Human Genetics, Radboud University Nijmegen, Nijmegen, The Netherlands

A.P.M. de Brouwer
Department of Cognitive Neurosciences, Donders Institute for Brain, Cognition and Behaviour, Radboud University Nijmegen, Nijmegen, The Netherlands

R.A. Wevers
Translational Metabolic Laboratory, Department of Laboratory Medicine, Radboud UMC, Nijmegen, The Netherlands

Introduction

Mitochondrial diseases are a heterogeneous group of disorders, caused by mutations in mitochondrial DNA (mtDNA) or nuclear DNA (nDNA). nDNA mutations can cause instability or a decreased quantity of mtDNA, or changed functioning of mitochondrial proteins. This will lead to dysfunction of the respiratory chain in mitochondria, where ATP is synthesised. Tissues highly dependent on oxidative energy supply (central nervous system, sensory organs, skeletal muscles and heart) are therefore most commonly affected in mitochondrial disease (Menezes et al. 2014).

Infantile mitochondrial encephalomyopathic depletion syndrome, which is associated with methylmalonic aciduria, has been connected to mutations in *SUCLA2* (MIM#612073, (Carrozzo et al. 2007; Ostergaard et al. 2007b)) and *SUCLG1* (MIM*611224, (Ostergaard et al. 2007a)). These genes encode for subunits of the adenosine diphosphate (ADP)-dependent isoforms of succinyl-coenzyme A synthase (SCS-A). SCS-A is a mitochondrial matrix enzyme that reversibly synthesises succinyl-coenzyme A from succinate and coenzyme A in the Krebs cycle. The hypothesis is that SCS-A forms a complex with mitochondrial nucleoside diphosphate kinase, an enzyme important in the dNTP salvage pathway in mtDNA replications. Disruption of SCS-A could thereby lead to impaired mtDNA synthesis and thus mtDNA depletion (Elpeleg et al. 2005).

SCS-A is a heterodimer that occurs in a G-SUCL and an A-SUCL form. They share an invariant alpha-subunit encoded by *SUCLG1*. The variable beta-subunit is encoded by *SUCLG2* or *SUCLA2* and determines the enzymatic nucleotide specificity (Johnson et al. 1998). The G-SUCL form initiates the reversible conversion of succinyl-CoA and GDP to succinate and GTP. A-SUCL reversibly converts succinyl-CoA and ADP to succinate and ATP in the Krebs cycle. A-SUCL is mainly expressed in testis, brain and skeletal muscle tissue, whereas G-SUCL is expressed in liver and anabolic tissues (Johnson et al. 1998; Lambeth 2006; Lambeth et al. 2004; Miller et al. 2011).

Mutations in *SUCLA2* give rise to a typical but rare combination of disorders: an early onset dystonia combined with deafness (MIM#612073, (Carrozzo et al. 2007; Ostergaard et al. 2007b)). In deafness-dystonia syndromes (e.g. Mohr-Tranebjaerg syndrome (*TIMM8A*, MIM#304700, (Jin et al. 1996)), Woodhouse-Sakati syndrome (*C2orf37*, *MIM#241080*, (Alazami et al. 2010) and MEGDEL (*SERAC1*, MIM#614739, (Wortmann et al. 2012)), these features dominate the clinical picture. Other causes for the rare association of dystonia and deafness are mitochondrial disorders and organic acidurias. Perinatal hypoxic-ischemic brain injury, kernicterus, head trauma and meningoencephalitis account for a small proportion of non-genetic causes (for review, see (Kojovic, et al. 2013)).

Here, we report one new patient with a homozygous intragenic deletion of a complete exon in *SUCLA2*. In addition, we compared the gen- and phenotypes of all 28 patients previously reported in literature.

Methods

Patients

We report one new patient who was under care of one of the authors (ADM) and performed a literature review on PubMed accessed on December 2014. We used the search term "SUCLA2" and had 44 hits. After reading the abstracts, eight relevant articles remained (Carrozzo et al. 2007; Elpeleg et al. 2005; Jaberi et al. 2013; Lamperti et al. 2012; Matilainen et al. 2014; Morava et al. 2009; Nogueira et al. 2015; Ostergaard et al. 2007b). No additional articles were found in the citation lists of used articles. All procedures followed were in accordance with the ethical standards of the responsible committee on human experimentation (institutional and national) and with the Helsinki Declaration of 1975, as revised in 2000. Informed consent was obtained from all patients for being included in the study.

DNA Sequence Analysis

DNA was extracted from peripheral venous blood samples using standard procedures. The complete coding region of *SUCLA2* (GenBank accession#NM_003850.2, chromosome 13q12.2-q13.3, 11 exons) was sequenced as described previously (Carrozzo et al. 2007).

Multiplex Ligation-Dependent Probe Amplification

MLPA (multiplex ligation-dependent probe amplification) to screen for deletions and duplications of exons 1, 2, 6, 9, 10 and 11 of *SUCLA2* was performed using the SALSA P089 probemix (MRC-Holland, The Netherlands), following the manufacturer's procedures.

Results

The patients' findings are summarised in Tables 1 and 2 and Fig. 1.

Clinical Report

The male patient was born at term as the 4th child of consanguineous healthy Turkish parents (first cousins) after an uneventful pregnancy and delivery. An older sister died due to cardiac failure at the age of 1.5 years; no more details have been documented. At the age of 2 months, generalised muscular hypotonia was noticed, followed by a severe delay in motor development. At the age of 5 months, hearing loss became apparent, and sensorineural hearing loss was proven with brainstem evoked potentials (BAEP). Cranial MRI findings at the age of 6 months revealed unspecific enlargement of ventricular system and delayed myelinisation. Echocardiography, electrocardiogram as well as electroencephalogram showed no abnormalities. At the age of 22 months, the patient was unable to sit independently or to turn himself from the prone to supine position. Proximal muscular hypotonia with reduced deep tendon reflexes and hyperkinetic-dystonic movements of his extremities and facial dyskinesia were noted. Facial features included high-arched palate, elongate facies and large ears. Eye movements were free in all directions, and the patient was able to follow objects. According to his parents, he was able to pronounce "mum", but no active speech was observed during clinical follow-up until 22 months. Feeding difficulties lead to failure to thrive with metric data for weight and head circumference on the 3rd percentile and length on the 25th percentile. The parents refused further academic care and follow-up, and we only know that the patient is alive at the age of 6 years but do not have further details.

Table 1 Clinical, radiological and metabolic findings in patients with *SUCLA2* deficiency

Symptoms	Patients reported in the literature ($n = 28$)[a]	This study	Total ($n = 29$)
Signs and symptoms			
Gender	19 males, 9 females	Male	20 males
Age of onset; birth–6 months	22/24	+	23/25
Age of death (12/28)	6 months–21 years	Alive 6 years	6 months–21 years
Muscle hypotonia	27/28	+	28/29
Delayed motor development	27/28	+	28/29
Sensorineural hearing loss	25/28	+	26/29
Dystonia/hyperkinesia	24/28	+	25/29
Absent speech	17/20	+	18/21
Feeding problems	22/28	+	23/29
Failure to thrive	20/27	+	21/28
Progressive spasticity	15/22	–	15/23
Ophthalmoplegia/strabismus/ptosis	17/26	–	17/27
Hyperhidrosis	4/14	NA	4/14
Epilepsy	4/21	–	4/22
Ataxia	1/1	–	1/2
Athetosis	2/2	–	2/3
Increased deep tendon reflexes	1/1	–	1/2
MRI			
Cerebral atrophy on MRI	12/24	+	13/25
Cerebellar atrophy on MRI	4/24	–	4/25
Basal ganglia lesions on MRI	18/24	–	18/25
Metabolic investigations			
Elevated serum lactate	17/19 (range 0.9–7.5; N < 2.2 mmol/l)	+	18/19
Elevated urinary lactate	2/2 (N < 150 μmol/mmol creatinine)	+	3/3
Elevated plasma methylmalonate	7/7 (range 0.8–33; N < 0.33 μmol/l)	+	8/8
Elevated urinary methylmalonate	17/18 (range "marginal"-212; N < 5 μmol/mmol creatinine)	+	18/19
Elevated plasma C4-dicarboxylic carnitine	4/4 (range 0.23–2.2; N <0.6 μmol/l)	+	5/5
Elevated urinary C4-dicarboxylic carnitine	3/3 (N 0.04–0.5 μmol/mmol creatinine)	+	4/4

N normal, *NA* not available

[a] Carrozzo et al. (2007), Elpeleg et al. (2005), Jaberi et al. (2013), Lamperti et al. (2012), Matilainen et al. (2014), Morava et al. (2009), Nogueira et al. (2015), Ostergaard et al. (2007b)

Metabolic Findings

Serum lactate was elevated (4.4 mmol/l, normal <2), the serum amino-acid profile was within the normal range, and in particular alanine was not elevated. The urinary C4-dicarboxylic carnitine (C4DC) excretion was strongly increased, as was urinary lactate (314 μmol/mmol creatinine, normal <150) and urine methylmalonate (47 μmol/mmol creatinine, normal <5). Homocysteine, vitamin B12 and folate in blood were all within normal limits.

Genetic Investigations

Sanger sequencing of the entire coding region of *SUCLA2* did not reveal any mutations, with the exception of exon 6 for which no PCR product could be obtained. Therefore, an MLPA analysis was performed, which confirmed the presence of a homozygous deletion of exon 6.

Review of Patients Reported in the Literature

A total of 28 patients were reported in literature (Carrozzo et al. 2007; Elpeleg et al. 2005; Jaberi et al. 2013; Lamperti et al. 2012; Matilainen et al. 2014; Morava et al. 2009; Nogueira et al. 2015; Ostergaard et al. 2007b) of whom nine were female.

In these patients, eight different disease-causing variants have been described in *SUCLA2*, two of which are splice site mutations and six missense mutations (Table 2). All are found in homozygous state in the affected patients except

Table 2 Genetic findings in patients with *SUCLA2* deficiency

Mutation	Predicted effect of the mutation on protein level	Type of mutation	Reference	Country of origin
c.308C>A	p.(Ala103Asp)	Missense	P I, II (Lamperti et al. 2012)	Italy
c.352G>A	p.(Gly118Arg)	Missense	P 2 (Carrozzo et al. 2007)	Italy
c.534+1G>A	p.(Pro125Valfs*4)	Splice	P 1–16 (Morava et al. 2009; Ostergaard et al. 2007b)	Faroe Islands
c.751G>A	p.(Asp251Asn)	Missense	P 1,2 (Jaberi et al. 2013)	Iran
c.789_802 +29delinsATAAA	p.(Tyr222Lysfs*51)	Splice	P II6, II7 (Elpeleg et al. 2005)	"Israelic muslim"
c.850C>T	p.(Arg284Cys)	Missense	P 1–3 (Carrozzo et al. 2007)	Italy
c.985A>G	p.(Met329Val)	Missense	P 1 (Nogueira et al. 2015)	Portugal
c.998A>G	p.(Asp333Gly)	Missense	P 1,2 (Matilainen et al. 2014)[a]	Finland
Deletion of exon 6	p.(Tyr222Lysfs*51)	Deletion	This study	Turkey

[a] Heterozygous mutation with additional deletion of 13q14 in P2

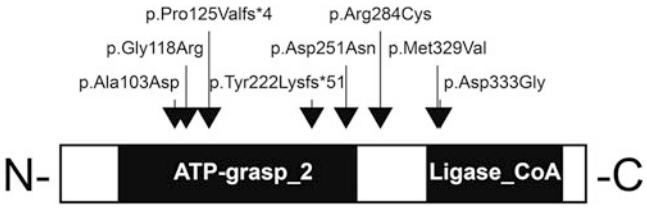

Fig. 1 The positions of all mutations identified in human

for one patient described with compound heterozygosity (Carrozzo et al. 2007) and one patient with a mutation of one of the alleles and a deletion of 13q14 (Matilainen et al. 2014).

Twenty-two of 24 patients presented symptoms within the first 6 months of life. Life span varies greatly, from 6 months to 21 years. Most prevalent clinical symptoms are muscle hypotonia and delayed motor development (27/28), sensorineural hearing loss (25/28), dystonia/hyperkinesia (24/28), absent speech (17/20), feeding problems (22/28), and failure to thrive (20/27). On MRI, basal ganglia lesions have been reported in 18 of 24 cases. Cerebral (12/24) or cerebellar (4/24) atrophy can also be part of the phenotype. The typical metabolic findings in *SUCLA2* deficiency encompass increased plasma (17/19) and urinary (2/2) lactate, increased plasma (7/7) and urinary (17/18) methylmalonic acid as well as increased plasma (4/4) and urinary (3/3) C4DC.

Discussion

Dystonia deafness syndromes are a rare and heterogeneous group of disorders. Known genetic causes include Mohr-Tranebjaerg syndrome (*TIMM8A*, MIM#304700, (Jin et al. 1996)), Woodhouse-Sakati syndrome (*C2orf37*, *MIM#241080*, (Alazami et al. 2010)) and mitochondrial disorders, such as MEGDEL syndrome (*SERAC*, MIM#614739,(Alexoudi and Schneider 2012)) and *SUCLA2* mutations (MIM#612073, Carrozzo et al. 2007; for review see (Kojovic, et al. 2013)). We show here that the dystonia deafness syndrome caused by *SUCLA2* dysfunction can also be caused by an intragenic deletion of *SUCLA2*.

Our patient presented with the same characteristic symptoms as other patients with a mutation of this gene. Most prevalent symptoms of this syndrome, apart from the dystonia (25/29 patients, 86%) and deafness (26/29, 90%), are failure to thrive (21/28, 75%), delayed motor development (28/29, 97%), muscle hypotonia (28/29, 97%), progressive spasticity (15/23, 65%) and ophthalmoplegia (17/27, 63%). Almost all patients present symptoms within the first 6 months of their lives (22/24, 92%), and in our patient, this was not different. Because follow-up of our patient was not possible beyond the age of nearly 4 years, a description of progressiveness in this specific intragenic *SUCLA2* deletion in comparison to other *SUCLA2* mutations cannot be given. Review of the previously described cases shows there are no patients with a mild disease presentation and/or course of disease reported to date. In the patient described in this paper, there was only one MRI made at the age of 6 months. It showed widening of the ventricle system, which is fairly unspecific and can be seen in early stages of many neurodegenerative diseases. MRIs of patients with *SUCLA2* mutations can show no abnormalities or mild cerebral atrophy with widened ventricle system and subarachnoid spaces in the first year. As patients grow older, Leigh-like lesions of the basal ganglia appear,

starting in the putamen and caudate nucleus being the cause of dystonia development.

Our patient had increased lactate in urine and plasma, as well as elevated urinary excretion of methylmalonate and C4DC. Also the biochemical parameters are strikingly similar amongst patients. The most important indicators for a *SUCLA2* deficiency are a mild increase of methylmalonate in plasma and urine in combination with an abnormal profile of carnitine esters. C4DC in plasma and especially in urine is elevated. Because of the TCA cycle defect caused by these mutations, lactate builds up as well.

In conclusion, mutations in *SUCLA2* cause one of the rare but distinctive dystonia deafness syndromes. The clinical phenotype together with the metabolic findings in blood and urine is so specific that careful description without further investigations (e.g. brain MRI) would be enough to classify patients. Mutation analysis of the *SUCLA2* gene will be necessary to confirm the diagnosis. Both mutations and intragenic deletions of this gene can cause this disorder. Both Sanger sequencing and MLPA (or another method to detect single exon deletions and duplication) of the *SUCLA2* gene is subsequently needed to confirm the diagnosis.

Synopsis

A newly reported *SUCLA2* deletion gives rise to a distinct deafness-dystonia syndrome.

Compliance with Ethics Guidelines

Competing Interests

Adela Della Marina, Arjan P.M. de Brouwer, Richard J Rodenburg, Roeltje R. Maas, Ron A. Wevers and Saskia B. Wortmann declare that they have no competing interests.

Informed Consent

All procedures followed were in accordance with the ethical standards of the responsible committee on human experimentation (institutional and national) and with the Helsinki Declaration of 1975, as revised in 2000. Informed consent was obtained from all patients for being included in the study.

Authors' Contribution

ADM provided the clinical data. AB, RW, RR and SW were involved in obtaining the biochemical data and genetic investigation, the data acquisition and analysis. RM and SW wrote the manuscript; all authors read and approved the final manuscript.

References

Alazami AM, Schneider SA, Bonneau D et al (2010) C2orf37 mutational spectrum in Woodhouse–Sakati syndrome patients. Clin Genet 78(6):585–590

Alexoudi A, Schneider SA (2012) Mutations in the phospholipid remodeling gene SERAC1 cause MEGDEL syndrome. Mov Disord 27(14):1738

Carrozzo R, Dionisi-Vici C, Steuerwald U et al (2007) SUCLA2 mutations are associated with mild methylmalonic aciduria, Leigh-like encephalomyopathy, dystonia and deafness. Brain 130(Pt 3): 862–874

Elpeleg O, Miller C, Hershkovitz E et al (2005) Deficiency of the ADP-forming succinyl-CoA synthase activity is associated with encephalomyopathy and mitochondrial DNA depletion. Am J Hum Genet 76(6):1081–1086

Jaberi E, Chitsazian F, Ali Shahidi G et al (2013) The novel mutation p.Asp251Asn in the beta-subunit of succinate-CoA ligase causes encephalomyopathy and elevated succinylcarnitine. J Hum Genet 58(8):526–530

Jin H, May M, Tranebjaerg L, Kendall E et al (1996) A novel X-linked gene, DDP, shows mutations in families with deafness (DFN-1), dystonia, mental deficiency and blindness. Nat Genet 14(2):177–180

Johnson JD, Mehus JG, Tews K, Milavetz BI, Lambeth DO (1998) Genetic evidence for the expression of ATP- and GTP-specific succinyl-CoA synthetases in multicellular eucaryotes. J Biol Chem 273(42):27580–27586

Kojovic M, Parees I, Lampreia T et al (2013) The syndrome of deafness-dystonia: clinical and genetic heterogeneity. Mov Disord 28(6): 795–803

Lambeth DO (2006) Reconsideration of the significance of substrate-level phosphorylation in the citric acid cycle. Biochem Mol Biol Educ 34(1):21–29

Lambeth DO, Tews KN, Adkins S, Frohlich D, Milavetz BI (2004) Expression of two succinyl-CoA synthetases with different nucleotide specificities in mammalian tissues. J Biol Chem 279(35):36621–36624

Lamperti C, Fang M, Invernizzi F et al (2012) A novel homozygous mutation in SUCLA2 gene identified by exome sequencing. Mol Genet Metab 107(3):403–408

Matilainen S, Isohanni P, Euro L et al (2015) Mitochondrial encephalomyopathy and retinoblastoma explained by compound heterozygosity of SUCLA2 point mutation and 13q14 deletion. Eur J Hum Genet 23:325–330

Menezes MJ, Riley LG, Christodoulou J (2014) Mitochondrial respiratory chain disorders in childhood: insights into diagnosis and management in the new era of genomic medicine. Biochim Biophys Acta 1840(4):1368–1379

Miller C, Wang L, Ostergaard E, Dan P, Saada A (2011) The interplay between SUCLA2, SUCLG2, and mitochondrial DNA depletion. Biochim Biophys Acta 1812(5):625–629

Morava E, Steuerwald U, Carrozzo R et al (2009) Dystonia and deafness due to SUCLA2 defect; clinical course and biochemical markers in 16 children. Mitochondrion 9(6):438–442

Nogueira C, Meschini MC, Nesti C et al (2015) A novel SUCLA2 mutation in a portuguese child associated with "mild" methylmalonic aciduria. J Child Neurol 30(2):228–232

Ostergaard E, Christensen E, Kristensen E et al (2007a) Deficiency of the alpha subunit of succinate-coenzyme A ligase causes fatal

infantile lactic acidosis with mitochondrial DNA depletion. Am J Hum Genet 81(2):383–387

Ostergaard E, Hansen FJ, Sorensen N et al (2007b) Mitochondrial encephalomyopathy with elevated methylmalonic acid is caused by SUCLA2 mutations. Brain 130(Pt 3):853–861

Wortmann SB, Vaz FM, Gardeitchik T et al (2012) Mutations in the phospholipid remodeling gene SERAC1 impair mitochondrial function and intracellular cholesterol trafficking and cause dystonia and deafness. Nat Genet 44(7):797–802

JIMD Reports
DOI 10.1007/8904_2015_489

RESEARCH REPORT

Diagnostic Value of Urinary Mevalonic Acid Excretion in Patients with a Clinical Suspicion of Mevalonate Kinase Deficiency (MKD)

Jerold Jeyaratnam · Nienke M. ter Haar · Monique G.M. de Sain-van der Velden · Hans R. Waterham · Mariëlle E. van Gijn · Joost Frenkel

Received: 28 February 2015 / Revised: 28 July 2015 / Accepted: 29 July 2015 / Published online: 27 September 2015
© SSIEM and Springer-Verlag Berlin Heidelberg 2015

Abstract *Objective*: In patients suffering from mevalonate kinase deficiency (MKD), the reduced enzyme activity leads to an accumulation of mevalonic acid which is excreted in the urine. This study aims to evaluate the diagnostic value of urinary mevalonic acid measurement in patients with a clinical suspicion of mevalonate kinase deficiency.

Methods: In this single-center, retrospective analysis, all patients in whom both measurement of mevalonic acid and genetic testing had been performed in the preceding 17 years have been included. The presence of two pathogenic *MVK* mutations or demonstration of decreased enzyme activity was considered to be the gold standard for the diagnosis of MKD.

Results: Sixty-one patients were included in this study. Thirteen of them harbored two *MVK* mutations; twelve of them showed elevated levels of mevalonic acid. Forty-eight patients did not harbor any *MVK* mutations, yet five of them excreted increased amounts of mevalonic acid. This corresponds to a sensitivity of 92%, a specificity of 90%, a positive predictive value of 71%, and a negative predictive value of 98%. The positive likelihood ratio is 10 and the negative likelihood ratio is 0.09.

Conclusion: MKD seems very unlikely in patients with a normal mevalonic acid excretion, but it cannot be excluded completely. Further, a positive urinary mevalonic acid excretion still requires *MVK* analysis to confirm the diagnosis of MKD. Therefore, detection of urinary mevalonic acid should not be mandatory before genetic testing. However, as long as genetic testing is not widely available and affordable, measurement of urinary mevalonic acid is a fair way to select patients for *MVK* gene analysis or enzyme assay.

Communicated by: Ivo Barić, M.D., PhD, Professor of Pediatrics

Competing interests: None declared

J. Jeyaratnam · J. Frenkel
Department of Pediatrics, University Medical Center Utrecht, Utrecht, The Netherlands

N.M. ter Haar (✉)
Laboratory of Translational Immunology, University Medical Center Utrecht, Utrecht, The Netherlands
e-mail: n.m.terhaar-2@umcutrecht.nl

M.G.M. de Sain-van der Velden · M.E. van Gijn
Department of Medical Genetics, University Medical Center Utrecht, Utrecht, The Netherlands

H.R. Waterham
Clinical Chemistry and Pediatrics, Academic Medical Center, Amsterdam, The Netherlands

Introduction

Mevalonate kinase deficiency (MKD) is a rare hereditary autoinflammatory syndrome which is inherited in an autosomal recessive manner. MKD has two phenotypes, known as hyperimmunoglobulinemia D and periodic fever syndrome (HIDS) and mevalonic aciduria (MA) (Prieur and Griscelli 1984; van der Meer et al. 1984; Berger et al. 1985). Both phenotypes are characterized by inflammation with fever accompanied by gastrointestinal complaints, lymphadenopathy, arthralgia, myalgia, skin rash, and mucosal ulcers. Besides these inflammatory attacks, patients affected by the more severe phenotype mevalonic aciduria have dysmorphic features, pre- and postnatal growth retardation, and neurological and ocular involvement (Simon et al. 2004).

MKD is caused by mutations in the mevalonate kinase gene *MVK*. Mevalonate kinase is an enzyme that is part of the mevalonate pathway. This pathway produces cholesterol and unsaturated lipid chains, known as isoprenoids

(van der Burgh et al. 2013). The mevalonate kinase activity is reduced in MKD patients. The enzyme kinase activity varies from 1.8% to 28% in patients with the HIDS phenotype to below 0.5% in patients affected by the MA phenotype (Houten et al. 1999; Cuisset et al. 2001). This enzyme activity does not correlate perfectly with the severity of the disease (Bader-Meunier et al. 2011). The reduced mevalonate kinase activity leads to an accumulation of its substrate, mevalonic acid, which is excreted in the urine. Elevated levels of urinary mevalonic acid are therefore suggestive of MKD. Examination of HIDS patients showed an increased excretion of mevalonic acid during febrile episodes, while normal levels of mevalonic acid were sometimes found between those episodes (van der Burgh et al. 2013; Poll-The et al. 2000).

Thus, urinary mevalonic acid levels are used as a tool in the diagnostic process of MKD. As clinical criteria are lacking, the diagnosis can only be confirmed by demonstration of decreased enzyme activity or by identification of two known pathogenic *MVK* mutations (Ammouri et al. 2007). However, although urinary mevalonic acid excretion is often used in the diagnostic evaluation of suspected MKD patients, the diagnostic value of this urinary analysis has not been investigated yet and remains unclear. This study aims to evaluate the diagnostic value of urinary mevalonic acid excretion.

Methods

This single-center retrospective study included patients analyzed in the Wilhelmina Children's Hospital. We included all patients in whom both measurement of urinary mevalonic acid and *MVK* analysis were performed in the preceding 17 years. A waiver of review was granted by the institutional ethical review board.

Analysis of Urinary Mevalonic Acid

Urinary mevalonic acid samples were analyzed at the department of medical genetics of the University Medical Center Utrecht. We quantified urinary mevalonic acid using isotope dilution technique. For the determination of mevalonic acid, $^{2}H_{7}$- mevalonolactone as internal standard is used. To convert mevalonic acid to the lactone form, urine was acidified. The acidified sample was extracted twice with ethyl acetate. The organic phase was dried over anhydrous Na_2SO_4 and evaporated under nitrogen at room temperature. The samples are then hydrolyzed with sodium hydroxide. The dry samples were then dissolved in acetone/ethyl acetate dried and derivatized with BSTFA (bis(trimethylsilyl)trifluoroacetamide). Samples are measured using gas chromatography–mass spectrometry (GC–MS) in the positive electron impact mode. The concentration of mevalonic acid in the urine is calculated using a calibration curve and was expressed as mmol/mol creatinine. (Lindenthal and von Bergmann 1994). The excretion of mevalonic acid was compared with age-dependent reference values, validated in our hospital. These reference values were 0.2–1.9 for patients between 0 and 0.5 year, 0.2–1.0 for patients between 0.5 and 1 year, 0.1–0.7 for patients between 1 and 5 years, and 0.1–0.7 for patients >5 years.

Analysis of Mevalonate Kinase Genes

DNA analysis was performed by extracting DNA from whole blood. Primers were designed for the coding exons, including the intron–exon boundaries (available upon request). The fragments were amplified and sequenced on an ABI 3100 automated sequencer (PE Applied Biosystems, Foster City, CA, USA). Data were analyzed with Sequence Pilot (JSI medical systems GmbH, Kippenheim, Germany). The presence of two pathogenic *MVK* mutations or demonstration of decreased enzyme activity was considered to be the gold standard for the diagnosis of MKD.

Data Analysis

Data were analyzed by using Statistical Package for the Social Sciences (SPSS) 20. The specificity, sensitivity, predictive values, and likelihood ratios of excess urinary mevalonic acid for the diagnosis of mevalonate kinase deficiency were calculated. Differences in clinical features between patients with two *MVK* mutations (MKD patients), patients with elevated mevalonic acid but without *MVK* mutations (false positives), and patients with normal mevalonic acid and without *MVK* mutations (true negatives) were analyzed by using Pearson's chi-square test. The ROC analysis was performed with GraphPad Prism 6.

Results

This study included 61 patients with a clinical suspicion of MKD (32 male and 29 female patients, aged 0.4–36 years). Thirteen patients harbored two *MVK* mutations; 12 of them excreted elevated amounts of mevalonic acid. Forty-eight patients harbored no *MVK* mutations; five of them had at least one elevated mevalonic acid excretion (Table 1). The characteristics of all patients are described in Table 2. The distribution of mevalonic acid excretions is displayed in Fig. 1.

Test Results

The characteristics derived from this study led to a sensitivity of 92%, a specificity of 90%, a positive predictive value (PPV) of 71%, and a negative predictive value (NPV) of 98%. The positive likelihood ratio is 10 and the negative likelihood ratio is 0.09. The area under the curve (AUC) of the receiver operating characteristic (ROC) curve is 0.911 (Fig. 2).

Table 1 Overview of results of mevalonic acid excretion

	MK deficient	MK sufficient	Total
Elevated mevalonic acid	12	5	17
Normal mevalonic acid	1	43	44
Total	13	48	61

MK deficient: presence of two *MVK* mutations. MK sufficient: absence of any *MVK* mutation
This resulted in a sensitivity of 92%, a specificity of 90%, a positive predictive value of 71%, and a negative predictive value of 98%. Positive likelihood ratio 10; negative likelihood ratio 0.09

Clinical Features

Patients with Two MVK Mutations

Thirty-four assessments of mevalonic acid excretion were performed in thirteen MKD patients. In all but one of them, excretion was elevated. The median excretion in patients with *MVK* mutations was 11 mmol/mol creatinine. Enzymatic studies were performed in eight MKD patients, which corresponded to residual activities ranging from 0.12% to 15% (Table 3).

In one patient with a homozygous V377I mutation, mevalonic acid could not be detected in urine collected during a febrile episode. Febrile episodes were accompanied by stomatitis, rash, arthralgia, diarrhea, abdominal pain, and arthritis. Activity of mevalonate kinase in leukocytes was impaired (2–3%). Thus, although mevalonate kinase activity in leukocytes was impaired in this genetically confirmed MKD patient, urinary mevalonic acid level was not increased. At last follow-up, she experienced only mild MKD attacks, without organ damage.

Table 2 Characteristics of patients with MKD, false-positive tests, and true-negative tests

Characteristics	MK-deficient patients		MK sufficient, mevalonic acid↑		MK sufficient, mevalonic acid↓	
Baseline	*n*	(%)	*n*	(%)	*n*	(%)
Patients	13		5		43	
Gender						
(M)	5	(38)	3	(60)	24	(56)
(F)	8	(62)	2	(40)	19	(44)
Febrile episodes	13	(100)	5	(100)	40	(93)
Mevalonic acid	Median	Range	Median	Range	Median	Range
Age at test (years)	3.7	0.6–11.8	3.5	1.6–6.7	5.6	0.4–36.6
Median excretion	11	0–5,461	3.3	0.9–8.1	0.1	0.01–0.7
Symptoms	*n*	(%)	*n*	(%)	*n*	(%)
Abdominal pain	13	(100)	4	(80)	20***	(47)
Diarrhea	13	(100)	2**	(40)	12***	(28)
Rash	9	(69)	1	(20)	12**	(28)
Arthralgia	12	(92)	1**	(20)	10***	(23)
Arthritis	6	(46)	0	(0)	4**	(9)
Stomatitis	10	(77)	1*	(20)	8***	(19)
Lymphadenopathy	11	(85)	2	(40)	14***	(33)
Mental retardation	2	(15)	2	(40)	2	(5)
Dysarthria	1	(8)	0	(0)	0	(0)
Retinitis pigmentosa	1	(8)	0	(0)	0	(0)

MK deficient: presence of two *MVK* mutations. MK sufficient: absence of any *MVK* mutation
MK sufficient, mevalonic acid↑ (false positives). MK sufficient, mevalonic acid↓ (true negatives)
Asterisks indicate significant different frequencies compared to MK-deficient patients: *$p \leq 0.05$; **$p \leq 0.01$; ***$p \leq 0.001$

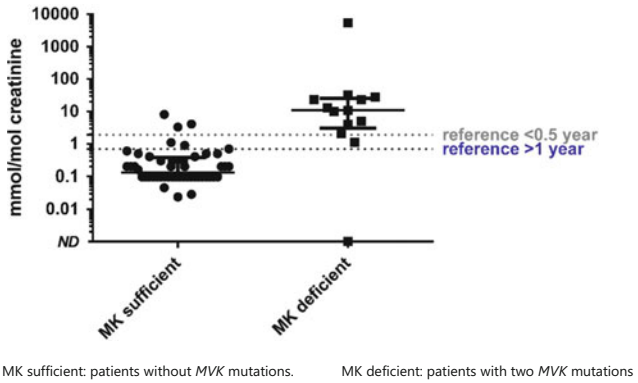

Fig. 1 Distribution of mevalonic acid excretions in patients without *MVK* mutations and with two *MVK* mutations

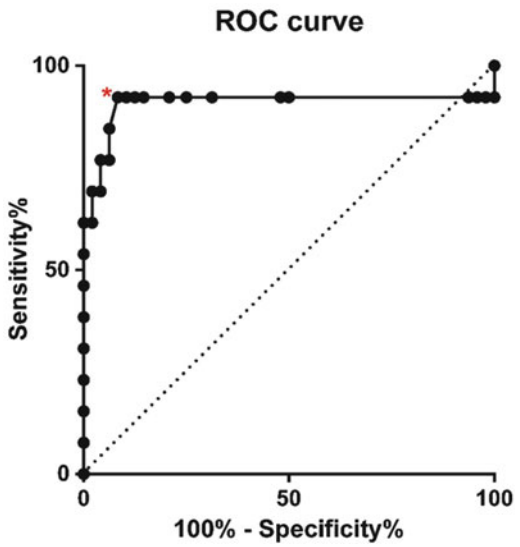

Fig. 2 The diagnostic accuracy of urinary mevalonic acid displayed in a receiver operating characteristic (ROC) curve. The mevalonic acid excretion is expressed as mmol/mol creatinine. *Asterisk* represents a cutoff value of 1 mmol/mol creatinine. This value has a sensitivity of 92% and a specificity of 92%. The area under the curve (AUC) is 0.911

Patients with Elevated Urinary Mevalonic Acid, Without *MVK* Mutations

Five patients did not bear any *MVK* mutations, but had at least one elevated measurement of urinary mevalonic acid. Fifteen measurements were performed in these patients. Six measurements were elevated, while nine measurements showed normal excretions of mevalonic acid. All five patients suffered from febrile episodes; in four patients, the episodes started within the first year of life. The enzyme activity was measured in fibroblasts in two patients; in both of them, the activity was normal in comparison to healthy individuals. Further, there were no indications for other metabolic disorders that could explain the elevated mevalonic acid excretion.

Table 3 Characteristics of patients with elevated mevalonic acid excretions

Patient	Mevalonic acid excretion	Age at test	Mutations	Mevalonate kinase enzyme activity
Mevalonate kinase-deficient patients				
1	2.1	3.3	V377I V377I	
2	13.1	0.7	V377I I268T	
3	1.1	4.9	V377I V377I	
4	11.0	1.0	I268T P167L	1%
5	5,461	1.1	A334T A141fs	0.15%
6	5	11.8	V377I R215Q	
7	32	3.7	V377I I268T	
8	27.5	1.6	V377I I268T	2.5%
9	22.8	7.8	V377I H20P	2.5%
10	10	7.9	V377I I268T	2%
11	4	8.8	N205A V321A	15%
12	23.7	0.6	V377I W62X	3.5%
Mevalonate kinase-sufficient patients				
13	1.1	2.7	–	
14	8.1	3.5	–	
15	4.1	6.7	–	Normal
16	0.9	4.4	–	
17	3.3	1.6	–	Normal

Two patients with an elevated measurement suffered from febrile episodes and typical MKD symptoms, such as pharyngitis, arthralgia, lymphadenopathy, diarrhea, abdominal pain, and stomatitis. Two other patients experienced predominantly neurological impairment, accompanied by febrile episodes. These two patients suffered from childhood absence epilepsy and mental retardation, one of them also had ataxia. In one patient with fever and headache without other specific MKD complaints, genetic analysis for Familial Mediterranean fever (FMF), TNF receptor-associated periodic fever syndrome (TRAPS), and MKD was all negative. Currently, she is not suffering from fever anymore, but the headache is still present.

Patients with Normal Urinary Mevalonic Acid and Without *MVK* Mutations

Fifty-four measurements of urinary mevalonic acid were performed in 43 patients. All of them were normal and none of these patients harbored any *MVK* mutations. Among those forty-three, forty patients suffered from febrile episodes. Those patients suffered predominantly from abdominal pain, diarrhea, lymphadenopathy, arthralgia, rash, and stomatitis. However, these were significantly less often seen compared to patients with *MVK* mutations (Table 2).

Discussion

Assessment of mevalonic acid excretion is often performed in patients with clinical features suggestive of MKD. Nonetheless, the diagnostic value of this assessment was unclear, and genetic testing and enzyme assay are still the only manner to definitely diagnose patients with MKD. Therefore, we examined the diagnostic value of this assessment in a group of patients with a phenotype of periodic fever.

In our cohort, patients with an elevated mevalonic acid excretion had a 71% chance to be suffering from mevalonate kinase deficiency. Examination of MKD patients and those with a false-positive test result showed many similarities and some discrepancies as well. Typical MKD symptoms such as abdominal pain, diarrhea, arthralgia, and lymphadenopathy were less prominent in patients with a false-positive test. In two of these patients, MKD was ruled out completely by detecting a normal enzyme activity. Although enzyme activity was not measured in the other three patients with elevated urinary mevalonic acid, the absence of *MVK* mutations made MKD extremely unlikely.

In this study, mevalonic acid could not be detected in one patient with MKD when urine was collected during fever. However, the clinical features of this patient were similar to MKD patients with elevated mevalonic acid excretions. Because there is only one false-negative patient in our series, the negative predictive value is high (98%), but it does show that we cannot rule out MKD in patients with a normal mevalonic acid excretion. We have no explanation for the fact that mevalonic acid was not elevated in this patient.

The reference values used to determine whether the mevalonic acid excretion was elevated are 95% confidence intervals, which means that 5% of all patients excrete higher or lower amounts of mevalonic acid. This might explain why some patients without *MVK* mutations had an elevated mevalonic acid excretion. Other metabolic disorders which might cause an elevated excretion of mevalonic acid, such as cerebrotendinous xanthomatosis and abetalipoproteinemia, were not found in these five patients (Lindenthal et al. 1996; Illingworth et al. 1989).

Currently, mevalonic acid excretion is often collected during febrile episodes (Ammouri et al. 2007). It is assumed that the excretion of mevalonic acid is elevated during febrile MKD episodes. In our study, it was not possible to collect urines exclusively during fever due to the retrospective design of this research. In some cases, it was not possible to trace whether urine samples had been collected during a febrile episode. This might have led to a lower diagnostic accuracy of this test.

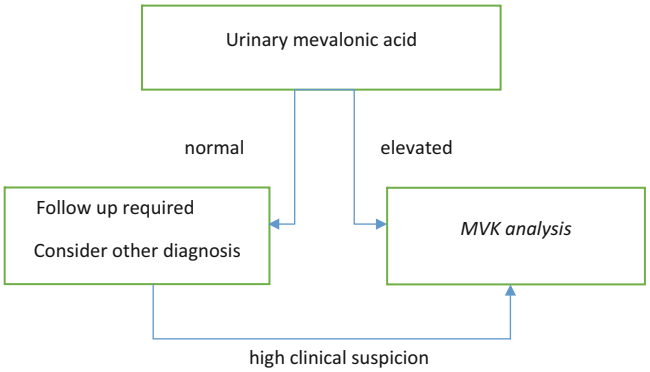

Fig. 3 Diagnostic tree in the diagnostic process of MKD

This single-center study was performed in a center with expertise in diagnosis and treatment of MKD. This might have led to a more accurate selection of patients before metabolic and genetic testing are performed and a better handling of the urine samples and thus better test characteristics than would be the case in a hospital with less expertise.

Although this is not a perfect diagnostic study due to the small number of patients and the retrospective design, the rarity of this disease hampers a proper diagnostic study. Therefore, by including all patients suspected of MKD, this study approaches a diagnostic study as close as possible. Based on the reported findings, we made a diagnostic algorithm (Fig. 3).

Several studies have described the phenomenon of elevated mevalonic acid levels in patients with MKD (Simon et al. 2004; Bader-Meunier et al. 2011; Poll-The et al. 2000; Prietsch et al. 2003; Hoffmann et al. 1993; Prasad et al. 2012). Hoffmann et al. have shown in a series of eleven MA patients that highly elevated levels of mevalonic acid occur in urine and that the levels of mevalonic acid in urine correlated with the severity of the disease (Hoffmann et al. 1993). Poll-The et al. described a series of twelve patients with the HIDS phenotype. Mildly increased excretions of mevalonic acid were found in these patients during febrile episodes. In comparison, patients suffering from the MA phenotype excreted higher levels of mevalonic acid (Poll-The et al. 2000). In contrary, Prasad et al. described two cases of severely affected patients with relatively low amounts of mevalonic acid excretion (Prasad et al. 2012).

In conclusion, MKD seems very unlikely in patients with a normal mevalonic acid excretion, but it cannot be excluded completely. Further, a positive urinary mevalonic acid excretion still requires *MVK* analysis to confirm the diagnosis of MKD. Therefore, detection of urinary mevalonic acid

should not be mandatory before genetic testing. However, as long as genetic testing is not widely available and affordable, measurement of urinary mevalonic acid is a fair way to select patients for *MVK* gene analysis or enzyme assay.

One Sentence

Measurement of urinary mevalonic acid is a fair way to select patients for *MVK* gene analysis or enzyme assay, as false-positive or false-negative mevalonic acid measurements can occur.

Compliance with Ethics Guidelines

Conflict of Interest

Joost Frenkel received consultancy fees from NOVARTIS and speaker's fees from SOBI.

Jerold Jeyaratnam, Nienke ter Haar, Monique de Sain-van der Velden, Hans Waterham, and Mariëlle van Gijn declare that they have no conflict of interest.

Informed Consent

All procedures followed were in accordance with the ethical standards of the responsible committee on human experimentation (institutional and national) and with the Helsinki Declaration of 1975, as revised in 2000 (5). A waiver of review was granted by the institutional ethical review board.

Details of the Contributions of Individual Authors

Jerold Jeyaratnam and Nienke te Haar contributed equally to this study

Jerold Jeyaratnam, Nienke ter Haar, and Joost Frenkel: coordination of the study, data analysis, and draft of the manuscript

Monique de Sain-van der Velden, Hans Waterham, and Mariëlle van Gijn: acquisition of data and final approval of the manuscript

References

Ammouri W, Cuisset L, Rouaghe S et al (2007) Diagnostic value of serum immunoglobulinaemia D level in patients with a clinical suspicion of hyper IgD syndrome. Rheumatology (Oxford) 46:1597–1600

Bader-Meunier B, Florkin B, Sibilia J et al (2011) Mevalonate kinase deficiency: a survey of 50 patients. Pediatrics 128:e152–e159

Berger R, Smit GP, Schierbeek H et al (1985) Mevalonic aciduria: an inborn error of cholesterol biosynthesis? Clin Chim Acta 152: 219–222

van der Burgh R, Ter Haar NM, Boes ML et al (2013) Mevalonate kinase deficiency, a metabolic autoinflammatory disease. Clin Immunol 147:197–206

Cuisset L, Drenth JP, Simon A et al (2001) Molecular analysis of MVK mutations and enzymatic activity in hyper-IgD and periodic fever syndrome. Eur J Hum Genet 9:260–266

Hoffmann GF, Charpentier C, Mayatepek E et al (1993) Clinical and biochemical phenotype in 11 patients with mevalonic aciduria. Pediatrics 91:915–921

Houten SM, Kuis W, Duran M et al (1999) Mutations in MVK, encoding mevalonate kinase, cause hyperimmunoglobulinaemia D and periodic fever syndrome. Nat Genet 22:175–177

Illingworth DR, Pappu AS, Gregg RE (1989) Increased urinary mevalonic acid excretion in patients with abetalipoproteinemia and homozygous hypobetalipoproteinemia. Atherosclerosis 76: 21–27

Lindenthal B, von Bergmann K (1994) Determination of urinary mevalonic acid using isotope dilution technique. Biol Mass Spectrom 23:445–450

Lindenthal B, Simatupang A, Dotti MT et al (1996) Urinary excretion of mevalonic acid as an indicator of cholesterol synthesis. J Lipid Res 37:2193–2201

van der Meer JW, Vossen JM, Radl J et al (1984) Hyperimmunoglobulinaemia D and periodic fever: a new syndrome. Lancet 1: 1087–1090

Poll-The BT, Frenkel J, Houten SM et al (2000) Mevalonic aciduria in 12 unrelated patients with hyperimmunoglobulinaemia D and periodic fever syndrome. J Inherit Metab Dis 23:363–366

Prasad C, Salvadori MI, Rupar CA (2012) Severe phenotypic spectrum of mevalonate kinase deficiency with minimal mevalonic aciduria. Mol Genet Metab 107:756–759

Prietsch V, Mayatepek E, Krastel H et al (2003) Mevalonate kinase deficiency: enlarging the clinical and biochemical spectrum. Pediatrics 111:258–261

Prieur AM, Griscelli C (1984) Nosologic aspects of systemic forms of very-early-onset juvenile arthritis. Apropos of 17 cases. Sem Hop 60:163–167

Simon A, Kremer HP, Wevers RA et al (2004) Mevalonate kinase deficiency: evidence for a phenotypic continuum. Neurology 62: 994–997

JIMD Reports
DOI 10.1007/8904_2015_481

CASE REPORT

Hyperprolinemia in Type 2 Glutaric Aciduria and MADD-Like Profiles

Clément Pontoizeau · Florence Habarou · Anaïs Brassier · Alice Veauville-Merllié · Coraline Grisel · Jean-Baptiste Arnoux · Christine Vianey-Saban · Robert Barouki · Bernadette Chadefaux-Vekemans · Cécile Acquaviva · Pascale de Lonlay · Chris Ottolenghi

Received: 08 June 2015 / Revised: 29 June 2015 / Accepted: 02 July 2015 / Published online: 27 September 2015
© SSIEM and Springer-Verlag Berlin Heidelberg 2015

Abstract Classical neonatal-onset glutaric aciduria type 2 (MAD deficiency) is a severe disorder of mitochondrial fatty acid oxidation associated with poor survival. Secondary dysfunction of acyl-CoA dehydrogenases may result from deficiency for riboflavin transporters, leading to severe disorders that, nevertheless, are treatable by riboflavin supplementation. In the last 10 years, we identified nine newborns with biochemical features consistent with MAD deficiency, only four of whom survived past the neonatal period. A likely iatrogenic cause of riboflavin deficiency was found in two premature newborns having parenteral nutrition, one of whom recovered upon multivitamin supplementation, whereas the other died before diagnosis. Four other patients had demonstrated mutations involving ETF or ETF-DH flavoproteins, whereas the remaining three patients presumably had secondary deficiencies of unknown mechanism. Interestingly, six newborns among the seven tested for plasma amino acids had pronounced hyperprolinemia. In one case, because the initial diagnostic workup did not include organic acids and acylcarnitine profiling, clinical presentation and hyperprolinemia suggested the diagnosis. Analysis of our full cohort of >50,000 samples from >30,000 patients suggests that the proline/alanine ratio may be a good marker of MAD deficiency and could contribute to a more effective management of the treatable forms.

Communicated by: Michael J Bennett, PhD

Competing interests: None declared

C. Pontoizeau and F. Habarou equally contributed to this book.

C. Pontoizeau · F. Habarou · A. Brassier · C. Grisel · J.-B. Arnoux · R. Barouki · B. Chadefaux-Vekemans · P. de Lonlay · C. Ottolenghi
Centre de Référence des Maladies Héréditaires du Métabolisme, Hôpital Necker-Enfants Malades, Assistance Publique-Hôpitaux de Paris, University of Paris Descartes, Institut Imagine, Paris, France

C. Pontoizeau (✉) · F. Habarou · R. Barouki · B. Chadefaux-Vekemans · C. Ottolenghi
Service de Biochimie Métabolomique et Protéomique, Hôpital Necker-Enfants Malades, Assistance Publique-Hôpitaux de Paris, 149 rue de Sèvres, 75015 Paris, France
e-mail: clement.pontoizeau@aphp.fr

F. Habarou · R. Barouki · B. Chadefaux-Vekemans · C. Ottolenghi
INSERM UMR-S 1124, University of Paris Descartes, Sorbonne Paris Cité, Paris, France

A. Veauville-Merllié · C. Vianey-Saban · C. Acquaviva
Service Maladies Héréditaires du Métabolisme et Dépistage Néonatal, Centre de Biologie et Pathologie Est, CHU Lyon, Bron, France

Introduction

Multiple acyl-CoA dehydrogenase deficiency (MADD), also known as glutaric aciduria type 2 (GA2, OMIM 231680), is a rare autosomal recessive metabolic disease, caused by defects in the mitochondrial electron transfer flavoprotein (ETF) or, in its electron acceptor counterpart, the electron transfer flavoprotein dehydrogenase (ETF-DH or ETF-QO) (Frerman and Goodman 1985). Neonatal-onset forms are characterized by nonketotic hypoglycemia, metabolic acidosis, hepatomegaly, and hypotonia, usually with fatal outcome during the neonatal period or the first months of life (Frerman and Goodman 2001). A few of these patients have congenital anomalies, such as renal cystic dysplasia, facial dysmorphism, rocker bottom feet, and abnormalities of external genitalia (Frerman and Goodman 2001), while the others often develop severe cardiomyopathy during the neonatal period. Cases of

secondary MADD related to riboflavin deficiency have been described in neonates of mothers carrying heterozygous mutations in a riboflavin transporter (deficiency for GPR172B/SLC52A1) and showed a good response to transient riboflavin supplementation (Chiong et al. 2007; Harpey et al. 1983; Ho et al. 2011). A different entity with later presentation, Brown–Vialetto–Van Laere syndrome, is caused by mutations in two related riboflavin transporters SLC52A2 and SLC52A3 (Bosch et al. 2011; Green et al. 2010; Johnson et al. 2012).

Important biochemical anomalies guide the diagnosis of primary or secondary MADD. Plasma acylcarnitine profiles show an increase of all chain-length acylcarnitines, while urine organic acid profiles display high concentrations of glutaric, 2-hydroxyglutaric, ethylmalonic and other dicarboxylic acids, and several glycine derivatives (Frerman and Goodman 2001). Early studies reported that a marked increase of plasma proline is common in neonatal-onset patients (Frerman and Goodman 2001; Goodman et al. 1983; Przyrembel et al. 1976; Sweetman et al. 1980), but plasma amino acid analysis does not usually play a part in the diagnostic workup.

In this report, we have identified nine newborns with biochemical features consistent with primary or secondary MAD deficiency in our local cohort and investigated the potential clinical interest of amino acid analyses in this context by comparison to a large cohort of patients.

Subjects and Methods

Between 2003 and 2014, we have identified four neonates with primary MAD deficiency and five others with suspected secondary MAD deficiency. Of these, 1/4 and 3/5 patients, respectively, survived past the neonatal period. Table 1 summarizes the relevant clinical and biochemical features and further details are presented in this section.

We observed primary neonatal MADD in four newborns (patients 1–4). Patients 1 and 2 showed typical neonatal MADD onset with hypoglycemia, metabolic acidosis with hyperlactatemia, mild hyperammonemia, hepatomegaly and hypotonia, and classical biochemical profiles associating very high glutaric levels (7,080 and 5,280 mmol/mol creatinine, respectively) with increased ethylmalonic acid, 2-hydroxyglutaric acid, dicarboxylic acids, and multiple acylglycines in urine, along with multiple acylcarnitines in plasma. Both died at a few days of life. Patient 1 showed compound heterozygosity for *ETFDH* mutations (c.50dup/p.His17GlnfsX6 in exon 2 and c.313A>G/p.Lys105Glu in exon 3). Patient 2 had a complete loss of ETF-DH activity and a homozygous mutation involving *ETFDH* (c.34+5G>C, donor splice site of intron 1). Patient 3 was the sister of patient 2 and MADD diagnosis was obtained during pregnancy. The child died at 38 days of life of respiratory failure following aspiration pneumonia. Patient 4 made good progress under treatment (Table 1), yet primary MADD was confirmed by molecular genetic testing (homozygous known pathogenic mutations in *ETFA*: c.797C>T, p.Thr266Met, in exon 9). She is now 9 years old. Of note, levels of glutaric acid (1,669 vs 5,280–7,980 mmol/mol creatinine) and other markers in urine were lower for patient 4 than patients 1–3.

The remaining five patients with biochemical features of MADD were suspected of having secondary MADD.

Riboflavin deficiency linked to riboflavin deficiency in the mothers was suspected for three of these patients (referred to as 5–7). Their clinical presentations were comparable to neonatal MADD but biochemical abnormalities were milder. Notably, urine glutaric acid levels were between 175 and 2,272 mmol/mol creatinine (patients 5 and 6). For patients 5 and 6, vitamin supplementation completely normalized clinical and biochemical features. The patients did not have further episodes of decompensation under riboflavin supplementation and eventually without any therapy. Normalization of biochemical parameters and uneventful evolution after discontinuation of therapy are not consistent with the diagnosis of primary MADD. In addition, for patient 5, fatty acid oxydation flux analysis was normal in fibroblasts, and for patient 6, we did not detect mutations of *ETFA*, *ETFB*, or *ETFDH*. Patient 7 died at 3 days of life, and we suspect a secondary MADD deficiency, because only moderate abnormalities were detected for acylcarnitines and organic acids in plasma (urine analysis unavailable).

Our last two cases (patients 8 and 9) likely suffered from iatrogenic riboflavin deficiency. Both were premature newborns (32 and 31 weeks gestation, respectively), fed by parenteral nutrition for over 2 weeks. Clinical signs and metabolic acidosis appeared after 2 and 3 weeks, respectively. They showed milder but suggestive biochemical profiles of MADD. Patient 8 recovered upon multivitamin supplementation while patient 9 died before diagnosis.

All procedures were in accordance with the ethical standards of the local committees on human experimentation (institutional and national) and with the Helsinki Declaration of 1975, as revised in 2000. Informed consent was obtained from all patients for being included in the study.

Amino Acid Analyses and Statistics

Quantitative plasma amino acid analysis was performed by ion-exchange chromatography: 40-μL deproteinized samples were injected into a JEOL AminoTac JLC-500/V

Table 1 Summary of clinical and biochemical findings in patients with MADD or MADD-like presentation

Patient n/sex	Age of onset	Survival	Clinical picture	Glutaric acid (mmol/mol of creatinine) in urine	Other anomalies[a]	Proline/ alanine (μmol/L) in plasma	Diagnosis
1/F	34 h	Deceased at 8 days	Hypoglycemia, feeding difficulties, hypotonia, mild hyperammonemia, hyperlactatemia, convulsion, hepatomegaly	7,080	Urine: EMA, IBG, BG, HG, 2-hydroxyglutaric acid, adipic acid, suberic acid	369/130	Primary MADD (ETF-DH deficiency)
2/M	1 h	Deceased at 4 days	Hypoglycemia, metabolic acidosis, mild hyperammonemia, lethargic coma, hypotonia, hepatomegaly, subependymal hemorrhage, PAH	6,507	Urine: EMA, 2-hydroxyglutaric acid, adipic acid, suberic acid, sebacic acid, HG, IBG, BG, IVG	622/126	Primary MADD (ETF-DH deficiency)
3/F	Antenatal diagnosis	Deceased at 38 days	Macrocephaly, dysmorphia, hepatomegaly, metabolic acidosis, hyperlactatemia, mild hyperammonemia, hypotonia	5,280	Urine: EMA, adipic acid, 2-hydroxyglutaric acid, IBG, IVG	NR/NR	Primary MADD (ETF-DH deficiency)
4/F	1 day	Alive	Feeding difficulties, hypotonia, hypothermia, hepatomegaly, hypoglycemia, hyperammonemia, hyperlactatemia, renal insufficiency	1,669	Urine: EMA, adipic acid, suberic acid, sebacic acid, HG, IBG, BG, IVG Plasma acylcarnitines: C4–C16:1	272/905	Primary MADD (ETFA deficiency)
5/F	12 h	Alive	Hypoglycemia, hyperlactatemia, pulmonary distress, metabolic acidosis, subependymal hemorrhage,	175	Urine: EMA, 2-hydroxyglutaric, IBG, IVG, HG, adipic acid, suberic acid, sebacic acid	1,152/1,134	Suspected secondary MADD
6/M	2 days	Alive after the neonatal period lost to follow-up	Hypoglycemia, hypotonia, feeding difficulties, hyperammonemia	2,272	Urine: adipic acid, suberic acid, sebacic acid, HG, SG, PG, BG, IVG	NR/NR	Suspected secondary MADD
7/F	1 day	Deceased at 3 days	Cardiorespiratory arrest, metabolic acidosis with hyperlactatemia, hepatomegaly, dilated left ventricle, PAH, liver dysfunction, pulmonary hemorrhage, multiorgan failure	2.87[b]	Plasma: 2-hydroxyglutaric acid, EMA, adipic acid, suberic acid Plasma acylcarnitines: C16-OH, C14-DC, C18-DC, glutarylcarnitine	1,457/429	Suspected secondary MADD
8/M	35 days	Alive	Metabolic acidosis, mild hyperlactatemia, pancytopenia, lethargy, hypotonia, myoclonia, hepatomegaly	535	Urine: EMA, 2-hydroxyglutaric, adipic acid, suberic acid, HG, SG, BG, IVG Plasma acylcarnitines: C3-C14	1,181/247	Iatrogenic riboflavin deficiency
9/M	13 days	Deceased at 17 days	Abnormal movements, anemia, thrombopenia, and severe metabolic acidosis	1,018	Urine: EMA, 2-hydroxyglutaric, adipic acid, suberic acid, HG, SG, BG, IVG Plasma acylcarnitines: C4-C14	1,230/599	Iatrogenic riboflavin deficiency
Control				<14		83–281/ 166–514	

EMA ethylmalonic, *BG* butyrylglycine, *HG* hexanoylglycine, *IVG* isovalerylglycine, *SG* suberylglycine, *PG* propionylglycine, *IBG* isobutyrylglycine, *PAH* pulmonary arterial hypertension, *NR* not reported

[a] Increase of the reported metabolites

[b] Plasma value in μmol/L (normal values 0.53 μmol/L)

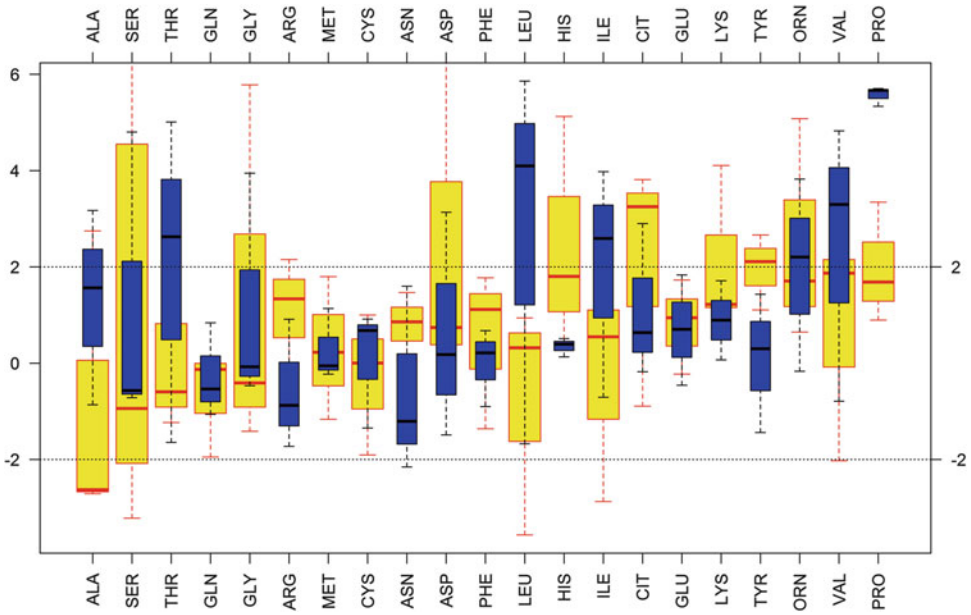

Fig. 1 Box plots of age-normalized levels of 21 plasma amino acids for samples from patients with primary (*yellow*) or presumably secondary (*blue*) MAD deficiency at presentation. *Y*-axis: age-normalized standard deviations from a hospital reference population. Amino acids are ordered from the lowest (alanine, ALA) to the highest median levels (proline, PRO) across all samples. The *boxes* cover the ±25th percentile from the median (*horizontal line* in the *boxes*); the *dotted lines* cover the ±95th percentile from the median

amino acid analyzer calibrated according to standards of known concentration. Amino acid identification was based on retention time and quantification was obtained by integration. Statistical analyses were performed in R (cran.r-project.org). In particular, the ellipse of Fig. 2 was obtained by robust covariance estimation (*covRob* module).

Results

We first investigated individual amino acid profiles to assess the degree of hyperprolinemia relative to reference intervals. Of the seven cases tested for plasma amino acids, six patients showed hyperprolinemia (Table 1). Two of four cases of primary MADD had only mild hyperprolinemia, yet contrasting with a paradoxical, moderate decrease of alanine concentration below the normal/reference interval. The only primary MADD patient who survived (patient 4) never showed marked hyperprolinemia at diagnosis or during follow-up. All the informative cases suspected of secondary MADD (patients 5, 7, 8, 9) showed much more pronounced hyperprolinemia (1,152–1,457 vs 272–622 μmol/L), whereas alanine levels were only moderately increased. For patient 7, as the initial diagnostic workup did not include organic acid or acylcarnitine profiling, clinical presentation and hyperprolinemia suggested to complete biochemical investigations leading to the diagnosis.

To evaluate the relevance of the association between hyperprolinemia and biochemical features of MADD, we noticed that alanine showed the minimum median levels across all the patients compared to 20 additional amino acids (Fig. 1). Because of the observed dissociation between proline and alanine levels, we reasoned that the ratio or the difference between the levels of these two amino acids could be of diagnostic relevance. Figure 2 plots proline against alanine in our entire cohort of plasma amino acid profiles archived since 1995 including patients with known metabolic disorders ($N = 53{,}338$). Figure 2 shows a clear correlation between alanine and proline, with on average higher concentrations of the former amino acid. We observed that some MADD-like profiles clearly deviate from this trend, characterized by high proline concentrations relative to alanine.

The plot shows that 3/4 tested patients with suspected secondary MADD were very unusual in having very high proline levels (>1,000 μM) contrasting with lower alanine levels (<1,000 μM). Two of three tested patients with primary MADD were also unusual in having moderate increases of proline (>300 μM) contrasting with reduced alanine (<200 μM). The plot also suggests that a potentially useful, continuous cutoff could be plasma proline at levels greater than 1.4 × (alanine concentration) + 140 (red line in Fig. 2; in micromoles/liter). Only 153 of the 53,338 samples show proline values above such cutoff and would be regarded as consistent with MADD,

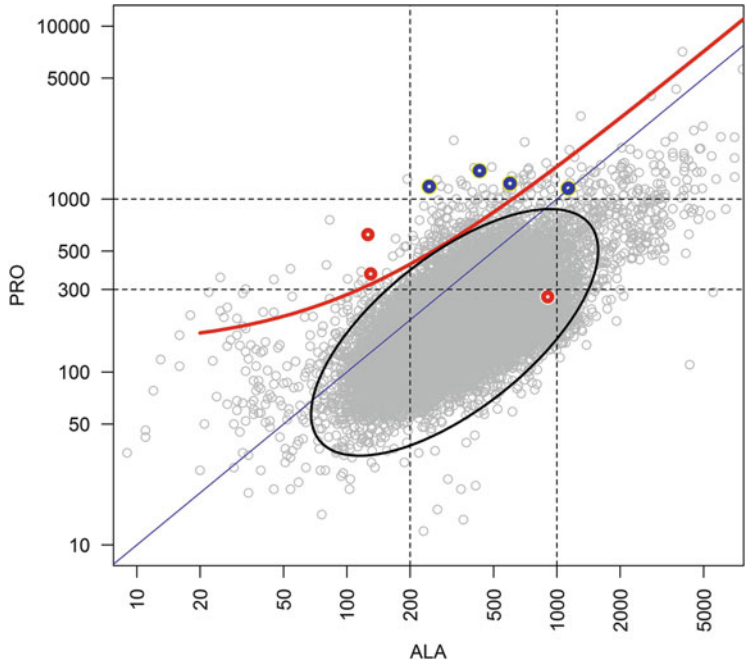

Fig. 2 The plasma levels of alanine ("ALA", *x*-axis) and proline ("PRO", *y*-axis) in micromoles/liter are shown for 53,338 samples corresponding to our complete cohort (*gray*). The samples collected at presentation from the patients reported in this study are shown as *red* (newborns with primary MADD) or *blue circles* (newborn with suspected secondary MADD). The *equality line* is *blue*, indicating that average reference alanine levels are greater than proline. Useful cutoffs are shown by *black dashed lines* and a proposed continuous cutoff by a *red line* (corresponding to the equation PRO = 1.4 × ALA + 140) (see text). The *black ellipse* represents the estimated bivariate normal distribution at alpha = 10^{-5}

with a *p*-value <0.003 (the same *p*-value is obtained by restricting the analysis to the first sample of each patient in the cohort, which yields 35 positive out of 34,525 patients). This cutoff is a tangent to the ellipse of Fig. 2, corresponding to a bivariate reference distribution, at alpha error of 10^{-5}, thus supporting the conclusion that the values associated with most neonatal MADD or MADD-like samples are highly deviant.

These analyses showed an overrepresentation of MADD-like cases among patients with hyperprolinemia, confirming the relevance of the association between these biochemical features. In addition, we suggest that hyperprolinemia with dissociated alanine levels can be useful to suggest a MADD-like disorder. Of note, other etiologies with proline much greater than alanine were primary hyperprolinemia, E3 (DLD) deficiency, lysinuric protein intolerance, and peri-mortem conditions.

Discussion

Early reports pointed to hyperprolinemia as a common feature of MADD, yet plasma proline is currently not regarded as a marker of the disease. Our study indicates that it is a frequent finding both in primary and in suspected cases of secondary early-onset forms of MADD. Our uniquely large cohort of >50,000 plasma amino acid samples also indicates that the simple dissociation between high proline and lower alanine levels may be suggestive of the diagnosis, by using simple cutoffs such as proline levels greater than 140% of alanine levels plus 140 μM. This is of particular interest considering that secondary MADD readily responds to riboflavin supplementation, provided that the diagnosis is suggested promptly. In addition, a small fraction of primary MADD cases can also respond to therapy involving riboflavin, carnitine, and appropriate diet.

Proline dehydrogenase (or proline oxidase (POX)) is a flavoprotein, well characterized in microorganisms and highly conserved throughout eukaryotes and bacteria (Servet et al. 2012; Tanner 2008). POX oxidizes proline to produce Δ^1-pyrroline-5-carboxylate (P5C), the first step of proline catabolism. Reduced POX may then give electrons to the electron transfer chain directly via the ubiquinone pool (Moxley et al. 2011), thus without requiring ETF (Wanduragala et al. 2010). Gene sequence comparison and absorption spectral characterization of its catalytic site have suggested that human POX features are comparable to those in microorganisms (Tallarita et al. 2012; Tanner 2008). Because POX is a flavoprotein, it is reasonable to propose that hyperprolinemia observed in riboflavin deficiency may be secondary to depletion in the FAD cofactor. The reason why hyperprolinemia is observed

in MADD is still unclear. Secondary coenzyme Q10 deficiency has been observed in riboflavin-responsive MADD (Cornelius et al. 2013). It is tempting to speculate that MADD might induce alterations of the ubiquinone pool or of riboflavin metabolism leading to hyperprolinemia.

Plasma proline was most prominently elevated in the suspected cases of secondary MADD at the time of presentation and was also found in a patient with Brown–Vialetto–Van Laere syndrome during a period of cardiorespiratory distress that preceded death (data not shown). Therefore, we suggest that hyperprolinemia may be a marker of acute decompensation. Nevertheless, it was not found at any time point in a primary MADD case that survived, and the other patients with primary MADD had absolute levels of proline that were not very elevated, except if compared to alanine.

Furthermore, proline levels were higher in secondary MADD, offering the opportunity to quickly refine MADD diagnoses.

We cannot completely rule out differential diagnoses for hyperprolinemia such as medical treatment containing proline, parenteral nutrition, or gelatin administration (Illsinger et al. 2006). However, the degree of hyperprolinemia relative to other amino acids such as alanine, and its association with biochemical features of MADD in different contexts, times, and geographical areas, is not really consistent with this association being coincidental. Hyperlactatemia also induces hyperprolinemia by inhibition of proline oxidase (Kowaloff et al. 1977). However, alanine and proline are both known to increase concomitantly with increased lactate concentrations, yet alanine did not increase as much as proline or actually decreased in some cases (Fig. 2). Hyperprolinemia can also be observed in peri-mortem profiles, characterized by generalized hyperaminoacidemia with very low arginine concentrations, which was clearly different from our profiles.

Our study highlighted the clinical heterogeneity associated with biochemical profiles of MADD. A significant part of suspected neonatal MADD may be secondary forms, treatable with riboflavin. For populations at risk of riboflavin deficiency like preterm newborns under parenteral nutrition, riboflavin supplementation should be considered with particular attention. Critical care recommendations may include riboflavin supplementation as part of a multivitamin cocktail as a first-line therapy for severely ill newborns. Based on our data, in some areas, education of neonatologists may be required to ensure complete prevention of iatrogenic or other causes of secondary MADD.

As shown by our study based on >50,000 plasma amino acid profiles, biochemical profiles of MADD were overrepresented among cases of hyperprolinemia with simple cutoffs ($p < 0.003$), and other diagnoses with similar alanine and proline levels are associated with very different clinical pictures (see above). This observation is particularly relevant for countries like France where plasma amino acid profiles are ordered before acylcarnitines and urine organic acids profiles. Of particular interest, proline concentrations were more pronounced in secondary MADD that is treatable but can lead to death if untreated. Hyperprolinemia may be a first-line indication of the diagnosis prompting the introduction of MADD therapy.

Our study suggests that the absolute difference between proline to alanine levels in plasma may be a good marker of MAD deficiency, in particular for secondary etiologies, and could contribute to a more effective management of this disorder.

Acknowledgments We thank Jacqueline Bardet, Odile Beaugendre, Marie Bisançon, Martine Gasquet, and Sabine Leroy for excellent technical assistance.

Synopsis

Hyperprolinemia and more precisely high proline/alanine ratio may be a good marker of MAD deficiency.

Compliance with Ethics Guidelines

Conflict of Interest

Clément Pontoizeau, Florence Habarou, Anaïs Brassier, Alice Veauville-Merllié, Coraline Grisel, Jean-Baptiste Arnoux, Christine Vianey-Saban, Robert Barouki, Bernadette Chadefaux-Vekemans, Cécile Acquaviva, Pascale de Lonlay, and Chris Ottolenghi declare that they have no conflict of interest.

Informed Consent

All procedures followed were in accordance with the ethical standards of the responsible committee on human experimentation (institutional and national) and with the Helsinki Declaration of 1975, as revised in 2000. Informed consent was obtained from all patients for being included in the study.

Details of the Contributions of Individual Authors

AB, CG, J-BA, and PdL collected the data. CP, FH, AVM, CVS, CA, PdL, and CO analyzed the data. CP, FH, CVS,

CA, PdL, and CO wrote the manuscript. All authors read and approved the final manuscript.

References

Bosch AM, Abeling NGGM, Ijlst L et al (2011) Brown-Vialetto-Van Laere and Fazio Londe syndrome is associated with a riboflavin transporter defect mimicking mild MADD: a new inborn error of metabolism with potential treatment. J Inherit Metab Dis 34:159–164

Chiong MA, Sim KG, Carpenter K et al (2007) Transient multiple acyl-CoA dehydrogenation deficiency in a newborn female caused by maternal riboflavin deficiency. Mol Genet Metab 92:109–114

Cornelius N, Byron C, Hargreaves I et al (2013) Secondary coenzyme Q10 deficiency and oxidative stress in cultured fibroblasts from patients with riboflavin responsive multiple Acyl-CoA dehydrogenation deficiency. Hum Mol Genet 22:3819–3827

Frerman FE, Goodman SI (1985) Deficiency of electron transfer flavoprotein or electron transfer flavoprotein:ubiquinone oxidoreductase in glutaric acidemia type II fibroblasts. Proc Natl Acad Sci U S A 82:4517–4520

Frerman FE, Goodman SI (2001) Defects of electron transfer flavoprotein and electron transfer flavoprotein-ubiquinone oxidoreductase: glutaric acidemia type II. In: Scriver CR, Sly WS, Childs B et al (eds) The metabolic and molecular basis of inherited disease. McGraw-Hill, New York, pp 2357–2365

Goodman SI, Reale M, Berlow S (1983) Glutaric acidemia type II: a form with deleterious intrauterine effects. J Pediatr 102:411–413

Green P, Wiseman M, Crow YJ et al (2010) Brown-Vialetto-Van Laere syndrome, a ponto-bulbar palsy with deafness, is caused by mutations in c20orf54. Am J Hum Genet 86:485–489

Harpey JP, Charpentier C, Goodman SI et al (1983) Multiple acyl-CoA dehydrogenase deficiency occurring in pregnancy and caused by a defect in riboflavin metabolism in the mother. Study of a kindred with seven deaths in infancy: value of riboflavin therapy in preventing this syndrome. J Pediatr 103:394–398

Ho G, Yonezawa A, Masuda S et al (2011) Maternal riboflavin deficiency, resulting in transient neonatal-onset glutaric aciduria Type 2, is caused by a microdeletion in the riboflavin transporter gene GPR172B. Hum Mutat 32:E1976–E1984

Illsinger S, Lücke T, Offner G et al (2006) Status epilepticus and hyperprolinaemia following recurrent gelatine administrations in a patient on peritoneal dialysis. Nephrol Dial Transplant 21:1417–1419

Johnson JO, Gibbs JR, Megarbane A et al (2012) Exome sequencing reveals riboflavin transporter mutations as a cause of motor neuron disease. Brain J Neurol 135:2875–2882

Kowaloff EM, Phang JM, Granger AS et al (1977) Regulation of proline oxidase activity by lactate. Proc Natl Acad Sci U S A 74:5368–5371

Moxley MA, Tanner JJ, Becker DF (2011) Steady-state kinetic mechanism of the proline:ubiquinone oxidoreductase activity of proline utilization A (PutA) from Escherichia coli. Arch Biochem Biophys 516:113–120

Przyrembel H, Wendel U, Becker K et al (1976) Glutaric aciduria type II: report on a previously undescribed metabolic disorder. Clin Chim Acta 66:227–239

Servet C, Ghelis T, Richard L et al (2012) Proline dehydrogenase: a key enzyme in controlling cellular homeostasis. Front Biosci Landmark Ed 17:607–620

Sweetman L, Nyhan WL, Tauner DA et al (1980) Glutaric aciduria type II. J Pediatr 96:1020–1026

Tallarita E, Pollegioni L, Servi S et al (2012) Expression in Escherichia coli of the catalytic domain of human proline oxidase. Protein Expr Purif 82:345–351

Tanner JJ (2008) Structural biology of proline catabolism. Amino Acids 35:719–730

Wanduragala S, Sanyal N, Liang X et al (2010) Purification and characterization of Put1p from Saccharomyces cerevisiae. Arch Biochem Biophys 498:136–142

JIMD Reports
DOI 10.1007/8904_2015_490

RESEARCH REPORT

IgG *N*-Glycosylation Galactose Incorporation Ratios for the Monitoring of Classical Galactosaemia

Henning Stockmann · Karen P. Coss · M. Estela Rubio-Gozalbo · Ina Knerr · Maria Fitzgibbon · Ashwini Maratha · James Wilson · Pauline Rudd · Eileen P. Treacy

Received: 22 June 2015 / Revised: 25 June 2015 / Accepted: 29 July 2015 / Published online: 30 September 2015
© SSIEM and Springer-Verlag Berlin Heidelberg 2015

Abstract Classical galactosaemia (OMIM #230400) is a rare disorder of carbohydrate metabolism caused by deficiency of the galactose-1-phosphate uridyltransferase enzyme (EC 2.7.7.12). The cause of the long-term complications, including neurological, cognitive and fertility problems in females, remains poorly understood. The relatively small number of patients with galactosaemia and the lack of validated biomarkers pose a substantial challenge for determining prognosis and monitoring disease progression and responses to new therapies. We report an improved method of automated robotic hydrophilic interaction ultra-performance liquid chromatography *N*-glycan analysis for the measurement of IgG *N*-glycan galactose incorporation ratios applied to the monitoring of adult patients with classical galactosaemia. We analysed 40 affected adult patients and 81 matched healthy controls. Significant differences were noted between the G0/G1 and G0/G2 incorporation ratios between galactosaemia patients and controls ($p < 0.001$ and <0.01, respectively). Our data indicate that the use of IgG *N*-glycosylation galactose incorporation analysis may be now applicable for monitoring patient dietary compliance, determining prognosis and the evaluation of potential new therapies.

Communicated by: Jaak Jaeken

Competing interests: None declared

H. Stockmann · P. Rudd
National Institute for Bioprocessing Research and Training (NIBRT), Glycoscience Group, Mount Merrion, Blackrock, Dublin University College, Dublin, Ireland

K.P. Coss
Department of Infectious Diseases, King's College London, Faculty of Life Sciences and Medicine, Guy's Hospital, London, UK

M.E. Rubio-Gozalbo
Maastricht University Medical Centre, Minderbroedersberg 4, Maastricht, The Netherlands

I. Knerr
National Centre for Inherited Metabolic Disorders, Childrens University Hospital, Dublin, Ireland

M. Fitzgibbon · E.P. Treacy (✉)
Mater Misericordiae University Hospital, Eccles St, Dublin, Ireland
e-mail: etreacy@mater.ie

A. Maratha · E.P. Treacy
University College Dublin Clinical Research Centre, Eccles St, Dublin, Ireland

J. Wilson
Centre for Population Health Sciences, Medical School, Teviot Place, Edinburgh EH8 9AG, Scotland

E.P. Treacy
Trinity College, Dublin, Ireland

Abbreviations

G0	Agalactosylated
G1	Monogalactosylated
G2	Digalactosylated
Gal-1-P	Galactose-1-phosphate
GALT	Galactose-1-phosphate uridyltransferase
HILIC-UPLC	Hydrophilic interaction ultra-performance liquid chromatography

Introduction

Classical galactosaemia (OMIM #230400) is a rare disorder of carbohydrate metabolism caused by profound deficiency of the galactose-1-phosphate uridyltransferase (GALT) enzyme (EC 2.7.7.12). The disease is life-threatening if left untreated in neonates. The only current treatment available is a lifelong galactose-restricted diet. While this is life-saving in the neonate, long-term complications persist in treated patients

despite early diagnosis, initiation of treatment and shared genotypes. These complications include cognitive impairment, neurological and speech abnormalities and fertility issues in female patients. The cause of the complications remains poorly understood (Fridovich-Keil and Walter 2008; Coss et al. 2014; Jumbo-Lucioni et al. 2012).

Reduced GALT activity results in decreased UDP-galactose bioavailability and the toxic build-up of intermediates of the galactose metabolism pathway. GALT maintains the balance between UDP-glucose (glc), UDP-galactose (gal), *N*-acetylgalactosamine (GalNAc) and *N*-acetylglucosamine (GlcNAc) (Frey 1996). These four UDP-hexoses are rate limiting for the biosynthesis of glycoproteins and proteoglycans, which form the foundation of the extracellular synaptomatrix of synaptic cleft and perisynaptic space (Dani and Broadie 2012).

Galactosaemia intoxicated neonates exhibit profound glycan assembly defects demonstrable in circulating transferrin and IgG. Galactosaemia patients (children and adults), on dietary galactose restriction, also have demonstrable defects in both assembly and processing of *N*-glycans (Charlwood et al. 1998; Sturiale et al. 2005; Quintana et al. 2009; Coman et al. 2010; Coss et al. 2012, 2013). These biochemical defects resemble those observed in a number of congenital disorders of glycosylation (CDG) types I (*N*-glycan assembly defects) and II (*N*-glycan processing defects) (Freeze 2013). The glycan synthesis abnormalities in galactosaemia are proposed to result from a combination of decreased UDP-hexose substrates and increased levels of galactose-1-phosphate (gal-1-p) which cause ER stress and in turn disrupt glycosylation and subsequently cause systemic genomic dysregulation (Petry et al. 1991; Ornstein et al. 1992; Ng et al. 1989; Lai et al. 2003; Slepak et al. 2007; Coman et al. 2010; Jumbo-Lucioni et al. 2014; Coss et al. 2014). The proposed alternative pathways of galactose metabolism may be more active in some patients, offering a protective role against gal-1-p intoxication, e.g. UDP-glucose pyrophosphorylase (UGP), which has the ability to convert both gal-1-p and glucose-1-phosphate to UDP-galactose and UDP-glucose, respectively (Fridovich-Keil and Walter 2008).

In our previous studies, we have shown the presence of ongoing IgG *N*-glycan processing defects in adults and children with galactosaemia maintained on a galactose-restricted diet. It is accepted that dietary restriction of galactose is life-saving in the neonate. We have queried whether over-restriction of galactose after the initial perinatal galactose detoxication dietary treatment could have an additive effect on the ongoing pathophysiology on account of the continuing systemic glycosylation abnormalities observed (Hughes et al. 2009; Coman et al. 2010; Coss et al. 2013, 2014).

The absence of reliable sensitive markers to monitor the proposed cellular and systemic glycosylation abnormalities is problematic. Measuring the proximal metabolite markers, red blood cell (RBC) gal-1-p and urinary galactitol, is very informative in the initial neonatal confirmation of satisfactory treatment with a marked decrease noted in these metabolites. After the neonatal stage of galactosaemia, measuring red blood cell (RBC) gal-1-p and urinary galactitol, however, does not identify minor deviations in the diet or differentiate between patients. We (and others) have shown that RBC gal-1-p and urinary galactitol measurements do not distinguish optimum biochemical control in a gradual galactose diet liberalisation study (Hutchesson et al. 1999; Hughes et al. 2009; Bosch et al. 2004; Coss et al. 2012; Krabbi et al. 2011), whereas the analysis of IgG *N*-glycan profiles measured by normal-phase high-performance liquid chromatography (NP-HPLC) showed consistent individual responses to diet liberalisation (Coss et al. 2012).

We have recently reported an improved automated hydrophilic interaction ultra-performance liquid chromatography (HILIC-UPLC) method of glycan analysis which has allowed for more high-throughput processing of total IgG, with improved glycan peak (GP) resolution (Stöckmann et al. 2013). In our earlier preliminary studies reporting IgG *N*-glycan galactose incorporation ratios (G-ratios) as potential biomarkers for determining galactose tolerance in classical galactosaemia, we have applied this to small studies in children and adults (Coss et al. 2012, 2013). Of note, we have now reported this method in a moderate galactose relaxation dietary study in children (using galactose content of 300–500 mg/day). The method identified a number of favourable responders with improved glycosylation ratios with increasing galactose intake and an inverse relationship between the G0/G2 ratio and circulating leptin receptor (sOb-R) in the supplementation group (Knerr et al. 2015).

We now report the development and improvement of this rapid automated method of measuring IgG *N*-glycan galactose incorporation ratios (G-ratios), with a sample of 40 adult galactosaemia individuals from two populations and the characterisation of adult healthy control ratios from a large adult control dataset (81 matched healthy controls). We have also increased the efficiency and turnaround time of the test with development of the analysis now of undigested IgG glycans, which bypasses the time required for the glycan enzymatic digestion step.

Materials and Methods

Study Subjects and Characterisation

The study consisted of 32 classical Irish galactosaemia patients, 14 female and 18 males, 28 homozygous for Q188R, 2 heterozygous for Q188R/R333W and 2 heterozygous for Q188R/K285N, with age range 13 to 36 years

Table 1 Galactosaemia patients' clinical characteristics

Ethnicity	Irish	Dutch
Patients	32	8
Age	21 (13–36)	18 (14–26)
Sex	14 F, 18 M	5 F, 3 M
Genotype	28: Q188R/Q188R, 2: Q188R/R333W, 2: Q188R/K285N	Q188R/Q188R
FSIQ	81 (47–126)	71 (56–97)

and average age 21 years, and 8 Dutch patients, 5 female and 3 males, all homozygous for Q188R, with age range 14 to 26 years and average age 18 years (Table 1). The full-scale intelligence quotient (FSIQ) range for the Irish patients at last testing was FSIQ range 47 to 126, with an average FSIQ of 81. The FSIQ range for the Dutch group of patients at last testing was FSIQ range 56 to 97, with an average FSIQ of 71. The controls consisted of 81 healthy adults (25 Irish adults, average age 35 years, obtained from a healthy population health insurance screening panel and 56 Scottish healthy controls, average age 29 years, from an Orkney Islands, Scotland, healthy population epidemiological study). All galactosaemia adult study patients were maintained on a dietary galactose intake of less than 500 mg gal/day.

Ethical approval for this study was obtained from the Ethics Committee of the Children's University Hospital, Dublin, Ireland, and the Ethics Committee of Maastricht University Hospital. All procedures followed were in accordance with the ethical standards of the responsible committee on human experimentation (institutional and national) and with the Helsinki Declaration of 1975, as revised in 2000. Informed consent was obtained from all patients for inclusion in the study.

Biochemical *N*-Glycan IgG Analysis

Isolation of IgG from Whole Serum

Whole serum was prepared from freshly spun blood samples and immediately frozen at −20°C. IgG was isolated from patient serum samples using a Protein G 96-well Spin Plate for IgG Screening (Thermo Scientific, Dublin, Ireland), as previously described (Stöckmann et al. 2013). The purity of the isolated IgG was assessed using 10% reducing SDS–PAGE gel in an XCell SureLock Mini-Cell (Invitrogen, Carlsbad, CA) according to the manufacturer.

Removal of N-Linked Glycans from IgG

N-glycans were released from the total IgG glycoproteins (heavy and light chains) using the ultrafiltration plate high-throughput method previously described.

2-Aminobenzamide (2-AB) Labelling of N-Glycans

Released *N*-glycans were labelled via reductive amination with the fluorophore 2-AB as previously described. Tagging the glycans with the fluorescent label, 2-AB, allows for their detection at femtomole levels (Stöckmann et al. 2013).

Hydrophilic Interaction Ultra-performance Liquid Chromatography (HILIC-UPLC)

2-AB-labelled *N*-glycans were separated by HILIC-UPLC with fluorescence detection on a Waters ACQUITY™ UPLC H-Class instrument consisting of a binary solvent manager, sample manager and fluorescence detector under the control of Empower 3 chromatography workstation software (Waters, Milford, MA, USA), as previously described (Stöckmann et al. 2013). The HILIC separations were performed using Waters BEH Glycan column, 150 × 2.1 mm i.d., 1.7 µm BEH particles, using a linear gradient of 70–53% acetonitrile at 0.56 ml/min in 16.5 min for IgG separation and a linear gradient of 70–53% acetonitrile at 0.56 ml/min in 24.81 min. Solvent A was 50 mM formic acid adjusted to pH 4.4 with ammonia solution. Solvent B was acetonitrile. An injection volume of 10 µl sample prepared in 70% v/v acetonitrile was used throughout. Samples were maintained at 5°C prior to injection and the separation temperature was 40°C. The fluorescence detection excitation/emission wavelengths were $\lambda_{ex} = 330$ nm and $\lambda_{em} = 420$ nm, respectively.

Method Validation The recovery of the total IgG is estimated to be 40%. The coefficient of variation for all the 28 IgG *N*-glycan peaks (with peak % areas greater than 1%) was based on quadruplicate assays performed on four different days and was below 10% for all major peaks as published previously (Stöckmann et al. 2013). To assess biological variation, samples were taken from one galactosaemia patient on three separate days. The biological replicate CV for the total G0 peaks was 2%, and this was 3% for G1 and 2% for G2.

The system was calibrated using an external standard of hydrolyzed and 2-AB-labelled glucose oligomers to create a dextran ladder, as described previously (Stöckmann et al. 2013; Royle et al. 2008).

IgG N-Glycan G-Ratios

G-ratios are informative indicators of the level of galactose incorporation into the *N*-glycan structures. The peak % areas of agalactosylated (G0), monogalactosylated (G1) and digalactosylated (G2) structures were determined to provide a quantitative measurement of the incorporation of galactose

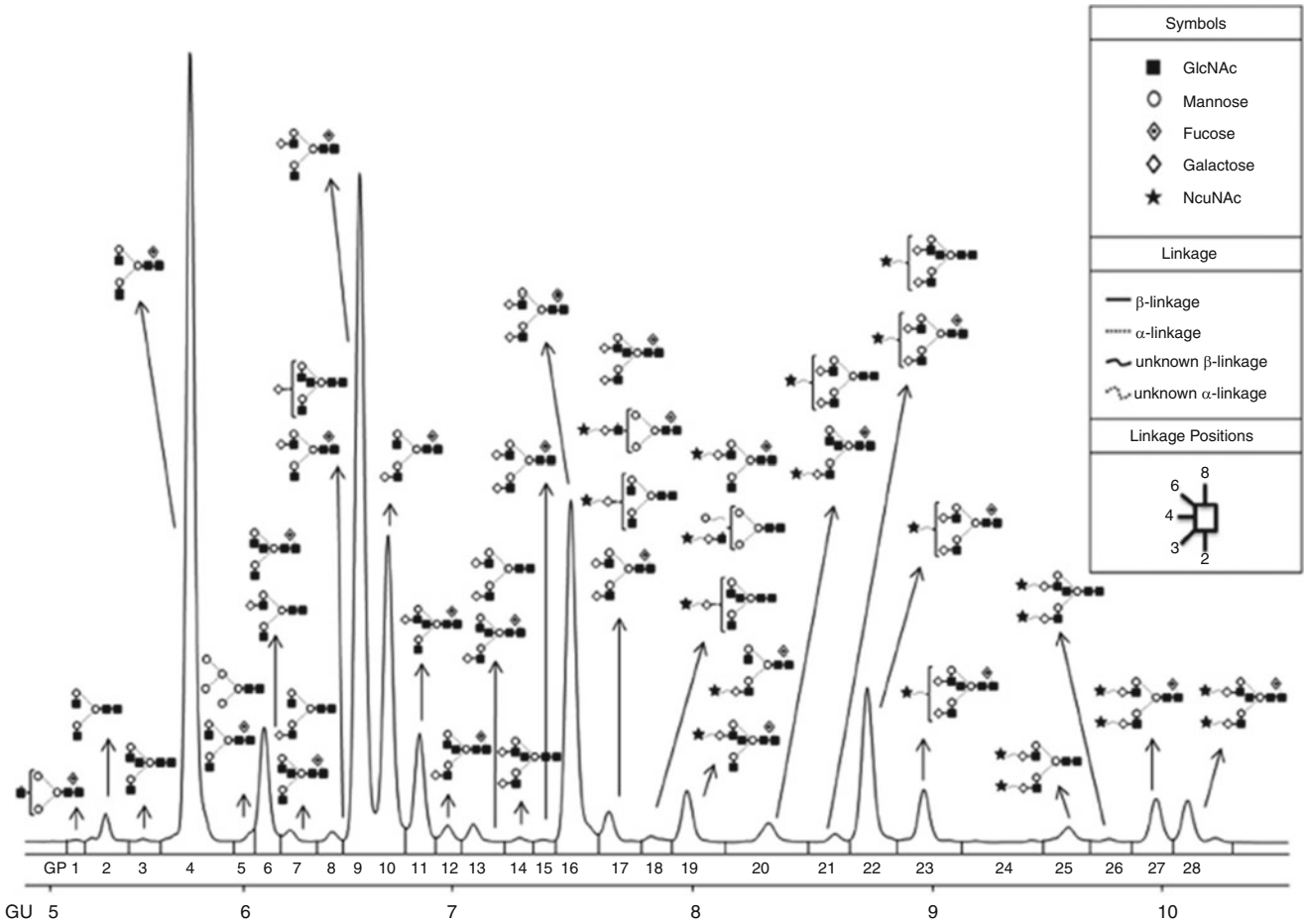

Fig. 1 Representation of released undigested human IgG *N*-glycosylation profile and glycan structures. The linkages and abbreviations used are seen in the boxed inset, and the major structures assigned are based on the structural annotations for IgG described in Stöckmann et al. (2013). *GP* glycan peak number, *GU* glucose units. Reprinted with permission from Stöckmann et al. (2013). Copyright 2013 American Chemical Society

into IgG *N*-glycans as we have previously described (Coss et al. 2012, 2013).

Glycan Feature Statistical Analysis

A nonparametric, Wilcoxon–Mann–Whitney test was used to examine potential differences in the G0/G1, (G0/G1)/G2 and G0/G2 ratios between the galactosaemia cases and controls. The analysis was performed using R software (www.r-project.org) with the R base package. Box plots were constructed using GraphPad Prism.

Oxford Glycan Annotation System

The specific *N*-glycans were annotated according to the Oxford notation system representing *N*-linked glycan composition and structure. The assignment of glycan structures by HILIC-UPLC in serum was performed by comparison with an updated GlycoBase 3.2 (http://glycobase.nibrt.ie/), as well as assignments published (Royle et al. 2008; Stöckmann et al. 2013). Assignment of the IgG glycans in each peak was based on the analysis in Pučić et al. 2011.

Results

The characteristics of the 40 adult galactosaemia study patients for the serum IgG *N*-glycosylation are shown in Table 1. The study group consisted of 32 Irish and 8 Dutch adult galactosaemia patients. All patients have classical galactosaemia, and 36 of the 40 patients are homozygous for the severe *GALT* mutation Q188R. The mean FSIQ of the 32 Irish patients was 81 (range 47–126). The mean FSIQ of the Dutch patients was 71 (range 56–97).

Figure 1 illustrates the peak assignments of the IgG *N*-glycan profile as previously published (Stöckmann et al. 2013).

In Table 2, the G-ratios for galactosaemia patients and controls are shown with means and standard deviations. The differences in G0/G1 and G0/G2 ratios between patients and controls are all statistically significant ($p < 0.001$ and <0.01, respectively), indicating the presence of continuing *N*-glycan processing defects in these galactosaemia patients on dietary galactose restriction.

Table 2 Adult undigested IgG *N*-glycan galactosylation average ratios and SD

Group	*n*	G0/G1	G0/G2
Controls	81	0.65 (± SD 0.14)	0.78 (± SD 0.29)
Galactosaemia	40	0.75 (0.15)	0.95 (0.39)
Irish	32	0.73 (0.14)	0.95 (0.36)
Dutch	8	0.75 (0.18)	0.94 (0.50)
p-value[a, b]		0.0004658	0.007318

[a] Statistical analysis (MANOVA)
[b] Controls vs. total galactosaemia patients

Figure 2 illustrates box–scatter plots of the distribution of G-ratios between patients and controls. As noted in our previous paediatric study, there may be overlap between outlier control and galactosaemia patients (Coss et al. 2013; Knerr et al. 2015). In this context, as previously noted, the test may be best utilised to monitor intervention changes using the patient acting as their own individual control. As with our earlier studies, the adult galactosaemia patients have higher levels of agalactosylated structures relative to the controls (Coss et al. 2012, 2013).

Discussion

The development of informative and accurate biomarkers which reflect the disease pathogenesis is paramount for the management of galactosaemia, in view of the heterogeneity and disappointing clinical outcomes, identifiable in at least 50% of treated individuals.

In our earlier studies, we have proposed that early stage developmental, and later ongoing, disruptions to

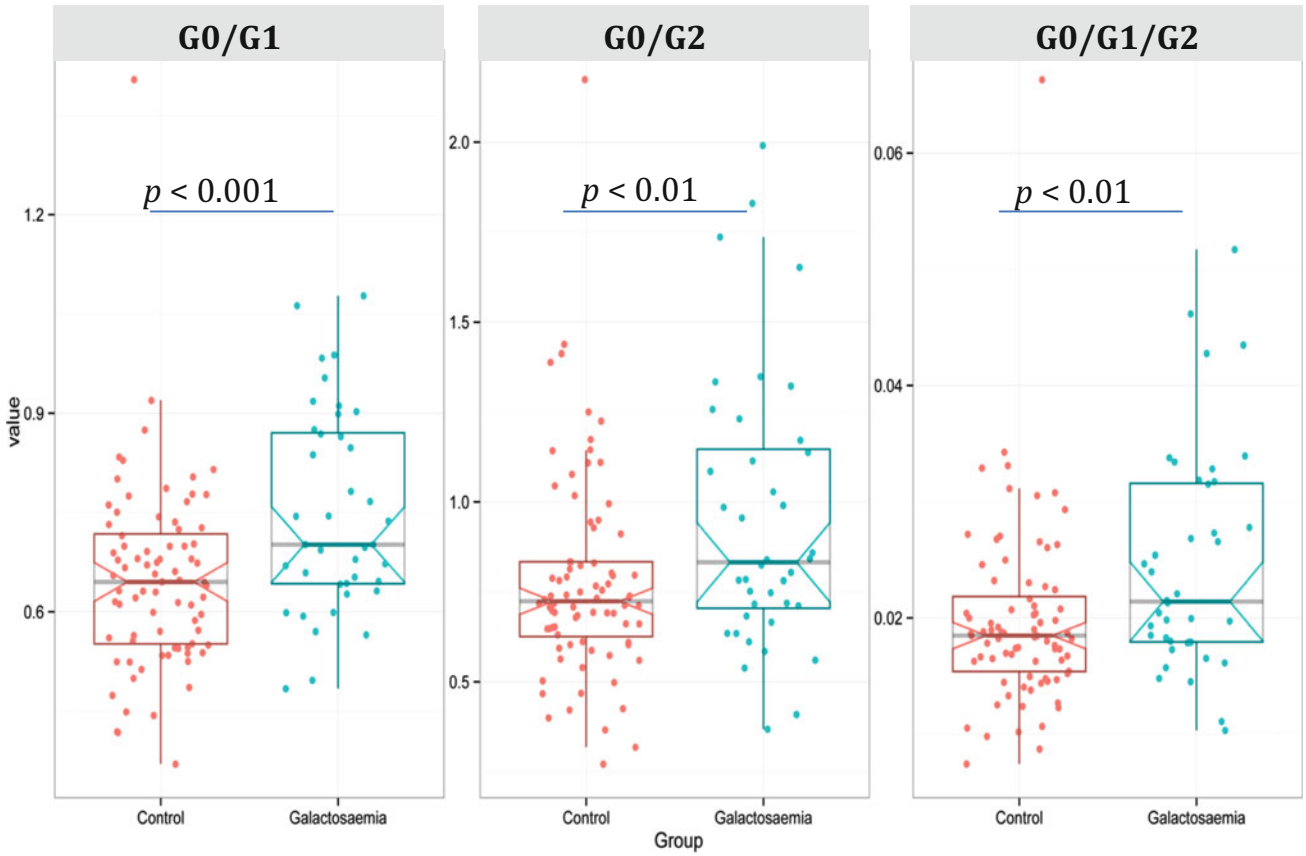

Fig. 2 Box–scatter plots of statistically significant G0/G1, G0/G2 and G0/G1/G2 ratios from adult undigested IgG *N*-glycans between the total galactosaemia group and controls, with respective average G-ratios and SD indicated in Table 2. Data are given in a box–scatter plot to show the spread of the individual values. The diagram is made up of a 'box', which lies between the upper and lower quartiles. The median level divides the 'box' into two. Values for healthy controls are shown in *red* and total galactosaemia patients are shown in *blue*

glycosylation and related gene expression pathways may have a role in the pathophysiology of classical galactosaemia. Perturbations to glycosylation during prenatal galactose intoxication could lead to systemic defects affecting long-term development in patients (Coss et al. 2013, 2014).

We have previously observed the correction of the gross assembly defects in young galactosaemia children following treatment with galactose restriction (Coss et al. 2013). In addition, we have observed improved glycosylation profiles in a number of adults with short-term moderate dietary galactose liberalisation and now recently in children, suggesting the upregulation of accessory glycosylation pathways (Coss et al. 2012; Knerr et al. 2015).

Beyond the untreated neonatal period, analysis of the whole serum or plasma *N*-glycome is largely uninformative in identifying subtle differences in glycosylation between adults with galactosaemia (Liu et al. 2012).

Our automated high-throughput HILIC-UPLC method applied to measure *N*-glycan abnormalities has been applied to the study of IgG *N*-glycan synthesis abnormalities and to the monitoring of a pilot study of moderate dietary relaxation in children with galactosaemia (Coss et al. 2013; Knerr et al. 2015). We now report the improvement of this method, now applied to a larger cohort of adult patients and controls, with the use of a large independent control dataset. Also of note, the G-ratios observed are similar in the Irish and Dutch classical galactosaemia cohorts (Table 2).

In summary, we have now refined the recently improved high-throughput automated HILIC-UPLC methodology of the IgG *N*-glycan galactose ratios, (G0/G1) and (G1/G2) as an indicator of processing defects in galactosaemia. In agreement with our earlier studies, in the current study, we have illustrated that treated adult galactosaemia patients generally have increased agalactosylated (G0) and monogalactosylated (G1) structures, with decreases in certain digalactosylated (G2) structures compared to healthy controls. These reductions would seem to indicate a continued lower percentage of galactose incorporation into serum glycoproteins and continuing *N*-glycan processing defects, in comparison to healthy individuals even after the prenatal, neonatal and childhood periods of intervention.

This further development of the IgG *N*-glycan G-ratios provides a tool to monitor therapeutic interventions and individualised metabolic/dietary control in affected adults with classical galactosaemia. Further studies will study this application in variant galactosaemia.

Acknowledgements Funding for these studies was granted by the Irish Medical Research Charities Group (CFFH/TSCUH)/ Health Research Board (No 2) was supported by the EU FP7 Research Framework Program 'HighGlycan' (Grant Reference No. 278535).

Synopsis

The use of IgG *N*-glycosylation galactose incorporation analysis by HILIC-UPLC analysis can be applied for monitoring of optimum metabolic control for individuals with classical galactosaemia.

Compliance with Ethics Guidelines

Conflict of Interest

The authors, Henning Stockmann, Karen P. Coss, M. Estela Rubio-Gozalbo, Ina Knerr, Maria Fitzgibbon, Ashwini Maratha, James Wilson, Pauline Rudd and Eileen P. Treacy, declare that they have no conflict of interest.

All procedures regarding the galactosaemia patient studies and sampling were followed in accordance with the ethical standards of the responsible committee on human experimentation (institutional and national) and with the Helsinki Declaration of 1975, as revised in 2000. Informed consent was obtained from all patients for being included in the study.

All authors listed above have been involved in the conception or design of this study and in drafting/revising the submitted article. Henning Stockmann and Karen Coss were involved in the direct planning and conduct of the study and experiments. The other authors were involved in interpreting the results, drafting and revising the manuscript.

References

Bosch AM, Bakker HD, Wenniger-Prick LJ, Wanders RJ, Wijburg FA (2004) High tolerance for oral galactose in classical galactosaemia: dietary implications. Arch Dis Child 89:1034–1036

Charlwood J, Clayton P, Keir G, Mian N, Winchester B (1998) Defective galactosylation of serum transferrin in galactosemia. Glycobiology 8:351–357

Coman DJ, Murray DW, Byrne JC, Rudd PM, Bagaglia PM, Doran PD, Treacy EP (2010) Galactosemia, a single gene disorder with epigenetic consequences. Pediatric Res 67:286–292

Coss K, Byrne J, Coman D, Adamczyk B et al (2012) IgG N-glycans as potential biomarkers for determining galactose tolerance in Classical Galactosaemia. Mol Genet Metab 105:212–220

Coss KP, Hawkes CP, Adamczyk B et al (2013) N-glycan abnormalities in children with galactosemia. J Proteome Res 13:385–394

Coss K, Treacy E, Cotter E, Knerr I, Murray D, Shin Y, Doran P (2014) Systemic gene dysregulation in classical Galactosaemia: is there a central mechanism? Mol Genet Metab 113:177–187

Dani N, Broadie K (2012) Glycosylated synaptomatrix regulation of trans-synaptic signalling. Dev Neurobiol 72(1):2–21

Freeze HH (2013) Understanding human glycosylation disorders: biochemistry leads the charge. J Biol Chem 288:6936–6945

Frey PA (1996) The Leloir pathway: a mechanistic imperative for three enzymes to change the stereochemical configuration of a single carbon in galactose. FASEB J 10:461–470

Fridovich-Keil JL, Walter JH (2008) Galactosaemia Chapter 72. The online metabolic and molecular bases of inherited disease, OMMBID. McGraw Hill, New York

Hughes J, Ryan S, Lambert D et al (2009) Outcomes of siblings with classical galactosemia. J Pediatr 154:721–726

Hutchesson AC, Murdoch-Davis C, Green A, Preece MA, Allen J, Holton JB, Rylance G (1999) Biochemical monitoring of treatment for galactosaemia: biological variability in metabolite concentrations. J Inherit Metab Dis 22:139–148

Jumbo-Lucioni P, Garber K, Kiel J et al (2012) Diversity of approaches to classic galactosaemia around the world: a comparison of diagnosis, intervention and outcomes. J Inherit Metab Dis 35(6):1037–1049

Jumbo-Lucioni P, Parkinson W, Broadie K (2014) Altered synaptic architecture and glycosylated synaptomatrix composition in a Drosophila classic galactosemia disease model. Dis Model Mech 7(12):1365–1378

Knerr I, Coss KP, Kratzsch J et al (2015) Effects of temporary low-dose galactose supplements in children aged 5–12 years with Classical Galactosaemia: a pilot study. Pediatr Res. doi:10.1038/pr.2015.107

Krabbi K, Uudelepp ML, Joost K, Zordania R, Ounap K (2011) Long-term complications in Estonian galactosemia patients with a less strict lactose-free diet and metabolic control. Mol Genet Metab 103(3):249–253

Lai K, Langley SD, Khwaja FW, Schmitt EW, Elsas LJ (2003) GALT deficiency causes UDP-hexose deficit in human galactosemic cells. Glycobiology 13:285–294

Liu Y, Xia B, Gleason TJ, Castañeda U, He M, Berry GT, Fridovich-Keil JL (2012) N-and O-linked glycosylation of total plasma glycoproteins in galactosemia. Mol Genet Metab 106:442–454

Ng WG, Xu YK, Kaufman FR, Donnell GN (1989) Deficit of uridine diphosphate galactose in galactosaemia. J Inherit Metab Dis 12: 257–266

Ornstein KS, McGuire EJ, Berry GT, Roth S, Segal S (1992) Abnormal galactosylation of complex carbohydrates in cultured fibroblasts from patients with galactose-1-phosphate uridyltransferase deficiency. Pediatr Res 31:508–511

Petry K, Greinix HT, Nudelman E, Eisen H, Hakomori S, Levy HL, Reichardt JK (1991) Characterization of a novel biochemical abnormality in galactosemia: deficiency of glycolipids containing galactose or N-acetylgalactosamine and accumulation of precursors in brain and lymphocytes. Biochem Med Metab Biol 46: 93

Pučić M, Knežević A, Vidič J et al (2011) High throughput isolation and glycosylation analysis of IgG–variability and heritability of the IgG glycome in three isolated human populations. Mol Cell. Proteomics 10:M111.010090

Quintana E, Navarro-Sastre A, Hernández-Pérez JM et al (2009) Screening for congenital disorders of glycosylation (CDG): transferrin HPLC versus isoelectric focusing (IEF). Clin Biochem 42:408–415

Royle L, Campbell MP, Radcliffe CM, White DM et al (2008) HPLC-based analysis of serum N-glycans on a 96-well plate platform with dedicated database software. Anal Biochem 376:1–12

Slepak TI, Tang M, Slepak VZ, Lai K (2007) Involvement of endoplasmic reticulum stress in a novel Classic Galactosemia model. Mol Genet Metab 92:78–87

Stöckmann H, Adamczyk B, Hayes J, Rudd PM (2013) Automated, high-throughput IgG-antibody glycoprofiling platform. Anal Chem 85: 8841–8849

Sturiale L, Barone R, Fiumara A et al (2005) Hypoglycosylation with increased fucosylation and branching of serum transferrin N-glycans in untreated galactosemia. Glycobiology 15: 1268–1276

JIMD Reports
DOI 10.1007/8904_2015_486

CASE REPORT

Intracranial Pressure Monitoring Demonstrates that Cerebral Edema Is Not Correlated to Hyperammonemia in a Child with Ornithine Transcarbamylase Deficiency

Julie Chantreuil · Géraldine Favrais · Nadine Fakhri · Marine Tardieu · Nicolas Roullet-Renoleau · Thierry Perez · Nadine Travers · Laurent Barantin · Baptiste Morel · Elie Saliba · François Labarthe

Received: 23 March 2015 / Revised: 31 May 2015 / Accepted: 15 July 2015 / Published online: 2 October 2015
© SSIEM and Springer-Verlag Berlin Heidelberg 2015

Abstract *Background*: Ornithine transcarbamylase deficiency (OTCD) is an inborn error of urea cycle resulting in increased plasma levels of ammonia and glutamine and cerebral edema. However, the underlying mechanism of brain cytotoxicity remains controversial. Our objective is to present an unusual acute hyperammonemic crisis suggesting a key role of brain glutamine to mediate ammonia neurotoxicity and the interest of intracerebral pressure (ICP) monitoring to maintain adequate cerebral perfusion pressure and to prevent neurological damages.

Patient: A 6-year-old boy with OTCD was admitted for an acute hyperammonemic encephalopathy following viral infection. At admission, he presented vomiting, confusion, lethargy (Glasgow scale 7/15), and bilateral papilledema, suggesting cerebral edema. Plasma ammonia level was slightly increased (194 μmol/L, rr 25–50 μmol/L), contrasting with the severity of neurological deterioration and with high levels of glutamine in plasma (1,949 μmol/L, rr 335–666 μmol/L) and the brain (10-fold increase on in vivo MR spectroscopy). The patient was placed on neuroprotective treatments and respiratory support.

Main Results: With a hypercaloric protein-free diet and nitrogen scavenger drugs, plasma levels of ammonia and glutamine rapidly decreased without neurological improvement. Continuous ICP monitoring showed repetitive peaks of pressure up to 60 mmHg in the first four days and was helpful to manage neuroprotective treatments. After several days, the patient progressively recovered without cognitive or motor disability.

Conclusion: This case report highlights the discrepancy between the severity of neurological impairment, presumably related to high level of brain glutamine, and plasma levels of ammonia or glutamine in a child with acute hyperammonemic encephalopathy related to OTCD. In this situation, continuous ICP monitoring was helpful to manage neuroprotective treatments and prevent brain damages.

Communicated by: Pascale de Lonlay

Competing interests: None declared

J. Chantreuil · G. Favrais · N. Fakhri · N. Roullet-Renoleau · T. Perez · E. Saliba
CHRU de Tours, Services de Réanimation Pédiatrique et Néonatologie, Tours, France

M. Tardieu · F. Labarthe (✉)
CHRU de Tours, Médecine Pédiatrique, Tours, France
e-mail: labarthe@med.univ-tours.fr

N. Travers
CHRU de Tours, Neurochirurgie Pédiatrique, Tours, France

L. Barantin · B. Morel
CHRU de Tours, Radiopédiatrie, Tours, France

G. Favrais · L. Barantin · E. Saliba
Inserm U930, Université François-Rabelais de Tours, PRES Centre-Val de Loire Université, Tours, France

F. Labarthe
Inserm U1069, Université François-Rabelais de Tours, PRES Centre-Val de Loire Université, Tours, France

Abbreviations

CPP	Cerebral perfusion pressure
ICP	Intracranial pressure
OTCD	Ornithine transcarbamylase deficiency
rr	Reference range

Introduction

Ornithine transcarbamylase deficiency (OTCD, MIM#311250) is an X-linked inborn error of metabolism of the urea cycle,

which converts ornithine and carbamoyl phosphate into citrulline in the hepatic mitochondria (Lichter-Konecki 2008). Enzyme dysfunction results in an increase of plasma levels of ammonia and its metabolites, glutamine and glutamate. Hyperammonemia may cause astrocyte swelling, cytotoxic edema, and increased intracranial pressure (ICP) with a high risk of irreversible damage to the brain (Albrecht et al. 2010; Braissant et al. 2013). In fact, cerebral ammonia is metabolized to glutamine by astrocytes, a process that is the principal means of ammonia detoxification into the brain. Glutamine is an essential precursor of the neuronal synthesis of the neurotransmitters glutamate and GABA, as well as an important energy metabolite in the brain (Albrecht et al. 2010). However, brain glutamine synthesis in excess has been recently reported to mediate key aspects of ammonia neurotoxicity (Albrecht et al. 2010; Braissant et al. 2013). Increased brain glutamine levels have a huge toxicity for astrocytes and other cerebral cells, inducing cellular swelling, cerebral edema, and neuronal cell death due to increased excitotoxicity (Pichili et al. 2007; Lichter-Konecki 2008). In contrast, the inhibition of glutamine synthesis by methionine sulfoximine reverses a spectrum of manifestations of ammonia toxicity, including brain edema and increased intracranial pressure (see Ref (Albrecht et al. 2010) for review). Therefore, brain glutamine metabolism may be viewed as the principal mediator of ammonia neurotoxicity (Albrecht et al. 2010; Braissant et al. 2013). Classically in children with urea cycle disorders (UCD), hyperammonemic encephalopathy is associated with severe hyperammonemia, and its management is based on the follow-up of plasma ammonia level (Haberle et al. 2012). However, ammonia level is not a reliable tool to predict raised ICP, and severe neurological crises have been reported in some patients with only mild increase in plasma ammonia level, suggesting that brain glutamine level will be a better marker of cerebral dysfunction than blood ammonia or glutamine levels (Kojic et al. 2005; Mak et al. 2007; Gropman et al. 2008). Brain glutamine level may be estimated by analysis of cerebrospinal fluid obtained by lumbar puncture or by brain magnetic resonance spectroscopy. These two methods can be performed punctually but do not allow a follow-up of brain glutamine level during acute crises. Therefore, monitoring ICP may be helpful to manage acute hyperammonemic encephalopathy and to prevent neurological damages (Wendell et al. 2010). We report the case of a 6-year-old OTCD boy who presented a severe and acute hyperammonemic encephalopathy that was managed with ICP monitoring to prevent decline of cerebral perfusion pressure (CPP) and neurological damages.

Case Report

A 6-year-old boy with OTCD was admitted to pediatric intensive care unit for an acute hyperammonemic encephalopathy following viral infection. He had a familial history of severe neonatal OTCD confirmed by genotyping (mutation C584G in the exon 6). Despite prenatal diagnosis of OTCD and very low protein diet supplemented with essential amino acid mixture, citrulline, L-arginine, and sodium benzoate, he experienced previously more than ten acute episodes of hyperammonemia (maximal ammonia level between 70 and 170 μmol/L, reference range rr 25–50 μmol/L) rapidly resolving with stopping protein intake and nitrogen scavenger drugs and never requiring admission in intensive care unit. Apart from these acute crises, his metabolic status was relatively acceptable, with normal ammonemia and slightly increased plasma levels of glutamine (827 ± 143 μmol/L, rr 335–666 μmol/L), alanine (659 ± 268 μmol/L, rr 134–502 μmol/L), glycine (350 ± 126 μmol/L, rr 149–301 μmol/L), and citrulline (47 ± 54 μmol/L, rr 16–40 μmol/L) during the two previous years. For this new acute episode, this boy was asymptomatic the day before, presenting only a rhinitis without fever or neurological symptom. Upon waking, he remained sleepy and presented three hours later at admission vomiting, confusion, and lethargy with a Glasgow scale 7/15 and bilateral papilledema on fundus examination, suggesting cerebral edema. Biochemical investigations revealed compensated metabolic acidosis (pH 7.39, Pco_2 29 mmHg [3.9 kPa], HCO_3 17 mmol/L [2.3 kPa]) with hyperlactatemia (4.9 mmol/L, rr <2.2 mmol/L). Initial plasma levels of ammonia (194 μmol/L, rr 25–50 μmol/L) and glutamine (1,949 μmol/L, rr 335–666 μmol/L) were increased, contrasting with normal values of transaminases, gamma-glutamyl transferase, bilirubin, and prothrombin time test (80% initially, controlled to 25% few hours later, rr 70–100%). Other plasma levels of amino acids related to urea cycle were in normal range (alanine 295 μmol/L, glycine 297 μmol/L) except those of citrulline that was near undetectable (3 μmol/L). The electroencephalogram showed slow delta waves at one Hertz and reactivity to stimulation without seizures. Brain MRI revealed small ventricles and a slightly restricted diffusion in the occipital lobes suggesting cerebral edema with a huge peak of glutamine on MR spectroscopy performed at the level of the occipital white matter, whereas glutamate level remained normal (Fig. 1a). It was concluded to a severe acute metabolic crisis with hyperammonemia and cerebral edema.

Following initial evaluation, he was intubated, ventilated, and sedated with midazolam (50 μg/kg/h) and sufentanil

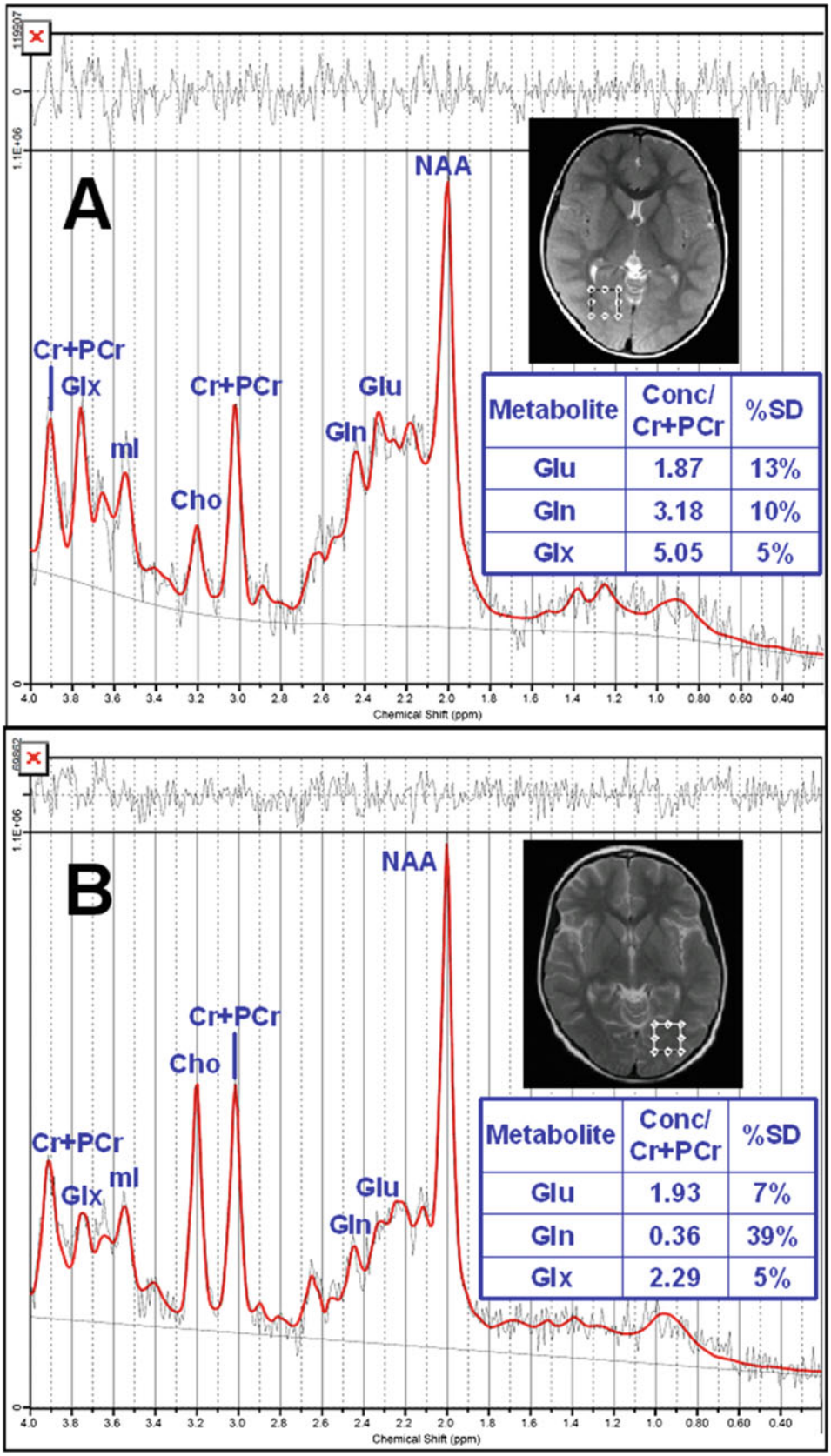

Fig. 1 MR spectroscopy during and after an acute episode of hyperammonemic encephalopathy in a 6-year-old boy with ornithine transcarbamylase deficiency. Brain glutamine (Gln) and glutamate (Glu) levels were estimated by in vivo MR spectroscopy (1.5T)

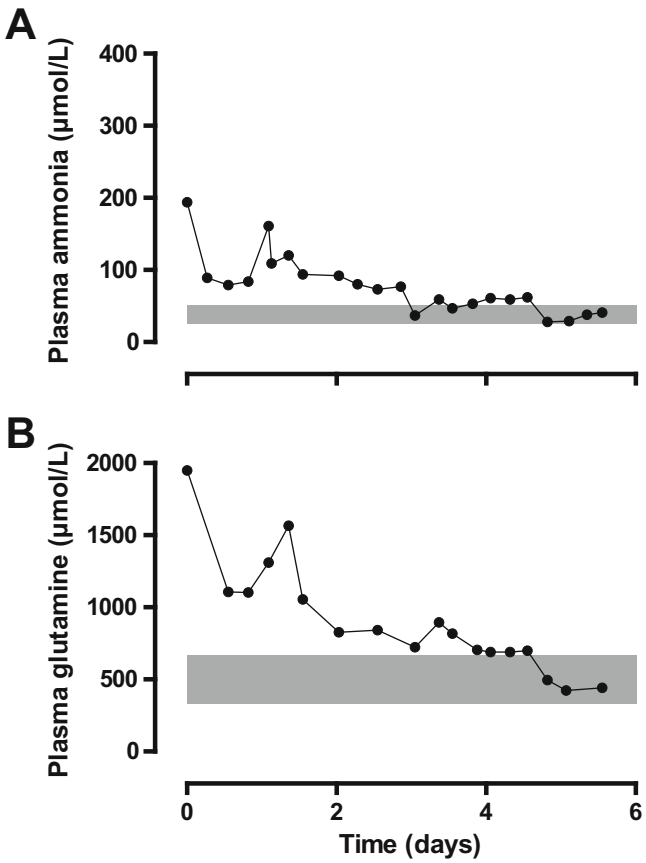

Fig. 2 Plasma ammonia (**a**) and glutamine (**b**) levels during an acute episode of hyperammonemic encephalopathy in a 6-year-old boy with ornithine transcarbamylase deficiency. Normal range is in *gray*

(0.2 µg/kg/h) to protect upper airways and to manage cerebral edema and intracranial hypertension. Hypercaloric protein-free diet was started by total parenteral nutrition, and intravenous treatment by sodium phenyl acetate and sodium benzoate (Ammonul®) was initiated 3 h after admission (loading dose infusion of 250 mg/kg administered over 90 min, followed by an equivalent maintenance dose infusion administered over 24 h). With these treatments, plasma levels of ammonia and glutamine progressively decreased to normal range since the fifth day (Fig. 2a, b). Proteins were reintroduced in the diet from the third day (0.2 g/kg/day) and gradually increased up to 0.8 g/kg/day at day 6, with a progressive switch from parenteral to continuous enteral nutrition. Intravenously treatment with sodium phenyl acetate and sodium benzoate was switched to enteral sodium phenylbutyrate (250 mg/kg/day in four doses) and intravenous sodium benzoate (continuous infusion of 250 mg/kg/day) from day 4. Due to neurological deterioration, an ICP monitoring (Codman® MicroSensor basic kit, Johnson & Johnson Professional Inc, MA, USA) was set in the first 24 h after correction of coagulation disorders. The monitoring of ICP showed repetitive peaks of pressure up to 60 mmHg in the first four days and was helpful to manage and adapt the neuroprotective treatments in the aim to maintain an adequate CPP (Fig. 3). Continuous neuroprotective treatments with midazolam and sufentanil were rapidly increased up to 1,200 µg/kg/h and 0.5 µg/kg/h, respectively, associated with bolus of both treatments and atracurium besylate (0.5 mg/kg/dose) at the time of ICP peaks. Vasoactive support (norepinephrine up to 0.12 µg/kg/min) was associated from day 2 to maintain arterial pressure and CPP. The frequency of ICP peaks decreased after few days, boluses of neuroprotective treatments were progressively spaced, and continuous treatments with midazolam, sufentanil, and norepinephrine were discontinued after eight days. Due to favorable outcome, ventilation support can be

Fig. 1 (continued) performed at the level of the occipital white matter during (**a**, day 1) and after (**b**, day 16) an acute episode of hyperammonemic encephalopathy. Data were analyzed using LCModel, 6.3-1H version, and concentrations were expressed related to Cr+PCr (standard deviation expressed in percentage, %SD). Cho, choline; Cr+PCr, creatine + phosphocreatine; Glx, Glu+Gln; mI, myoinositol; NAA, *n*-acetyl-aspartic acid

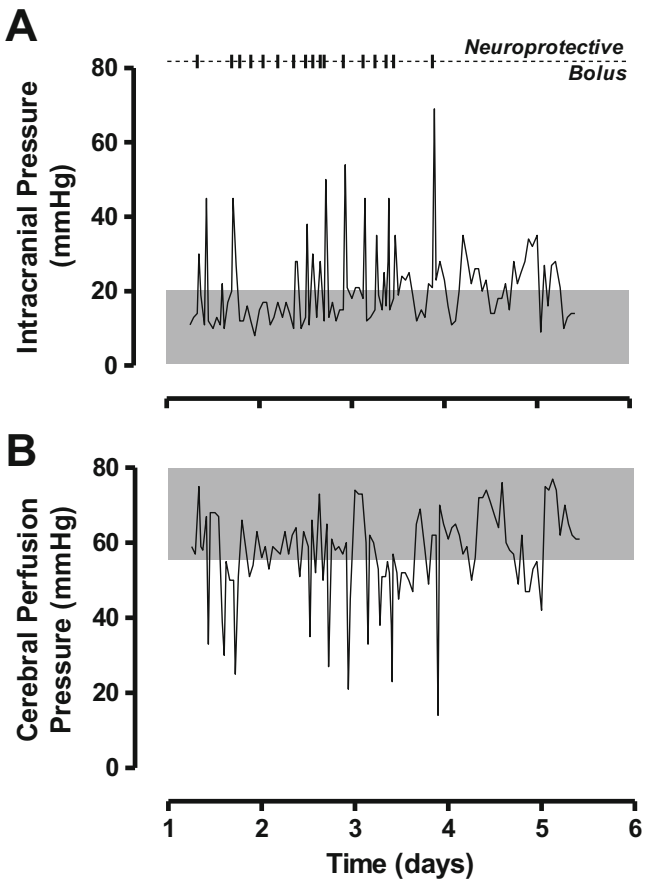

Fig. 3 Evolution of intracranial pressure and cerebral perfusion pressure during an acute episode of hyperammonemic encephalopathy in a 6-year-old boy with ornithine transcarbamylase deficiency. Intracranial pressure (**a**) was monitored invasively and cerebral perfusion pressure (**b**) was calculated from the difference between mean arterial pressure and intracranial pressure. Normal range is in *gray*. Bolus of neuroprotective treatments (midazolam, sufentanil, and atracurium besylate) are represented as *bars* at the top of the graph

stopped on day 8 and the boy was discharged from intensive care unit at day 12 without apparent severe damage.

He progressively recovered and a second brain MRI realized four days after discharge was considered as normal, with a reduced peak of glutamine on MR spectroscopy (Fig. 1b). At the same time, plasma levels of ammonia and glutamine were normal (21 and 534 μmol/L, respectively). A clinical evaluation 6 months later found no cognitive or motor disability.

Discussion

Acute hyperammonemic encephalopathy is a medical emergency for which the aim of treatment is to prevent irreversible brain damage by timely action (Haberle et al. 2012). This case report highlights the key role of brain glutamine to mediate ammonia neurotoxicity and the interest of monitoring ICP to maintain adequate CPP and to prevent neurological damages. The first hallmark of this case report is the discrepancy between the level of plasma ammonia, only moderately increased, and the severity of neurological impairment. This boy has previously experienced recurrent episodes of acute hyperammonemic crises but without the same degree of neurologic impairment. The absence of intoxication symptom the day before suggested a very acute and sudden crisis. Lactic acidosis at admission is unusual in OTCD crises but may be explained in the present case by either an initial vasomotor instability related to brain edema or by transient ischemic brain damage, in accordance with the severity of this episode. The presence of a coma at admission was reported to be associated with a lower survival rate, particularly in OTCD patients (Enns et al. 2007), and neurological symptoms persisted even after decreasing ammonemia levels under 100 μmol/L. In UCD, the function of excretion of nitrogen as urea is impaired and leads to accumulate ammonia and glutamine, two toxic molecules for the brain. The severity of neurologic impairment and survival are classically related to age and peak ammonia level (Enns et al. 2007). Acute hyperammonemic crises in the neonatal period are typically most severe, with a peak ammonia level >500 μmol/L. In older children, peak

ammonia levels are generally lower but remains >200 μmol/L in most of the patients during acute crises (Enns et al. 2007). However, severe neurological crises have been reported even in the absence of severe hyperammonemia (Kojic et al. 2005; Mak et al. 2007; Gropman et al. 2008). This apparent discrepancy between neurological impairment and plasma ammonia level may be explained in part by the mechanisms of hyperammonemia neurotoxicity. Following its uptake by the brain, ammonia is mainly metabolized to glutamine by astrocytes, leading to high levels of cerebral glutamine that may be viewed as the principal mediator of ammonia neurotoxicity (Albrecht et al. 2010; Braissant et al. 2013). Glutamine is osmotically active and its concentration increase leads to cytotoxic edema by astrocyte swelling possibly related to glutamine transport into mitochondria, thereby increasing ammonia synthesis from glutamine into mitochondria, inducing apoptosis and producing reactive oxygen species. A significant proportion of newly synthesized glutamine will also exit astrocytes and enter neurons to give rise to glutamate into the intercellular space which is excitotoxic, essentially through NMDA receptor activation, altering neurotransmission and NO synthesis and inducing neuronal cell death. Finally, glutamine efflux across the blood-brain barrier would favor the removal of brain glutamine and decrease its toxic effect. Brain concentrations of ammonia and glutamine are not strictly related to plasma levels, possibly due to variations of brain ammonia uptake and glutamine synthesis and transport (Pichili et al. 2007; Lichter-Konecki 2008; Zwirner et al. 2010). In our case, brain glutamine estimated by MR spectroscopy appeared to be largely increased (about tenfold, compared to 2 weeks later), contrasting with the moderate increase of ammonemia, then possibly explaining the discrepancy between neurological impairment and plasma concentrations of ammonia.

Classically, the management of hyperammonemic encephalopathy is based on the follow-up of plasma ammonia level (Haberle et al. 2012). In fact, increased plasma levels of ammonia and glutamine are indicators of the increased nitrogen load of the organism and must be closely monitored for optimal treatment (Enns et al. 2007). However, their plasma concentrations are not a predictor of their brain concentrations and are not a reliable guide to manage cerebral edema (Haberle et al. 2012). The clinical situation of the patient should guide clinical decisions and the rather low ammonia levels should never prevent from aggressive intervention in such comatose patient. Clearly, there is a need to identify predictors of cerebral injury. As in our case, brain glutamine level can be appreciated by MR spectroscopy, a simple and reliable method to assess in vivo the cerebral concentration of several brain metabolites. The acquisition of spectroscopy measurements takes only about ten additional minutes during a conventional structural MRI. This gives a first spectrum that can estimate concentration of the different metabolites. A more precise estimation of each metabolite concentration needs to model the in vivo spectrum as a linear combination of adequately line-broadened individual metabolite spectra. This can be achieved using an analysis program such as "LCModel," but this step needs most of the time the assistance of a specialist. The use and the accuracy of this method have been clearly validated to evaluate brain metabolism in OTCD patients (see Gropman et al. 2008) for details), but this investigation cannot be regularly repeated (Connelly et al. 1993). In contrast, continuous ICP monitoring was very useful to detect ICP peaks and to treat them immediately, in the aim to maintain adequate CPP and to prevent cerebral damages. High doses of neuroprotective therapies were used because of the recurrence of ICP peaks higher than 40 mmHg and were associated with treatment bolus at the time of ICP peaks (Rabinstein 2010). In the case of persistent intracranial hypertension refractory to maximal medical management, the next therapeutic step would have been to propose a decompressive craniectomy (Wendell et al. 2010). An associated hypothermia protocol has also been proposed in some cases. In contrast, ventricular drainage is the treatment of choice when intracranial hypertension is due to hydrocephaly; it has also been proposed to treat refractory cerebral edema after traumatic brain injury, but its use is not classical for cytotoxic cerebral edema, as occurred during hyperammonemia. Continuous ICP monitoring was also helpful to evaluate improvement of cerebral hypertension and to decide time to discontinue neuroprotective therapy. The use of ICP monitoring has not been frequently reported in comatose patients related to urea cycle disorders, excepted in a recent adult case report (Wendell et al. 2010), but its utilization is validated in other pediatric conditions as traumatic brain injury (Exo et al. 2011). Treatment of cerebral edema is more effective when it is based on direct monitoring of ICP, with evidence of improved outcomes (Barlow and Minns 1999). However, coagulopathy associated with acute liver failure is often considered a contraindication for invasive monitoring of ICP due to risk for intracranial bleeding (Vaquero et al. 2005). Correction of coagulopathy disorders prior to ICP monitor placement may decrease rate of complications (Kamat et al. 2012).

Since the main mechanism for brain toxicity seems to be high intracerebral levels of glutamine rather than hyperammonemia itself, the aims of the treatment would be to decrease plasma levels of ammonia, the precursor of glutamine synthesis into the brain, and of plasma glutamine to favor removal of brain glutamine. In addition to symptomatic and nutritional therapies, the use of nitrogen scavenger drugs is also recommended. Intravenous treatments with sodium phenyl acetate and sodium benzoate are the mainstay drugs

for bypassing the urea cycle, by conjugation of benzoate with glycine to generate hippurate or of phenyl acetate with glutamine to generate phenylacetylglutamine, both conjugates being excreted in the urine. Their use without delay results in survival in the majority of patients (Enns et al. 2007). Extracorporeal detoxification, most of the time by continuous venovenous hemodiafiltration, can also be associated in severe hyperammonemic crises. Its use is classically indicated for children who have ammonia levels upper than 500 μmol/L or if there has been an inadequate response to initial medical treatment (Haberle et al. 2012). However, its utilization for children requires a solid expertise in the field of dialysis therapy to avoid technical problems and hypotension that should be deleterious in the context of cerebral edema (Picca et al. 2008). Furthermore, continuous hemodiafiltration is not really efficient to detoxify glutamine with plasma concentration remaining high, in contrast to the effects on ammonia level (Chen et al. 2007).

To summarize, this case report highlights the absence of correlation between the severity of neurological impairment and plasma levels of nitrogen metabolites in a child with acute decompensation of urea cycle disorder. In this situation, invasive ICP monitoring appeared to be feasible and very helpful to manage hyperammonemic encephalopathy and neuroprotective treatments, in the aim to maintain adequate CPP and to prevent brain injury. Nitrogen scavenger drugs were efficient to decrease plasma levels of ammonia and glutamine, without resorting to hemodiafiltration.

Conflicts of Interest

The authors declare no disclosure.

Take-Home Message

This case report highlights the key role of brain glutamine to mediate ammonia neurotoxicity in urea cycle disorders and the interest of monitoring intracranial pressure to maintain adequate cerebral perfusion pressure and to prevent neurological damages.

Compliance with Ethics Guidelines

All the authors declare no conflict of interest.

All procedures followed were in accordance with the ethical standards of the responsible committee on human experimentation (institutional and national) and with the Helsinki Declaration of 1975, as revised in 2000. Informed consent was obtained from all patients for being included in the study.

The following are the details of the contributions of individual authors: JC, GF, NF, NRR, TP, and ES for patient management in ICU; MT and FL for metabolic management; NT for surgical placement of intracranial pressure monitoring; and LB and BM for MRI analyses. JC and FL wrote the paper. All coauthors have read the manuscript and approved its submission to the JIMD Reports.

References

Albrecht J, Zielinska M, Norenberg MD (2010) Glutamine as a mediator of ammonia neurotoxicity: a critical appraisal. Biochem Pharmacol 80:1303–1308

Barlow KM, Minns RA (1999) The relation between intracranial pressure and outcome in non-accidental head injury. Dev Med Child Neurol 41:220–225

Braissant O, McLin VA, Cudalbu C (2013) Ammonia toxicity to the brain. J Inherit Metab Dis 36:595–612

Chen CY, Tsai TC, Lee WJ, Chen HC (2007) Aminograms during continuous hemodiafiltration in the treatment of hyperammonemia due to ornithine transcarbamylase deficiency. Ren Fail 29: 661–665

Connelly A, Cross JH, Gadian DG, Hunter JV, Kirkham FJ, Leonard JV (1993) Magnetic resonance spectroscopy shows increased brain glutamine in ornithine carbamoyl transferase deficiency. Pediatr Res 33:77–81

Enns GM, Berry SA, Berry GT, Rhead WJ, Brusilow SW, Hamosh A (2007) Survival after treatment with phenylacetate and benzoate for urea-cycle disorders. N Engl J Med 356:2282–2292

Exo J, Kochanek PM, Adelson PD et al (2011) Intracranial pressure-monitoring systems in children with traumatic brain injury: combining therapeutic and diagnostic tools. Pediatr Crit Care Med 12:560–565

Gropman AL, Fricke ST, Seltzer RR et al (2008) 1H MRS identifies symptomatic and asymptomatic subjects with partial ornithine transcarbamylase deficiency. Mol Genet Metab 95:21–30

Haberle J, Boddaert N, Burlina A et al (2012) Suggested guidelines for the diagnosis and management of urea cycle disorders. Orphanet J Rare Dis 7:32

Kamat P, Kunde S, Vos M et al (2012) Invasive intracranial pressure monitoring is a useful adjunct in the management of severe hepatic encephalopathy associated with pediatric acute liver failure. Pediatr Crit Care Med 13:e33–e38

Kojic J, Robertson PL, Quint DJ, Martin DM, Pang Y, Sundgren PC (2005) Brain glutamine by MRS in a patient with urea cycle disorder and coma. Pediatr Neurol 32:143–146

Lichter-Konecki U (2008) Profiling of astrocyte properties in the hyperammonaemic brain: shedding new light on the pathophysiology of the brain damage in hyperammonaemia. J Inherit Metab Dis 31:492–502

Mak CM, Siu TS, Lam CW et al (2007) Complete recovery from acute encephalopathy of late-onset ornithine transcarbamylase deficiency in a 3-year-old boy. J Inherit Metab Dis 30:981

Picca S, Bartuli A, Dionisi-Vici C (2008) Medical management and dialysis therapy for the infant with an inborn error of metabolism. Semin Nephrol 28:477–480

Pichili VB, Rao KV, Jayakumar AR, Norenberg MD (2007) Inhibition of glutamine transport into mitochondria protects astrocytes from ammonia toxicity. Glia 55:801–809

Rabinstein AA (2010) Treatment of brain edema in acute liver failure. Curr Treat Options Neurol 12:129–141

Vaquero J, Fontana RJ, Larson AM et al (2005) Complications and use of intracranial pressure monitoring in patients with acute liver failure and severe encephalopathy. Liver Transpl 11:1581–1589

Wendell LC, Khan A, Raser J et al (2010) Successful management of refractory intracranial hypertension from acute hyperammonemic encephalopathy in a woman with ornithine transcarbamylase deficiency. Neurocrit Care 13:113–117

Zwirner K, Thiel C, Thiel K, Morgalla MH, Konigsrainer A, Schenk M (2010) Extracellular brain ammonia levels in association with arterial ammonia, intracranial pressure and the use of albumin dialysis devices in pigs with acute liver failure. Metab Brain Dis 25:407–412

JIMD Reports
DOI 10.1007/8904_2015_468

RESEARCH REPORT

No Evidence for Association of *SCO2* Heterozygosity with High-Grade Myopia or Other Diseases with Possible Mitochondrial Dysfunction

Dorota Piekutowska-Abramczuk · Beata Kocyła-Karczmarewicz · Maja Małkowska · Sylwia Łuczak · Katarzyna Iwanicka-Pronicka · Stephanie Siegmund · Hua Yang · Quan Wen · Quan V. Hoang · Ronald H. Silverman · Paweł Kowalski · Olga Szczypińska · Kamila Czornak · Janusz Zimowski · Rafał Płoski · Jacek Pilch · Elżbieta Ciara · Jacek Zaremba · Małgorzata Krajewska-Walasek · Eric A. Schon · Ewa Pronicka

Received: 23 March 2015 / Revised: 14 May 2015 / Accepted: 26 May 2015 / Published online: 2 October 2015
© SSIEM and Springer-Verlag Berlin Heidelberg 2015

Abstract *SCO2* mutations cause recessively inherited cytochrome *c* oxidase deficiency. Recently Tran-Viet et al. proposed that heterozygosity for pathogenic *SCO2* variants, including the common E140K variant, causes high-grade myopia. To investigate the association of *SCO2* mutations with myopia, ophthalmic examinations were performed on 35 E140K carriers, one homozygous infant, and on a mouse model of Sco2 deficiency. Additionally, a screen for other putative effects of *SCO2* heterozygosity was carried out by comparing the prevalence of the common E140K variant in a population of patients with undiagnosed diseases compatible with *SCO2*-related pathogenesis to that in a general population sample. High-grade myopia was not identified in any of the studied individuals. Of the carriers, 17 were emmetropic, and 18 possessed refractive errors. Additionally, no significant axial elongation indicative of high-grade myopia was found in mice carrying E129K (corresponding to E140K in humans) knock-in mutations. The prevalence of E140K carriers in the symptomatic cohort was evaluated as 1:103 (CI: 0.44–2.09) and did not differ significantly from the population prevalence (1:147, CI: 0.45–1.04).

Our study demonstrates that heterozygosity for pathogenic *SCO2* variants is not associated with high-grade myopia in either human patients or in mice.

Communicated by: Verena Peters

Competing interests: None declared

D. Piekutowska-Abramczuk · M. Małkowska · S. Łuczak · K. Iwanicka-Pronicka · P. Kowalski · O. Szczypińska · K. Czornak · E. Ciara · M. Krajewska-Walasek · E. Pronicka (✉)
Department of Medical Genetics, The Children's Memorial Health Institute, 04-730 Warsaw, Poland
e-mail: e.pronicka@czd.pl

B. Kocyła-Karczmarewicz
Department of Ophthalmology, The Children's Memorial Health Institute, 04-730 Warsaw, Poland

S. Siegmund · H. Yang · E.A. Schon
Department of Neurology, Columbia University Medical Center, New York, NY 10032, USA

Q. Wen · Q.V. Hoang · R.H. Silverman
Department of Ophthalmology, Columbia University Medical Center, New York, NY 10032, USA

J. Zimowski · J. Zaremba
Department of Genetics, Institute of Psychiatry and Neurology, 02-957 Warsaw, Poland

R. Płoski
Department of Medical Genetics, Medical University of Warsaw, 02-106 Warsaw, Poland

J. Pilch
Department of Child Neurology, Medical University of Silesia, 0-055 Katowice, Poland

E.A. Schon
Department of Genetics and Development, Columbia University Medical Center, New York, NY 10032, USA

E. Pronicka
Department of Pediatrics, Nutrition and Metabolic Diseases, The Children's Memorial Health Institute, 04-730 Warsaw, Poland

Introduction

Pathogenic mutations in *SCO2* (RefSeq: NM_005138.2; NP_005129.2) are a frequent cause of cytochrome *c* oxidase deficiency, with symptoms including neonatal encephalocardiomyopathy and mortality by three months of life (OMIM 604377). The typical form of the disease is associated with compound heterozygosity, with at least one allele expressing the common c.418G>A (p.E140K) variant (Pronicka et al. 2013).

When homozygous, E140K presents with delayed onset and death by the age of ~9 months. Hypotonia generally precedes onset, and up to 70% of cases are screened for *SMN1/NAIP* deletion prior to detection of Sco2 mutations, causing delay in diagnosis (Pronicki et al. 2010).

Recently, Tran-Viet et al. (2013) proposed that heterozygous *SCO2* mutations are not phenotypically neutral but cause high-grade myopia. They identified four mutations in *SCO2* from unrelated high-myopic individuals. Additionally, using a mouse model of lens-induced myopia, they provided evidence for *SCO2* expression in the retina, which is downregulated in myopic mouse eyes.

The aim of our study was to verify the findings of Tran-Viet et al., by investigating Sco2 mutations in both patients and a mouse model. We compared the incidence of ophthalmologic phenotypes in a group of families with the E140K variant and undiagnosed disorders compatible with *SCO2* deficiency, to the incidence in the general population. Additionally, we investigated the putative ophthalmologic phenotype in mice carrying a heterozygous *Sco2* E129K mutation (the homolog of the human E140K mutation) (KI) and/or a knockout allele (KO) (Yang et al. 2010). Previous characterization of this mouse model of Sco2 deficiency revealed that heterozygous KI/WT, homozygous KI/KI, and compound heterozygous KI/KO mice were viable but had muscle weakness and respiratory chain deficiencies in multiple tissues (most prominently in the KI/KO mice) (Brosel et al. 2010; Yang et al. 2010); however, no ophthalmologic analysis had been performed. High-grade myopia is associated with globe axial elongation sufficient to cause a refractive distortion of at least −6.0 diopters, and the level of myopia in mouse models has previously been assessed by measuring globe axial length (Park et al. 2012).

Materials and Methods

Ophthalmic Examination of Patients

Using our database of 34 *SCO2*-deficient families (Pronicka et al. 2013), the confirmed/obligate carriers were polled for their results of recent ophthalmic examinations. Thirty-five subjects responded, representing six different pathogenic *SCO2* variants. Individual family members (Family 16, Table 1) and one homozygous patient were reexamined in the Children's Memorial Health Institute (CMHI). The refraction was expressed as spherical equivalent (SE) calculated as sphere plus half of the cylinder. The total refractions in children were measured after cycloplegia.

Screening of the Symptomatic and Population Cohorts

DNA samples from 626 patients with diseases of unknown cause (symptomatic cohort) were next screened for the E140K variant allele, in order to identify alternative symptomatic conditions associated with heterozygosity of this Sco2 mutation. The material consisted of (1) 468 blood samples negative for the *SMN1/NAIP* homozygous deletion, selected from 932 cases referred to the Institute of Psychiatry and Neurology (Warsaw, Poland) for early SMA screening in the 1998–2010 time period, and (2) 158 dry blood spots of the patients with increased lactate excretion who died undiagnosed. These samples were sent to the CMHI for selective metabolic screening in the 2000–2013 time period. Probing for the E140K variant was part of an ongoing diagnostic study of suspected mitochondrial disorders, which also included the search for mtDNA deletions and common pathogenic SNV in mtDNA, *SURF1*, *SCO2*, and *POLG*. The material for analysis in the general population consisted of 3,080 dried blood spots collected for newborn screening for phenylketonuria in the 2002–2006 time period. Written informed consent was obtained from the parents or guardians of investigated children, and the study was approved by the Bioethical Commission of CMHI.

Genotyping for the E140K variant was performed by allele-specific TaqMan assay (Life Technologies). In all cases, a positive result was confirmed by Sanger sequencing with BigDye terminators (Applied Biosystems). Confidence intervals (CI) were calculated as 95% CI according to Wilson (1927). Whole exome sequencing (WES) was performed using HiSeq 1500 (Illumina) at the Warsaw Medical University as described previously (Płoski et al. 2014).

Generation and Animal Care of Sco2-Deficient Mice

Two mouse models of Sco2 deficiency generated as described previously (Yang et al. 2010), an E129K mutation in *Sco2* (KI) and a knockout allele (KO), were used in this study. Experiments were performed by mating KI/KI and KI/+ mice with KO/+ heterozygotes and then comparing KI/+, KI/KI, and KI/KO mice with wild-type littermate control mice. All mouse experiments were performed according to a protocol approved by the

Table 1 Refraction in 36 individuals studied

Individual/family number	Age (years)	Mutation	Right eye refraction	Left eye refraction
Confirmed or obligatory carriers				
f/3	43	[E140K]	E	E
m/3	42	[E140K]	+0.75	+0.5
m/5	44	[E140K]	E	E
f/5	43	[E140K]	−1.0	E
f/9	36	[E140K]	E	E
m/9	35	E140K	+1.25	+0.75
m/12	26	[E140K]	E	E
f/12	28	[E140K]	E	E
m/13	41	E140K	−0.5	−0.75
f/13	42	E140K	−1.0	−0.75
f/14	34	E140K	−1.25	−0.75
m/14	30	E140K	E	E
f/16	35	E140K	+0.25	+0.25
m/16	34	E140K	+0.75	+0.25
b1/16	14	E140K	+1.0	+0.75
m/17	27	E140K	−0.25	−0.25
f/17	29	E140K	E	E
f/18	54	E140K	−0.75	−0.5
m/18	53	E140K	+1.0	+1.0
f/19	50	[E140K]	E	E
m/19	48	E140K	−0.5	E
f/23	46	Q53*	−2.0	−3.25
gm/23	70	Q53*	+2.5	+2.5
m/23	45	E140K	−0.5	−0.25
m/24	30	M177T	E	E
f/24	30	E140K	E	E
m/27	40	E140K	E	E
f/27	46	W75R	−4.5	−4.5
s/27	5	E140K	E	E
m/31	33	E140K	E	E
m/32	33	E140K	E	E
f/32	34	E140K	E	E
m/33	28	E140K	E	E
f/33	31	Y241*	−0.5	−0.1
p/34	47	E140K	E	E
Homozygous patient	1.3	E140K/E140K	+1.75	+2.0
Carriership excluded				
b3/16	6	E140K negative	+2.25	+2.75
b2/16	11.5	E140K negative	+0.0	+0.25

f father, *m* mother, *b* brother, *s* sister, *gm* grandmother, *p* patient with *SCO2* unrelated disease, *E* emmetropic, *[E140K]* obligatory heterozygote

Columbia University Medical Center Institutional Animal Care and Use Committee, which is consistent with the National Institutes of Health Guide for the Care and Use of Laboratory Animals. Mice were housed and bred according to international standard conditions, with a 12-h light, 12-h dark cycle.

Mouse Globe Axial Length Measurement by Ultrasound Biomicroscopy

Adult mice (approximately 14 weeks of age) were anesthetized with intraperitoneal ketamine (100 mg/kg) and xylazine (8 mg/kg). The axial lengths were followed with an adapted immersion B-scan ultrasound (Quantel Aviso, Bozeman, MT, USA) employing a 50 MHz ultrasound biomicroscopy (UBM) probe attached to a water-filled ClearScan bubble-tip (ESI, Inc., Plymouth, MN, USA) (Pavlin et al. 1991; Pavlin and Foster 1995; Coleman et al. 2006). After placing a drop of GenTeal (hypromellose, 0.3%, Alcon) on the open eye, the ClearScan was placed in contact with the cornea and the range between probe and eye adjusted to place the eye in the focal region. Two cineloop videos were acquired imaging the entire length of the eye in UBM mode, and two individual frames that contained proper reflections from the cornea, lens, iris, and posterior wall were selected from each cineloop for biometric analysis. Axial length was measured along the visual axis from the anterior surface of the cornea to the posterior wall, and the average from the four measurements was recorded.

Results

Ophthalmic Examination

None of the *SCO2* carriers examined demonstrated high-grade myopia as defined by Tran-Viet (>−6 diopters). Seventeen carriers were emmetropic. In the homozygous infant, mild physiologic hyperopia (+1.75 diopters in the right eye and +2.0 diopters in the left eye) was identified. Refractive errors occurred in 18 carriers (33 eyes): hyperopia up to +1.0 diopter in 13 eyes and myopia in 20 eyes. Of these 20 myopic eyes, 17 were categorized as mild myopia (16 eyes up to −1.25 diopters) and 3 demonstrated moderate myopia. The highest myopia level of 4.5 diopters occurred in an individual with a c.223T>C (p.W75R) variant, rather than the E140K variant. In a family carrying a c.157C>T (p.Q53*) variant, both moderate myopia (−3.5 diopters) and hyperopia (+2.0 diopters) were found (Family 23, Table 1). An individual bearing a different severe variant, c.723C>G (p.Y241*), had no refractive error. We did not find significant refractive differences among three E140K carriers (6 eyes, mean 0.54; $p = 0.35$, *t*-test) vs. two healthy individuals in the same family (4 eyes, mean 1.31; Family 16, Table 1).

Screening of the Symptomatic and Population Cohorts

Screening of a symptomatic patient cohort with previously unidentified disease yielded eleven subjects possessing the E140K allele (1:59). Sequencing of the *SCO2* gene in all of these subjects showed five homozygotes (Pronicka et al. 2013), whereas in the six remaining cases no pathogenic variant was found on the other allele. Thus, the apparent prevalence of random carriers was 6:621 (1:103, 0.96%, CI: 0.44–2.09). Thorough investigations led to the identification of spinal muscular atrophy with respiratory distress (SMARD1) (Jędrzejowska et al. 2014) in one case and to the identification of candidate genes responsible for neurological symptoms in two other patients (data not shown). Twenty-one E140K carriers were found in the population cohort (1:147), indicating the carrier frequency of 0.68% (CI: 0.45–1.04%).

Mouse Globe Axial Length Measurement by Ultrasound Biomicroscopy

High-grade myopia, corresponding to a refractive error of at least −6.0 diopters, correlates with an axial length (AL) elongation of over 30–40 micrometers in mouse eyes (Schmucker and Schaeffel 2004); likewise the average distortion of −22 diopters described by Tran-Viet et al. would correspond to a mouse globe AL elongation over control of approximately 120 μm. We measured mouse globe axial length in adult Sco2-deficient mice (KI/+, KI/KI and KI/KO) and wild-type littermate controls, using ultrasound biomicroscopy (Coleman et al. 2006; Pavlin et al. 1991; Pavlin and Foster 1995). For each genotype, the left and right eyes of six mice (three males and three females) were analyzed, with no significant differences found between right vs. left eye or male vs. female. No significant axial length elongation was found in mice carrying Sco2 mutations (Fig. 1), with average lengths of 3,020 ± 70 μm for +/+ control mice, 2,950 ± 40 μm for KI/+ mice, 2,950 ± 40 μm for KI/KI mice, and 2,950 ± 60 μm for KI/KO mice. Surprisingly, all Sco2-variant mice exhibited slightly shorter average axial length, despite no significant difference in animal size/weight (data not shown), although this difference was not statistically significant.

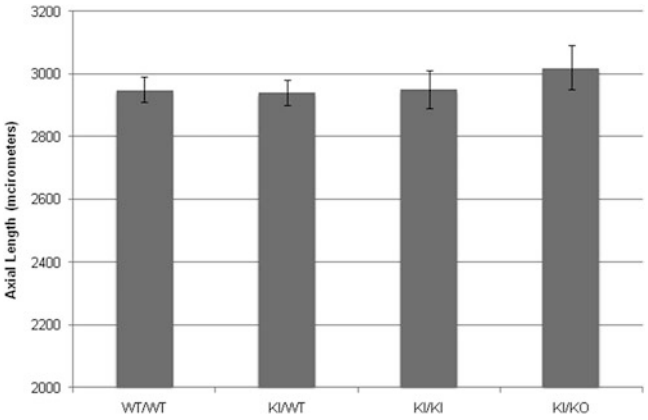

Fig. 1 Ultrasound biomicroscopy measurement of Sco2-deficient mouse eye axial lengths. Axial length is given in microns. *Each bar* with indicated genotype represents the average of the left and right eyes (3–6 independent axial length measurements per eye) for 6 adult mice (3 males, 3 females) of approximately 14 weeks' age. *Bars* represent standard deviation

Discussion

Our results do not support the hypothesis that heterozygosity for deleterious *SCO2* variants is pathogenic, as none of 35 subjects examined in this study displayed high-grade myopia and mice carrying heterozygous, compound heterozygous, or homozygous pathogenic *Sco2* mutations revealed no axial elongation indicative of high-grade myopia. Furthermore, analysis of undiagnosed patients with symptoms related to *SCO2* pathology showed a carriage rate with CI largely overlapping the carriage rate for general population (0.96%, CI: 0.44–2.09 vs. 0.68%, CI: 0.45–1.04%, respectively). Noteworthy, this is a first study documenting the presence of E140K mutation in the large cohort of 468 symptomatic infants with a histological pattern resembling SMA and negative for the *SMN1/NAIP* deletion.

Similar E140K carrier frequency (1:140) was reported by Tran-Viet et al. in high-myopic individuals (Tran-Viet et al. 2013). The nature of visual impairment in the studied patients did not differ from that diagnosed in the general population (Nowak et al. 2008).

The discrepancy between our results and those reported previously (Tran-Viet et al. 2013) may be caused by very low penetrance of heterozygous pathogenic *SCO2* variants. However, an unrecognized population heterogeneity seems more probable. The E140K variant is quite rare worldwide, as it was not reported in the 1000 Genomes Database and had a prevalence of only 3/8597 (0.035%) among European alleles in the NHLBI Exome Sequencing Project (ESP). The high prevalence of E140K carriers in Poland is in agreement with a frequent occurrence of SCO2 deficiency in Slavic regions and with an uneven distribution of homozygous patients who, in the majority, were born in Central-Eastern Europe (Böhm et al. 2006; Papadopoulou et al. 1999; Pronicka et al. 2013). Since >20 million Poles live abroad, the high prevalence of E140K indicates that patients and controls used in *SCO2* population studies should be matched carefully, not only for broad ethnicity but also specifically for Polish (Central European) admixture.

Acknowledgements We are grateful to parents of affected infants participating in the survey.

The study was supported by grants from the National Science Centre 1154/B/P01/2011/40, 2012/05/B/NZ2/01627 and the CMHI projects S211/10, S136/13, and S126/12; grants from the US National Institutes of Health (EY013435, EY019007, EY023595, HD032062, and HD080642) and the US Department of Defense (W911NF-12-1-9159 and W911F-15-1-0169); and an unrestricted grant to the Department of Ophthalmology of Columbia University from Research to Prevent Blindness, the Muscular Dystrophy Association, and the J. Willard and Alice S. Marriott Foundation. This publication was also supported by Career Development Awards from Research to Prevent Blindness, the Louis V. Gerstner Jr. Scholars Program, and the AR and JR Peacock Trust.

Take-Home Message

The heterozygosity for pathogenic *SCO2* variants is not associated with high-grade myopia in either human patients or in mice.

Compliance with Ethics Guidelines

Conflict of Interest Statement

The authors of this manuscript declare that there are no conflicts of interest.

Informed Consent

All procedures followed were in accordance with the ethical standards of the responsible committee on human experimentation (institutional and national) and with the Helsinki Declaration of 1975, as revised in 2000. Informed consent was obtained from all patients for being included in the study.

Animal Rights

All institutional and national guidelines for the care and use of laboratory animals were followed.

Details of the Contributions of Individual Authors

DPA devised study protocol, analyzed the data, conceived the purpose of the manuscript, and wrote the article.

BKK performed ophthalmological assessments analysis and assisted in writing the manuscript.

SŁ and MM performed population studies and analyzed the data.

OS, KC, and PK performed population studies.

KIP, JP, JZ, JZ, MKW, and EC collected previous data and assisted in reviewing and editing the manuscript.

RP conducted whole genome sequencing experiments and assisted in writing the manuscript.

EAS designed experiments, analyzed the data, and assisted in writing the paper.

SS designed experiments, assisted with experiments, and analyzed the data.

HY designed experiments and assisted with experiments.

QW assisted with experiments and analyzed the data.

QH designed experiments, assisted with experiments, analyzed the data, and assisted in writing the manuscript.

RS assisted with experiments.

EP conceived the purpose of the manuscript, analyzed the data, and involved in writing and editing the manuscript.

References

Böhm M, Pronicka E, Karczmarewicz E et al (2006) Retrospective, multicentric study of 180 children with cytochrome c oxidase deficiency. Pediatr Res 59:21–26

Brosel S, Yang H, Tanji K et al (2010) Unexpected vascular enrichment of SCO1 over SCO2 in mammalian tissues: implications for human mitochondrial disease. Am J Pathol 177: 2541–2548

Coleman DJ, Silverman RH, Lizzi FL et al (2006) Ultrasonography of the eye and orbit, 2nd edn. Lippincott Williams & Wilkins, Philadelphia

Jędrzejowska M, Madej-Pilarczyk A, Fidziańska A et al (2014) Severe phenotypes of SMARD1 associated with novel mutations of the IGHMBP2 gene and nuclear degeneration of muscle and Schwann cells. Eur J Paediatr Neurol 18:183–192

Nowak MS, Goś R, Smigielski J (2008) Character of refractive errors in population study performed by the Area Military Medical Commission in Lodz. Klin Oczna 110:55–59 (in Polish)

Papadopoulou LC, Sue CM, Davidson MM et al (1999) Fatal infantile cardioencephalomyopathy with COX deficiency and mutations in *SCO2*, a COX assembly gene. Nat Genet 23:333–337

Park H, Qazi Y, Tan C et al (2012) Assessment of axial length measurements in mouse eyes. Optom Vis Sci 89:296–303

Pavlin CJ, Foster FS (1995) Ultrasound biomicroscopy of the eye. Springer-Verlag, New York

Pavlin CJ, Harasiewicz K, Foster FS (1991) Clinical application of ultrasound biomicroscopy. Ophthalmology 98:287–295

Płoski R, Pollak A, Müller S et al (2014) Does p.Q247X in TRIM63 cause human hypertrophic cardiomyopathy? Circ Res 114: e2–e5

Pronicka E, Piekutowska-Abramczuk D, Szymańska-Dębinska T et al (2013) The natural history of SCO2 deficiency in 36 Polish children confirmed the genotype-phenotype correlation. Mitochondrion 13:810–816

Pronicki M, Kowalski P, Piekutowska-Abramczuk D et al (2010) A homozygous mutation in the SCO2 gene causes a spinal muscular atrophy like presentation with stridor and respiratory insufficiency. Eur J Paediatr Neurol 14:253–260

Schmucker C, Schaeffel F (2004) A paraxial schematic eye model for the growing C57BL/6 mouse. Vis Res 44:1857–1867

Tran-Viet KN, Powell C, Barathi VA et al (2013) Mutations in SCO2 are associated with autosomal-dominant high-grade myopia. Am J Hum Genet 92:820–825

Wilson EB (1927) Probable interference, the law of succession, and statistical interference. J Am Stat Assoc 22:209–212

Yang H, Brosel S, Acin-Perez R et al (2010) Analysis of mouse models of cytochrome *c* oxidase deficiency owing to mutations in *Sco2*. Hum Mol Genet 19:170–180

JIMD Reports
DOI 10.1007/8904_2015_498

RESEARCH REPORT

Voluntary Exercise Prevents Oxidative Stress in the Brain of Phenylketonuria Mice

Priscila Nicolao Mazzola • Vibeke Bruinenberg • Karen Anjema • Danique van Vliet • Carlos Severo Dutra-Filho • Francjan J. van Spronsen • Eddy A. van der Zee

Received: 27 May 2015 / Revised: 14 September 2015 / Accepted: 15 September 2015 / Published online: 7 October 2015
© SSIEM and Springer-Verlag Berlin Heidelberg 2015

Abstract *Background*: High phenylalanine levels in phenylketonuria (PKU) have been associated with brain oxidative stress and amino acid imbalance. Exercise has been shown to improve brain function in hyperphenylalaninemia and neurodegenerative diseases. This study aimed to verify the effects of exercise on coordination and balance, plasma and brain amino acid levels, and brain oxidative stress markers in PKU mice.

Methods: Twenty wild-type (WT) and 20 PAH^{enu2} (PKU) C57BL/6 mice were placed in cages with (exercise, Exe) or without (sedentary, Sed) running wheels during 53 days. At day 43, a balance beam test was performed. Plasma and brain were collected for analyses of amino acid levels and the oxidative stress parameters superoxide dismutase (SOD) activity, sulfhydryl and reduced glutathione (GSH) contents, total radical-trapping antioxidant potential (TRAP), and total antioxidant reactivity (TAR).

Results: SedPKU showed poor coordination ($p < 0.001$) and balance ($p < 0.001$), higher plasma and brain phenylalanine ($p < 0.001$), and increased brain oxidative stress ($p < 0.05$) in comparison to SedWT. ExePKU animals ran less than ExeWT ($p = 0.018$). Although no improvement was seen in motor coordination and balance, exercise in PKU restored SOD, sulfhydryl content, and TRAP levels to controls. TAR levels were increased in ExePKU in comparison to SedPKU ($p = 0.012$). Exercise decreased plasma and brain glucogenic amino acids in ExePKU, but did not change plasma and brain phenylalanine in both WT and PKU.

Conclusions: Exercise prevents oxidative stress in the brain of PKU mice without modifying phenylalanine levels. Hence, exercise positively affects the brain, demonstrating its value as an intervention to improve brain quality in PKU.

Abbreviations

BCAA	Branched-chain amino acid
Exe	Exercise
GSH	Reduced glutathione
PAH	Phenylalanine hydroxylase
Phe	Phenylalanine
PKU	Phenylketonuria
Sed	Sedentary
SOD	Superoxide dismutase
TAR	Total antioxidant reactivity
TRAP	Total radical-trapping antioxidant potential
WT	Wild type

Communicated by: Nenad Blau, PhD

Competing interests: None declared

Electronic supplementary material: The online version of this chapter (doi:10.1007/8904_2015_498) contains supplementary material, which is available to authorized users.

P.N. Mazzola (✉) · V. Bruinenberg · E.A. van der Zee
Department of Molecular Neurobiology, Groningen Institute for Evolutionary Life Sciences (GELIFES) – University of Groningen, Nijenborgh 7, 9747 AG Groningen, The Netherlands
e-mail: pku@priscilamazzola.com

P.N. Mazzola · K. Anjema · D. van Vliet · F.J. van Spronsen
Beatrix Children's Hospital, University Medical Center Groningen, University of Groningen, Groningen, The Netherlands

P.N. Mazzola · C.S. Dutra-Filho
Programa de Pós-Graduação em Ciências Biológicas: Bioquímica, Universidade Federal do Rio Grande do Sul (UFRGS), Porto Alegre, Brazil

Introduction

Phenylketonuria (PKU, MIM 261600) is characterized by accumulation of phenylalanine (Phe) to toxic levels due to absent activity of Phe hydroxylase (PAH, EC 1.14.16.1).

High Phe concentration can impair brain function even in early-treated PKU patients, who have shown poor cognitive function (Gonzalez et al. 2011; Weglage et al. 2013; Jahja et al. 2014). Although the mechanisms are not yet fully understood, oxidative stress and brain amino acid imbalance caused by high Phe levels are speculated to underlie the impaired clinical outcomes. At the biochemical level, high blood Phe disturbs the concentration of other large neutral amino acids in the brain (de Groot et al. 2010; Martynyuk et al. 2010). Moreover, high Phe levels have been related to oxidative stress in blood from patients (Sierra et al. 1998; van Bakel et al. 2000; Schulpis et al. 2005; Sitta et al. 2009a, b; Sanayama et al. 2011), in the brain of animal models of the disease (Ercal et al. 2002; Moraes et al. 2014) and in in vitro experiments (Hagen et al. 2002; Sitta et al. 2009b; Fernandes et al. 2010; Moraes et al. 2010).

PKU treatment is based on a Phe-restricted diet, which aims to prevent high Phe concentrations in blood and tissues (Surtees and Blau 2000). Although efficient in lowering Phe levels, this diet is extremely hard to follow (Vilaseca et al. 2010). Therefore, other treatment strategies are still needed for PKU in order to improve patients' clinical and biochemical outcomes. In this way, exercise could be a concomitant treatment in PKU. Exercising regularly can lead to peripheral and central adaptations such as strengthening brain antioxidant capacity (Elokda and Nielsen 2007; Radak et al. 2007; Tsou et al. 2015) and improving dopaminergic and serotoninergic systems (Stroth et al. 2010; Wipfli et al. 2011; Chang et al. 2012; Lin and Kuo 2013). Additionally, aerobic exercise has improved cognition in elderly individuals (Kirk-Sanchez and McGough 2014) and in patients with neurodegenerative diseases (Petzinger et al. 2013; Radak et al. 2010). Moreover, in rats chemically subjected to hyperphenylalaninemia, regular exercise improved the brain antioxidant system (Mazzola et al. 2011). However, little is known about the effects of exercise in PKU and whether it can be beneficial for patients. Therefore, this study aimed to determine the effects of voluntary exercise on behavioral and biochemical parameters in a genetic mouse model of PKU, by the means of motor coordination and balance performance, plasma and brain amino acid concentrations, and brain oxidative stress parameters.

Methods

Animals

All the experimental procedures were approved by the Animal Welfare Committee of the University of Groningen, the Netherlands. A total of 40 adult (4 months old) C57Bl/6 homozygous (−/−) PAH^{enu2} (PKU) and (+/+) PAH^{enu2} (wild type, WT) female mice were used in this experiment. WT and PKU animals were individually housed and randomly assigned to sedentary (Sed) or exercise (Exe) groups. Mice were given water and regular chow ad libitum, while kept in a 12:12-h light–dark regime and weighed weekly.

Voluntary Exercise

Mice from ExeWT and ExePKU had free access to a running wheel placed in their home cage throughout the experiment, i.e., 4 days of acclimatization plus 53 days of voluntary training. Daily running wheel activity was calculated as described before (Mulder et al. 2014).

Balance Beam Test

The balance beam is a sensorimotor integration test, which focuses on hind limb functioning (Carter et al. 1999; Soderling et al. 2003). The apparatus consisted of a 50-mm wide beam with a "safe cage" placed at the end of it. Animals performed nonconsecutive four trials (5, 10, 40, and 100 cm) on the beam, which were recorded. The number of hind limb steps and slips was counted in the 100-cm trial using the video files.

Tissue Preparation

Animals were sacrificed by cervical dislocation. Blood was centrifuged at 1,500 × *g* for 10 min and then plasma was harvested and stored at −80°C. The total brain was immediately frozen in liquid nitrogen. Shortly before analysis, brain tissue was grinded in liquid nitrogen and then divided into weighed aliquots. Later, the aliquots were homogenized in specific buffers as required for each technique and sonified (30 s per sample at 11–12 W). The brain homogenates were then centrifuged at 1,000 × *g* for 10 min at 4°C, and the supernatant was used for the biochemical measurements.

Plasma and Brain Amino Acid Levels

Brain homogenates were prepared using phosphate-buffered saline (pH 7.4) at a 1:4 weight to volume ratio (mg/μL). Plasma and brain amino acid concentrations were determined using HPLC coupled to derivatization with ninhydrin, according to the manufacturer's protocol (Pharmacia Biotech, Cambridge, UK).

Oxidative Stress Parameters

Cerebral tissue was homogenized in 50 mM Tris–HCl buffer containing 1 mM EDTA (pH 8.2) at a 1:10 (w/v)

ratio. All measurements were normalized by protein concentration using albumin as standard (Lowry et al. 1951).

Superoxide Dismutase (SOD) Activity Assay

This assay is based on the capacity of pyrogallol to autoxidize and on the ability of SOD to inhibit this reaction (Marklund 1985). Therefore, SOD activity can be indirectly assayed spectrophotometrically at 420 nm by comparing the samples' values with a standard curve. These data are expressed as percentage of control (%SedWT).

Sulfhydryl Content

5,5′dithiobis(2-nitrobenzoic acid) (DTNB) color reagent is reduced by thiols, thus generating a yellow derivative (TNB) which can be spectrophotometrically read at 412 nm (Aksenov and Markesbery 2001). Oxidation of free thiol groups in proteins leads to the formation of disulfide bonds, which will not react with DTNB. Therefore, the sulfhydryl content is inversely correlated to oxidative damage to proteins. The results are expressed as nmol TNB/mg protein.

Reduced Glutathione (GSH) Content

This method is based on the reaction of GSH with the fluorophore *ortho*-phthalaldehyde (Browne and Armstrong 1998). Briefly, metaphosphoric acid was used to deproteinize samples, which were then centrifuged at 1,000 × *g* for 10 min. Then, sodium phosphate buffer at pH 8.0 and *ortho*-phthalaldehyde 1 mg/mL solution were added to the samples' supernatants. After standing in the dark for 15 min, the fluorescence of this mixture was measured at excitation 350 nm and emission 420 nm. A calibration curve was made with a commercial GSH solution, and the results were expressed as μmol GSH/mg protein.

Total Radical-Trapping Antioxidant Potential (TRAP) and Total Antioxidant Reactivity (TAR)

TRAP and TAR were determined by measuring the chemiluminescence intensity of luminol induced by ABAP thermolysis (free radical source) in a scintillation counter (Evelson et al. 2001). After adding 3 mL of 10 mM ABAP and 10 μL of 5.6 mM luminol to scintillation vials, the initial light intensity was obtained. Ten microliters of 160 μM Trolox or 30 μL of sample was added to assess antioxidant content. At this point, the luminescence intensity is practically abolished. The consumption of active antioxidants present in samples results in the return of the luminescence (TRAP). For each sample, the time required to return of luminescence (TAR) was compared to that obtained by employing Trolox under identical experimental conditions. Values were calculated as Trolox equivalents and were represented as nmol Trolox/mg protein.

Statistical Analysis

The statistical analyses were performed with the Pearson's correlation coefficient, independent Student's *t*-test, or two-way ANOVA followed by the Tukey post hoc test for multiple comparisons and repeated measures ANOVA for longitudinal analyses. The SPSS was used and $p < 0.05$ was considered to be statistically significant. Number of animals per group varied due to technical sampling problems or due to exclusion of outliers (values that were two or more SDs away from the group mean).

Results

In order to evaluate the effects of voluntary exercise in PKU mice, we performed a study in which WT and PKU animals had free access to running wheels (Exe groups) and compared these to animals that did not have the apparatus in their home cages (Sed groups). As shown in Fig. 1, ExePKU group ran significantly less than did the ExeWT group (6,064 ± 1,937 m/day and 10,627 ± 4,868 m/day, respectively, $p = 0.018$), and the effect of the genotype was significant ($p = 0.027$). Exercise did not modify body weight ($p = 0.758$), and both PKU groups were lighter than WT groups throughout the experiment ($p = 0.001$) (Fig. 1).

PKU animals from both Sed and Exe groups showed poor performance in the balance beam test as compared to WT mice, as shown in Table 1. When crossing the beam, both PKU groups had a higher number of steps ($p < 0.001$) and slips ($p < 0.001$) in comparison to SedWT, representing deficits in motor coordination and balance, respectively. Neither Exe group differed from the Sed groups, therefore showing no exercise effect for this task.

As shown before (Ney et al. 2008; Solverson et al. 2012; Sawin et al. 2014), Phe levels in plasma and brain of SedPKU mice were higher in comparison to respective levels in SedWT group ($p < 0.001$). Exercise did not modify Phe levels when comparing each Exe group to its Sed control (Fig. 1). A comparison of plasma values between PKU groups showed that exercise decreased levels of alanine ($p = 0.038$), citrulline ($p = 0.002$), glutamine ($p = 0.040$), glycine ($p = 0.006$), ornithine ($p = 0.008$), and proline ($p = 0.028$) (Fig. 2). Furthermore, exercise reduced brain amino acid levels in ExePKU compared to SedPKU for histidine ($p = 0.036$), isoleucine ($p = 0.011$),

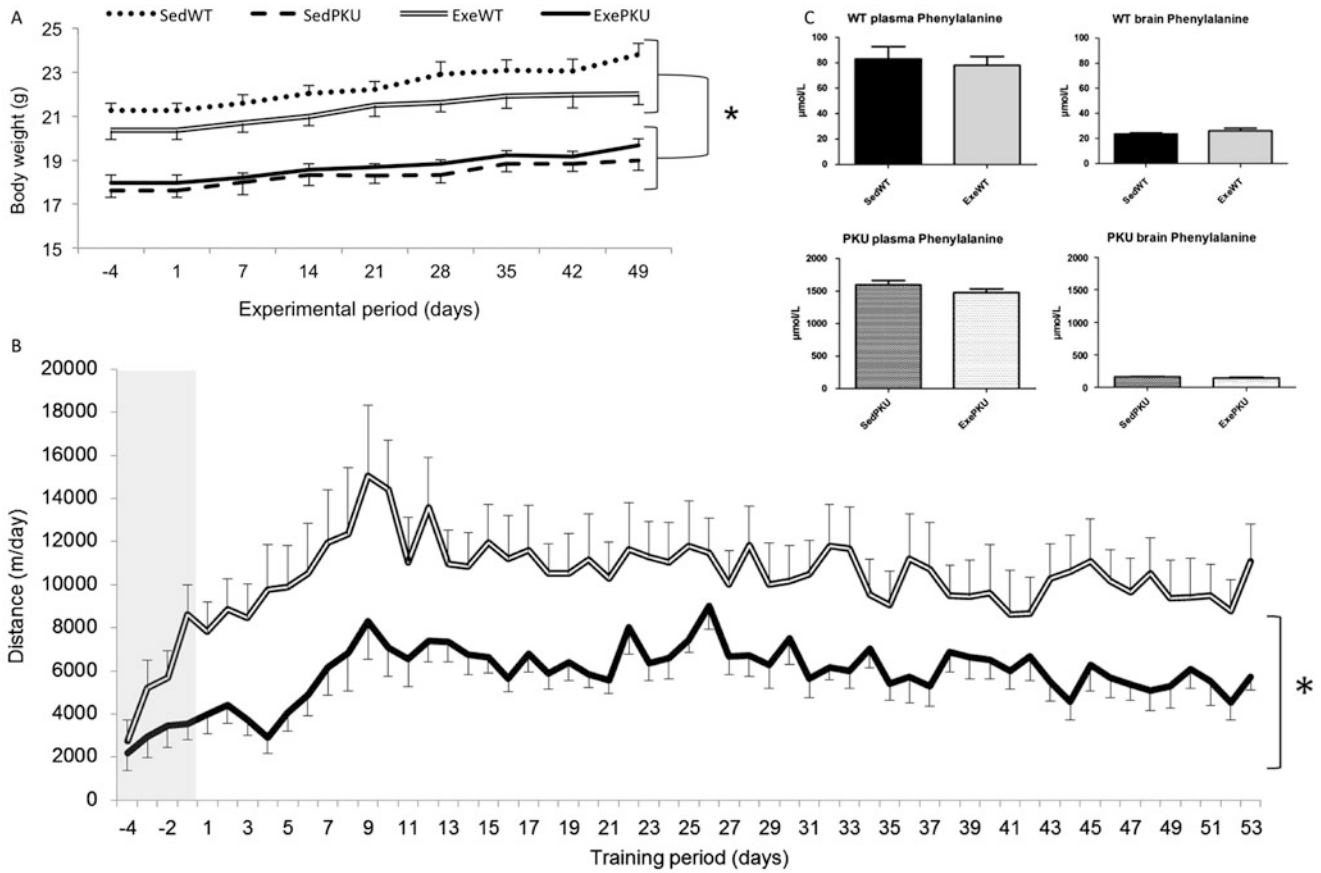

Fig. 1 (**a**) Body weight from sedentary (Sed) and exercise (Exe) wild-type (WT) and PAH^{enu2} (PKU) mice, (**b**) daily running wheel activity ExeWT and ExePKU mice during the 4-day acclimatization period (*gray area*) followed by 53 days of training and (**c**) phenylalanine levels in the plasma and brain of Sed and Exe WT and PKU. Data are shown as mean ± SEM ($n = 10$/group, except for plasma phenylalanine in SedPKU where $n = 8$). *$p < 0.05$, repeated measures ANOVA

Table 1 Balance beam test outcomes

	SedWT	SedPKU	ExeWT	ExePKU
Time (s)	19 ± 9	22 ± 9	11 ± 5	17 ± 5
Number of steps	40 ± 3	54 ± 7*	39 ± 6	50 ± 7*
Number of slips	8 ± 5	29 ± 10*	9 ± 8	27 ± 11*

Results are expressed as mean ± SD ($n = 10$/group)
*$p < 0.001$, compared to SedWT (Tukey post hoc)

methionine ($p = 0.005$), proline ($p = 0.005$), and valine ($p = 0.010$), and a positive correlation ($r = 0.817$; $p = 0.004$) between brain proline levels and distance run was found only for ExePKU (Fig. 2). No effects of exercise were found on plasma and brain amino acid levels for WT mice (Supplemental Table 1).

Regarding oxidative stress in the brain, the SedPKU group showed lower superoxide dismutase activity ($p = 0.029$), sulfhydryl ($p = 0.043$), GSH ($p = 0.007$), and TRAP ($p = 0.003$) in comparison to the SedWT group (Fig. 3). Exercise prevented those changes, so the ExePKU group reached levels similar to SedWT for SOD, sulfhydryl, TRAP and also tended to restore GSH levels ($p = 0.049$). Furthermore, exercise led to higher levels of TAR only for the ExePKU group in comparison to the SedPKU group ($p = 0.012$), although TAR levels were not lower in SedPKU in comparison to SedWT. No exercise effect was found for WT animals (ExeWT group).

Discussion

To the best of our knowledge, this study was the first to evaluate the long-term effects of voluntary exercise in a genetic mouse model of PKU. The protocol used was voluntary exercise by animals having free access to running wheels in their home cages. Therefore, Exe animals could run whenever and for as long as they desired. PKU mice, although running less than controls, improved brain oxidative stress markers, while no changes in plasma and blood Phe levels were found.

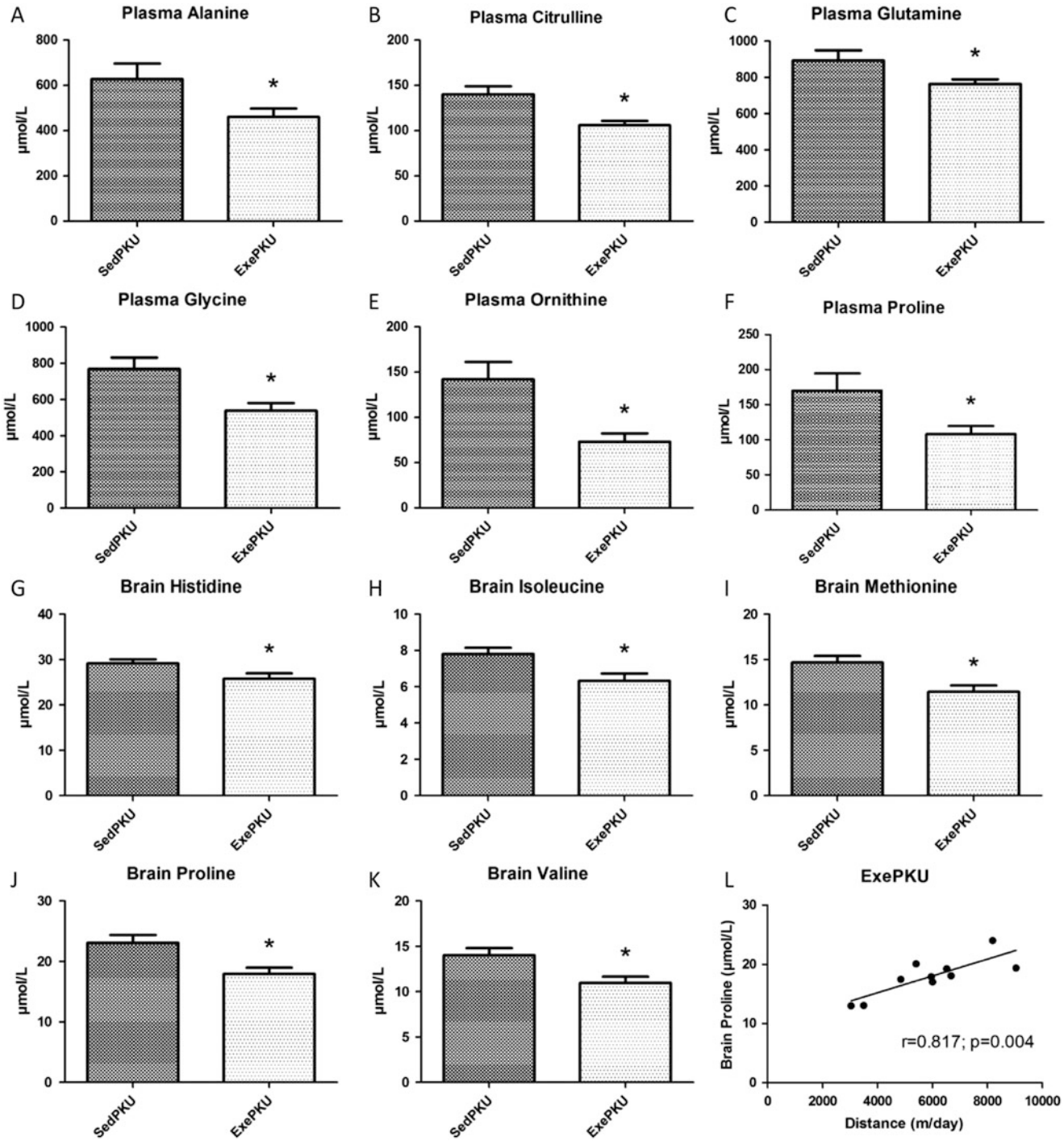

Fig. 2 Plasma amino acid levels of (**a**) alanine, (**b**) citrulline, (**c**) glutamine, (**d**) glycine, (**e**) ornithine, and (**f**) proline and brain amino acid levels of (**g**) histidine, (**h**) isoleucine, (**i**) methionine, (**j**) proline, (**k**) valine, and (**l**) correlation between brain proline levels and distance ran in sedentary (Sed) and exercise (Exe) PAH^{enu2} (PKU) mice. Results are expressed as mean ± SEM ($n = 10$/group, except for plasma levels in SedPKU where $n = 8$). *$p < 0.05$

The lower running wheel activity of the ExePKU group might be caused by their specific motor problems and/or early fatigue. Both SedPKU and ExePKU groups showed worse performance in the balance beam task than WT mice. As various brain regions are affected by Phe toxicity (Qin and Smith 2007; Fernandes et al. 2010), the balance beam findings indicate possible motor cortex and cerebellum impairments in this PKU mouse model. Voluntary training has been effective in improving motor performance in the rotarod test in healthy mice (Clark et al. 2008). However,

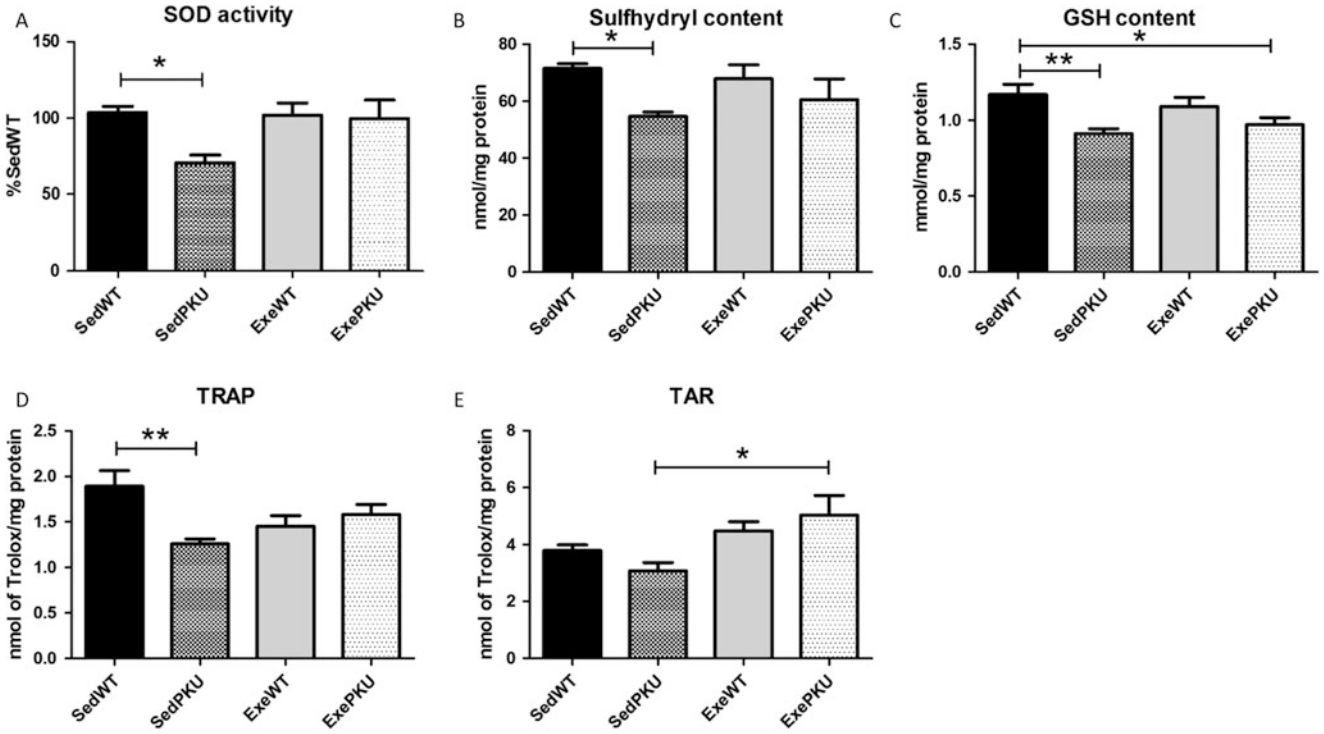

Fig. 3 Oxidative stress parameters (**a**) superoxide dismutase (SOD) activity, (**b**) sulfhydryl and (**c**) reduced glutathione (GSH) contents, (**d**) total radical-trapping antioxidant potential (TRAP), and (**e**) total antioxidant reactivity (TAR) in the brain of sedentary (Sed) and exercise (Exe) wild-type (WT) and PAH^{enu2} (PKU) mice. Results are expressed as mean ± SEM (n = 8–10/group). *$p < 0.05$ and **$p < 0.01$

the exercise used in the present study did not improve balance beam outcomes in both PKU and WT groups. In this way, perhaps this exercise protocol was not able to address those skills specifically necessary for crossing a narrow beam. On the other hand, the exercise used in the present study decreased plasma glucogenic amino acid levels only in the PKU mice. Skeletal muscles produce alanine to get rid of nitrogen groups during amino acid catabolism, thus preventing accumulation of ammonia to toxic levels (Graham and MacLean 1998). The lower plasma levels of alanine, glutamate precursors (glutamine and proline), and urea cycle intermediates (ornithine and citrulline) in ExePKU may indicate that trained PKU mice did not have an efficient nitrogen buffering mechanism. Supporting this hypothesis, supplementations of ornithine, citrulline, and glutamine have shown to postpone fatigue by decreasing blood ammonia in rodents (Meneguello et al. 2003; Takeda et al. 2011; Kim and Kim 2013). In this way, the PKU mice in the present study might have run less than WT due to fatigue, besides motor problems.

Exercise decreased brain levels of glucogenic amino acids, including branched-chain amino acids (BCAA) that were not changed in plasma. Lower availability of brain large neutral amino acids in PKU has been related to the clinical problems caused by high Phe levels, and this can be explained by the a critical imbalance in the competition to cross the blood–brain barrier when Phe is relatively more concentrated (de Groot et al. 2010). However, in the present study, among the amino acids that were decreased in plasma of ExePKU mice, proline was the only amino acid also decreased in the brain in comparison to SedPKU. Moreover, as concentrations of Phe and other large neutral amino acids did not change in the brain due to exercise, competition between aromatic amino acids and BCAA might not have hampered BCAA uptake in ExePKU in comparison to SedPKU. This observation could indicate an increased amino acid metabolism to yield energy, as the brain has high activity of the key enzymes especially for BCAA catabolism (Piscopo et al. 2011). Furthermore, brain proline levels show a positive correlation with the daily distance run only for PKU mice ($r = 0.817$; $p = 0.004$); therefore, the amount of running, and hence the amount of training, might have influenced this result.

The PKU mouse model used in this study showed oxidative stress in the brain by lower levels of SOD activity, sulfhydryl, and GSH contents and TRAP levels, which was mostly prevented by the voluntary exercise.

Solverson et al. (2012) have found metabolic stress in the same strain of PKU mice (C57BL/6). As the brain is the most affected organ in PKU, our results corroborate the already stated hypothesis that oxidative stress is involved in the pathophysiology of the disease (Ribas et al. 2011). While exercise did not change any oxidative stress parameter in the control (WT) mice, the PKU group benefitted from exercising. ExePKU had SOD, sulfhydryl content and TRAP restored to control levels, and increased TAR in comparison to SedPKU. In this study, PKU animals that voluntarily exercised showed similar oxidative stress parameters to those of controls, thus preventing the impairments caused by PKU without changing brain Phe levels. Previous research on voluntary wheel running has shown enhancement of antioxidant enzymatic activity in arteries of old mice thus preventing age-related oxidative stress (Durrant et al. 2009). Furthermore, exercise has been shown to prevent oxidative stress in the brain of animal models of neurodegenerative diseases (Ang et al. 2010; Souza et al. 2013) as well as in hyperphenylalaninemia (Mazzola et al. 2011). In the same way, exercise improved brain oxidative stress parameters in PKU animals in the present study.

The focus of PKU treatment strategies should not only be on reducing Phe but also on enhancing central parameters that are impaired by high Phe levels (van Spronsen et al. 2009; van Vliet et al. 2015). In this way, the intermittent stress caused by exercise might be able to overcome high Phe issues and improve PKU outcomes. Moreover, even though PKU animals showed less physical activity than WT mice, only the PKU group showed changes in amino acid and oxidative stress levels. Therefore, PKU mice were more responsive to exercise effects. Future studies might evaluate the effects of exercise when introduced at early ages as well as in male mice, therefore shedding light in the importance of physical activity in this population. Although therapeutic strategies in PKU primarily address high Phe-related problems, the beneficial effects of exercise on other PKU-related problems as shown here should open new avenues in combined treatment strategies.

Conclusions

Exercise decreased levels of glucogenic amino acids in plasma and brain of PKU mice, but did not improve motor coordination or balance. Voluntary exercise training prevented oxidative stress in the brain of PKU mice without changing Phe levels in the plasma or brain. Therefore, exercise may be a concomitant strategy for PKU patients to improve brain redox status and hence brain biochemistry and function.

Acknowledgments This research project has been made possible thanks to a fellowship from PKU Academy under the auspices of EXCEMED, Excellence in Medical Education, the Abel Tasman Talent Program from the University Medical Center Groningen and the University of Groningen. We thank Pim de Blaauw for the amino acid analyses and Wanda Douwenga and Jan Keijser for their technical support.

Concise 1: Sentence Take-Home Message

Voluntary training improved brain oxidative stress and reduced brain and plasma glucogenic amino acids in phenylketonuria mice without changing phenylalanine levels.

Compliance with Ethics Guidelines

Conflict of Interest

Priscila Nicolao Mazzola, Vibeke Bruinenberg, Karen Anjema, Danique van Vliet, Carlos Severo Dutra-Filho, Francjan J. van Spronsen, and Eddy A. van der Zee declare that they have no conflict of interest.

Animal Rights

All institutional and national guidelines for the care and use of laboratory animals were followed.

Details of the Contribution of Individual Authors

Priscila Nicolao Mazzola, Vibeke Bruinenberg, Karen Anjema, and Danique van Vliet collected the data. Priscila Nicolao Mazzola performed the statistical analyses and drafted the manuscript. All authors participated in the study design, contributed to the interpretation of the results, and revised the manuscript.

References

Aksenov MY, Markesbery WR (2001) Changes in thiol content and expression of glutathione redox system genes in the hippocampus and cerebellum in Alzheimer's disease. Neurosci Lett 302:141–145

Ang ET, Tai YK, Lo SQ, Seet R, Soong TW (2010) Neurodegenerative diseases: exercising toward neurogenesis and neuroregeneration. Front Aging Neurosci 2:25

Browne RW, Armstrong D (1998) Reduced glutathione and glutathione disulfide. Methods Mol Biol 108:347–352

Carter RJ, Lione LA, Humby T et al (1999) Characterization of progressive motor deficits in mice transgenic for the human Huntington's disease mutation. J Neurosci 19:3248–3257

Chang YK, Liu S, Yu HH, Lee YH (2012) Effect of acute exercise on executive function in children with attention deficit hyperactivity disorder. Arch Clin Neuropsychol 27:225–237

Clark PJ, Brzezinska WJ, Thomas MW, Ryzhenko NA, Toshkov SA, Rhodes JS (2008) Intact neurogenesis is required for benefits of exercise on spatial memory but not motor performance or contextual fear conditioning in C57BL/6J mice. Neuroscience 155:1048–1058

de Groot MJ, Hoeksma M, Blau N, Reijngoud DJ, van Spronsen FJ (2010) Pathogenesis of cognitive dysfunction in phenylketonuria: review of hypotheses. Mol Genet Metab 99(Suppl 1):S86–S89

Durrant JR, Seals DR, Connell ML et al (2009) Voluntary wheel running restores endothelial function in conduit arteries of old mice: direct evidence for reduced oxidative stress, increased superoxide dismutase activity and down-regulation of NADPH oxidase. J Physiol 587:3271–3285

Elokda AS, Nielsen DH (2007) Effects of exercise training on the glutathione antioxidant system. Eur J Cardiovasc Prev Rehabil 14:630–637

Ercal N, Aykin-Burns N, Gurer-Orhan H, McDonald JD (2002) Oxidative stress in a phenylketonuria animal model. Free Radic Biol Med 32:906–911

Evelson P, Travacio M, Repetto M, Escobar J, Llesuy S, Lissi EA (2001) Evaluation of total reactive antioxidant potential (TRAP) of tissue homogenates and their cytosols. Arch Biochem Biophys 388:261–266

Fernandes CG, Leipnitz G, Seminotti B et al (2010) Experimental evidence that phenylalanine provokes oxidative stress in hippocampus and cerebral cortex of developing rats. Cell Mol Neurobiol 30:317–326

Gonzalez MJ, Gutierrez AP, Gassio R, Fuste ME, Vilaseca MA, Campistol J (2011) Neurological complications and behavioral problems in patients with phenylketonuria in a follow-up unit. Mol Genet Metab 104(Suppl):S73–S79

Graham TE, MacLean DA (1998) Ammonia and amino acid metabolism in skeletal muscle: human, rodent and canine models. Med Sci Sports Exerc 30:34–46

Hagen MEK, Pederzolli CD, Sgaravatti AM et al (2002) Experimental hyperphenylalaninemia provokes oxidative stress in rat brain. Biochim Biophys Acta 1586:344–352

Jahja R, Huijbregts SC, de Sonneville LM, van der Meere JJ, van Spronsen FJ (2014) Neurocognitive evidence for revision of treatment targets and guidelines for phenylketonuria. J Pediatr 164:895.e2–899.e2

Kim DI, Kim KS (2013) Walnut extract exhibits anti-fatigue action via improvement of exercise tolerance in mice. Lab Anim Res 29:190–195

Kirk-Sanchez NJ, McGough EL (2014) Physical exercise and cognitive performance in the elderly: current perspectives. Clin Interv Aging 9:51–62

Lin TW, Kuo YM (2013) Exercise benefits brain function: the monoamine connection. Brain Sci 3:39–53

Lowry OH, Rosebrough NJ, Farr AL, Randall RJ (1951) Protein measurement with the Folin phenol reagent. J Biol Chem 193:265–275

Marklund SL (1985) Pyrogallol autoxidation. In: Greenwald RA (ed) Handbook of methods for oxygen radical research. CRC, Boca Raton, pp 243–247

Martynyuk AE, van Spronsen FJ, Van der Zee EA (2010) Animal models of brain dysfunction in phenylketonuria. Mol Genet Metab 99(Suppl 1):S100–S105

Mazzola PN, Terra M, Rosa AP et al (2011) Regular exercise prevents oxidative stress in the brain of hyperphenylalaninemic rats. Metab Brain Dis 26:291–297

Meneguello MO, Mendonca JR, Lancha AH Jr, Costa Rosa LF (2003) Effect of arginine, ornithine and citrulline supplementation upon performance and metabolism of trained rats. Cell Biochem Funct 21:85–91

Moraes TB, Zanin F, da Rosa A et al (2010) Lipoic acid prevents oxidative stress in vitro and in vivo by an acute hyperphenylalaninemia chemically-induced in rat brain. J Neurol Sci 292:89–95

Moraes TB, Dalazen GR, Jacques CE, de Freitas RS, Rosa AP, Dutra-Filho CS (2014) Glutathione metabolism enzymes in brain and liver of hyperphenylalaninemic rats and the effect of lipoic acid treatment. Metab Brain Dis 29:609–615

Mulder CK, Papantoniou C, Gerkema MP, Van Der Zee EA (2014) Neither the SCN nor the adrenals are required for circadian time-place learning in mice. Chronobiol Int 31:1075–1092

Ney DM, Hull AK, van Calcar SC, Liu X, Etzel MR (2008) Dietary glycomacropeptide supports growth and reduces the concentrations of phenylalanine in plasma and brain in a murine model of phenylketonuria. J Nutr 138:316–322

Petzinger GM, Fisher BE, McEwen S, Beeler JA, Walsh JP, Jakowec MW (2013) Exercise-enhanced neuroplasticity targeting motor and cognitive circuitry in Parkinson's disease. Lancet Neurol 12:716–726

Piscopo P, Crestini A, Adduci A et al (2011) Altered oxidative stress profile in the cortex of mice fed an enriched branched-chain amino acids diet: possible link with amyotrophic lateral sclerosis? J Neurosci Res 89:1276–1283

Qin M, Smith CB (2007) Regionally selective decreases in cerebral glucose metabolism in a mouse model of phenylketonuria. J Inherit Metab Dis 30:318–325

Radak Z, Kumagai S, Taylor AW, Naito H, Goto S (2007) Effects of exercise on brain function: role of free radicals. Appl Physiol Nutr Metab 32:942–946

Radak Z, Hart N, Sarga L et al (2010) Exercise plays a preventive role against Alzheimer's disease. J Alzheimers Dis 20:777–783

Ribas GS, Sitta A, Wajner M, Vargas CR (2011) Oxidative stress in phenylketonuria: what is the evidence? Cell Mol Neurobiol 31:653–662

Sanayama Y, Nagasaka H, Takayanagi M et al (2011) Experimental evidence that phenylalanine is strongly associated to oxidative stress in adolescents and adults with phenylketonuria. Mol Genet Metab 103:220–225

Sawin EA, Murali SG, Ney DM (2014) Differential effects of low-phenylalanine protein sources on brain neurotransmitters and behavior in C57Bl/6-Pah(enu2) mice. Mol Genet Metab 111:452–461

Schulpis KH, Tsakiris S, Traeger-Synodinos J, Papassotiriou I (2005) Low total antioxidant status is implicated with high 8-hydroxy-2-deoxyguanosine serum concentrations in phenylketonuria. Clin Biochem 38:239–242

Sierra C, Vilaseca MA, Moyano D et al (1998) Antioxidant status in hyperphenylalaninemia. Clin Chim Acta 276:1–9

Sitta A, Barschak AG, Deon M et al (2009a) L-carnitine blood levels and oxidative stress in treated phenylketonuric patients. Cell Mol Neurobiol 29:211–218

Sitta A, Manfredini V, Biasi L et al (2009b) Evidence that DNA damage is associated to phenylalanine blood levels in leukocytes from phenylketonuric patients. Mutat Res 679:13–16

Soderling SH, Langeberg LK, Soderling JA et al (2003) Loss of WAVE-1 causes sensorimotor retardation and reduced learning and memory in mice. Proc Natl Acad Sci U S A 100:1723–1728

Solverson P, Murali SG, Brinkman AS et al (2012) Glycomacropeptide, a low-phenylalanine protein isolated from cheese whey, supports growth and attenuates metabolic stress in the murine model of phenylketonuria. Am J Physiol Endocrinol Metab 302: E885–E895

Souza LC, Filho CB, Goes AT et al (2013) Neuroprotective effect of physical exercise in a mouse model of Alzheimer's disease

induced by beta-amyloid(1)(-)(4)(0) peptide. Neurotox Res 24:148–163

Stroth S, Reinhardt RK, Thone J et al (2010) Impact of aerobic exercise training on cognitive functions and affect associated to the COMT polymorphism in young adults. Neurobiol Learn Mem 94:364–372

Surtees R, Blau N (2000) The neurochemistry of phenylketonuria. Eur J Pediatr 159(Suppl 2):S109–S113

Takeda K, Machida M, Kohara A, Omi N, Takemasa T (2011) Effects of citrulline supplementation on fatigue and exercise performance in mice. J Nutr Sci Vitaminol 57:246–250

Tsou YH, Shih CT, Ching CH et al (2015) Treadmill exercise activates Nrf2 antioxidant system to protect the nigrostriatal dopaminergic neurons from MPP+ toxicity. Exp Neurol 263:50–62

van Bakel MM, Printzen G, Wermuth B, Wiesmann UN (2000) Antioxidant and thyroid hormone status in selenium-deficient phenylketonuric and hyperphenylalaninemic patients. Am J Clin Nutr 72:976–981

van Spronsen FJ, Hoeksma M, Reijngoud DJ (2009) Brain dysfunction in phenylketonuria: is phenylalanine toxicity the only possible cause? J Inherit Metab Dis 32:46–51

van Vliet D, Anjema K, Jahja R et al (2015) BH4 treatment in BH4-responsive PKU patients: preliminary data on blood prolactin concentrations suggest increased cerebral dopamine concentrations. Mol Genet Metab 114:29–33

Vilaseca MA, Lambruschini N, Gomez-Lopez L et al (2010) Quality of dietary control in phenylketonuric patients and its relationship with general intelligence. Nutr Hosp 25:60–66

Weglage J, Fromm J, van Teeffelen-Heithoff A et al (2013) Neurocognitive functioning in adults with phenylketonuria: results of a long term study. Mol Genet Metab 110(Suppl): S44–S48

Wipfli B, Landers D, Nagoshi C, Ringenbach S (2011) An examination of serotonin and psychological variables in the relationship between exercise and mental health. Scand J Med Sci Sports 21:474–481

JIMD Reports
DOI 10.1007/8904_2015_460

RESEARCH REPORT

Seizures Due to a *KCNQ2* Mutation: Treatment with Vitamin B_6

Emma S. Reid · Hywel Williams · Polona Le Quesne Stabej · Chela James · Louise Ocaka · Chiara Bacchelli · Emma J. Footitt · Stewart Boyd · Maureen A. Cleary · Philippa B. Mills · Peter T. Clayton

Received: 09 April 2015 / Revised: 13 May 2015 / Accepted: 19 May 2015 / Published online: 8 October 2015
© SSIEM and Springer-Verlag Berlin Heidelberg 2015

Abstract There is increasing evidence that vitamin B_6, given either as pyridoxine or pyridoxal 5′-phosphate, can sometimes result in improved seizure control in idiopathic epilepsy. Whole-exome sequencing was used to identify a *de novo* mutation (c.629G>A; p.Arg210His) in *KCNQ2* in a 7-year-old patient whose neonatal seizures showed a response to pyridoxine and who had a high plasma to CSF pyridoxal 5′-phosphate ratio, usually indicative of an inborn error of vitamin B_6 metabolism. This mutation has been described in three other patients with neonatal epileptic encephalopathy. A review of the literature was performed to assess the effectiveness of vitamin B_6 treatment in patients with a KCNQ2 channelopathy. Twenty-three patients have been reported to have been trialled with B_6; in three of which B_6 treatment was used alone or in combination with other antiepileptic drugs to control seizures. The anticonvulsant effect of B_6 vitamers may be propagated by multiple mechanisms including direct antagonist action on ion channels, antioxidant action on excess reactive oxygen species generated by increased neuronal firing and replenishing the pool of pyridoxal 5′-phosphate needed for the synthesis of some inhibitory neurotransmitters. Vitamin B_6 may be a promising adjunctive treatment for patients with channelopathies and the wider epileptic population. This report also demonstrates that an abnormal plasma to CSF pyridoxal 5′-phosphate ratio may not be exclusive to inborn errors of vitamin B_6 metabolism.

Communicated by: Nicole Wolf, MD PhD

Competing interests: None declared

Emma S. Reid and Hywel Williams contributed equally to the manuscript.

Electronic supplementary material: The online version of this chapter (doi:10.1007/8904_2015_460) contains supplementary material, which is available to authorized users.

E.S. Reid · H. Williams · P.L.Q. Stabej · C. James · L. Ocaka · C. Bacchelli · P.B. Mills · P.T. Clayton (✉)
Centre for Translational Omics, Genetics and Genomic Medicine, UCL Institute of Child Health, 30 Guilford Street, London, UK WC1N 1EH
e-mail: peter.clayton@ucl.ac.uk

E.J. Footitt · M.A. Cleary
Metabolic Medicine Department, Great Ormond Street Hospital NHS Foundation Trust, Great Ormond Street, London, UK WC1N 3JH

S. Boyd
Electrophysiology Department, Great Ormond Street Hospital NHS Foundation Trust, Great Ormond Street, London, UK WC1N 3JH

Introduction

Pyridoxine-dependent epilepsy (PDE) (OMIM 266100) was first described by Hunt et al. (1954). Typically patients present with antiepileptic drug-resistant seizures in the neonatal period that respond dramatically to pyridoxine (PN) and remain seizure-free on this treatment. This metabolic defect has been shown to be due to a deficiency of α-aminoadipic semialdehyde (α-AASA) dehydrogenase, an enzyme on the lysine catabolic pathway (Mills et al. 2010). The accumulating upstream metabolite, L-Δ^1-piperideine-6-carboxylate (P6C), forms an adduct with pyridoxal 5′-phosphate (PLP), the active form of vitamin B_6, rendering it inactive as a cofactor. P6C is in equilibrium with α-AASA, and it is the measurement of these compounds in urine, CSF or plasma that now forms the biochemical basis for diagnosis, alongside molecular genetic analysis of *ALDH7A1*. Patients with pyridox(am)ine 5′-phosphate oxidase (PNPO) deficiency (OMIM 610090) are also now being recognised as responding to

PN, despite early patient cohorts only showing a clinical response to PLP (Mills et al. 2014).

In the majority of patients with PDE, treatment with intravenous PN (50 or 100 mg single dose) followed by a maintenance oral dosing regimen of 5–15 mg/kg/day (maximum 200 mg/day) results in seizure resolution. Whilst the long-term outcome is variable, most children have a degree of developmental delay involving cognitive impairment and speech and language problems. However, a recent review reports 31% of patients having normal developmental outcome (Guerin et al. 2014).

Many reports suggest that a variety of children with epilepsy can respond, either long term or transiently, to vitamin B_6 treatment (Ohtahara et al. 2011). One study suggested that PLP was effective in controlling up to 46% of children with intractable infantile spasms and 11.7% with idiopathic intractable epilepsy, the oldest of which was 15 years old (Wang et al. 2005). Whilst the genetic and biochemical basis for the response of many of these patients has not been investigated, the proportion responding is so high that it is unlikely that they all have antiquitin or PNPO deficiency. Whole-exome sequencing is one method that can be used to investigate the genetic aetiologies of cases such as these. We present the case of a girl whose neonatal seizures appeared to respond to a vitamin supplement containing PN and who had a high plasma to CSF PLP ratio indicative of a vitamin B_6 disorder. However, at 7 years of age, she was shown to have a channelopathy caused by a *de novo* mutation in the potassium voltage-gated channel, KQT-like subfamily, member 2 (*KCNQ2)* gene.

Case Report

The patient, a daughter of unrelated parents, was born by spontaneous labour at 38+6 weeks after an uneventful pregnancy. Good foetal movements were reported. The baby had hiccoughs during the last trimester, although similar movements were also reported during the mother's first pregnancy with an unaffected child.

She was born in good condition and discharged on day three of life. Prior to this, she suffered two episodes of facial reddening, stiffening and then becoming pale; these were associated with feeding and thus assumed to be reflux. One day post-discharge, she had episodes of choking and cyanosis, associated with stiffening after which she became floppy. Further seizures on day 4 were documented at her local hospital; these were accompanied by 'cycling' movements of her arms with oxygen saturations dropping to 68%, lasting less than 1 min. A full septic screen including a lumbar puncture was negative and she was given a loading dose of phenobarbitone. Seizures continued following this requiring control with phenobarbitone, phenytoin and lorazepam.

At 9 days of age, she had a normal cranial ultrasound and CT scan but an electroencephalogram (EEG) demonstrated some asymmetry with larger amplitude responses on the right and abnormal paroxysmal components. A brain MRI on day 28 demonstrated normal brain structures with appropriate maturation but some increased signal intensity in the subthalamic nuclei around the lateral geniculate nuclei bilaterally.

A series of biochemical investigations (7 days–1 month) demonstrated mild, but likely insignificant, abnormalities of plasma amino acids (Data S2). Urine analysis showed widespread mild elevation of multiple amino acids and organic acid analysis revealed mildly elevated 2-oxoglutarate and pyruvate interpreted as a possible renal tubule leak or immaturity. Other analytes found to be high were gamma-glutamyl transferase 256 U/L (ref: 12–43 U/L) and alkaline phosphatase 342 U/L (ref: 129–291 U/L), a common finding in children on anticonvulsants.

By 6 weeks of age, seizures continued to occur sporadically, beginning with both eyes staring towards the corner of the room, mouth pouting, clonic movements of both limbs and respiratory grunting sounds. A repeat EEG at this time demonstrated abnormal delta activities and intermittently occurring angular or sharp waves, mainly anteriorly whilst at rest. Conversely, when she cried or had been alerted, the recording was of lower voltage without sharp waves but the content was abnormal. An electrocardiogram showed a normal corrected QT interval. At 2 months of age, she was commenced on 0.3 mL of DaliVit multivitamin oral drops per day, a dose which contained 0.25 mg of PN. Seizures were reported to have ceased 6 days after this, at a time when she was also receiving 6.7 mg/kg/day of phenytoin and 11 mg/kg/day of carbamazepine. Further biochemical testing (3 months) revealed a plasma PLP level of 670 nmol/L (ref: 15–73 nmol/L) but a CSF PLP level of 12 nmol/L (ref: 14–92 nmol/L). This high plasma to CSF PLP gradient suggested an abnormality of vitamin B_6 metabolism; thus, she was commenced on 5 mg/kg/day of PN. Urinary α-AASA was not elevated and no mutations were detected in *ALDH7A1* or *PNPO*.

Throughout the following 2 years, she continued to have seizures, mainly during intercurrent illness, requiring 15 mg/kg/day of carbamazepine for control, in addition to PN supplementation. An MRI and EEG were unremarkable; therefore, weaning of carbamazepine was carried out over a period of 2 months. Three days after weaning, she had two generalised seizures lasting between 3 and 4 min, consisting of tongue biting, stiffening, going pale, grunting, frothing at the mouth and becoming floppy afterwards. The carbamazepine was recommenced at her original dose but

she became very ataxic (a side effect of this medication); therefore, the dose was halved (7.3 mg/kg/day). Neurotransmitter analysis (4 years) revealed a slightly low level of methyltetrahydrofolate of 41 nmol/L (ref: 52–178 nmol/L); thus she was started on calcium folinate (7.5 mg/day).

Since commencing PN treatment (at four months), her dose had been increased to 15.6 mg/kg/day in addition to 7.3 mg/kg/day of carbamazepine, in line with weight gain. She is developmentally delayed (7 years old) with minimal expressive language and attends a special school but remains healthy except for seizures in the context of intercurrent illness. A recent EEG has shown a change to a left temporal lobe focus. Since genetic diagnosis, weaning of PN has commenced and her dose has been halved with no increase in seizures.

Methods

This study was approved by the ethics committee of Great Ormond Street Hospital for Children and National Research Ethics Committee London (Bloomsbury). Whole-exome sequencing (WES) was carried out for the proband and parents (BGI Genomics, Hong Kong). Further details of sequencing and data analysis techniques can be found in Data S3.

Results

WES data was analysed initially assuming that this disorder had been inherited in an autosomal recessive manner. No plausible variants were identified that fitted a homozygous or compound heterozygous inheritance pattern. Since there was no family history of the disorder, data was reanalysed to look for *de novo* variants. Stringent filtering identified 7 variants (7 genes). The best candidate was a known pathogenic *de novo* missense change (c.629G>A; p.Arg210His) in exon 1 of *KCNQ2* (Fig. 1). WES data was also scrutinised for potentially pathogenic variants in genes known to cause inborn errors of B_6 metabolism, a high plasma to CSF PLP ratio or hyperphosphatasia, namely, *PNPO*, *ALDH7A1*, *ALPL* and genes involved in glycosylphosphatidylinositol (GPI) anchor synthesis. None were identified.

A comprehensive literature review of reports indexed in PubMed describing patients with *KCNQ2* mutations who have had a trial of vitamin B_6 was performed using the terms KCNQ2 and epilepsy. Ten reports detailing 23 patients with mutations in *KCNQ2* having been trialled on vitamin B_6, either transiently or on a long-term basis (Data S1) were found. Three of these were reported to have had a clinical response to varying degrees. The first, a patient with a 1.5-Mb terminal deletion of the long arm of chromosome 20 which included deletion of *KCNQ2*, masqueraded as pyridoxine-dependent epilepsy with a 95% reduction in seizure activity seen within 1 min of administration of intravenous PN (Mefford et al. 2012). The others included a child with benign familial neonatal seizures (BFNS) reported to have been treated acutely with PLP (Allen et al. 2014) and a child with neonatal epileptic encephalopathy (NEE) in which a combination of topiramate, vigabatrin and PN controlled seizures (Weckhuysen et al. 2012). 6/23 additional patients were treated with vitamin B_6 during the first month of life; however, responses to each antiepileptic drug (AED) were not stated. Whilst in the majority of patients no clinical improvement was noted, this may be related to the length of trial they received and other AEDs that were being taken concurrently. None of the patients were documented as having CSF PLP measured.

Discussion

The patient described here had an apparent improvement in seizure control on PN treatment and had an abnormally high plasma to CSF PLP ratio prior to PN supplementation. Antiquitin and PNPO deficiency were both ruled out biochemically and/or genetically. The high plasma PLP level whilst on only 0.25 mg/day (0.07 mg/kg/day) PN was noteworthy, being much higher than levels reported in healthy individuals and similar to levels in adults taking 40 mg/day (0.63 mg/kg/day) PN (Midttun et al. 2005) and in fact more comparable to children taking 200 mg/day (8 mg/kg/day) for treatment of PDE (Footitt et al. 2013). Moreover, the plasma to CSF PLP ratio of 55.8 was very striking, being much higher than the upper limit of 4.4 in paediatric patients with neurological disease (Footitt et al. 2011). The only other genetically defined disorder in which a high plasma to CSF PLP ratio has been documented is hypophosphatasia due to mutations in alkaline phosphatase (*ALPL*). Defects in GPI anchor biosynthesis can also cause B_6-responsive epilepsy (Kuki et al. 2013) due to a decrease of the membrane-associated tissue non-specific alkaline phosphatase required to allow PLP to enter the brain. No potentially pathogenic variants were found in these genes. This report confirms the utility of WES for the diagnosis of childhood epilepsy and reveals that this patient's neonatal epilepsy and developmental disorder were caused by a *de novo* dominant mutation in *KCNQ2*. With the benefit of hindsight, this patient may have been diagnosed using a targeted epilepsy gene panel. Targeted gene panel sequencing has advantages over WES, including increased depth of gene coverage, more robust coverage of regions of interest and reduced incidental findings. WES was employed in this case due to the atypical presentation and biochemical

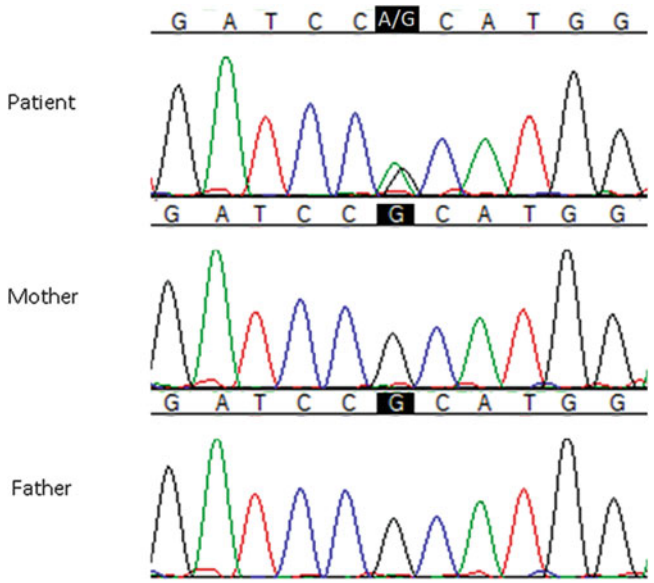

Fig. 1 *KCNQ2* sequence analysis of affected family. The affected individual shows a heterozygous missense change from G to A at position 629 of the cDNA (c.629G>A) causing a change of amino acid 210 from arginine to histidine (p.Arg210His)

findings; however, diagnostic panels remain a timely and cost-effective alternative for the diagnostic workup of children with neonatal/infantile epilepsies.

KCNQ2 encodes a voltage-gated potassium channel expressed in the brain (Biervert et al. 1998) and plays a critical role in determining response to synaptic inputs and subthreshold electroexcitability of neurons. Dominant mutations in *KCNQ2* result in a range of epileptic disorders including Ohtahara syndrome, NEE and 60–70% of BFNS (Weckhuysen et al. 2013). The evidence that the mutation found in our patient causes epileptic encephalopathy is strong. Three patients have been reported previously to have the same *de novo* p.Arg210His mutation (Weckhuysen et al. 2013; Numis et al. 2014). All had NEE presenting with seizures on the first day of life and, similarly to our patient, two became seizure-free on administration of carbamazepine after failure of other AEDs. Carbamazepine acts to stabilise the inactive state of voltage-gated sodium channels which co-localise with KCNQ potassium channels in neuronal membranes (Pan et al. 2006). Thus modulation of one channel may affect the function of the channel complex. The other patient showed no improvement on carbamazepine treatment and died shortly afterwards due to respiratory failure in the context of infection (Numis et al. 2014). None of these three patients were trialled on vitamin B_6.

Whilst KCNQ2-related epilepsy is very variable phenotypically, seizures, characterised by cyanosis or apnoea as seen in the case described, are a common presentation (Allen et al. 2014). The tonic stiffening and choking seen initially, associated with asynchronous discontinuity of EEG activities, have some parallels with the much more severe electro-clinical phenotype described in KCNQ2 encephalopathy. However, in this case, the EEG abnormalities remained mild, with resolution of any discontinuity within 2 weeks and normal findings during initial treatment with vitamin B_6. All EEG changes were non-specific and no distinctive electro-clinical pattern was discernible.

One of the most striking features seen in our patient, which directed further metabolic investigations, was her abnormally high plasma to CSF PLP ratio. The role of oxidative stress resulting from excessive free-radical production in epilepsy initiation and propagation is becoming a well-accepted paradigm and may explain this biochemical finding in our patient. Many studies have demonstrated that repeated seizure activity results in increased oxidation of cellular macromolecules such as proteins, lipids and nucleotides, which in turn can lead to neuronal death. It has been hypothesised that a cascade of events including excessive neuronal firing, increased glutamate release, N-methyl-D-aspartate receptor activation, influx of calcium into the cytosol and mitochondria and increased ATP consumption leads to abundant production of reactive oxygen species (ROS) (Shin et al. 2011). The brain is rich in mitochondria due to its high metabolic demand and it is plausible that this ROS production may overwhelm the normal mitochondrial antioxidant defences leading to mitochondrial dysfunction and greater superoxide production through a damaged respiratory chain, thus producing a self-perpetuating vicious cycle of oxidative stress. B_6 vitamers can also be attacked by oxygen-derived free radicals (Footitt et al. 2011) thereby depleting PLP in the CSF, as seen in our patient. Indeed ROS can also react with and deplete folates (Footitt et al. 2011) which would explain the low 5-methyltetrahydrofolate seen in our patient.

There is increasing evidence that vitamin B_6, given either as PN or PLP, can result in improved seizure control in idiopathic epilepsy (Ohtahara et al. 2011). However, the mechanisms underlying this response are unknown. Our patient showed an apparent improvement in seizure control upon starting multivitamin drops containing 0.25 mg of PN. If excessive ROS production due to unregulated neuronal firing results in the CSF PLP deficiency seen in our patient, it is intuitive that PN supplementation should correct this abnormality. In addition to this, a number of studies have demonstrated the antioxidant properties of the B_6 vitamers by preventing oxygen radical generation and lipid peroxidation (Chumnantana et al. 2005). Treatment with PN/PLP may therefore prevent secondary seizures due to oxidative stress-induced PLP depletion cause by unregulated neuronal firing, as well as curtailing the cycle of mitochondrial and neuronal dysfunction.

PLP has recently been shown to inhibit P2X receptors in vitro (Thériault et al. 2014). These receptors are cation-permeable ligand-gated ion channels that are activated by ATP and gate fast depolarising sodium and calcium entry. Effects of their activation include neuromodulation under conditions of excessive firing and indirect effects on excitability by control of neuroinflammation and gliosis (Henshall et al. 2013). Certain P2X receptors, particularly P2X7R, have been shown to be activated during pathologic brain activity including neuronal necrosis due to excitotoxicity and prolonged or repeated brief seizures. This activation modulates neurotransmitter release, promotes activation and release of interleukin 1β (a proconvulsant) from microglia and acts on oligodendrocytes and astrocytes to trigger cell death (Henshall et al. 2013). P2X7R antagonists have been reported to have potent anticonvulsant effects (Jimenez-Pacheco et al. 2013); thus, it is possible that PLP is having anticonvulsant effects by acting as a P2X7R antagonist. It is also possible that the action of PLP is not only limited to P2X receptors. Perhaps PLP is also a ligand of the KCNQ family of potassium channels; the clinical improvement seen in our patient upon PN supplementation may then be due to PLP modulation of excessive firing due to the lack of inhibitory potassium current due to *KNCQ2* mutations.

Finally, one effect of the lack of inhibitory current and thus excessive neuronal firing is a depletion of inhibitory neurotransmitters, for example, γ-aminobutyric acid (GABA). GABA is synthesised from glutamate by the enzyme L-glutamic acid decarboxylase for which PLP is a cofactor. Supplementation with either PN or PLP may favour conversion of glutamate to GABA, leading to anticonvulsant effects.

Unfortunately, there are no prospective studies observing CSF PLP levels in seizure patients on various AEDs to determine whether low PLP is a general finding in all patients independent of underlying genetic defect. In addition, there are no studies of CSF PLP levels in healthy newborns or infants. All reference ranges are generated from neurologically abnormal children undergoing CSF metabolite measurement for diagnostic workup. Thus there are limitations in establishing a true reference range and these vary throughout the literature, making interpretation of low values such as those seen in our patient difficult.

Despite the potential benefits of vitamin B_6 as an anticonvulsant, there are well-documented adverse effects that can occur in patients taking high doses, namely, peripheral neuropathy for PN and liver toxicity for PLP (Mills et al. 2014). We recommend that patients with intractable epilepsy, including those with channelopathies, should be trialled on B_6 and in those showing a response liver function and nerve conduction should be tested periodically. In addition, a trial of discontinuation should be carried out to confirm that there is a real necessity for PN/PLP supplementation.

Conclusions

We present the case of a girl whose neonatal seizures showed an apparent improvement on PN treatment and had an abnormally high plasma to CSF PLP ratio, who at 7 years of age was shown to have a channelopathy disorder caused by a *de novo* mutation in *KCNQ2*. In previous reports, the anticonvulsant effect of vitamin B_6 was assumed to be coincidental or not discussed further, perhaps due to the lack of dramatic response. We hypothesise that the anticonvulsant effect of B_6 vitamers may be more universal than previously thought and may be propagated by multiple mechanisms: (1) direct antagonist action on ion channels, (2) antioxidant action on excess ROS generated by increased neuronal firing and (3) replenishing the pool of PLP needed for the synthesis of some inhibitory neurotransmitters. Further work is required to understand these proposed mechanisms and its utility as an adjunctive treatment for patients with *KNCQ2* mutations and the wider epileptic population.

Acknowledgements We would like to thank the child and her family for participating in this study and for consenting to this report. Additional thanks to Emma Wakeling and Frances Cowen for consenting and referring the patient to our centre, respectively. PBM and PTC are supported by Great Ormond Street Hospital Children's Charity (GOSHCC). This project was funded by grants from the University College London Impact Award and GOSHCC Metabolic Fund. GOSgene is supported by the NIHR BRC at GOSH for Children NHS Foundation Trust and UCL Institute of Child Health. Views expressed are those of the author(s) and not necessarily those of the NHS, the National Institute for Health Research or the Department of Health.

Take-Home Message

This paper presents a case of KCNQ2 channelopathy showing an apparent response to pyridoxine treatment and indicates that a high plasma to CSF pyridoxal 5′-phosphate ratio is not specific for disorders directly affecting vitamin B_6 metabolism.

Compliance with Ethics Guidelines

Conflict of Interest

Emma S. Reid, Hywel Williams, Polona Le Quesne Stabej, Chela James, Louise Ocaka, Chiara Bacchelli, Emma J. Footitt, Stewart Boyd, Maureen A. Cleary, Philippa B. Mills and Peter T. Clayton declare that they have no conflict of interest.

All procedures followed were in accordance with the ethical standards of the responsible committee on human experimentation (institutional and national) and with the Helsinki Declaration of 1975, as revised in 2000 (5). Informed consent was obtained from all patients for being included in the study.

All authors have read the manuscript and agreed to it being submitted for publication. All individuals listed as authors meet the appropriate authorship criteria, nobody who qualifies for authorship has been omitted from the list, contributors and their funding sources have been properly acknowledged, and all authors and contributors have approved the acknowledgement of their contributions. Emma Reid contributed to data analysis and wrote and submitted the manuscript. Hywel Williams, Polona Le Quesne Stabej, Chela James and Louise Ocaka together prepared the DNA samples for whole-exome sequencing, analysed the data and confirmed the pathogenic mutation. Emma Footitt submitted the initial application for whole-exome sequencing to be carried out. Chiara Bacchelli considered and accepted the application for sequencing. Peter Clayton, Maureen Cleary, Emma Footitt and Emma Reid consulted with the patient and her family regarding the research and the results of the study. Stewart Boyd reviewed all EEGs from the patient. Philippa Mills and Peter Clayton made large contributions to the critical revision of the manuscript. All authors had access to the study data that support this publication.

References

Allen NM, Mannion M, Conroy J et al (2014) The variable phenotypes of KCNQ-related epilepsy. Epilepsia 55(9):e99–e105

Biervert C, Schroeder BC, Kubisch C et al (1998) A potassium channel mutation in neonatal human epilepsy. Science 279(5349):403–406

Chumnantana R, Yokochi N, Yagi T (2005) Vitamin B_6 compounds prevent the death of yeast cells due to menadione, a reactive oxygen generator. Biochim Biophys Acta 1722(1):84–91

Footitt EJ, Heales SJ, Mills PB, Allen GF, Oppenheim M, Clayton PT (2011) Pyridoxal 5′-phosphate in cerebrospinal fluid; factors affecting concentration. J Inherit Metab Dis 34 (2):529–538

Footitt EJ, Clayton PT, Mills K et al (2013) Measurement of plasma B6 vitamer profiles in children with inborn errors of vitamin B6 metabolism using an LC-MS/MS method. J Inherit Metab Dis 36(1):139–145

Guerin A, Aziz AS, Mutch C et al (2014) Pyridox(am)ine-5-phosphate oxidase deficiency treatable cause of neonatal epileptic encephalopathy with burst suppression: case report and review of the literature. J Child Neurol. doi:10.1177/0883073814550829

Henshall DC, Diaz-Hernandez M, Miras-Portugal MT, Engel T (2013) P2X receptors as targets for the treatment of status epilepticus. Front Cell Neurosci 7:237

Hunt AD, Stokes J, McCrory WW, Stroud HH (1954) Pyridoxine dependency: report of a case of intractable convulsions in an infant controlled by pyridoxine. Pediatrics 13(2):140–145

Jimenez-Pacheco A, Mesuret G, Sanz-Rodriguez A et al (2013) Increased neocortical expression of the P2X7 receptor after status epilepticus and anticonvulsant effect of P2X7 receptor antagonist A-438079. Epilepsia 54(9):1551–1561

Kuki I, Takahashi Y, Okazaki S et al (2013) Vitamin B6-responsive epilepsy due to inherited GPI deficiency. Neurology 81 (16):1467–1469

Mefford HC, Cook J, Gospe SM Jr (2012) Epilepsy due to 20q13.33 subtelomere deletion masquerading as pyridoxine-dependent epilepsy. Am J Med Genet A 158A(12):3190–3195

Midttun O, Hustad S, Solheim E, Schneede J, Ueland PM (2005) Multianalyte quantification of vitamin B6 and B2 species in the nanomolar range in human plasma by liquid chromatography-tandem mass spectrometry. Clin Chem 51(7):1206–1216

Mills PB, Footitt EJ, Mills KA et al (2010) Genotypic and phenotypic spectrum of pyridoxine-dependent epilepsy (ALDH7A1 deficiency). Brain 133(Pt 7):2148–2159

Mills PB, Camuzeaux SS, Footitt EJ et al (2014) Epilepsy due to PNPO mutations: genotype, environment and treatment affect presentation and outcome. Brain 137(Pt 5):1350–1360

Numis AL, Angriman M, Sullivan JE et al (2014) KCNQ2 encephalopathy: delineation of the electroclinical phenotype and treatment response. Neurology 82(4):368–370

Ohtahara S, Yamatogi Y, Ohtsuka Y (2011) Vitamin B(6) treatment of intractable seizures. Brain Dev 33(9):783–789

Pan Z, Kao T, Horvath Z et al (2006) A common ankyrin-G-based mechanism retains KCNQ and NaV channels at electrically active domains of the axon. J Neurosci 26(10):2599–2613

Shin EJ, Jeong JH, Chung YH et al (2011) Role of oxidative stress in epileptic seizures. Neurochem Int 59(2):122–137

Thériault O, Poulin H, Thomas GR, Friesen AD, Al-Shaqha WA, Chahine M (2014) Pyridoxal-5′-phosphate (MC-1), a vitamin B6 derivative, inhibits expressed P2X receptors. Can J Physiol Pharmacol 92(3):189–196

Wang HS, Kuo MF, Chou ML et al (2005) Pyridoxal phosphate is better than pyridoxine for controlling idiopathic intractable epilepsy. Arch Dis Chil 90(5):512–515

Weckhuysen S, Mandelstam S, Suls A et al (2012) KCNQ2 encephalopathy: emerging phenotype of a neonatal epileptic encephalopathy. Ann Neurol 71(1):15–25

Weckhuysen S, Ivanovic V, Hendrickx R et al (2013) Extending the KCNQ2 encephalopathy spectrum: clinical and neuroimaging findings in 17 patients. Neurology 81(19):1697–1703

JIMD Reports
DOI 10.1007/8904_2015_435

RESEARCH REPORT

The Frequencies of Different Inborn Errors of Metabolism in Adult Metabolic Centres: Report from the SSIEM Adult Metabolic Physicians Group

S. Sirrs • C. Hollak • M. Merkel • A. Sechi • E. Glamuzina • M.C. Janssen • R. Lachmann • J. Langendonk • M. Scarpelli • T. Ben Omran • F. Mochel the SFEIM-A Study Group • M.C. Tchan

Received: 16 November 2014 / Revised: 19 March 2015 / Accepted: 23 March 2015 / Published online: 9 October 2015
© SSIEM and Springer-Verlag Berlin Heidelberg 2015

Communicated by: Francois Feillet, MD, PhD

For the SFEIM-A (Société Française des Erreurs Innées du Métabolisme Adulte) Study Group: Besson G (Grenoble), Bienvenu B (Caen), Corne C (Grenoble), Douillard C (Lille), Garnotel R (Reims), Goizet C (Bordeaux), Jaussaud R (Reims), Kaminsky P (Nancy), Kaphan E (Marseille), Laforêt P (Pitié-Salpêtrière hospital, Paris), Lavigne C (Angers), Leguy-Seguin V (Dijon), Maillot F (Tours), Mazodier K (Marseille), Mochel F (Pitié-Salpêtrière Hospital, Paris), Nadjar Y (Pitié-Salpêtrière Hospital, Paris), Noel E (Strasbourg), Read MH (Caen), Servais A (Necker Hospital, Paris), Thauvin C (Dijon) and Tourbah A (Reims).

Electronic supplementary material: The online version of this chapter (doi:10.1007/8904_2015_435) contains supplementary material, which is available to authorized users.

S. Sirrs
Vancouver General Hospital, Vancouver, BC, Canada

C. Hollak
Amsterdam Medical Centre, Amsterdam, The Netherlands

M. Merkel
Asklepios Klinik St. Georg, Hamburg, Germany

A. Sechi
Azienda Ospedaliero-Universitaria S. Maria della Misericordia, Udine, Italy

E. Glamuzina
Starship Children's Hospital, Auckland, New Zealand

M.C. Janssen
Nijmegen Medical Centre, Nijmegen, The Netherlands

R. Lachmann
National Hospital for Neurology and Neurosurgery, London, UK

J. Langendonk
Erasmus Medical Centre, Rotterdam, The Netherlands

M. Scarpelli
University Hospital GB Rossi, Verona, Italy

T. Ben Omran
Qatar Medical Genetic Centre, Doha, Qatar

Abstract *Background*: There are few centres which specialise in the care of adults with inborn errors of metabolism (IEM). To anticipate facilities and staffing needed at these centres, it is of interest to know the distribution of the different disorders.

Methods: A survey was distributed through the list-serve of the SSIEM Adult Metabolic Physicians group asking clinicians for number of patients with confirmed diagnoses, types of diagnoses and age at diagnosis.

Results: Twenty-four adult centres responded to our survey with information on 6,692 patients. Of those 6,692 patients, 510 were excluded for diagnoses not within the IEM spectrum (e.g. bone dysplasias, hemochromatosis) or for age less than 16 years, leaving 6,182 patients for final analysis. The most common diseases followed by the adult centres were phenylketonuria (20.6%), mitochondrial disorders (14%) and lysosomal storage disorders (Fabry disease (8.8%), Gaucher disease (4.2%)). Amongst the disorders that can present with acute metabolic decompensation, the urea cycle disorders, specifically ornithine transcarbamylase deficiency, were most common (2.2%), followed by glycogen storage disease type I (1.5%) and maple syrup urine disease (1.1%). Patients were frequently diagnosed as adults, particularly those with mitochondrial disease and lysosomal storage disorders.

Conclusions: A wide spectrum of IEM are followed at adult centres. Specific knowledge of these disorders is needed to provide optimal care including up-to-date

F. Mochel
Hospitalier Pitié-Salpêtrière, Paris, France

M.C. Tchan (✉)
Westmead Hospital, Sydney, Australia
e-mail: michelt@gmp.usyd.edu.au

knowledge of treatments and ability to manage acute decompensation.

Abbreviations

ACE	Angiotensin-converting enzyme
CESD	Cholesteryl ester storage disease
CPEO	Chronic progressive external ophthalmoplegia
CPT1	Carnitine palmitoyltransferase 1
CPT2	Carnitine palmitoyltransferase 2
GSDb	Glycogen storage disease
IEM	Inborn errors of metabolism
LCHAD	Long-chain 3-hydroxyacyl-CoA dehydrogenase deficiency
MCAD	Medium-chain acyl-CoA dehydrogenase deficiency
MELAS	Mitochondrial myopathy, encephalitis, lactic acidosis and stroke-like episodes
MERRF	Myoclonic epilepsy with ragged red fibres
MIDD	Maternally inherited diabetes and deafness
MMA	Methylmalonic aciduria
MPS	Mucopolysaccharidosis
MSUD	Maple syrup urine disease
MTHFR	Methylenetetrahydrofolate reductase deficiency
MTP	Mitochondrial trifunctional protein deficiency
NAGS	*N*-Acetyl glutamate synthase deficiency
OTC	Ornithine transcarbamylase deficiency
PKU	Phenylketonuria
SCAD	Short-chain acyl-CoA dehydrogenase deficiency
SSIEM	Society for the Study of Inborn Errors of Metabolism
TMAU	Trimethylaminuria
VLCAD	Very-long-chain acyl-CoA dehydrogenase deficiency
X-ALD	X-linked adrenoleukodystrophy

Introduction

The care of adults with inborn errors of metabolism (IEM) is an expanding subspecialty due to the improved survival of children with classical IEM, the recognition of milder forms of disease diagnosed in adulthood and late-onset disorders presenting in adulthood. Reflecting this increased interest, the Adult Metabolic Physicians working group of the Society for the Study of Inborn Errors of Metabolism (SSIEM) was formed in 2010 under the leadership of Frederic Sedel (Pitié-Salpêtrière Hospital, Paris, France) (http://www.ssiem.org/amp/welcome.asp). Clinical departments with a particular adult interest have developed in various countries, including large and well-established centres in the United Kingdom, Canada and the Netherlands and national networks such as in France the SFEIM-A – Société Française des Erreurs Innées du Métabolisme Adulte.

The prevalence of IEM in the adult population is unknown, as are the number and types of these patients being seen by metabolic physicians. How many of these patients were diagnosed and managed in childhood, as opposed to presenting with an adult-age diagnosis, is also unknown. Further information regarding the care of this patient population would thus be useful to anticipate needs for adult services, provide rationale for development of protocols and education, serve as a background for awareness amongst other physicians and identify centres with specific expertise for consultation, research and training.

Methods

All physicians who participate in the SSIEM Adult Metabolic Physicians group were contacted through e-mail in 2011 to submit anonymised patient data including diagnosis, age group at diagnosis (unknown, newborn screen, neonatal (week 1 of life), infantile (0–2 years), childhood (3–10 years), juvenile (11–16 years), adult (>16 years)) and current age. Initial data included all patients seen at each centre; hence, a number of patients with diagnoses not traditionally categorised as IEM were submitted but subsequently excluded from the analysis (excluded diagnoses list available from authors on request). Patients submitted who were younger than 16 years were also excluded. Only patients with a biochemical or genetically confirmed diagnosis were included in the analysis.

The numbers of each disorder were counted and grouped into metabolic subtypes. The median current age and age group at diagnosis for each disorder were calculated.

Updated total patient numbers were requested in 2014 to assess growth in service demand over this time. A number of French centres submitted initial limited data sets at this time which included patient numbers and diagnoses at each centre, but without current patient age or age at diagnosis.

Results

Initially 15 centres responded to our survey with data on 4,998 patients. With the addition of data from the French centres that are organised through a dedicated national society (the SFEIM-A, 1,694 patients), data was available on a total of 6,692 patients (Supplementary Table S1). Five hundred and ten patients were excluded from analysis for diagnoses not within the IEM spectrum (e.g. bone dysplasias, haemochromatosis) or for age less than 16 years (Supplementary Table S2), leaving 6,182 patients for final analysis. Two hundred and thirty-six separate diagnoses

Table 1 Submitted patient numbers from each clinical centre. Patients in the 2011 column were included in age and age at diagnosis analysis. Patients in the 2014 column were included in total patient numbers for each diagnosis

Centre location	Number of patients with confirmed metabolic diagnoses in 2011	Number of patients with confirmed metabolic diagnoses in 2014
London, United Kingdom	1,418	1,940
Vancouver, Canada	753	795 (estimated)
Rotterdam, Netherlands	551	564
Amsterdam, Netherlands	540	600
Sydney, Australia	499	583
Nijmegen, Netherlands	291	447
Auckland, New Zealand	278	358
Hamburg, Germany	132	155
Lille, France	124	126
Udine, Italy	117 (submitted in 2013)	117
Tours, France	106	100
Paris, France (Dr Mochel)	76	93
Doha, Qatar	71	95
Grenoble, France	35	43
Verona, Italy	7	12
Paris (Pitié-Salpêtrière hospital minus Dr Mochel patients), France		734
Paris (Necker Hospital), France		385
Angers, France		113
Marseille, France		98
Strasbourg, France		97
Reims, France		92
Bordeaux, France		63
Nancy, France		53
Dijon, France		49
Caen, France		10

Table 2 Thirty most frequent diagnoses and ages, including French patients added in 2014 in the total number, but not in the analysis of median age and age range which were not available for French patients. Four thousand eight hundred and seventy-one patients are included in this group of thirty diagnoses

Disorder	Number	Median age	Age range	Percentage of total patients
PKU	1,274	34	16–83	20.6
Fabry	544	45	19–82	8.8
Mitochondrial – CPEO	263	59.5	18–85	4.3
Gaucher	261	48	17–90	4.2
Mitochondrial	253	49	19–84	4.1
Homocystinuria	244	35	16–84	3.9
X-ALD	237	47	16–82	3.8
GSD II	220	55	18–83	3.6
Galactosaemia	165	29	18–64	2.7
Mitochondrial – MELAS	159	42	19–71	2.6
TMAU	146	44	20–79	2.4
GSD V	145	51.5	20–80	2.3
OTC	136	33	20–79	2.2
Hypophosphataemic rickets	87	36	18–79	1.4
MSUD	69	27	16–52	1.1
GSD III	60	38	21–67	1.0
GSD Ia	59	29	20–59	1.0
Niemann-Pick C	56	35	18–59	0.9
Mitochondrial – POLG	50	50	20–67	0.8
MCAD	48	23	18–49	0.8
MMA	48	25	19–44	0.8
Niemann-Pick B	45	39	0–60	0.7
MPS I	45	33.5	18–59	0.7
CPT2 deficiency	43	36	20–77	0.7
Carnitine transporter deficiency	40	31	17–61	0.6
Mitochondrial – MERRF	36	42	22–66	0.6
Porphyria	36	53	18–82	0.6
Porphyria – acute intermittent	35	51	25–81	0.6
MPS IV	35	35	19–59	0.6
Alkaptonuria	32	52	20–86	0.5

were documented, although in some disorders there was the potential for diagnostic overlap or ambiguity; for example, 12 patients were labelled with hyperhomocystinaemia, 244 were labelled with homocystinuria and a single patient was labelled as homocystinuria and MTHFR deficiency. The number of patients submitted from each centre varied from 7 to 1,418 (Table 1).

As expected, the most frequent disorder was phenylketonuria (PKU), representing 1,274 (20.6%) cases. The median age of PKU patients was 34 years, and diagnosis was predominantly via a newborn screening programme (413 of 499 (82.8%) patients with age of diagnosis data). Forty-six PKU patients were diagnosed as juveniles (13) or adults (33). The next most common diagnosis was Fabry disease (544 patients, 8.8%), followed by CPEO (263 patients, 4.3%) and Gaucher disease (261 patients, 4.2%). The 30 most common diagnoses are listed in Table 2.

Table 3 Number of patients grouped by disease categories, as defined in Saudubray et al. (2012). The urea cycle disorders are counted amongst the aminoacidopathies. The patient numbers for the lysosomal storage disorders do not include the mucopolysaccharidoses or peroxisomal disorders as they are counted in separate disease categories. A more detailed table is available in Supplementary Table S4

Disorder type	Number
Aminoacidopathy	2,061
Lysosomal	1,220
Mitochondrial	867
Peroxisomal	258
Glycogen storage	370
Fatty acid oxidation	221
Mucopolysaccharidoses	141
Porphyrias	101
Vitamin and cofactor	93

Disorders of amino acid metabolism (2,061 patients) were the most frequent when data were analysed according to types of disease (Table 3). Lysosomal storage disorders were the next most prevalent (1,220 patients) and were predominately Fabry (544), Gaucher (261) and Pompe (220) diseases. The broad group of mitochondrial disorders was strongly represented with 867 patients. Within these 867 patients, 253 did not have their phenotype described further, 162 had MELAS, 263 had CPEO, 23 had MIDD, 19 had Kearns-Sayre and other mitochondrial phenotypes were present to lesser degrees. The age group at onset was documented for 377 of these mitochondrial patients, and of these 317 were diagnosed in adulthood. Out of 258 patients with peroxisomal disorders, 237 had X-ALD. Patient numbers for each condition within the urea cycle disorders (201), disorders of fatty acid oxidation (225), mucopolysaccharidoses (141) and glycogen storage diseases (370, excluding Pompe) are shown in Table 4.

Data for the age group at diagnosis was available for 2,022 patients, all of whom were submitted in the initial group of cases (Table 5). Many were diagnosed as adults (925 patients, 45.7%), with the known remainder predominantly diagnosed via newborn screening (455 patients, 22.5%), although this number is largely patients with PKU (413 patients). Mitochondrial diseases accounted for the largest number of adult diagnoses (317 patients) followed by Fabry disease (137 patients) and then homocystinuria (45 patients).

Of the conditions that may present with fatal decompensations at any time of life, 29 patients with OTC deficiency were diagnosed as adults (age at diagnosis was available for 46 patients); however, patient gender was not

Table 4 Patient numbers for each diagnosis in the urea cycle disorders, fatty acid oxidation disorders, mucopolysaccharidoses, glycogen storage diseases (excluding GSD II) and total lysosomal disorders. Some disorders are divided into separate categories, depending on the amount of diagnostic detail submitted by the clinician; e.g. 11 patients with citrullinaemia may be type I or type II, but were not specified in the data submitted. Patient numbers include the French data from 2014

Disorder	Number of patients
Urea cycle	
OTC deficiency	136
Argininosuccinic aciduria	31
Citrullinaemia	11
Arginase deficiency	8
CPS	7
NAGS	4
Citrullinaemia type I	2
Fatty acid oxidation	
MCAD	48
CPT2 deficiency	43
Carnitine transporter deficiency	40
VLCAD	32
LCHAD	19
CPT1 deficiency	15
GA2	13
SCAD	7
MTP deficiency	4
Mucopolysaccharidoses	
MPS I	45
MPS IV	35
MPS III	20
MPS VI	17
MPS II	16
MPS IIIA	5
MPS IIIB	2
MPS VII	1
Glycogen storage diseases	
GSD V	145
GSD III	60
GSD Ia	59
GSD	25
GSD Ib	24
GSD IX	14
GSD IIIa	12
GSD VI	9
GSD IIIb	5
GSD IV	4
GSD VII	4
GSD IIId	1
GSD VIII	1

(continued)

Table 4 (continued)

Disorder	Number of patients
Total lysosomal	
Sphingolipidoses	965
Peroxisomal disorders	258
Pompe disease	220
Mucopolysaccharidoses	141
Oligosaccharidoses	30
Cystinosis	28
CESD	10
Ceroid lipofuscinoses	7

Table 5 Patient age group at diagnosis. French data submitted in 2014 was not included in this analysis

Age group at diagnosis	Number of patients	% of total with data (2022)
Unknown	2,466	n/a
Adult	925	45.7
Newborn screen	455	22.5
Juvenile	334	16.5
Infantile	255	12.6
Neonatal	44	2.2
Childhood	9	0.4

requested and so the proportion of these that are female is not known. Where age at diagnosis was submitted, all of the acute porphyrias were diagnosed in adulthood. Others with potentially unstable conditions were generally diagnosed in infancy or early childhood, although five patients with MSUD and two patients with MMA were diagnosed as juveniles.

Conditions where some form of treatment is available, whether dietary, enzyme replacement or other pharmacological means, were represented by 4,649 (75%) patients (Supplementary Table S3). Disorders in which bone marrow transplant may be offered, such as metachromatic leukodystrophy, were not included in this "treatable" cohort, although we appreciate that an argument could be made to include them.

Discussion

This paper is the first analysis of patient data from a group of clinical centres with a dedicated interest in adult patients with IEM. It demonstrates the wide spectrum of disease seen and is striking for the large numbers of patients that were diagnosed as adults and the growth in demand for these services in a relatively short period of time. We recognise that this data set is limited due to its ascertainment biases and as such does not represent a true picture of the burden of IEM in adults; however, it does make apparent that IEM in adults is far from restricted to PKU, mitochondrial disease and the lysosomal disorders.

Disease Frequencies

Newborn screening for PKU was instituted in many countries in the late 1960s and early 1970s, and this in combination with its relatively high prevalence (1 in 10,000 in Australia) makes it unsurprising that it is the most common disorder in this cohort. All centres saw patients with PKU, although the proportion varied widely. The frequency of mitochondrial patients is perhaps lower than expected as various studies have indicated that around 1 in 7,000 adults have a mitochondrial disorder (Schaefer et al. 2008). Given this prevalence we might have expected to see similar numbers of mitochondrial and PKU patients, however various factors likely account for this discrepancy – many patients will be seen by neurologists or other specialty facilities (such as that at Newcastle upon Tyne in the United Kingdom), as well as an incomplete diagnostic rate in adults. As our study only included patients with confirmed diagnoses, patients with "possible" or "probable" mitochondrial disease (a group which is expected to be significantly larger than the group of patients with a confirmed molecular diagnosis of mitochondrial disease) are not included in our data.

This data set is a "snapshot" of the patients that adult metabolic physicians care for and is a useful tool for service planning and building an awareness of the significant burden of adult metabolic disease. It is not however a comprehensive description of the epidemiology of these patients. For example, the number of patients with MCAD (48) is less than expected from prevalence data (1 in 4,900 (Sander et al. 2001) to 1 in 25,000 (Carpenter et al. 2001)). Fifty percent of MCAD patients remain undetected in the absence of screening (Wilcken et al. 2007), with the risk of death in this group about 5–7% in the first 6 years and very low thereafter (Wilcken 2010), although there are case reports of previously undiagnosed adults dying (Lang 2009). Thus, a good proportion of unscreened MCAD patients would be expected to reach adulthood undiagnosed. Some diagnosed MCAD patients would not be transitioned to adult services as a result of being lost to follow-up, and some may have been transitioned to alternative services such as adult endocrinology. The sample is also biased by the relative expertise and historical interests of each centre; for example, many of the Pompe patients come from the Rotterdam centre (106 of the 220

patients), and other centres see fewer patients. Similarly, 120 of the 146 TMAU patients and 70 of the 87 hypophosphataemic rickets were seen at the Charles Dent Metabolic Unit in London. Data was submitted from the European, Canadian and Asia-Pacific centres only; hence, our data may be different from patient populations seen at centres in the United States and elsewhere.

Age Group at Diagnosis

Age group at diagnosis was available for approximately 2,000 patients and showed that more than 40% were diagnosed in adulthood. This demonstrates the importance of adult physicians being aware of metabolic diseases as a diagnostic possibility. Mitochondrial disorders may present with any combination of organ dysfunctions and at any stage of life and may therefore be seen by nearly any type of specialist physician, although neurologists are perhaps the most likely to be involved given the strong representation of MELAS and CPEO patients in this group. Fabry disease was also diagnosed almost exclusively in adulthood (137 of 147 patients with age at diagnosis data), and given its prevalence in hypertrophic cardiomyopathy, stroke and end-stage renal failure cohorts (Rolfs et al. 2005; Gaspar et al. 2010; Palecek et al. 2014), its importance to adult physicians is noteworthy. It is, however, important to realise that a diagnosis of Fabry disease can be difficult. The availability of enzyme replacement therapy since 2,000 has triggered screening for this disorder, showing a steep rise in prevalence of genetic and enzymatic diagnoses. Traditionally, the prevalence of classical Fabry disease is estimated to be around 1 in 40,000 (Desnick et al. 2007), but this has changed to almost 1 in 3,000 in newborn screening programmes (Spada et al. 2006). Since most mutations in the *GLA* gene are private (Garman 2007), the pathogenicity of newly identified variants is not always clear. Many individuals picked up during screening do not fulfil the classic criteria, and hence, there may be an overestimation of cases (van der Tol et al. 2014).

Increasing Service Demands

Since these data was originally collected in 2011, each of these clinical centres has experienced growth in patient numbers (Table 1). The numbers listed in Table 1 include only those patients with confirmed metabolic diagnoses. Similar to paediatric services, many of the adult centres follow a large number of patients who are either in the process of undergoing diagnostic evaluation or in whom the results of such evaluation are inconclusive (such as patients with "possible" or "probable" mitochondrial disease) and these patients need also to be considered in the human resource requirements of adult clinics. The proportion of patients requiring ongoing follow-up but in whom a confirmed diagnosis had not yet been reached varied from 15% to 50% in those centres where it was known – these patients were not included in our analysis. Increasing awareness of adult metabolic services is responsible in part, as is ongoing transition of paediatric patients.

We are aware that there is a sizable population of paediatric metabolic patients who have been diagnosed by tandem mass spectrometry newborn screening. In New South Wales, Australia (population approximately 7.2 million), around twenty-five new patients with IEM are diagnosed each year and the oldest of these patients is 15 years. This approaching cohort of transitioning paediatric patients needs to be considered in future service planning.

There are an increasing number of previously rare metabolic defects, like carnitine transporter deficiency, being diagnosed in adult women when their infants have positive results on expanded newborn screening panels (Vijay et al. 2006). Although it is likely that many of these women will be asymptomatic for life, there are case reports suggesting that this disorder in adult women may be associated with adverse health consequences such as pregnancy loss (El-Hattab et al. 2010) and cardiomyopathy (Lee et al. 2010). These patients will need to be followed to clarify the long-term health consequences of these disorders, and thus, the expanded newborn screening panels adopted in many countries around the world have immediate resource implications for adult centres.

The majority of patients described in this cohort potentially have some form of treatment available to them; although in some localities ultra-expensive therapies like enzyme replacement may be unavailable. Given that many adult patients with IEM can be offered therapy, it would seem sensible that treatment be guided by physicians with expertise in these rare disorders. It should also not be forgotten that amongst these diseases are those that, even though extremely rare, can be well treated if diagnosed early, such as tyrosinaemia type II (5 patients) and cobalamin E deficiency (1 patient).

These data are also helpful in designing training programmes for physicians who wish to care for adults with inborn errors of metabolism. Training programmes need to include exposure to acute metabolic medicine, such as patients with decompensated urea cycle defects. However, such physicians also need expertise in adult neurology, allowing for the evaluation of myopathies, leukodystrophies, ataxic disorders and progressive cognitive impairment, and experience in general internal medicine to allow them to care for patients with lysosomal storage diseases (who require a wide range of common adult therapies such as ACE inhibitors, statins, antiplatelet agents and therapies for osteoporosis).

Conclusion

Our data show the wide range of paediatric and adult-onset IEM seen in these clinical centres. The increase in adult patient numbers is important to recognise, as it indicates an increasing need for specialty services to be available to these patients. Specialised knowledge of these disorders is needed to provide optimal care, including up-to-date monitoring and treatments and the ability to manage acute decompensation. We consider that care for this growing adult IEM patient population is important, as the vast majority of these people participate fully in society and the consequences of failed care can be catastrophic. This study also demonstrates useful collaboration between members of the SSIEM Adult Metabolic Physicians group and provides information that will hopefully pave the way for future cohort studies and clinical trials in adults with these rare disorders.

Acknowledgement The authors would like to dedicate this work to the memory of Dr Philip Lee, a pioneer in the care of adult patients with IEM.

Compliance with Ethics Guidelines

Conflict of Interest

Sandra Sirrs, Carla Hollak, Martin Merkel, Annalisa Sechi, Emma Glamuzina, Miriam Janssen, Robin Lachmann, Janneke Langendonk, Mauro Scarpelli, Tawfeg Ben Omran, Fanny Mochel, members of the SFEIM-A Study Group and Michel Tchan declare that they have no conflict of interest.

All procedures followed were in accordance with the ethical standards of the responsible committee on human experimentation (institutional and national) and with the Helsinki Declaration of 1975, as revised in 2000 (5). Informed consent was not obtained for each participant in this study.

Author Contributions

Sandra Sirrs, Carla Hollak and Martin Merkel planned the study and reviewed the draft article.

Annalisa Sechi, Emma Glamuzina, Miriam Janssen, Robin Lachmann, Janneke Langendonk, Mauro Scarpelli, Tawfeg Ben Omran, Fanny Mochel and members of the SFIEM-A Study Group submitted patient data and reviewed the draft article.

Michel Tchan planned the study, analysed the data and wrote the draft article.

References

Carpenter K, Wiley V, Sim KG, Heath D, Wilcken B (2001) Evaluation of newborn screening for medium chain acyl-CoA dehydrogenase deficiency in 275,000 babies. Arch Dis Child Fetal Neonatal Ed 85(2):F105–F109

Desnick RJ, Ioannou YA, Eng CM (2007) Alpha galactosidase A deficiency: Fabry disease. Online Metab Mol Bases Inherited Dis 3733–3774

El-Hattab AW, Li FY, Shen J et al (2010) Maternal systemic primary carnitine deficiency uncovered by newborn screening: clinical, biochemical, and molecular aspects. Genet Med 12 (1):19–24

Garman SC (2007) Structure-function relationships in alpha-galactosidase A. Acta Paediatr Suppl 96(455):6–16

Gaspar P, Herrera J, Rodrigues D et al (2010) Frequency of Fabry disease in male and female haemodialysis patients in Spain. BMC Med Genet 11:19

Lang TF (2009) Adult presentations of medium-chain acyl-CoA dehydrogenase deficiency (MCADD). J Inherit Metab Dis 32 (6):675–683

Lee NC, Tang NL, Chien YH et al (2010) Diagnoses of newborns and mothers with carnitine uptake defects through newborn screening. Mol Genet Metab 100(1):46–50

Palecek T, Honzikova J, Poupetova H et al (2014) Prevalence of Fabry disease in male patients with unexplained left ventricular hypertrophy in primary cardiology practice: prospective Fabry cardiomyopathy screening study (FACSS). J Inherit Metab Dis 37(3):455–460

Rolfs A, Bottcher T, Zschiesche M et al (2005) Prevalence of Fabry disease in patients with cryptogenic stroke: a prospective study. Lancet 366(9499):1794–1796

Sander S, Janzen N, Janetzky B et al (2001) Neonatal screening for medium chain acyl-CoA deficiency: high incidence in Lower Saxony (northern Germany). Eur J Pediatr 160(5):318–319

Saudubray JM, Walter JH, van der Berghe G (eds) (2012) Inborn metabolic diseases: diagnosis and treatment. Springer, Berlin, Heidelberg, New York.

Schaefer AM, McFarland R, Blakely EL et al (2008) Prevalence of mitochondrial DNA disease in adults. Ann Neurol 63(1):35–39

Spada M, Pagliardini S, Yasuda M et al (2006) High incidence of later-onset Fabry disease revealed by newborn screening. Am J Hum Genet 79(1):31–40

van der Tol L, Smid BE, Poorthuis BJ et al (2014) A systematic review on screening for Fabry disease: prevalence of individuals with genetic variants of unknown significance. J Med Genet 51(1):1–9

Vijay S, Patterson A, Olpin S et al (2006) Carnitine transporter defect: diagnosis in asymptomatic adult women following analysis of acylcarnitines in their newborn infants. J Inherit Metab Dis 29 (5):627–630

Wilcken B (2010) Fatty acid oxidation disorders: outcome and long-term prognosis. J Inherit Metab Dis 33(5):501–506

Wilcken B, Haas M, Joy P et al (2007) Outcome of neonatal screening for medium-chain acyl-CoA dehydrogenase deficiency in Australia: a cohort study. Lancet 369(9555):37–42

JIMD Reports
DOI 10.1007/8904_2015_497

RESEARCH REPORT

Electroclinical Features of Early-Onset Epileptic Encephalopathies in Congenital Disorders of Glycosylation (CDGs)

Agata Fiumara • Rita Barone • Giuliana Del Campo • Pasquale Striano • Jaak Jaeken

Received: 10 June 2015 / Revised: 05 September 2015 / Accepted: 14 September 2015 / Published online: 10 October 2015
© SSIEM and Springer-Verlag Berlin Heidelberg 2015

Abstract Congenital disorders of glycosylation (CDG) are a constantly growing group of genetic defects of glycoprotein and glycolipid glycan synthesis. CDGs are usually multisystem diseases, and in the majority of patients, there is an important neurological involvement comprising psychomotor disability, hypotonia, ataxia, seizures, stroke-like episodes, and peripheral neuropathy. To assess the incidence, among early-onset epileptic encephalopathies (EOEE), of patients with identified congenital disorders of glycosylation (CDG), we made a review of clinical, electrophysiological, and neuroimaging findings of 27 CDG patients focusing on seizure onset, semiology and frequency, response to antiepileptic drugs (AED), and early epileptic manifestations. Epilepsy was uncommon in PMM2-CDG (11%), while it was a main concern in other rare forms. We describe a series of patients with EOEE and genetically confirmed CDG (ALG3-CDG, ALG6-CDG, DPM2-CDG, ALG1-CDG). Epileptic seizures at onset included myoclonic and clonic fits and focal seizures. With time, patients developed recurrent and intractable seizures principally tonic–clonic seizures, infantile spasms, and myoclonic seizures. Electrophysiological correlates included focal and multifocal epileptic discharges, slowed background rhythm, and generalized epileptic activity including burst suppression pattern and status epilepticus. We propose a diagnostic flowchart for the early diagnosis of CDG in patients presenting with EOEE and suggest to perform serum transferrin IEF (or capillary zone electrophoresis) as a first-line screening in early-onset epilepsy.

Communicated by: Stephanie Gruenewald, MD

The present study emphasizes the importance of increased awareness that among subjects with early-onset epileptic encephalopathies (EOEEs), patients with congenital disorders of glycosylation (CDGs) may be detected. We propose a diagnostic flowchart for the early diagnosis of CDG in patients presenting with EOEE.

Competing interests: None declared

A. Fiumara (✉) · G. Del Campo
Department of Clinical and Experimental Medicine, Regional Referral Center for Inborn Errors Metabolism, Pediatric Clinic, University of Catania, via Santa Sofia 78, 95123 Catania, Italy
e-mail: agafiu@virgilio.it

R. Barone
Child Neuropsychiatry, Department of Clinical and Experimental Medicine, University of Catania, Catania, Italy

R. Barone
CNR Institute for Polymers, Composites and Biomaterials IPCB, Catania, Italy

P. Striano
Pediatric Neurology and Muscular Diseases Unit, Department of Neurosciences, Rehabilitation, Ophthalmology, Genetics, Maternal and Child Health, The Giannina Gaslini Institute, University of Genoa, Genoa, Italy

J. Jaeken
Department of Pediatrics, Center for Metabolic Disease, KU Leuven, Leuven, Belgium

Introduction

Early-onset epileptic encephalopathies (EOEE) are challenging conditions in newborns and infants, characterized by recurrent seizures, with onset in the first year of life, and impaired cognitive and motor development (Holland and Hallinan 2010). They include Ohtahara syndrome, early myoclonic epileptic encephalopathy, malignant migrating partial seizures of infancy, and others. EOEE may have different origins (anoxic–ischemic events, intracranial bleeding, infections, brain malformations, genetic/metabolic defects, drugs abstinence) although the cause is not always identified. The incidence of inborn errors of

metabolism (IEM) causing epilepsy is rated differently in published series, ranging from 0.1 to 300/100,000 live births (Mastrangelo and Leuzzi 2012; Mastrangelo et al. 2012). Nevertheless, a significant bias can derive from the specific experience of caring physicians and the availability of diagnostic tests.

Among IEM, congenital disorders of glycosylation (CDG) are a rapidly growing group of genetic defects of glycoprotein and glycolipid glycan synthesis (Freeze 2006). Since their first description by Jaeken in 1980, some 80 CDG have been identified, classified as defects of protein *N*-glycosylation, protein *O*-glycosylation, lipid, and GPI anchor glycosylation and combined defects (Barone et al. 2014). The screening technique for *N*-glycosylation disorders is serum transferrin (Tf) isoelectric focusing (IEF), although in rare instances Tf IEF profile can be normal in the first weeks of life in affected subjects (Clayton et al. 1993). CDG with type 1 IEF pattern (increase of asialo- and disialoforms and decreased tetrasialoforms) (CDG-I) are defects of *N*-glycan assembly and/or transfer to the glycosylation site of a protein. CDG with type 2 IEF pattern (increase of asialo-, monosialo-, disialo-, and/or trisialoforms) are due to *N*-glycan processing defects (Jaeken 2010). After finding a type 1 pattern, further biochemical characterization can be performed by fibroblast dolichol-linked oligosaccharide analysis. In the case of type 2 pattern, mass spectrometry profiling of *N*-glycans from serum Tf or total serum glycoproteins may be performed. In both instances, the next step is mutation analysis of a panel of genes known to be involved in CDG. If the latter is normal, whole-exome/whole-genome sequencing is increasingly used.

CDG are usually multisystem diseases, and in the majority of patients, there is an important neurological involvement comprising psychomotor disability, hypotonia, ataxia, seizures, stroke-like episodes, and peripheral neuropathy. Seizures have been reported in almost all types of CDG, often without an accurate description of semiology, EEG patterns, and therapeutic response. In this study, we describe the electroclinical features of a series of patients with EOEE and genetically confirmed CDG. In addition, we propose a diagnostic flowchart for the early diagnosis of CDG in patients presenting with EOEE.

Methods

Out of 3,700 samples referred for serum Tf IEF screening test to the Regional Center for Inborn Errors of Metabolism at the Pediatric Clinic, University of Catania, Italy, from 2005 to 2014, 29 showed a pattern compatible with the clinical diagnosis of CDG. Two subjects showed a type 2 IEF pattern suggesting a glycoprotein processing defect. In the 27 patients showing a type 1 pattern, PMM enzyme assay and/or PMM2 gene analyses were performed as PMM2-CDG is by far the most common *N*-glycosylation disorder. If PMM2-CDG was ruled out, dolichol-linked oligosaccharide (DLO) analysis was assessed in fibroblasts, and genetic testing for the putative CDG genes by Sanger was eventually performed. Thus, we reached a genetically confirmed diagnosis of PMM2-CDG in 17 out of 27 patients. Among the remaining ten non-PMM2-CDG subjects, ALG6-CDG, DPM2-CDG, and ALG3-CDG were each diagnosed in one patient. Furthermore, two ALG1-CDG patients were identified. In the other patients, including five CDG-I and two CDG-II subjects, we did not define yet the molecular defect, and whole-exome sequencing is ongoing.

The clinical records of all patients were reviewed with regard to the electroclinical features of epilepsy (onset, seizure semiology and frequency, response to antiepileptic drugs), EEG, and brain MRI findings. Seizures and epileptic syndromes were classified according to the International Classification (Commission on Classification and Terminology of the International League Against Epilepsy 1989).

Results

Epilepsy was uncommon in PMM2-CDG, as it was present in 2 (11%) out of the 17 genetically confirmed cases. Six patients experienced stroke-like episodes manifested as recurrent episodes of amaurosis, painful paresthesias, headache, and aphasia. Stroke-like episodes with transient hemiparesis or hemiplegia were initially diagnosed as partial crises followed by Todd paralysis for a few hours or days. On the contrary, epilepsy was the main complaint in patients with other CDG types. Four cases, each with a different CDG, were classified as having EOEE (Table 1).

Patient 1

This 7-year-old child of unrelated parents was born at the 38th week of gestation, after a pregnancy complicated by threats of miscarriage. Physical parameters were normal for his gestational age. He had respiratory distress and since his first week of life massive myoclonic jerks during sleep, hypotonia, and hypoglycemia. The boy presented sudden episodes of crying followed by apnea and cyanosis, lasting up to 15 min. Interictal electroencephalogram (EEG) showed slowed background and rare sharp waves over the posterior areas of the left hemisphere switching to synchronous and asynchronous epileptic discharges. The electroclinical picture was suggestive of early myoclonic encephalopathy of infancy (EMEI). Therapy with pheno-

Table 1 Clinical and molecular data of the present non-PMM2-CDG cases with EOEE

Case	1	2	3	4
Age/sex	7 y/M	30 m/F	22 m/F	10 m/F
Age at diagnosis (positive IEF test)	24 m	24 m	8 m	4 m
Type	ALG6-CDG	DPM2-CDG	ALG3-CDG	ALG1-CDG
Seizure onset	1st w	1st w	1st m	1st d
Seizure type	EMEI	EMEI	EMEI	Ohtahara syndrome
AED	PB, VGB, VPA	VPA, LTG	PB, VGB	PB, LEV, VPA, DZP, CLB
Current therapy/ outcome	LEV	Dead at age 30 m	Dead at age 22 m	Dead at age 10 m
Brain MRI	Cortical atrophy, thin corpus callosum	Periventricular and subcortical demyelination	Hypoplasia of corpus callosum	Delayed myelination, cortical subcortical atrophy

y year, *m* month, *w* week, *d* day, *M* male, *F* female, *EMEI* early myoclonic encephalopathy of infancy, *AEDs* antiepileptic drugs, *PB* phenobarbital, *VGB* vigabatrin, *VPA* valproate, *LTG* lamotrigine, *LEV* levetiracetam, *DZP* diazepam, *CLZ* clonazepam

barbital was started. At age 6 months, he started to experience daily tonic seizures with truncal hypertonia and sialorrhea, lasting more than 10 min. Treatment with vigabatrin and then valproate was unsuccessful.

The patient was admitted to our department at age 24 months. He showed slowed growth of head circumference and facial dysmorphism (coarse face with high forehead, esotropia, hypertelorism, large ears, depressed nasal root, bulbous nose) and bilateral cryptorchidism. Psychomotor development was severely delayed: he had poor gaze fixation and pursuit eye movements, axial hypotonia (he did not sit unaided), and dyskinetic limb movements (Fig. 1a). Fundoscopy revealed initial signs of chorioretinal dystrophy and optic nerve atrophy. Blood investigation revealed increased prothrombin time (PT), decreased coagulation factor XI, and pseudocholinesterase; serum Tf IEF showed a type 1 pattern. PMM activity was normal in fibroblasts. Dolichol-linked oligosaccharide (DLO) analysis in fibroblasts suggested an ALG6 defect, and molecular investigation revealed a homozygous mutation (c.250G>A/p.A84T) in this gene. Levetiracetam was started with partial benefit. Follow-up brain MRI revealed delayed myelination, thinning of corpus callosum, and progression of cerebral cortical atrophy (Fig. 1b).

Patient 2

This 30-month old girl (Fig. 1c) has been previously reported (patient 1 in Barone et al. 2012) without describing electroclinical features of epilepsy. She started to present myoclonic jerks of the four limbs at 6 days of life. She showed facial dysmorphism (hypertelorism, small rounded nose, pronounced philtrum, thin upper lip, ogival palate, and micrognathia); keel thorax; multiple contractions of elbows, wrists, fingers, and knees; and mild hepatomegaly. Spontaneous movements as well as plantar and palmar reflexes were absent. Brain ultrasound showed periventricular matter abnormalities. She was admitted for respiratory distress at age 3 months. Blood investigation showed increased serum transaminases and CK and decreased AT-III levels. Her EEG showed slowed background and low-voltage spikes over the left fronto-central areas. Seizures were refractory to antiepileptic therapy with valproate and then lamotrigine. The electroclinical features suggested EMEI. At 20 months, the patient showed profound psychomotor disability with generalized severe hypotonia, and she still experienced daily tonic–clonic seizures and limb myoclonus. At age 2 years, fundoscopy showed optic atrophy. Brain MRI revealed loss of myelin in the periventricular and subcortical areas and widening of the lateral ventricles. She died at the age of 30 months. A type 1 pattern was found on serum Tf IEF. DLO analysis in fibroblasts showed an accumulation of the glycan assembly intermediate Dol-PP-$GlcNAc_2Man_5$. She was found to be compound heterozygous for two mutations in DPM2: c.68A>G (p.Y23C) of maternal origin and c.4-1G>C from the father.

Patient 3

This patient was born at the 35th week, with a birth weight of 2,550 g (50th centile) by natural delivery. Around the 12th gestational week, threats of miscarriage were pharmacologically treated. She had respiratory distress at birth, severe hypotonia, and arthrogryposis. At 1 month, she developed cyanotic spells. The EEG showed continuous, generalized, slow spike/waves and polyspike waves configuring a nonconvulsive status epilepticus. Vigabatrin and phenobarbital were started. With time she developed focal motor and tonic–clonic seizures with multifocal epileptic

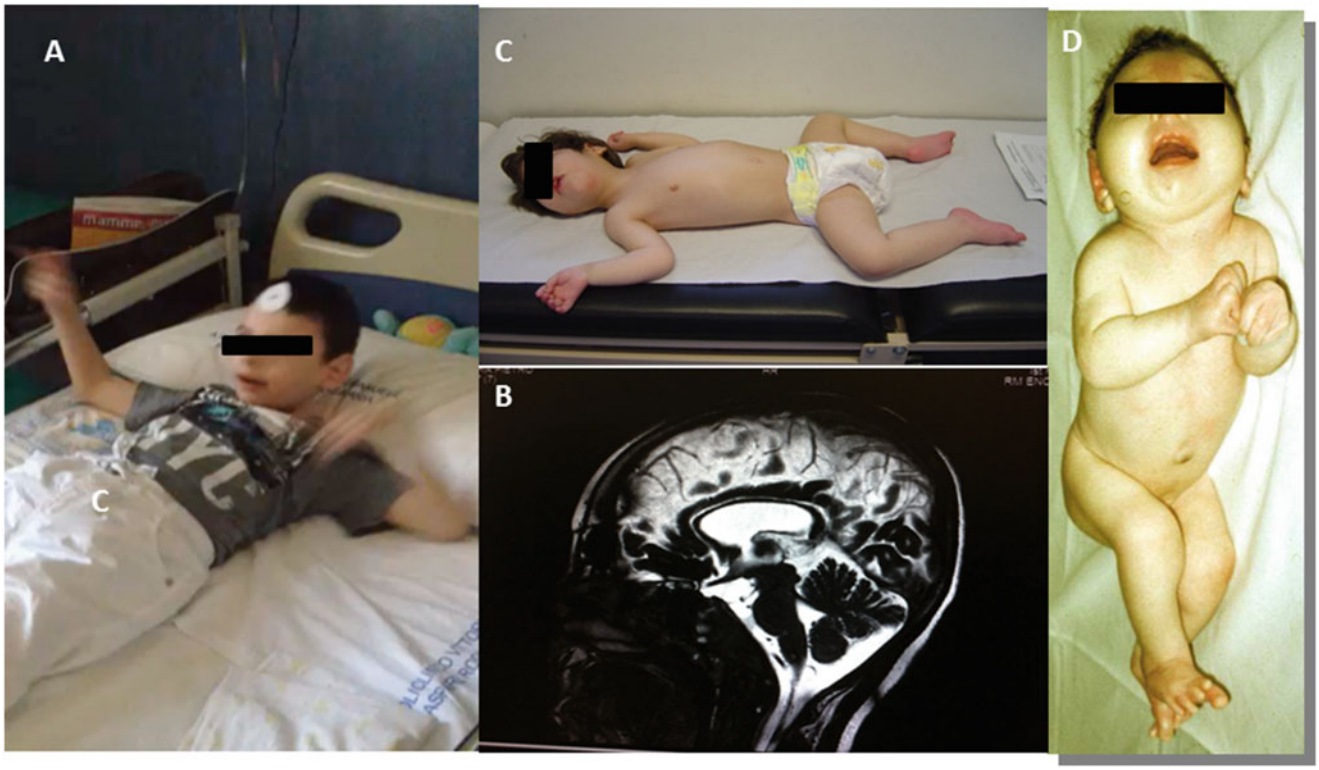

Fig. 1 Clinical and neuroimaging features of present patients with CDG and EOEE. (**a**) Case # 1 ALG6-CDG. (**b**) Case #1 MRI showing thin corpus callosum. (**c**) Case # 2 DPM2-CDG. (**d**) Case # 3 ALG3-CDG

abnormalities at the EEG compatible with early-onset multifocal epileptic encephalopathy. Brain MRI showed hypoplasia of the corpus callosum.

At age 8 months (Fig. 1d), she showed stunted growth, poor eye contact and head control, hypomotility, microcephaly, and craniofacial dysmorphism (plagiocephaly, short neck, low-set hairline, sparse hair, depressed nasal root, flat philtrum, large mouth with down-slanting lips, high-arched palate and micrognathia, and large and dysmorphic earlobes). There were also severe scoliosis, camptodactyly of hand and arm joints, pes cavus, and arthrogryposis of elbows, knees, ankles, and toes. Laboratory investigation showed increased serum transaminases and gamma-GT. Serum Tf IEF showed a type 1 pattern, and genetic testing revealed two ALG3 mutations: the c.564_566del CCT mutation and the combination of mutations c.1125G>A (p.Met375Ile) plus c.1127delC. She died at age 22 months with pulmonary infection and respiratory failure.

Patient 4

This girl was born to unrelated healthy parents after a 37 weeks pregnancy. The birth weight was 2,560 g (50th centile); length was 46 cm (50th centile); head circumference was 31 cm (<3rd centile); and APGAR at 1′ and 10′ was 9 and 10. From day 1 of life, she experienced daily clonic seizures, with cyanosis and oxygen desaturation (<92%) and burst suppression EEG pattern indicative of Ohtahara syndrome. Different AEDs were used (levetiracetam, valproate, diazepam, and clonazepam) without benefit.

At 3 months of age, neurological examination showed axial muscle hypotonia, weakness, hyperreflexia, and severe dysphagia; there were some dysmorphic features, as frontal bossing, short philtrum, and inverted nipples. The head circumference was 34 cm (<3rd centile). At that time, she suffered daily motor partial complex seizures, often with secondary generalization and oxygen desaturation. EEG showed multifocal anomalies, mainly on anterior areas, and brain MRI impaired myelination. Profound psychomotor disability, microcephaly, severe axial hypotonia, and intermittent dystonia of the arms were present. Swallowing impairment requested nose tube feeding since age 6 months. She died at age 10 months with pulmonary infection and respiratory failure. Because of a positive screening test for CDG by serum Tf IEF, mutation analysis of putative CDG genes showed a compound heterozygosity of ALG1 gene c.1076C>T (p.S359L) c.1250_1251insTG: (p.A418Efs*18).

Discussion

Epilepsy is reported in almost one-third of patients with PMM2-CDG (Monin et al. 2014), and it is generally controlled with one or more AEDs. On the other hand, the retrospective evaluation of this series of CDG patients shows that epilepsy can be the first and prominent sign of non-PMM2-CDG. They presented with epileptic encephalopathy within the first weeks of life. In the same 9-year period, we observed 122 EOEE patients, and thus these four account for the 3.3% of them. On the other hand, if we consider also the five cases of CDG-Ix still without a definitive molecular diagnosis, the incidence of CDG among EOEE in our center increases to 5%. In the present four CDG patients, epileptic seizures at onset included myoclonic and clonic fits and focal seizures with desaturation, apneic spells, and bradycardia. With time, all patients developed recurrent and intractable seizures, principally tonic–clonic seizures, infantile spasms, and myoclonic seizures. Electrophysiological correlates included focal and multifocal epileptic discharges, slowed background rhythm, and generalized epileptic activity including burst suppression pattern and status epilepticus. Associated neurological findings were severe developmental disability, acquired microcephaly, generalized hypotonia, and, in some, dyskinetic limb movements. Three out of four subjects died at an early age ranging from 6 to 30 months.

Among the *N*-glycosylation disorders, ALG6-CDG is the most frequent type, after PMM2-CDG. Fifty four cases have been described (review in Jaeken et al. 2015a). Although in most patients the neurological/epileptic phenotype is reported as a unique entity, it appears that most patients have epilepsy with early onset (between 5 months and 2 years). As illustrated by patient 1, ALG6-CDG epilepsy is difficult to treat and has variable features including tonic–clonic, partial complex, atonic, as well as myoclonic seizures. MRI brain findings frequently include corpus callosum hypoplasia; cerebellar involvement was described in one-third of cases (Barone et al. 2014).

The patient with DPM2-CDG started epileptic myoclonus on the sixth day of life, passing to generalized tonic fits associated with myoclonic jerks when she was 20 months old. Two other DPM2-CDG patients were reported so far: they both had severe epilepsy with focal and/or generalized seizures at 3 and 5 months, respectively (Barone et al. 2012).

The ALG3-CDG patient started to present epilepsy at age 1 month. She had been initially labeled with Pena–-Shokeir syndrome because of her peculiar dysmorphisms with arthrogryposis. She was the first reported CDG-Ix patient with a malformation syndrome (Fiumara et al. 2002). Since the first description, in 1999, ALG3-CDG was identified as a severe epileptic syndrome with neonatal onset and absent psychomotor development. Moreover, microcephaly; skeletal malformations, resembling those observed in the present patient; and ophthalmological anomalies were described (Korner et al. 1999). Nine patients have been reported (review in Riess et al. 2013). They all presented microcephaly, neonatal-onset intractable seizures with multiple patterns (West syndrome, tonic–clonic seizures, or combined types), and various degrees of corpus callosum involvement. Cerebral and/or cerebellar atrophy can be present.

Our ALG1-CDG patient had epileptic encephalopathy with electroclinical features of the Ohtahara syndrome. Severe hypotonia, dystonic posture of limbs, and swallowing impairment were additional features. At the time of writing, 19 ALG1-CDG patients have been reported (review in Jaeken et al. 2015b). Their clinical spectrum ranges from early-onset severe cases with rapid fatal outcome to milder, long-surviving cases. Most reported patients experienced intractable epilepsy with onset between birth and 8 months. Multifocal EEG activity and sharp wave pattern were observed. Stupor, probably masking status epilepticus, was also described in terminal patients (Rohlfing et al. 2014).

In addition to ALG6- (OMIM: 603147), ALG3- (601110), ALG1- (608540), and DPM2-CDG (603564), other *N*-glycosylation disorders in which epilepsy is usually severe and difficult to treat are DPM1- (603503), MPDU1- (608799), ALG2- (607906), DPAGT1- (608540), ALG12- (607143), ALG8- (608104), ALG9- (608776), ALG11- (613666), and RFT1-CDG (612015). They all are defects of *N*-glycan assembly located in the endoplasmic reticulum, leading to underoccupancy of *N*-glycosylation sites of glycoproteins (Clayton and Grünewald 2009). In addition, seizures have been reported in patients with dolichol biosynthesis defect SRD5A3-CDG (62379) and DOLK-CDG (610768) and in CDG-II including GCS1- (606056), SLC35C1 (266265), B4GALT1- (607091), COG1- (611209), COG4- (613489), COG5- (613612), COG6- (606977), COG7- (608779), COG8- (611182), and ATP6V0A2-CDG (219200). Recently, SLC35A2-CDG (de novo mutation in X-linked UDP-galactose transporter) due to defective galactosylation of glycoconjugates in the Golgi was identified by whole-exome sequencing (WES) in patients with West syndrome, dysmorphic features, and absence of hepatic and coagulation features usually observed in CDG (Ng et al. 2013; Kodera et al. 2013).

Pathophysiology of epilepsy in CDG is undoubtedly complex (defective glycosylation of signal transducers such as receptors, ion channels, etc.) and will not be discussed here. In early-onset epilepsy, a CDG has to be considered particularly in the presence of dysmorphic features and/or

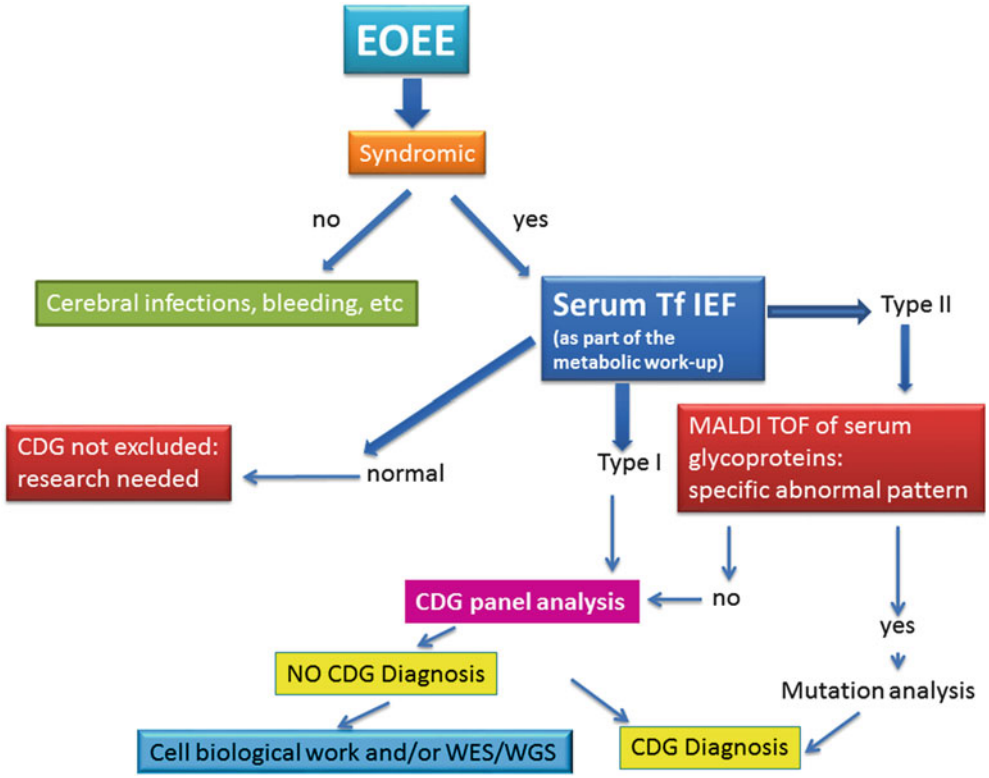

Fig. 2 EOEE diagnostic flowchart for CDG

signs of multisystemic involvement. We propose to perform serum Tf IEF (or capillary zone electrophoresis) as a first-line screening. The further differential diagnostic approach is depicted in Fig. 2. When serum transferrin IEF is not readily available, the decrease of other glycoproteins, such as haptoglobin, thyroxine-binding globulin, antithrombin III, protein C, and factor XI, can provide a hint to a glycosylation defect.

Compliance with Ethics Guidelines

Conflict of Interest

Agata Fiumara, Rita Barone, Giuliana Del Campo, Pasquale Striano, and Jaak Jaeken declare that they have no conflict of interest.

Informed Consent

All procedures followed were in accordance with the ethical standards of the responsible committee on human experimentation (institutional and national) and with the Helsinki Declaration of 1975, as revised in 2000. Informed consent was obtained from all patients for being included in the study.

Details of the Contributions of Individual Authors

Prof. Fiumara wrote the report with the contribution of Prof Barone.

Prof. Jaeken critically revised the manuscript and added his own data.

Dr. Del Campo collected all patients' data and wrote their case reports.

Prof. Striano cared for the electrophysiological aspects and contributed to the manuscript elaboration.

References

Barone R, Aiello C, Race V et al (2012) DPM2-CDG a muscular dystrophy-dystroglycanopathy syndrome with severe epilepsy. Ann Neurol 72(4):550–558

Barone R, Fiumara A, Jaeken J (2014) Congenital disorders of glycosylation with emphasis on cerebellar involvement. Semin Neurol 34(3):357–366

Commission on Classification and Terminology of the International League Against Epilepsy (1989) Proposal for revised classification of epilepsies and epileptic syndromes. Epilepsia 30 (4):389–399

Clayton PT, Grünewald S (2009) Comprehensive description of the phenotype of the first case of congenital disorder of glycosylation due to RFT1 deficiency (CDG In). J Inherit Metab Dis 32(Suppl 1): S137–S139

Clayton P, Winchester B, Di Tomaso E, Young E, Keir G, Rodeck C (1993) Carbohydrate-deficient glycoprotein syndrome: normal glycosylation in the fetus. Lancet 341(8850):956

Fiumara A, Sorge G, Meli C, Barone R, Pavone L (2002) IEF type 1 in COFS/Pena-Shokeir syndrome. A new form of CDG (CD Ix) with evidence of metabolic defect causing multiple malformations. J Inherit Metab Dis 25(Suppl 1):134

Freeze HH (2006) Genetic defects in the human glycome. Nat Rev Genet 7(7):537–551

Holland KD, Hallinan BE (2010) What causes epileptic encephalopathy in infancy?: the answer may lie in our genes. Neurology 75 (13):1132–1133

Jaeken J (2010) Congenital disorders of glycosylation. Ann N Y Acad Sci 1214:190–198

Jaeken J, Lefeber D, Matthijs G (2015a) Clinical utility gene card for: ALG6 defective congenital disorder of glycosylation. Eur J Hum Genet 23(2). doi:10.1038/ejhg.2014.146

Jaeken J, Lefeber D, Matthijs G (2015b) Clinical utility gene card for: ALG1 defective congenital disorder of glycosylation. Eur J Hum Genet. doi:10.1038/ejhg.2015.9

Kodera H, Nakamura K, Osaka H et al (2013) De novo mutations in SLC35A2 encoding a UDP-galactose transporter cause early-onset epileptic encephalopathy. Hum Mutat 4(12):1708–1714

Korner C, Knauer R, Stephani U, Marquardt T, Lehle L, Von Figura K (1999) Carbohydrate deficient glycoprotein syndrome type IV: deficiency of dolichyl-P-Man:Man5GlcNAc2-PP-dolichyl mannosyltransferase. EMBO J 18(23):6816–6822

Mastrangelo M, Leuzzi V (2012) Genes of early onset epileptic encephalopathies: from genotype to phenotype. Pediatr Neurol 46(1):24–31

Mastrangelo M, Celato A, Leuzzi V (2012) A diagnostic algorithm for the evaluation of early onset genetic-metabolic epileptic encephalopathies. Eur J Paediatr Neurol 16(2):179–191

Monin ML, Mignot C, De Lonlay P, Héron B, Masurel A, Mathieu-Dramard M et al (2014) 29 French adult patients with PMM2-congenital disorder of glycosylation: outcome of the classical pediatric phenotype and depiction of a late-onset phenotype. Orphanet J Rare Dis 11(9):207–215

Ng BG, Buckingham KJ, Raymond K et al (2013) Mosaicism of the UDP-galactose transporter SLC35A2 causes a congenital disorder of glycosylation. Am J Hum Genet 92(4):632–636

Riess S, Reidihough DS, Howell KB, Dagia C, Jaeken J, Matthijs G, Yaplito-Lee J (2013) ALG3-CDG (CDG ID) Clinical, biochemical and molecular findings in two siblings. Mol Genet Metab 110 (1–2):170–175

Rohlfing AK, Rust S, Reunert J et al (2014) ALG1 CDG A new case with early fatal outcome. Gene 534(2):345–351

JIMD Reports
DOI 10.1007/8904_2015_476

RESEARCH REPORT

The Newborn Screening Paradox: Sensitivity vs. Overdiagnosis in VLCAD Deficiency

Eugene Diekman · Monique de Sain-van der Velden · Hans Waterham · Leo Kluijtmans · Peter Schielen · Evert Ben van Veen · Sacha Ferdinandusse · Frits Wijburg · Gepke Visser

Received: 19 December 2014 / Revised: 11 June 2015 / Accepted: 12 June 2015 / Published online: 10 October 2015
© SSIEM and Springer-Verlag Berlin Heidelberg 2015

Abstract *Objective*: To improve the efficacy of newborn screening (NBS) for very long chain acyl-CoA dehydrogenase deficiency (VLCADD).

Patients and Methods: Data on all dried blood spots collected by the Dutch NBS from October 2007 to 2010 (742.728) were included. Based solely on the C14:1 levels (cutoff $\geq$0.8 μmol/L), six newborns with VLCADD had been identified through NBS during this period. The ratio of C14:1 over C2 was calculated. DNA of all blood spots with a C14:1/C2 ratio of $\geq$0.020 was isolated and sequenced. Children homozygous or compound heterozygous for mutations in the *ACADVL* gene were traced back and invited for detailed clinical, biochemical, and genetic evaluation.

Results: Retrospective analysis based on the C14:1/C2 ratio with a cutoff of $\geq$0.020 identified an additional five children with known *ACADVL* mutations and low enzymatic activity. All were still asymptomatic at the time of diagnosis (age 2–5 years). Increasing the cutoff to $\geq$0.023 resulted in a sensitivity of 93% and a positive predictive value of 37%. The sensitivity of the previously used screening approach (C14:1 $\geq$0.8) was 50%.

Conclusion: This study shows that the ratio C14:1/C2 is a more sensitive marker than C14:1 for identifying VLCADD patients in NBS. However, as these patients were all asymptomatic at the time of diagnosis, this suggests that a more sensitive screening approach may also identify individuals who may never develop clinical disease. Long-term follow-up studies are needed to establish the risk of these VLCADD-deficient individuals for developing clinical signs and symptoms.

Communicated by: Bridget Wilcken

Competing interests: None declared

E. Diekman · H. Waterham · S. Ferdinandusse · F. Wijburg
Department of Clinical Chemistry and Pediatrics, Laboratory Genetic Metabolic Diseases, Emma Children's Hospital, Academic Medical Centre, University of Amsterdam, Amsterdam, The Netherlands

E. Diekman · G. Visser (✉)
Department of Paediatric Gastroenterology and Metabolic Diseases, Wilhelmina Children's Hospital UMC Utrecht, Utrecht, The Netherlands
e-mail: gvisser4@umcutrecht.nl

M. de Sain-van der Velden
Department of Medical Genetics, Wilhelmina Children's Hospital UMC Utrecht, Utrecht, The Netherlands

L. Kluijtmans
Department of Laboratory Medicine, Translational Metabolic Laboratory, Radboud University Medical Center, Nijmegen, The Netherlands

P. Schielen · E.B. van Veen
National Institute for Public Health and the Environment (RIVM), Reference Laboratory for Pre- and Neonatal Screening, Bilthoven, The Netherlands

Introduction

Many newborn screening (NBS) programs in the world, including the Dutch NBS program, have very long chain acyl-CoA dehydrogenase deficiency (VLCADD) in their disease panel (Lindner et al. 2010; Loeber et al. 2012). VLCADD is a disorder of long-chain fatty acid beta-oxidation (OMIM 609575) that compromises energy homeostasis and leads to accumulation of long-chain fatty acids and derivatives. Patients may present with hypoglycemia, hepatomegaly, and cardiomyopathy in the neonatal period and rhabdomyolysis in early childhood. These features can be induced by fasting, exercise, illness, and fever (Vianey-Saban et al. 1998; Andresen et al. 1999;

Laforêt et al. 2009; Baruteau et al. 2014). VLCADD is included in NBS programs mainly because life-threatening symptoms as hypoglycemia and cardiomyopathy can be prevented by dietary measures.

NBS for VLCADD is performed by measuring the concentration of accumulating long-chain acylcarnitines in blood spots, especially tetradecenoyl carnitine (C14:1). In the Netherlands, the cutoff level of C14:1 for referral of newborns was initially ≥0.80 μmol/L (2007). However, because one patient was missed (detected via screening of the family of an index patient), the cutoff level for referral was reduced to ≥0.60 μmol/L (2010). Results of the Region 4 database (McHugh et al. 2011), which contains collaborative data on the outcome of NBS programs worldwide (Houten et al. 2013), indicated that the ratio of C14:1 over acetylcarnitine (C2) might further improve the sensitivity of the screening procedure (Hall et al. 2014). C2 concentrations are often, and also in the Netherlands, measured in NBS screening programs as secondary markers for screening of isovaleric acidemia. In order to improve the NBS on VLCADD, we retrospectively investigated whether the ratio C14:1/C2 is a better marker for VLCADD than the original marker C14:1.

Patients and Methods

We retrospectively calculated the C14:1/C2 ratios and C14:1 levels of all 742.728 NBS blood spots from the Dutch NBS program taken in the period 2007–2010. NBS blood spots are taken within 72–144 h from birth. The levels were measured within 7 days after birth. All blood spots with a C14:1/C2 cutoff value of ≥0.020 and/or C14:1 ≥0.60 μmol/L were selected for further analysis. DNA of the selected blood spots was isolated using the NucleoSpin Tissue genomic DNA purification kit (Macherey-Nagel, Düren, Germany). All exons plus flanking intronic regions of the *ACADVL* gene were subsequently sequenced. Three proven VLCADD patients were included in a blinded manner as positive controls.

VLCAD enzymatic activity was measured in lymphocytes by using ferrocenium hexafluorophosphate as the electron acceptor, followed by UPLC, to separate the different acyl-CoA species (Wanders et al. 2010). Acylcarnitines were measured as described previously (Vreken et al. 1999).

Based on the duty of care principle (Sokol 2012), the patients who were originally classified as nonaffected but who turned out positive upon evaluation of the C14:1/C2 ratio were traced back and contacted for care. All were alive and all accepted the invitation for neurological, cardiological, biochemical, and genetic evaluation.

Results

Acylcarnitine Measurement and Mutation Analysis in Blood Spots

We found a C14:1/C2 ratio of ≥0.020 in 67 blood spots. Sequence analysis of the ACADVL gene in this group revealed five children who were either homozygous for a single mutation or compound heterozygous for two different mutations. These mutations were confirmed in independent samples (blood spot and blood). In addition, we identified 18 children who were carriers of one mutation in the *ACADVL* gene (Table 1).

The enzymatic activity of VLCAD in lymphocytes was severely deficient in two of the five detected children (PID 1 and 2) and mildly reduced in the other three patients (PID 3-5). The parents of individual 5 with 46% VLCAD activity were analyzed to check for heterozygosity. Both parents were heterozygotes for the found mutations in patient 5. VLCADD was subsequently also confirmed in two siblings (Table 1).

In the period 2007–2010, six VLCADD patients had been identified by the Dutch NBS program based on the original screening selection criteria: C14:1 ≥0.80 μmol/L. The five additional children detected in this study were not referred at the time. However, based on the current cutoff value of C14:1 ≥0.6 μmol/L (adopted 2013), individual 1 would have been referred.

Two of the three plasma acylcarnitine levels were below the age-adjusted reference value (95th percentile) of <0.26 μmol/L (patients 3 and 5).

Clinical Phenotype

All newly identified children with VLCADD were evaluated for clinical symptoms (Table 1). None of these children reported muscle-related symptoms and none had neurological or cardiological abnormalities. All were normoglycemic upon evaluation and none had suffered metabolic decompensation. Growth varied with a length range < −1.5 SD below the target height to appropriate to target height and a weight-length range of −2.18 to +1.94. The median creatine kinase level at the first evaluation was 120 U/L (range 91–200 U/L).

Sensitivity and Positive Predictive Value

Our results indicate that the sensitivity of C14:1 (≥0.8) is 50% and the sensitivity of C14:1 (≥0.6) is 58%, while the

Table 1 Patient characteristics. Clinical, biochemical, and genetic details of each patient

ID	Age (year)	Gender	Blood spot [C14:1] (normal <0.60 µmol/L)	Blood spot C14:1/C2 (normal <0.020 µmol/L)	Plasma [C14:1] (normal <0.26 µmol/L)	C14:1/C2	Enzymatic activity Lymphocytes (% of controls)	Genotype Allele 1	Genotype Allele 2	Neurological examination	Cardiological examination	Other symptoms	Creatine kinase (normal <250)
1	5	M	0.70	0.058	0.60	0.220	<7	p.G441D *missense*	p.A490P *missense*	Normal (MRC 5)	Normal (no echo/ECG abnormalities)	No hepatomegaly, fatigue, sometimes myalgia	91
2	5	M	0.36	0.040	2.92	0.780	<7	p.P89HfsX28 *frameshift*	p.V283A *missense*	Normal	Normal	No hepatomegaly, no complaints	198
Sib of 2	11	F					11	p.P89HfsX28 *frameshift*	p.V283A *missense*			No complaints	n.a.
3	4	F	0.33	0.024	0.15	0.069	21	p.V283A *missense*	p.V283A *missense*	Normal	Normal	No hepatomegaly, no complaints	96
4	5	M	0.25	0.050	0.38	0.18	14	p.V283A *missense*	p.V283A *missense*	Normal	Normal	No hepatomegaly, no complaints	200
5	2	M	0.55	0.039	0.14	0.094	46	p.G441D *missense*	p.R615Q *missense*	Normal	Normal	No hepatomegaly, no complaints	120
Sib of 5	2	F					40	p.G441D *missense*	p.R615Q *missense*	Normal	Normal	No complaints	n.a.

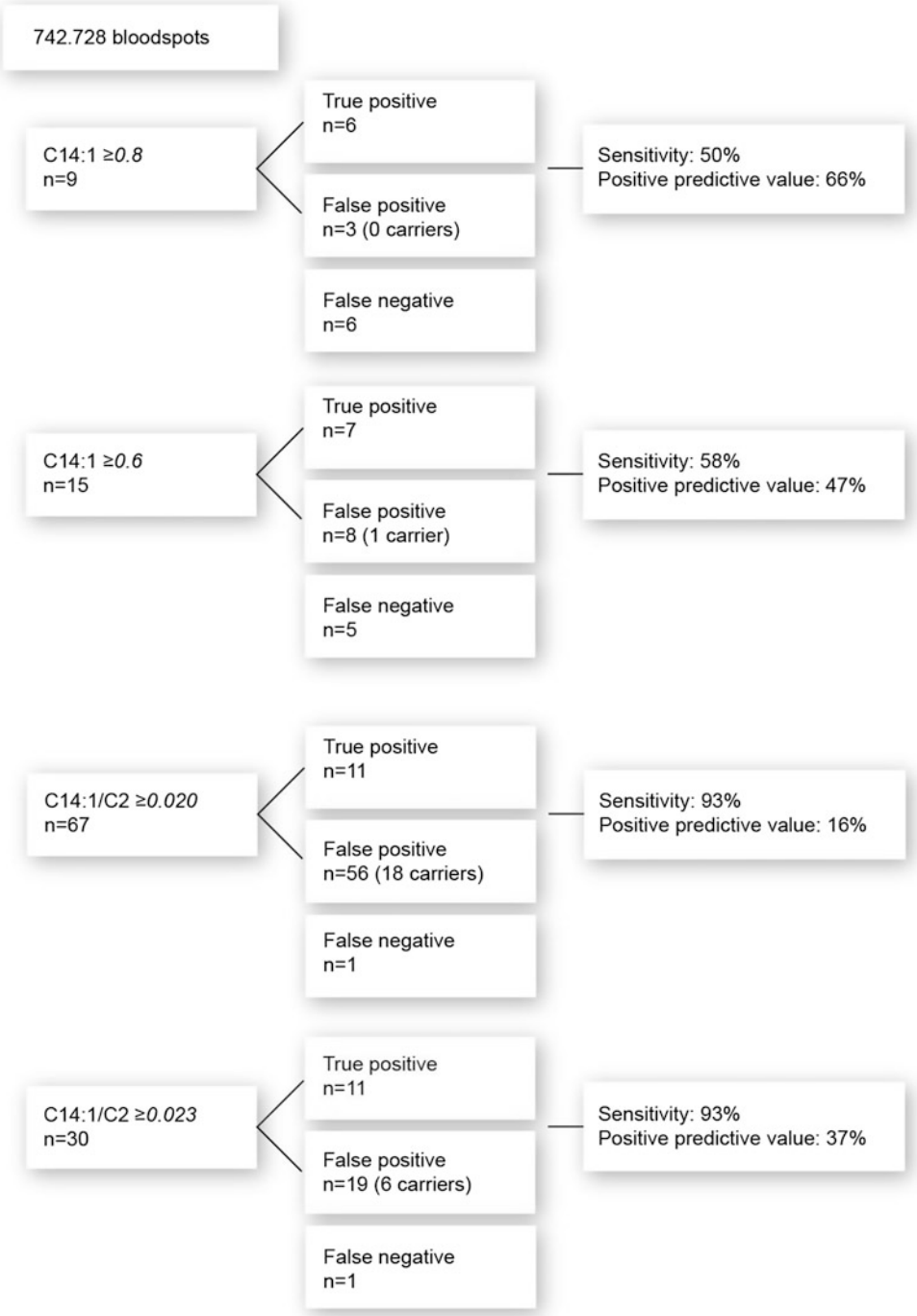

Fig. 1 Sensitivity and positive predictive value. Sensitivity and positive predictive values of C14:1 and C14:1/C2 with the various cutoff values

sensitivity of C14:1/C2 (≥0.020) is 93%. In addition, the positive predictive values of C14:1 (≥0.8 and ≥0.6) and C14:1/C2 (≥0.020) are 66%, 47%, and 16%, respectively (Fig. 1). With a C14:1/C2 cutoff value of ≥0.023, the sensitivity remains 93%, while the positive predictive value increases to 37% (Fig. 1).

Discussion

This study shows that inclusion of the ratio C14:1/C2 to the NBS increases the sensitivity to detect VLCADD. Accordingly, this ratio is now added to the Dutch NBS as primary marker for screening on VLCADD.

Introducing C14:1/C2 into the expanded NBS program has advantages as well as limitations. The inclusion of this ratio will increase the sensitivity from 50% to 93%, which leads to fewer false negative results and thus less missed patients. But, the increase of the sensitivity is at the expense of a lower positive predictive value. A false-positive NBS result may have great impact on the parents of newborns and the families involved (Waisbren et al. 2003; Gurian et al. 2006). Special care and a best practice for communication between healthcare providers and parents are therefore essential in mitigating the stress involved (Schmidt et al. 2012). Compared to other disease in the NBS, a positive predictive value of 37% is high (Hall et al. 2014).

Retrospective analyses allowed us to identify five children with reduced VLCAD activity who, on clinical evaluation, were all asymptomatic, but in whom the diagnosis VLCADD was confirmed by mutation analysis. These children may be at high risk of future metabolic crises and/or later-onset disease. However, it is not possible to define which outcomes are clinically relevant (Wilcken 2010; Bonham 2013). Children with a VLCAD activity of >20% appear to have no symptoms (Hoffmann et al. 2011). One could argue that individual 5 is therefore not a case. Even with a residual VLCAD activity <20%, the clinical outcome is not certain. Fatty acid oxidation flux might be a better biomarker to predict the clinical severity of VLCAD deficiency than enzyme activity (Diekman et al. 2015). With the current development rate of new techniques in genetics and biochemistry, sensitivity will probably increase even more in the coming years (Dixon et al. 2012; Bonham 2013). Although the introduction of worldwide NBS programs has offered significant health gain for many patients, it might be argued that too sensitive NBS methods can lead to "overdiagnosing" and as such may be harmful for patients and their families (Timmermans and Buchbinder 2010; Kwon and Steiner 2011).

Conclusion

In summary, we show that the biomarker C14:1/C2 (≥0.023) is a better marker (sensitivity 93%) compared to C14:1 (≥0.8, sensitivity 50%) to detect VLCADD patients and thus leads to fewer missed patients. However, the identified missed patients were all asymptomatic at the time of diagnosis. This suggests that a more sensitive screening approach may also identify individuals who may never develop clinical disease. Studies that evaluate the natural history of pre-NBS detected patients are needed to establish the risk of these VLCADD-deficient individuals for developing clinical signs and symptoms.

Acknowledgments We are most grateful to Dr. B. Elvers of the National Institute for Public Health and the Environment (RIVM) for providing the selected blood spots for further analyses and to Dr. P. Verkerk of TNO (Applied Scientific Research Institute) and Prof. Dr. E.E.S. Nieuwenhuis of the Wilhelmina's Children's Hospital/University Medical Centre Utrecht (WKZ/UMCU) for their biochemical and ethical advice. They were not compensated for their efforts.

Synopsis

We show that the C14:1/C2 (≥0.023) ratio is a better biomarker (sensitivity 93%) to detect patients with VLCADD compared to C14:1 (≥0.8, sensitivity 50%) and identified five additional patients.

Conflict of Interest

Eugene Diekman has no conflict of interest, Monique de Sain-van der Velden has no conflict of interest, Hans Waterham has no conflict of interest, Leo Kluijtmans has no conflict of interest, Peter Schielen has no conflict of interest, Evert Ben van Veen has no conflict of interest, Sacha Ferdinandusse has no conflict of interest, Frits Wijburg has no conflict of interest, and Gepke Visser has no conflict of interest.

Funding Source

This research was supported by ZonMW (dossier 200320006), Metakids (www.metakids.nl), and the ESN-stimuleringsprijs.

Compliance with Ethics Guidelines

Informed Consent

All procedures followed were in accordance with the ethical standards of the responsible committee on human experimentation (institutional and national) and with the Helsinki Declaration of 1975, as revised in 2000 (5). Informed consent was obtained from all patients for being included in the study.

References

Andresen BS, Olpin S, Poorthuis BJ et al (1999) Clear correlation of genotype with disease phenotype in very-long-chain acyl-CoA dehydrogenase deficiency. Am J Hum Genet 64:479–494. doi:10.1086/302261

Baruteau J, Sachs P, Broué P et al (2014) Clinical and biological features at diagnosis in mitochondrial fatty acid beta-oxidation defects: a French pediatric study from 187 patients. Complementary data. J Inherit Metab Dis 37:137–139. doi:10.1007/s10545-013-9628-9

Bonham JR (2013) Impact of new screening technologies: should we screen and does phenotype influence this decision? J Inherit Metab Dis 36:681–686. doi:10.1007/s10545-013-9598-y

Diekman EF, Ferdinandusse S, van der Pol WL et al (2015) Fatty acid oxidation flux predicts the clinical severity of VLCAD deficiency. Genet Med. doi:10.1038/gim.2015.22

Dixon S, Shackley P, Bonham J, Ibbotson R (2012) Putting a value on the avoidance of false positive results when screening for inherited metabolic disease in the newborn. J Inherit Metab Dis 35:169–176. doi:10.1007/s10545-011-9354-0

Gurian EA, Kinnamon DD, Henry JJ, Waisbren SE (2006) Expanded newborn screening for biochemical disorders: the effect of a false-positive result. Pediatrics 117:1915–1921. doi:10.1542/peds.2005-2294

Hall PL, Marquardt G, McHugh DMS et al (2014) Postanalytical tools improve performance of newborn screening by tandem mass spectrometry. Genet Med. doi:10.1038/gim.2014.62

Hoffmann L, Haussmann U, Mueller M, Spiekerkoetter U (2011) VLCAD enzyme activity determinations in newborns identified by screening: a valuable tool for risk assessment. J Inherit Metab Dis. doi:10.1007/s10545-011-9391-8

Houten SM, Herrema H, te Brinke H et al (2013) Impaired amino acid metabolism contributes to fasting-induced hypoglycemia in fatty acid oxidation defects. Hum Mol Genet 22:5249–5261. doi:10.1093/hmg/ddt382

Kwon JM, Steiner RD (2011) "I'm fine; I'm just waiting for my disease": the new and growing class of presymptomatic patients. Neurology 77:522–523. doi:10.1212/WNL.0b013e318228c15f

Laforêt P, Acquaviva-Bourdain C, Rigal O et al (2009) Diagnostic assessment and long-term follow-up of 13 patients with Very Long-Chain Acyl-Coenzyme A dehydrogenase (VLCAD) deficiency. Neuromuscul Disord 19:324–329. doi:10.1016/j.nmd.2009.02.007

Lindner M, Hoffmann GF, Matern D (2010) Newborn screening for disorders of fatty-acid oxidation: experience and recommendations from an expert meeting. J Inherit Metab Dis 33:521–526. doi:10.1007/s10545-010-9076-8

Loeber JG, Burgard P, Cornel MC et al (2012) Newborn screening programmes in Europe; arguments and efforts regarding harmonization. Part 1. From blood spot to screening result. J Inherit Metab Dis 35:603–611. doi:10.1007/s10545-012-9483-0

McHugh DMS, Cameron CA, Abdenur JE et al (2011) Clinical validation of cutoff target ranges in newborn screening of metabolic disorders by tandem mass spectrometry: a worldwide collaborative project. Genet Med 13:230–254. doi:10.1097/GIM.0b013e31820d5e67

Schmidt JL, Castellanos-Brown K, Childress S et al (2012) The impact of false-positive newborn screening results on families: a qualitative study. Genet Med 14:76–80. doi:10.1038/gim.2011.5

Sokol DK (2012) Law, ethics, and the duty of care. BMJ 345, e6804. doi:10.1212/WNL.0b013e318228c15f

Timmermans S, Buchbinder M (2010) Patients-in-waiting: Living between sickness and health in the genomics era. J Health Soc Behav 51:408–423. doi:10.1177/0022146510386794

Vianey-Saban C, Divry P, Brivet M et al (1998) Mitochondrial very-long-chain acyl-coenzyme A dehydrogenase deficiency: clinical characteristics and diagnostic considerations in 30 patients. Clin Chim Acta 269:43–62

Vreken P, van Lint AE, Bootsma AH et al (1999) Quantitative plasma acylcarnitine analysis using electrospray tandem mass spectrometry for the diagnosis of organic acidaemias and fatty acid oxidation defects. J Inherit Metab Dis 22:302–306

Waisbren SE, Albers S, Amato S et al (2003) Effect of expanded newborn screening for biochemical genetic disorders on child outcomes and parental stress. JAMA 290:2564–2572. doi:10.1001/jama.290.19.2564

Wanders RJA, Ruiter JPN, IJLst L, et al. (2010) The enzymology of mitochondrial fatty acid beta-oxidation and its application to follow-up analysis of positive neonatal screening results. J Inherit Metab Dis 33:479–494. doi: 10.1007/s10545-010-9104-8

Wilcken B (2010) Fatty acid oxidation disorders: outcome and long-term prognosis. J Inherit Metab Dis 33:501–506. doi:10.1007/s10545-009-9001-1

JIMD Reports
DOI 10.1007/8904_2015_504

RESEARCH REPORT

Further Delineation of the ALG9-CDG Phenotype

Sarah AlSubhi • Amal AlHashem • Anas AlAzami • Kalthoum Tlili • Saad AlShahwan • Dirk Lefeber • Fowzan S. Alkuraya • Brahim Tabarki

Received: 13 July 2015 / Revised: 14 September 2015 / Accepted: 18 September 2015 / Published online: 10 October 2015
© SSIEM and Springer-Verlag Berlin Heidelberg 2015

Abstract ALG9-CDG is one of the less frequently reported types of CDG. Here, we summarize the features of six patients with ALG9-CDG reported in the literature and report the features of four additional patients. The patients presented with drug-resistant infantile epilepsy, hypotonia, dysmorphic features, failure to thrive, global developmental disability, and skeletal dysplasia. One patient presented with nonimmune hydrops fetalis. A brain MRI revealed global atrophy with delayed myelination. Exome sequencing identified a novel homozygous mutation c.1075G>A, p.E359K of the ALG9 gene. The results of our analysis of these patients expand the knowledge of ALG9-CDG phenotype.

Communicated by: Eva Morava, MD PhD

Competing interests: None declared

S. AlSubhi · S. AlShahwan · B. Tabarki (✉)
Divisions of Pediatric Neurology, Prince Sultan Military Medical City, Riyadh, Saudi Arabia
e-mail: btabarki@hotmail.com

A. AlHashem
Division of Genetics, Department of Pediatrics, Prince Sultan Military Medical City, Riyadh, Saudi Arabia

A. AlAzami · F.S. Alkuraya
Department of Genetics, King Faisal Specialist Hospital and Research Center, Riyadh, Saudi Arabia

K. Tlili
Department of Radiology, Prince Sultan Military Medical City, Riyadh, Saudi Arabia

D. Lefeber
Department of Neurology, Translational Metabolic Laboratory of Genetic, Endocrine and Metabolic Diseases, Radboud University Medical Center, Nijmegen, The Netherlands

F.S. Alkuraya
Department of Anatomy and Cell Biology, College of Medicine, Alfaisal University, Riyadh, Saudi Arabia

Introduction

Congenital disorders of glycosylation (CDG) are genetic disorders caused by defects in the synthesis of the glycans of glycoproteins as well as glycolipids. More than 80 inborn errors of metabolism have been described due to congenital defects in protein N-linked glycosylation. CDG affect multiple organ systems. The severity of symptoms is highly variable and shows a broad clinical spectrum with considerable overlap. An increasing number of disorders have been discovered using new techniques that combine glycobiology with next-generation sequencing (Jaeken 2013; Timal et al. 2012). The majority of CDG known to date represent defects of the dolichol-linked oligosaccharide assembly classified as CDG-I. In 2004, a novel form of CDG, ALG9-CDG, was described caused by a deficiency of alpha-1,2-mannosyltransferase due to a defect in the ALG9 gene (Frank et al. 2004). Here, we describe the clinical, biochemical, and molecular features of four new cases of ALG9-CDG.

Methods

We retrospectively reviewed the clinical and genetic data of the patients. HPLC analysis of serum transferrin isoforms was performed as described (Arndt et al. 2007).The *ALG9* mutation was identified using the inborn errors of metabolism gene panel, part of the Mendeliome assay (Saudi Mendeliome Group 2015). Gene panel analysis consisted of removing all non-exonic and non-splice site variants, then utilizing population frequency from our in-house Saudi database to exclude benign polymorphisms. Once the patients were confirmed to have the mutation, the parents were tested. All four patients had a skeletal survey, a brain

MRI, US of the abdomen and kidneys, an echocardiogram, and an EEG.

Results

We have evaluated four patients from a large consanguineous family (pedigree). The main clinical features are summarized in Table 1.

The Mendeliome assay revealed a previously reported homozygous missense mutation (NM_024740.2: c.1588G>A:p.E530K) in the *ALG9* gene. Sanger sequencing confirmed this mutation. The parents were tested and found to be heterozygous for the mutation.

The index case (IV:5) is a 6-year-old female. The mother mentioned decreased fetal movements during pregnancy. The patient was the product of a full-term normal vertex delivery with a birth weight of 3,170 g, length of 49 cm, and head circumference of 34 cm. Apgar score was 8 at 1 min and 9 at 5 min. She was diagnosed since birth to have hip dislocation, dysmorphic features, and congenital heart disease in the form of minor tricuspid regurgitation.

At the age of 4 months, the patient started to develop frequent seizure attacks in the form of frequent clusters of clonic and tonic movements with up-rolling of the eyes. She was frequently admitted for uncontrolled seizures and unexplained febrile episodes. The EEG showed bursts of spikes/sharp waves in the left parieto-central area with slow background activity in favor of epileptic encephalopathy. After the first 5 years of life, the patient became seizure-free with a normal EEG.

The patient showed global developmental disability. At the age of 6 years, she can sit without support, reach for objects, make incomprehensible sounds, turn her head toward a voice, and recognize her family.

On examination at the age of 6 years, all growth parameters were at the 5th percentile. She was fixing but not following. She was hypotonic and showed exaggerated deep tendon reflexes but without clonus.

Facial dysmorphism includes frontal bossing, depressed nasal bridge, low seated ears, large mouth, and hypertelorism. Other associated abnormalities were inverted widely spaced nipples, abnormal distribution of fat on the buttocks, cutis marmorata, cutis aplasia congenita, and broad thumbs (Fig. 1). No organomegaly was noted.

HPLC analysis of the transferrin isoforms showed a type 1 pattern (elevated diasialotransferrin (28%; reference value: 1.10 ± 0.72) and asialotransferrin (2%; reference value: not detectable). The activity of phosphomannomutase and lipid-linked oligosaccharides in fibroblasts were normal. The skeletal survey showed delayed bone age and mild skeletal dysplasia including mesomelic brachymelia with thickening of frontal and occipital bone, mild kyphosis of thoracolumbar spine, bilateral hip dislocation, round pelvis, brachycephaly, and shortening of greater sciatic notch. There are 11 ribs, symmetric with normal shape. The electroretinogram was normal. Brain MRI showed global cerebrum and cerebellar atrophy with delayed myelination.

The family history revealed three affected cousins (Fig. 2). Patients IV:8 and IV:13 have a similar presentation as patient IV:5 (Table 1). The only difference is that patient IV:8 has less severe developmental disability.

Patient IV:3 is a 25-day-old boy. He was diagnosed by fetal ultrasonography at 28 weeks of gestation with hydrops fetalis, which consisted of severe skin edema, pericardial effusion, and ascites. At 37 weeks of gestation, a cesarean section was performed because of breech presentation. Birth weight was 3,700 g (above 97th centile). Apgar scores were 7 at 1 min and 9 at 5 min. He had neck, feet, and skin edema. He had facial dysmorphism including a short nose, with a long philtrum, and a short neck. Echocardiography showed an atrial septal defect and mild dilatation of the right ventricle. Abdominal ultrasound was normal. Skeletal survey showed mild skeletal dysplasia. Cranial ultrasound showed wide subarachnoid spaces.

Discussion

So far only six patients with an ALG9-related phenotype have been reported in the literature (Frank et al. 2004; Tham et al. 2015; Vleugels et al. 2009; Weinstein et al. 2005). In this paper we report four more patients. Our patients' phenotype, except patient IV:3, is similar to that of the patients described by Frank et al. (2004), Vleugels et al. (2009), and Weinstein et al. (2005). All of these patients, including our three, presented with a phenotype including infantile epileptic encephalopathy, progressive microcephaly, failure to thrive, and global developmental disability. Hepatomegaly, cardiac anomalies, mild skeletal dysplasia, and dysmorphism were observed in some patients. Hydrops fetalis was observed in only one patient. The three patients reported by Tham et al. had more severe phenotype (severe skeletal dysplasia, polycystic kidney, and multiple malformations) similar to that first reported by Gillessen-Kaesbach and Nishimura (Gillessen-Kaesbach et al. 1993; Nishimura et al. 1998). All of these patients died in utero. It is possible that the milder phenotypes of patients who were reported previously may be explained by a residual activity of the defective enzymes.

Our study confirms that skeletal dysplasia is a common symptom in ALG9-CDG syndrome, but this feature is also

Table 1 Clinical and molecular characteristics of reported and present patients with ALG9-CDG

	Patient (Frank et al. 2004)	Patient (Weinstein et al. 2005)	Patient (Vleugels et al. 2009)	Patients (3 patients) (Tham et al. 2015)	Patient 1	Patient 2	Patient 3	Patient 4 (25 days old)
Epilepsy	+	+	+		+	+	+	−
Developmental disability	+	+	+		+	+	+	−
Microcephaly	+	+	?		+	+	+	−
Dysmorphism	NA	+	+	+	+	+	+	+
Skeletal dysplasia	NA	NA	NA	Severe	Mild	Mild	Mild	+
Hepatomegaly	+	+	+		Mild	Mild	Mild	Mild
Failure to thrive	NA	+	+		+	+	+	−
Hydrops fetalis	−	−	−	−	−	−	−	+
Echocardiography	NA	Pericardial effusion	Pericardial effusion	CHD (1 patient): large ventricular septum defect and a double outlet right ventricle with anomalous outflow tracts No CHD in 2 patients	Mild tricuspid regurgitation	Normal	Mild pericardial effusion	Atrial septal defect, mild dilatation of right ventricle
US kidneys	NA	Polycystic kidneys	NA	Polycystic kidneys	Normal	Normal	Normal	Normal
Brain MRI	NA	Cerebral and cerebellar atrophy, delayed myelination	Normal (CT)		Cerebral and cerebellar atrophy, delayed myelination	Cerebral and cerebellar atrophy, delayed myelination	Cerebral and cerebellar atrophy, delayed myelination	US head normal
ALG9 mutation	c.1567G>A (p.E523K)	c.860A>G (p.Y286C)	c.860A>G (p.Y286C)	c.1173+2T>A (p.V340A*fs**57)	c.1588G>A (p.E530K)	c.1588G>A (p.E530K)	c.1588G>A (p.E530K)	c.1588G>A (p.E530K)

NA information not available, *CHD* congenital heart disease
Pease note that in Saudi Mendeliome Group (2015), there are three patients

Fig. 1 Photographs of the index case showing craniofacial dysmorphism (partial aplasia cutis congenita of the scalp, hypotelorism, broad base of nose, upturned nose, big mouth, prominent maxilla, large ears), inverted widely spaced nipples, abnormal distribution of fat at the buttocks, cutis marmorata, and broad thumbs

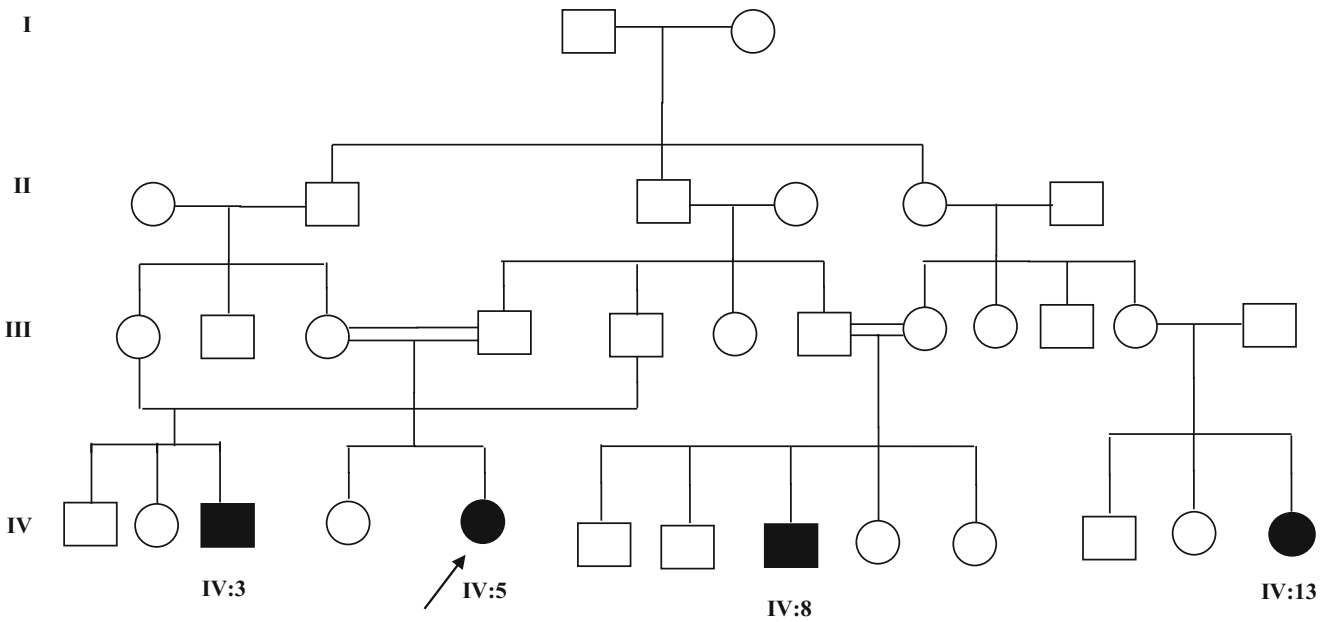

Fig. 2 Pedigree of the family. The index case is indicated by an *arrow*

observed in other CDG including ALG3-CDG and ALG12-CDG (Lepais et al. 2015; Murali et al. 2014). Our study reports for the first time hydrops fetalis in ALG9-CDG. Also patients with PMM2-CDG and ALG8-CDG may present with hydrops fetalis (Höck et al. 2015; van de Kamp et al. 2007).

Although the number of patients is still small, there seems to be some phenotype-genotype correlation (Table 1). Patients with the most severe phenotype exhibit severe lethal skeletal dysplasia with visceral malformations. Their genotype is homozygous for a deleterious variant in the splice donor site of exon 10 in ALG9 (NG_009210.1:g. also denoted NM_024740.2:c.1173+2T>A). This variant results in skipping of exon 10 and leads to a shorter transcript. The other patients exhibit epilepsy and microcephaly, developmental disability, hepatomegaly, mild skeletal dysplasia, and cardiac anomalies. Interestingly, after an aggressive phase after 4–5 years with drug-resistant epilepsy and severe hypotonia, these patients become more stable and show some improvement in their milestones and epilepsy. Their genotype is a homozygous missense mutation.

In conclusion, the clinical and the biochemical findings described in these patients add to the spectrum of presentations of ALG9-CDG. Skeletal dysplasia, ranging in severity from mild to severe, appears to be a consistent feature. Other clinical features common to other forms of CDG are often associated including nonimmune hydrops fetalis.

Synopsis

The ALG9-CDG phenotype commonly includes skeletal dysplasia and may present with hydrops fetalis. A review of the literature suggests genotype-phenotype correlation.

Compliance with the Ethics Guidelines

Conflict of Interest

Sarah AlSubhi, Amal Hashem, Kalthoum Tlili, Saad AlShahwan, Dirk Lefeber, Fowzan S. Alkuraya, and Brahim Tabarki declare that they have no conflict of interest.

Details of the Contributions of Individual Authors

All authors (Sarah AlSubhi, Amal Hashem, Kalthoum Tlili, Saad AlShahwan, Dirk Lefeber, Fowzan S. Alkuraya, Brahim Tabarki) contributed equally in the planning, conducting, and reporting of the work described in the article.

Name of one author who serves as guarantor for the article, accepts full responsibility for the work and/or the conduct of the study, had access to the data, and controlled the decision to publish: Brahim Tabarki

Details of Funding for All Research Studies

None.

"The authors confirm independence from the sponsors; the content of the article has not been influenced by the sponsors."

Details of Ethics Approval

All procedures followed were in accordance with the ethical standards of the responsible committee on human experimentation (institutional and national) and with the Helsinki.

In the declaration of 1975, as revised in 2000, informed consent was obtained from the family for being included in the study.

A Patient Consent Statement

A consent form for the figures has been signed by the parents.

References

Arndt T, Stanzel S, Sewell AC (2007) Paediatric age-dependent serum transferrin isoform distribution studied by HPLC. Clin Lab 53:575–582

Frank CG, Grubenmann CE, Eyaid W, Berger EG, Aebi M, Hennet T (2004) Identification and functional analysis of a defect in the human ALG9 gene: definition of congenital disorder of glycosylation type IL. Am J Hum Genet 75:146–150

Gillessen-Kaesbach G, Meinecke P, Garrett C et al (1993) New autosomal recessive lethal disorder with polycystic kidneys type Potter I, characteristic face, microcephaly, brachymelia, and congenital heart defects. Am J Med Genet 45:511–518

Höck M, Wegleiter K, Ralser E et al (2015) ALG8-CDG: novel patients and review of the literature. Orphanet J Rare Dis 10 (1):73

Jaeken J (2013) Congenital disorders of glycosylation. Handb Clin Neurol 113:1737–1743

Lepais L, Cheillan D, Collardeau Frachon S et al (2015) ALG3-CDG: Report of two siblings with antenatal features carrying homozygous p.Gly96Arg mutation. Am J Med Genet A. doi:10.1002/ajmg.a.37232

Murali C, Lu JT, Jain M et al (2014) Diagnosis of ALG12-CDG by exome sequencing in a case of severe skeletal dysplasia. Mol Genet Metab Rep 1:213–219

Nishimura G, Nakayama M, Fuke Y et al (1998) A lethal osteochondrodysplasia with mesomelic brachymelia, round pelvis, and congenital hepatic fibrosis: two siblings born to consanguineous parents. Pediatr Radiol 28:43–47

Saudi Mendeliome Group (2015) Comprehensive gene panels provide advantages over clinical exome sequencing for Mendelian diseases. Genome Biol 16(1):134

Tham E, Eklund EA, Hammarsjö A et al (2015) A novel phenotype in N-glycosylation disorders: Gillessen–Kaesbach–Nishimura skeletal dysplasia due to pathogenic variants in ALG9. Eur J Hum Genet. doi:10.1038/ejhg.2015.91

Timal S, Hoischen A, Lehle L et al (2012) Gene identification in the congenital disorders of glycosylation type I by whole-exome sequencing. Hum Mol Genet 21:4151–4161

van de Kamp JM, Lefeber DJ, Ruijter GJ et al (2007) Congenital disorder of glycosylation type Ia presenting with hydrops fetalis. J Med Genet 44:277–280

Vleugels W, Keldermans L, Jaeken J et al (2009) Quality control of glycoproteins bearing truncated glycans in an ALG9-defective (CDG-IL) patient. Glycobiology 19:910–917

Weinstein M, Schollen E, Matthijs G et al (2005) CDG-IL: an infant with a novel mutation in the ALG9 gene and additional phenotypic features. Am J Med Genet 136A:194–197